

Amrutha V Nair
Dr. Vipin Solanki



ANALOG AND DIGITAL COMMUNICATIONS



ALEXIS PRESS
JERSEY CITY, USA

ANALOG AND DIGITAL COMMUNICATIONS

ANALOG AND DIGITAL COMMUNICATIONS

Amrutha V Nair
Dr. Vipin Solanki





ALEXIS PRESS

Published by: Alexis Press, LLC, Jersey City, USA
www.alexispress.us

© RESERVED

This book contains information obtained from highly regarded resources.
Copyright for individual contents remains with the authors.
A wide variety of references are listed. Reasonable efforts have been made
to publish reliable data and information, but the author and the publisher
cannot assume responsibility for the validity of
all materials or for the consequences of their use.

No part of this book may be reprinted, reproduced, transmitted,
or utilized in any form by any electronic, mechanical, or other means,
now known or hereinafter invented, including photocopying,
microfilming and recording, or any information storage or retrieval system,
without permission from the publishers.

For permission to photocopy or use material electronically
from this work please access alexispress.us

First Published 2022

A catalogue record for this publication is available from the British Library

Library of Congress Cataloguing in Publication Data

Includes bibliographical references and index.

Analog and Digital Communications by *Amrutha V Nair, Dr. Vipin Solanki*

ISBN 978-1-64532-880-3

CONTENTS

Chapter 1. Introduction to Communication System.....	1
— <i>Mrs. Amrutha V Nair</i>	
Chapter 2. Application of Analog and Digital Communication.....	12
— <i>Mrs. Amrutha V Nair</i>	
Chapter 3. Transmission of Signals through Linear Systems: Convolution Revisited.....	23
— <i>Dr. Abhinav Bhawal</i>	
Chapter 4. Next-generation Mobile Networks	34
— <i>Dr. Saurav Ganguly</i>	
Chapter 5. Development of a System for Registration and Monitoring of UAVs Using 5g Cellular Networks.....	45
— <i>Dr. Prabhu T</i>	
Chapter 6. Wireless Sensor Network Protection System	54
— <i>Dr. K Gowri</i>	
Chapter 7. Massive MIMO Systems: A Family of Hybrid Analog-digital Beam Forming Methods	70
— <i>Dr. Ajit Kumar</i>	
Chapter 8. Time-to-digital Converter (TDC)	88
— <i>Dr. Vipin Solanki</i>	
Chapter 9. High-power Microwave Weapons.....	111
— <i>Dr. Rahul Kumar</i>	
Chapter 10. Digital Signal Processing.....	125
— <i>Dr. Vikram Singh</i>	
Chapter 11. IOT Application in Analog and Digital Communication	147
— <i>Ravendra Pratap Rana</i>	
Chapter 12. Modern Environmental Recording Devices.....	181
— <i>Dr. Vikas Sharma</i>	

CHAPTER 1

INTRODUCTION TO COMMUNICATION SYSTEM

Mrs. Amrutha V Nair, Assistant Professor

Department of Electronics and Communication Engineering, Presidency University, Bangalore, India

Email Id- amruthavnair@presidencyuniversity.in

In keeping with this quote from Auguste Comte, we start our introduction to communication systems study with a historical overview of this field that affects our everyday lives in some manner. This section's subsections each concentrate on certain significant and relevant occurrences in the communication industry's past development.

Telegraph

Samuel Morse, a painter, developed the telegraph. When Morse's electric telegraph sent the words "What hath God done" between Washington, D.C., and Baltimore, Maryland, in 1844, it started an entirely new method of real-time, long-distance communication. The telegraph is the predecessor of digital communications because it is well suited for manual keying. The four symbols that make up the Morse code's alphabet are a dot, a dash, a letter space, and a word space; short sequences stand in for common letters, while lengthy sequences stand in for rare letters.

Radio

The underlying system of equations carries his name. In 1864, James Clerk Maxwell developed the electromagnetic theory of light and predicted the emergence of radio waves. Heinrich Hertz performed an experimental verification of radio waves in 1887. Oliver Lodge demonstrated wireless communication in 1894 over a manageable 150-yard distance. Then, on December 12, 1901, Guglielmo Marconi at Signal Hill in Newfoundland picked up a radio signal that had originated 1700 miles distant in Cornwall, England. Thus, the path was cleared for a significant expansion in the reach of communications. The first radio transmission was made famous by self-educated professor Reginald Fessenden in 1906.

Edwin H. Armstrong created the superheterodyne radio receiver in 1918; nowadays, this kind of receiver makes up the majority of radios. Armstrong showed yet another ground-breaking idea in 1933, a modulation technique he named Frequency Modulation (FM). The article by Armstrong arguing the favour of FM radio was released in 1936.

A teacher of the deaf named Alexander Graham Bell created the telephone in 1875. Real-time voice communication through electrical encoding and sound reproduction became a possibility thanks to the telephone. The first telephone was rudimentary and inadequate, allowing only short-distance communication. Interest in automated telephone service emerged when it had just been around for a few years. Notably, the mechanical step-by-step switch that carries his name was created by Kansas City, Missouri-based undertaker A. B. Strowger in 1897. The Strowger

switch was the most well-liked and extensively utilised of all the electromechanical switches developed throughout the years.

Electronics

The vacuum-tube diode, created in 1904 by John Ambrose Fleming, served as a precursor to Lee de Forest's creation of the vacuum-tube triode in 1906. The triode was discovered in 1913, which marked the beginning of wireless voice communications and played a crucial role in the development of transcontinental telephony. The triode was the ultimate amplifier design tool up until the development and refinement of the transistor[1], [2].

Walter H. Brattain, John Bardeen, and William Shockley at Bell Laboratories created the transistor in 1948. Robert Noyce created the first silicon integrated circuit (IC) in 1958. These significant advancements in integrated circuits and solid-state technology paved the way for the creation of single-chip microprocessors and very-large-scale integrated (VLSI) circuits, which permanently altered the nature of signal processing and the telecommunications sector.

Television

Vladimir K. Zworykin and Philo T. Farnsworth both gave demonstrations of the first fully electronic television system in 1929. The British Transmission Corporation (BBC) began commercial television broadcasting in 1939. Harry Nyquist presented a seminal article on the telegraphic signal transmission theory in 1928. Nyquist, in particular, created standards for the proper receipt of telegraph messages sent across dispersive channels without noise. A significant portion of Nyquist's early research was eventually used to transmit digital data via dispersive channels.

Pulse-code modulation (PCM), developed by Alex Reeves in 1937, is used to digitally encode voice signals. The method was created during World War II to permit the encryption of voice communications; in fact, the US military deployed a full-scale, 24-channel system after the conflict. However, PCM had to wait until the transistor was discovered and large-scale circuit integration was developed before it could be used commercially. Figure 1 discloses the Communication system and the User Information.

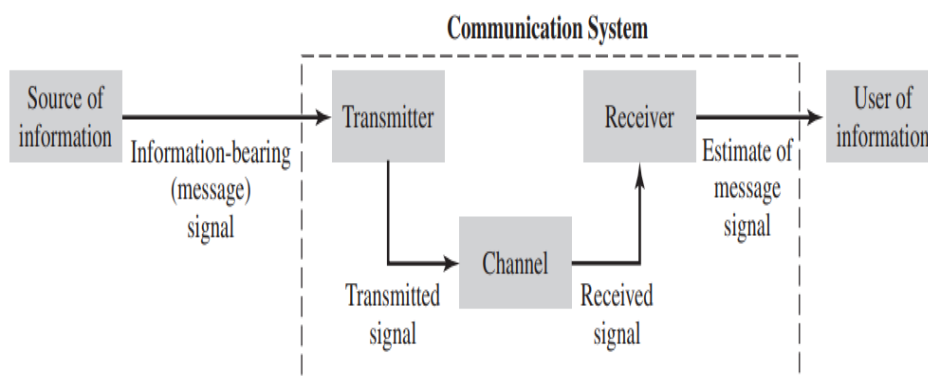


Figure 1: Discloses the Communication system and the User Information.

Electronics have been used in switching and digital communications since the 1948 introduction of the transistor. The goals were to increase capacity, lower cost, and enhance dependability. Bell Laboratories received the first call via a stored-program system in March 1958, and Morris, Illinois, in June 1960, saw the start of the first commercial telephone service using digital switching. Bell Laboratories implemented the first T-1 carrier system transmission in 1962.

The matching filter was created by D. O. North in 1943 to provide the best detection of a known signal in additive white noise. The phrase "matching filter" was first used by J. H. Van Vleck and D. Middleton in 1946 after they separately achieved a comparable result. A Mathematical Theory of Communication, a study written by Claude Shannon in 1948, provides the theoretical groundwork for modern digital communications. The response to Shannon's article was swift and fervent. The title of Shannon's article was changed to "The Mathematical Theory of Communications" when it was republished a year later in a book he co-wrote with Warren Weaver. Perhaps this answer gave Shannon the confidence to do so. It is interesting to note that before Shannon's 1948 classic article was published, it was thought that raising the pace at which information is sent through a channel would increase the likelihood of a mistake[3], [4]. When Shannon demonstrated that this was untrue, provided the transmission rate was below the channel capacity, the community of communication theory was taken aback. Figure 2 discloses the Communication system and the Satellite.

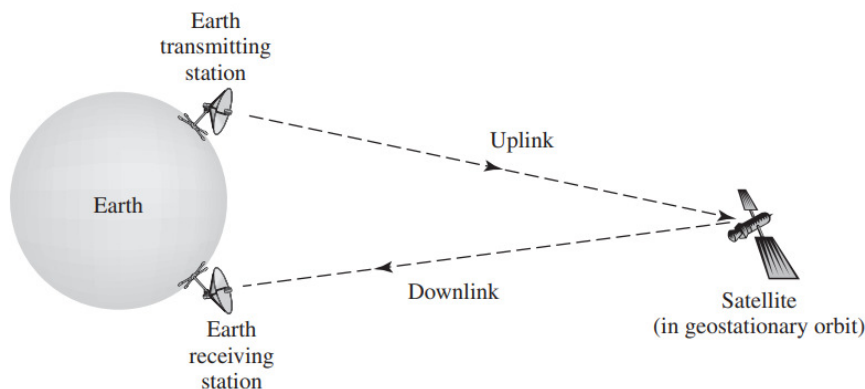


Figure 2: Discloses the Communication system and the Satellite.

Under the technical supervision of J. Presper Eckert, Jr. and John W. Mauchly, the first electronic digital computer, known as the ENIAC, was constructed at the Moore School of Electrical Engineering at the University of Pennsylvania between 1943 and 1946. However, starting with the initial draught of a paper made in 1945, John von Neumann's contributions were some of the first and most important to the theory, design, and use of digital computers. In the early 1950s, terminals and computers began talking with one another over great distances. Initially, voice-grade telephone circuits running at slow rates (300 to 1200 b/s) were employed as the connections. The concept of adaptive equalisation, developed by Robert Lucky in 1965, and effective modulation methods, developed by G. Ungerboeck in 1982, are only two of the many elements that have helped data transmission speeds rise dramatically. Another concept that's used often in computer communications is automated repeat-request (ARQ). H. C. A. van Duuren first

came up with the ARQ approach during World War II, and it was published in 1946. To facilitate long-distance telex transmission, it was employed to enhance radio-telephony. Numerous investigations on computer networks were conducted between 1950 and 1970. However, the Advanced Research Projects Agency Network (ARPANET), which went into operation for the first time in 1971, was the most important of them in terms of its influence on computer communications.

The Advanced Research Projects Agency of the United States Department of Defense funded the creation of ARPANET. On the ARPANET, groundbreaking work in packet switching was done. The ARPANET was dubbed the Internet in 1985. When Tim Berners-Lee suggested the World Wide Web, a hypermedia software interface to the Internet, in 1990, it marked a turning point in the development of the Internet. The Web moved from being unheard of to being widely recognized in only two years, reaching its peak of commercialization in 1994. We may suggest the following explanations for the Internet's rapid development:

The components for the formation of the Web were there before it sprang into reality. Particularly, personal computers (PCs) had already proliferated in households all over the globe as a result of VLSI, and they were progressively being fitted with modems for communication with the outside world. The Internet has been expanding gradually for almost 20 years but only among a small group of users, and it had now crossed a crucial barrier for electronic mail and file sharing. Hypertext markup language (HTML), hypertext transfer protocol (HTTP), and standards for document description and transport had been established. Figure 3 discloses the Communication system and the Boundry of subnet.

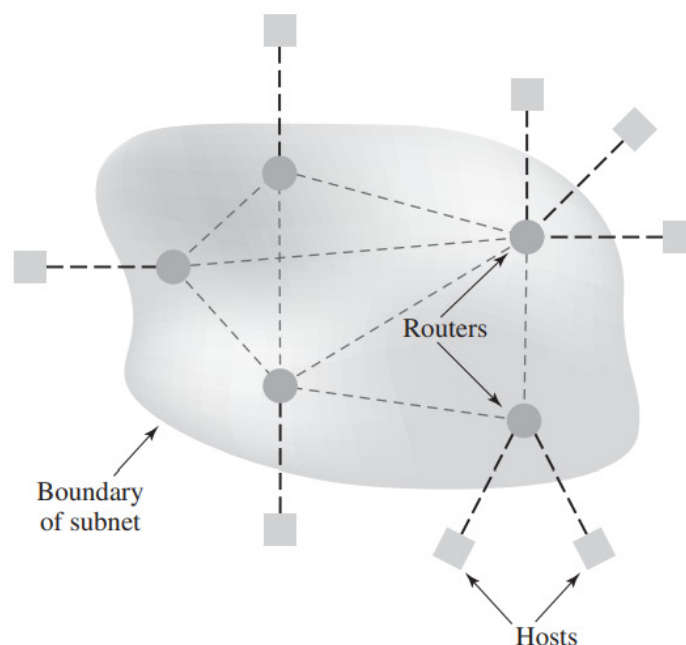


Figure 3: Discloses the Communication system and the Boundry of subnet.

Thus, everything required to create the Web was already present, except for two essential components: a straightforward user interface and an innovative service idea using satellite technology. John R. Pierce suggested using satellites for communications in 1955. However, Arthur C. Clark had already proposed the notion of employing an Earth-orbiting satellite as a relay point for communication between two Earth stations in a paper that was published in 1945, which came before this one. Sputnik I, launched by the Soviet Union in 1957, relayed telemetry data for 21 days. The American launch of Explorer I in 1958, which sent out telemetry signals for around five months, came soon after. On July 10, 1962, Telstar I was launched from Cape Canaveral, marking a significant advancement in communications satellite technology. Bell Laboratories, which had gained a great deal of information from Pierce's pioneering work, created the Telstar satellite. Only by using maser receivers and huge antennas was it feasible for the satellite to send TV shows over the Atlantic. Figure 4 discloses the Communication system and the subnet.

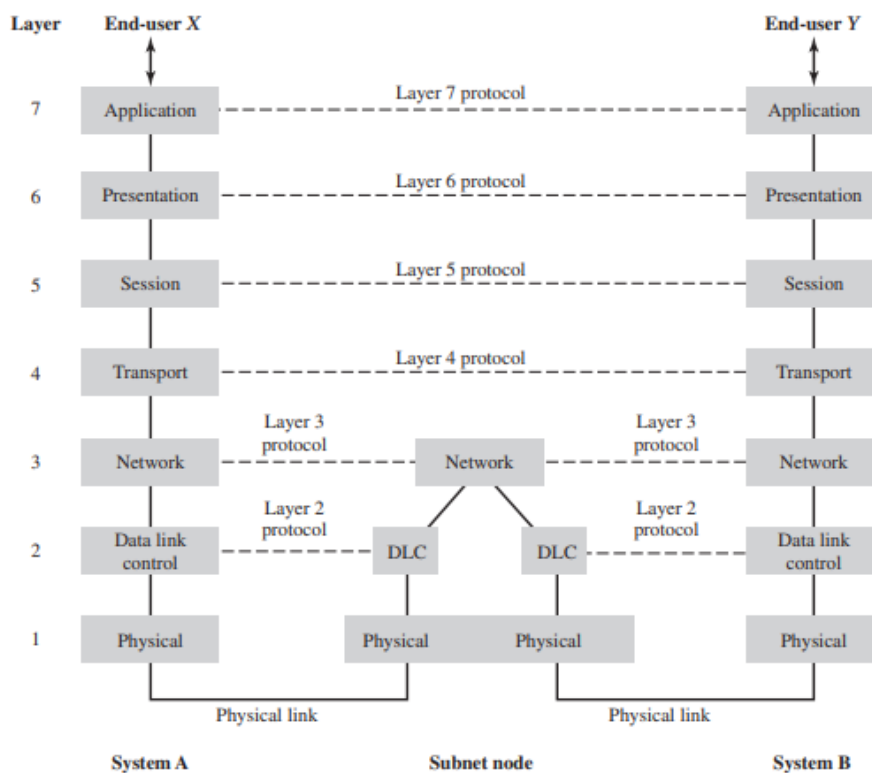


Figure 4: Discloses the Communication system and the subnet.

Optical Communications Information has been sent by optical methods since the dawn of time, such as smoke and fire signals. However, until 1966, when K. C. Kao and G. A. Hockham of Standard Telephone Laboratories, U. K., suggested the use of a clad glass fibre as a dielectric waveguide, no significant advancement in optical communications had been realised. In 1959 and 1960, the laser a.k.a. light amplification by stimulated emission of radiation was created and refined. Kao and Hockham made two points clear: the inherent loss, as estimated by Rayleigh scattering, is extremely minimal, and the attenuation in optical fibre was caused by imperfections

in the glass. They said that a loss of 20 dB/km ought to be possible. This amazing forecast, made when the power loss through a glass fibre was around 1000 dB/km, would subsequently be proven correct. Transmission losses as low as 0.1 dB/km are now possible.

Dramatic changes in the telecommunications environment are all a result of the phenomenal advancements in microelectronics, digital computers, and lightwave systems that we have seen to date and will continue to see in the future. Many of these modifications have already been made, and more will be made in the future. Use of a single, highly effective transmitter and several, easily constructed receivers is known as broadcasting. Information-carrying signals in this kind of communication system only go in one way, from the transmitter to each of the receivers out in the field.

Point-to-point communication is when a single transmitter and a single receiver communicate with each other across a single connection. There is often a bidirectional flow of information-bearing signals in this second type of communication networks signals, which in turn necessitates the employment of a transceiver (i.e., transmitter and receiver) at either end of the connection. The transmitter transforms the message signal generated by an information source into a format appropriate for transmission across the channel at some point in space. The channel then transmits the message signal to the receiver, who is located at a different position in space. However, channel defects cause signal distortion during transmission via the channel. Additionally, interference signals and noise from other sources are added to the channel output, causing the received signal to be a distorted copy of the broadcast signal. For the information user, the receiver's role is to process the received signal to approximate the original message signal. We use the word "estimate" because there will always be a little difference between the transmitter input and the receiver output due to noise, interference, and poor channels[3], [5].

RADIO

Depending on how it is utilised, the radio may serve as a point-to-point communication tool as well as a broadcasting tool. We are all quite used to both AM and FM radio. AM and FM are acronyms for amplitude and frequency modulation, respectively. We discover the two of them in every home and on every automobile; they are created in an integrated form inside of a single unit. We listen to the news on the radio that is aired from nearby radio stations, including local, national, and worldwide news, commentary, music, and weather predictions. AM radios and FM radios have historically been constructed utilising analogue technology. However, digital radio in both AM and FM variants is already in use today due to the continuously improving capabilities and low cost of digital electronics.

Radio uses electrical impulses to convey speech. Electrical impulses are used to convey visual pictures in television, which likewise functions on comparable electromagnetic and communication-theoretic principles. Since a speech signal is by definition a one-dimensional function of time, signal processing methods are naturally suited to it. A picture in motion, on the other hand, is a two-dimensional function of time, necessitating closer scrutiny. Each image at a given moment is perceived as a frame split into several tiny squares known as picture components, or pixels; the more pixels are utilised to depict an image, the higher its resolution

will be. The information in the picture is transformed into an electrical signal whose amplitude is proportional to the brightness level of the individual pixels by scanning the pixels in a systematic order. The electrical signal produced at the scanner's output is the transmission of the video stream. The receiver is aware of the well-defined mapping procedure that leads to the generation of the visual signal. The receiver can thus rebuild the original picture from the video feed. Television benefits from the same amazing developments in digital technology that digital radio does. High-definition television (HDTV), which significantly improves the quality of reconstructed pictures at the receiver output, was developed as a result of these developments, the use of sophisticated digital signal processing methods, and customer demands.

The point-to-point communication scenario is our next stop. Two more key ways that the radio has impacted our everyday lives are via satellite communications and wireless communications. Line-of-sight radio propagation is necessary for the functioning of both the uplink and the downlink in satellite communications, which are centred on a satellite in geostationary orbit. A transponder i.e., the satellite's electronic circuitry is connected to an Earth terminal through an uplink, and a transponder is connected to another Earth terminal via a downlink. Accordingly, as shown in Fig. 1.2, an information-carrying signal is transferred from the Earth terminal to the satellite through the uplink, amplified in the transponder, and then retransmitted from the satellite via the downlink to the other Earth terminal. By accomplishing this, a satellite communication system provides a special feature: worldwide coverage.

Wireless communications function somewhat similarly to satellite communications in that both a downlink and an uplink are required. The forward-link radio transmission from a base station to its mobile users is done through the downlink. The reverse-link radio transmission from mobile users to their base stations is handled by the uplink. Due to reflections of the broadcast signal from objects such as buildings, trees, etc. that are in the propagation path, wireless communications unlike satellite communications are dominated by the multipath phenomenon. The performance of the receiver tends to suffer as a result of this occurrence, making the receiver's design a difficult assignment. In any case, mobile communications have a special capacity all of their own. Additionally, the wireless communication system can reuse the radio spectrum across a huge region as often as feasible thanks to the utilisation of the cellular idea. Mobile users operating inside a cell may share the available communication resources within that cell.

TELEPHONE NETWORKS

The computer was first imagined as a standalone device that could conduct mathematical operations. However, it was quickly seen that the computer is well suited to the construction given the intrinsic capacity of a computer to conduct logical operations. Networked communications. A communication network is made up of several routers, which are composed of intelligent processors such as microprocessors. The term "routers" refers to the fact that the main function of these processors is to route speech or data via the network. A host is a device that communicates with another host; hosts are connected to every router. The conveyance or exchange of audio, video, or data between hosts is the primary function of a network, which is

made possible by the use of digital switching. Circuit switching and packet switching are the two main types of switching.

Circuit switching establishes specialized communication channels for the transfer of messages between two or more stations, often known as terminals. From source to destination, the communication circuit is made up of a linked series of connections. For instance, the connections could be made up of time slots as in time-division multiplexed systems, where numerous users can share a single channel. The crucial thing to remember is that once it is set up, the circuit stays open during transmission. A centralized hierarchical control mechanism with knowledge of the whole network's structure often manages circuit switching. A free channel via the phone network must be taken and then allocated to the exclusive usage of the two users who want to communicate to create a circuit-switched connection. For instance, before communication can start, the call-request signal must travel to the destination and be recognized. The network becomes practically transparent to the users at this point, meaning that the two users effectively "own" the resources allotted to the circuit for the duration of the connection. Until the circuit is severed, this situation persists [6], [7].

For telephone networks, where voice transmission makes up the majority of network traffic, circuit switching is a good fit. We claim this because speech generates a stream of traffic and voice discussions often last longer approximately two minutes on average than the time needed to set up the circuit (about 0.1 to 0.5 seconds). On the other hand, in packet switching, network resources are shared according to demand. Consequently, packet switching is superior to circuit switching in that P. Baran created packet switching in 1964 to meet a requirement for American national security. The initial requirement was to construct a distributed network with various degrees of redundancy, which is robust in the sense that it can withstand the loss of numerous nodes due to a coordinated attack while still allowing the remaining nodes to maintain intercommunication for carrying common and control information.

A subgroup of the International Organization for Standardization (ISO) created the OSI reference model in 1977. See Tannenbaum for a discussion of the ideas used to determine the initial seven levels of the OSI model as well as an explanation of the layers themselves (1996). A link is often used more completely when it has traffic to convey. Data transmissions, in contrast to spoken communications, may come in the form of bursts.

Store and forward is the packet switching network tenet. In a packet-switched network, in particular, every message longer than a defined size is broken into segments that do not exceed the required size before transmission. The resulting parts are known as packets. The original message is pieced back together packet by packet at the destination after being transported through several network regions. Thus, it is possible to think of the network as a collection of network resources such as channel bandwidth, buffers, and switching processors that are dynamically shared by a group of rival sites that want to connect. The circuit-switched network, where the resources are allocated to a pair of hosts for the whole time they are in contact, contrasts sharply with this dynamic sharing of network resources.

Networks for data

A data network is a kind of communication network where the hosts are all made up of computers and terminals. By considering the network in terms of a layered architecture, which is considered a hierarchy of nested layers, the design of such a network progresses in an orderly manner. A layer is a procedure or item within a computer system that is created to carry out a certain task. The internal workings and intricacies of a layer will be known to its creators. However, a user only sees the layer in question as a "black box" at the system level, where it is characterized in terms of inputs, outputs, and the functional relationship between the inputs and outputs. Each layer in a layered architecture views the layer below it as one or more "black boxes" with a defined set of functional requirements that the layer above it may utilise. Thus, the very challenging communication issue in data networks is reduced to a manageable collection of clearly defined, mutually exclusive roles. This type of thinking is what inspired the creation of the OSI reference model, which stands for open systems interconnection. The ability of any two systems to link is referred to be "open," given that those systems adhere to the reference model and the standards that go along with it.

The communications and related-connection functions are arranged in the OSI reference model as several layers with clearly defined interfaces. Every layer is built on the one before it. Each layer specifically carries out a related subset of basic operations and depends on the layer below it to carry out further primitive tasks. Additionally, each layer protects the layer above it from the specifics of how those services are implemented by providing it with certain services. There is an interface between each pair of layers that outlines the services the lower layer makes available to the top layer[8], [9]. The roles of each of the model's component layers are likewise described in the diagram. According to a set of guidelines and standards known as layer k protocol, layer k on system A, for example, connects with layer R on another system B. where $k = 1, 2, \dots, 7$. The word "protocol" is a borrowing from everyday speech that refers to customary human social conduct. Peer processes are the objects that make up the appropriate levels on various systems. In other words, communication between systems A and B is accomplished by protocol-based peer-to-peer communication between the two systems. Physical link between neighbouring processes giving end users access to the OSI environment

Data transformation is the process of transforming incoming data to provide services chosen by the application layer; encryption is one example of data transformation that provides security giving two collaborating users a control framework for communication and managing their conversation in an organized manner and control over the whole communication chain, from source to destination, between users flow control and packet routing via the network are intended to ensure excellent performance over a communication connection discovered by the packet routing process error prevention for secure information transmission via the channel.

Transmission of unprocessed data bits through a physical channel; this layer takes care of the functional, procedural, and mechanical needs to access the channel only exists at layer 1, or the physical layer. The subsequent layers, 2 through 7, are connected to their far-off colleagues virtually. Through layer-to-layer interfaces, each of these last six levels communicates data and control with layers above and below.

INTERNET

The Internet is reached from the topic of data networks that was just provided. The Internet paradigm adopts an abstract definition of network service to isolate the underlying network technology from the current applications. In additional detail, we might state the following: The technology used to build the network does not affect how the apps are run. Hosts, subnets, and routers are the three functional building pieces of the Internet application. The hosts, where data originates or is delivered, are the network's nodes. To bridge subnet borders, routers serve as intermediary nodes. All sites that are part of a subnet exchange data directly with one another; for instance, subnets. Generally speaking, a subnet's internal functioning is divided into two categories.

Connectionless mode, where the independent packets are known as datagrams, in analogy with telegrams, and connected approach, where the connections are known as virtual circuits, in analogy with actual circuits set up in a telephone system. The Internet has a tiered system of protocols, much like previous data networks. Data interchange between hosts and routers is specifically carried out via the Internet protocol (IP). It is straightforward, creating an addressing scheme with the ability to send packets of data from one node to another. The routers decide how the packets designated for a certain destination should be routed while crossing a sub-network border. This is carried out through routing tables that are created by using unique protocols to communicate important data with other routers. The provision of best-effort service is the end consequence of using the layered set of protocols. In other words, the Internet promises to send each data packet.

REFERENCES:

- [1] R. Surahmat, M. Neherta, and N. Nurariati, "Hubungan Karakteristik Perawat terhadap Pelaksanaan Sasaran Keselamatan Pasien Pasca Akreditasi Rumah Sakit 'X' di Kota Palembang Tahun 2018," *J. Ilm. Univ. Batanghari Jambi*, 2019, doi: 10.33087/jiubj.v19i1.493.
- [2] G. M. Talaue, A. AlSaad, N. AlRushaidan, A. AlHugail, and S. AlFahhad, "The Impact of Social Media on Academic Performance of Selected College Students," *Int. J. Adv. Inf. Technol.*, 2018, doi: 10.5121/ijait.2018.8503.
- [3] J. L. Darbyshire, M. Müller-Trapet, J. Cheer, F. M. Fazi, and J. D. Young, "Mapping sources of noise in an intensive care unit," *Anaesthesia*, 2019, doi: 10.1111/anae.14690.
- [4] J. van Dijck, "Governing digital societies: Private platforms, public values," *Comput. Law Secur. Rev.*, 2020, doi: 10.1016/j.clsr.2019.105377.
- [5] R. M. Chaerudin and T. E. Permana, "Analisis Pengaruh Citra Merek dan Kualitas Produk Terhadap Loyalitas Pengguna Smartphone Android dengan Kepuasan Sebagai Variabel Intervening Di Lingkungan Mahasiswa Universitas Bandung Raya," *Ekonom J. Ekon. Akunt. Manaj.*, 2020, doi: 10.37577/ekonom.v1i2.213.
- [6] F. Zezulka, P. Marcon, Z. Bradac, J. Arm, T. Benesl, and I. Vesely, "Communication Systems for Industry 4.0 and the IIoT," 2018. doi: 10.1016/j.ifacol.2018.07.145.

- [7] A. Kumar and M. Gupta, "A review on activities of fifth generation mobile communication system," *Alexandria Engineering Journal*. 2018. doi: 10.1016/j.aej.2017.01.043.
- [8] C. Y. Li *et al.*, "A High-Speed and Long-Reach PAM4 Optical Wireless Communication System," *IEEE Photonics J.*, 2018, doi: 10.1109/JPHOT.2018.2859321.
- [9] V. Raj and S. Kalyani, "Backpropagating through the air: Deep learning at physical layer without channel models," *IEEE Commun. Lett.*, 2018, doi: 10.1109/LCOMM.2018.2868103.

CHAPTER 2

APPLICATION OF ANALOG AND DIGITAL COMMUNICATION

Mrs. Amrutha V Nair, Assistant Professor

Department of Electronics and Communication Engineering, Presidency University, Bangalore, India

Email Id- amruthavnair@presidencyuniversity.in

Computers are now at the centre of a communication medium that is fundamentally altering our everyday lives at home and work thanks to the development of the Internet into a global network. One host in North America may send an email to another host in Australia at the other end of the world, and the message will get there in a couple of seconds. This is even more amazing considering that the message's constituent packets very well may have travelled wholly different routes across the network. Our usage of the Internet to browse the Web serves as another example of how powerful it is. To find references related to a certain topic of interest, for instance, we may utilise a search engine. Searching through books and journals at the library, which used to take hours or even days, just takes a few seconds today!

We need a wideband modem (i.e., modulator-demodulator) to provide a quick communication connection between that host and its subnet to fully leverage the processing capacity of the Internet from a host situated at a faraway location. When we use the term "fast," we refer to operational rates of at least a few megabits per second. The 'digital subscriber line' is a device that complies with this criterion (DSL). The DSL's ability to function across a linear wideband channel with an open frequency response makes it even more impressive. A typical telephone channel constructed employing twisted pairs for signal transmission serves as an example of such a channel. Two solid copper conductors wrapped in polyvinyl chloride (PVC) sheaths make up a twisted pair. Cables are often constructed from twisted pairs, with each cable including several twisted pairs that are near to one another. By using the well-known engineering concept of divide and conquer, the DSL meets the demanding criteria mentioned above from the perspective of signal transmission.

The wideband channel is specifically represented by a series of narrowband channels, each of which may then be handled in a reasonably simple way. Should make one more last point. Typically, hosts in the form of computer terminals are used to establish access to the Internet i.e., servers. By using portable devices that serve as hosts and connect with Internet subnets through wireless networks, access is widened. We now have a new communication medium with a vast array of practical applications by combining mobility via wireless communications with the processing power of the Internet.

Transmission of Voice over Internet Protocol (VoIP), which would make it feasible to combine telephone services with the quickly expanding Internet-based applications, is one of the significant issues confronting the telecoms sector. Because the IP is built to facilitate data interchange between hosts and routers, it is challenging to provide quality service for VoIP, which exacerbates the difficulty.

The number of packets lost during network transit compared to the overall number of packets pushed into the network is known as the packet loss ratio. The duration it takes for a specific host-to-host connection's packet to go across the network is known as the connection delay. According to subjective VoIP testing, the packet loss ratio and one-way connection time must both be kept below 1% to offer voice-grade telephone service. The packet loss ratio may increase by up to 160 ms without noticeably losing quality. Deployment of well-managed, well-designed VoIP networks that adhere to these requirements is taking place. The problem of initial-echo control is still difficult to solve. Initial echo describes the echo heard at the start of a call on the first word or a few syllables said by a user [1], [2].

An impedance mismatch anywhere in the network causes the incident signal to be reflected in the source, causing the echo. In the future, we may say the following about internet calling: Private branch exchanges (PBXs), which are distant switching devices with their independent controls, will be replaced by VoIP along with other types of office switches. VoIP is presently successful with longer distance calls as well, although this is mostly because long-haul networks now have extra capacity. A real-time service like VoIP would suffer if the demand on these long-haul networks rises, increasing the latency. Therefore, VoIP telephone may become commonplace and popular provided long-service providers continue to build capacity such that loading is constantly low and response time is quick, assuring the quality of service.

It is common to think of broadcasting and point-to-point communication systems when discussing significant applications of digital communication concepts. However, CD and DVD players serve as excellent examples of how the same ideas are used for the digital storage of audio and visual information. In that their storage capacity in the tens of gigabytes is orders of magnitude more than that of CDs, and they can also transport data at a much faster pace, DVDs are improvements to CDs. To store audio and video signals, the digital domain is preferable over the analogue domain for the reasons listed below. The digital-to-analogue conversion (DAC) process, whose parameterization is in the designer's control, determines the quality of a digitalized audio-video signal as assessed in terms of frequency response, linearity, and noise.

After the audio/video signal has been converted to digital form, we may utilise sophisticated and potent encoding methods to minimize bandwidth and defend against the danger of committing storage-related mistakes. The digital storage of audio and video signals does not deteriorate with time for the majority of real-world applications. The production of integrated circuits used to create CDs and DVDs continues to advance, ensuring the ever-rising cost-effectiveness of these digital storage media.

DVDs can store hours of high-quality audio-visual material because of the strong encoding methods included in their design, which makes them the perfect medium for interactive multimedia applications. However, the systems are made to allow for the effective use of two key communication resources in their unique ways. The average power of the signal being transferred is referred to as transmitted power. The breadth of the channel's pass band determines the channel bandwidth. We may categorize communication routes following which of these two resources is thought to be the limiting element as follows:

Channels with a restricted amount of transmitting power. Such channels include, for instance, the following: Low transmitted power is preferred on wireless channels to save battery life. It is necessary to maintain the broadcast power on the downlink at a modest level while using satellite channels since the available power on the satellite transponder is limited. Deep-space communications, where the amount of power a probe may use to go across space is severely constrained, necessitating keeping the average strength of the signals the probe sends to an Earth station as low as feasible.

Channels with a restricted amount of capacity, when bandwidth is scarce. The following are examples of this second type of communication channel. Telephone channels, where it is necessary to reduce the frequency band allotted to transmitting each voice signal while maintaining the quality of service for each user in a multi-user scenario. Channel bandwidth for television channels is restricted by regulatory bodies, and reception quality is ensured by utilizing a high enough transmitted power.

The inevitable existence of noise at a communication system's receiver input is another crucial consideration. Noise is a general term for unwanted signals that tend to degrade the quality of the signal that is received in a communication system. The sources of noise in the system might be internal or external. The common channel noise that results from the thermal movement of electrons in the receiver's front-end amplifier is an example of internal noise. External noise examples include ambient noise and interference from signals sent by other users[3], [4].

Thinking in terms of the signal-to-noise ratio (SNR), a dimensionless metric, allows one to quantitatively account for the positive impact of the transmitted power in comparison to the deteriorating effect of noise i.e., measure the quality of the received signal. For example, the formal definition of the SNR at the receiver input is the ratio of the average power of the received signal also known as the channel output to the average power of noise measured at the receiver input. The SNR is often expressed in decibels (dBs), which are equal to 10 times the power ratio's logarithm (to base 10) For instance, 10, 100, and 1000 have signal-to-noise ratios of 10, 20, and 30 dBs, respectively.

The fundamental theory for the study of communication systems is information theory. Due to this theory's extremely mathematical and hence complex character, which makes it unsuitable for an introductory book, we have not included it here. This talk has made it clear that there are only two system-design characteristics that matter in terms of performance evaluation: channel bandwidth and signal-to-noise ratio. In more precise language. Signal-to-noise ratio and channel bandwidth are the key design factors in communication systems. According to the limitations of the system, we may thus enhance system performance by using one of two possible design strategies:

1. The signal-to-noise ratio is improved to account for a channel bandwidth restriction.
2. The channel bandwidth is expanded to satisfy a signal-to-noise ratio restriction.
3. Because boosting the signal-to-noise ratio may be done by simply increasing the transmitted power, strategy 1 of these two design methods is often easier to execute than strategy 2. On the other hand, to take advantage of increased channel bandwidth, we must

also raise the broadcast signal's bandwidth, which calls for a corresponding rise in transmitter and receiver complexity.

It is difficult to understand communication networks from a theoretical and technological standpoint. Four ideas that are crucial for comprehending various facets of communication systems are highlighted in this section. Whether in the context of digital or analogue communications, modulation is a fundamental signal-processing operation for the transmission of an information-bearing signal through a communication channel. By altering a carrier wave's parameter in line with the information-bearing message signal, this process is carried out. Depending on the application, the carrier wave may take one of two fundamental forms:

Sinusoidal carrier wave in which the information-carrying signal chooses to modify the amplitude, phase, or frequency periodic series of pulses, where the information-carrying signal modifies one or more of the pulses' amplitude, breadth, or positions. Whatever method is used to carry out the modulation process, the following modulation theory problems must be resolved description of the modulated signal in the time domain description of the modulated signal in the frequency domain detection of the original information-carrying signal and assessment of the receiver's response to noise.

The Fourier transform is a linear mathematical operation that converts a signal's time-domain description into a frequency-domain description without losing any of the original signal's information, enabling accurate recovery of the original signal from the frequency-domain description. However, a few prerequisites must be met for the signal to be Fourier transformable. Fortunately, the signals that are encountered while researching communication systems satisfy these requirements. The following concerns may be assessed mathematically using Fourier analysis a modulated signal's frequency-domain description, including the transmission bandwidth signal transmission using a communication channel or (frequency-selective) filter as an example of a linear system correlation between two signals, or resemblance.

Due to the fast Fourier transform methodology, which offers a quick way to compute the Fourier transform, these assessments have even more significance. One of the challenges the receiver has is how to accurately identify the original information-bearing signal from a received signal that has been distorted by additive channel noise. Two factors make the signal-detection challenge more challenging there are noise present factors like the carrier wave's unexplained phase shift caused by the sinusoid ally modulated signal being sent through the channel[5], [6].

The way these problems are handled in analogue communications and digital communications are quite different from one another. The typical strategy in analogue communications concentrates on output signal-to-noise ratio and associated computations. On the other hand, the signal detection issue in digital communications is seen as a hypothesis-testing issue. What is the likelihood that the binary symbol 1 would be accurately identified, for instance, in the particular scenario of binary data transmission, assuming that it is communicated, and how is that likelihood impacted by a change in the signal-to-noise ratio at the receiver input?

Therefore, we address the following analogue communications concerns in dealing with detection theory: The score used to evaluate how well a certain modulation scheme performs in

noise threshold phenomena that happens when the signal-to-noise ratio of a signal is conveyed falls below a specific level.

1. Performance evaluation of various modulation techniques.
2. On the other hand, in digital communications, we consider:
3. The typical likelihood of a symbol mistake at the output of the receiver.
4. Coping with uncontrolled circumstances is a problem.
5. Contrasting different digital modulation techniques.

It is clear from the succinct exposition just given on the function of detection theory in the study of communication networks that we must get a thorough grasp of the following: Probability theory is a mathematical theory that explains how randomly occurring occurrences behave in statistical analysis of noise and random signals.

A random signal, in contrast to a deterministic signal, is unpredictable before occurrence. Due to the uncertainty, a random signal may be considered to be a part of an ensemble, or group, of signals, each of which has a unique waveform from the ensemble's other signals. Additionally, each signal in the ensemble has a certain chance of occurring. The term "random process" or "stochastic process" refers to the collection of signals. A random process includes examples like:

A radio or television receiver's front-end amplifier produces electrical noise.

1. Either a male or female speaker's speech signal.
2. A TV broadcasting station's antenna sends out a video signal.
3. We discuss the following topics about probability theory, random signals, and noise:
4. Fundamental ideas in probabilistic models and probability theory.
5. A random process' statistical description using ensemble and temporal averages.
6. Processing and analysis of random signals using mathematics.

In this chapter, we have provided a quick overview of the basic theories of communication systems as well as a historical description and applications of communications. Additionally, we made the following arguments to back up our assertion that studying this field is both very difficult and exciting. Communication systems include a wide range of applications, including radio, television, wireless, satellite, deep-space, telephone, data networks, the Internet, and many more. Digital communication is now the preeminent method of communication. Many of the developments in digital communication systems that we have seen may be attributed to the following enabling theories and technologies. A thorough knowledge of the processing of information-bearing signals and their transmission via physical mediums requires the application of abstract mathematical concepts.

Digital signal-processing techniques for effective signal filtering, correlation, and computing of spectra software development and cutting-edge CPU designs. Remarkable developments in the production of very large-scale integrated (VLSI) circuits and the physics of solid-state devices. The study of communication systems is a dynamic field that is always changing as a result of technology advancements in other fields of study as well as new social demands. Last but not least, communication systems have an impact on our everyday lives at home and work, and

without the accessibility of communication tools that we take for granted, our lives would be much less rich.

An overview of both analogue and digital types of communication systems is provided in the next eleven chapters of the book. The book should equip the reader to continue learning about a field that can best be defined as having an almost infinite range of applications. Given the trend towards combining wire line and wireless networks to provide the integrated transmission of voice, video, and data, this is particularly true. When a signal's waveform is presented on an oscilloscope, we often observe it as a function of time, which is how signals are typically characterized mathematically. However, as was said in Chapter 1, we must understand the signal's frequency content from the standpoint of a communication system. The Fourier transform is a mathematical technique that links the signal's time-domain description to its frequency-domain description. The Fourier transform is accessible in several different forms. We limit the discussion in this chapter largely to two distinct versions: The Fourier transform (FT), sometimes known as the continuous Fourier transform, operates on continuous functions in both the time and frequency domains. The discrete Fourier transform, sometimes known as DFT, is a mathematical algorithm that handles discrete data in both the time and frequency domains.

Since the main goal of this chapter is to determine the frequency content of a continuous-time signal or to assess what happens to this frequency content when the signal is passed through a linear time-invariant (LTI) system, a large portion of the information presented in this chapter focuses on the Fourier transform. The discrete Fourier transform, on the other hand, is useful when it is necessary to assess the frequency content of the signal on a digital computer or to assess what happens to the signal when it is processed by a digital device, such as in digital communications. It is discussed towards the end of the chapter.

These lessons are taught through the vast content in this chapter:

1. 1st lesson: A signal's complex amplitudes of the elements that make up its frequency-domain description or spectral content are specified by the Fourier transform of the signal.
2. Given its frequency-domain description, the signal can only be recovered through the inverse Fourier transform.
3. Lesson 2: The Fourier transform has several significant characteristics that, both individually and together, provide crucial insight into the link between a signal's frequency domain description and its time domain definition.
4. Lesson 3: Only the frequency domain or the time domain, not both, may be used to firmly restrict a signal.
5. Lesson 4: A linear time-invariant filter's frequency response and the spectral content of a signal are both described by a quantity known as bandwidth.

The Fourier Transform The early 19th century saw the study of heat flow by Joseph Fourier. At that time, figuring out how to understand heat movement meant solving the heat equation, a partial-differential equation with both practical and scientific implications. To solve partial differential equations, Fourier created a method known as the Fourier series. This method was

based on the idea that the solution was a weighted sum of harmonically linked sinusoids with unknown coefficients. After assessment by Lagrange, Laplace, and Legendre, Fourier's inaugural study on heat conduction was rejected by the Academy of Sciences of Paris in 1807. Despite his contemporaries criticizing him for lacking rigor, Fourier continued in refining his theories. Eventually, in 1822, he wrote *Theory analytique de la chaleur*, which is today recognized as one of the classics of mathematics and included much of his work. The fast Fourier transform method, which is a popular technique that is used to compute the discrete Fourier transform, is the mathematical instrument for Fourier transformation-related digital calculations.

The Relative Importance of Time and Frequency

The characteristics of the Fourier transform covered demonstrate an inverse relationship between the time-domain and frequency-domain representations of a signal. We may specifically express two key points here signal's frequency-domain description changes in the opposite direction of how its time-domain description does, and vice versa. Because of this inverse link, a signal cannot be specified arbitrarily in any domain. To put it another way, we can define either an arbitrary function of time or an arbitrary spectrum, but not both at once.

If a signal's frequency is rigorously constrained, its time-domain description will continue eternally even if its amplitude may gradually decrease. If a signal's Fourier transform is precisely 0 outside of a certain range of frequencies, it is said to be strictly frequency-restricted or strictly band-limited, a sinc pulse is an example of a signal that is strictly band-limited. The sinc pulse's temporal limit is merely asymptotically constrained, as this picture demonstrates. Inversely, even if the amplitude spectrum may take on increasingly decreasing values, a signal's spectrum is infinite in size if it is strictly time bound i.e., precisely 0 outside of a defined period. The triangular pulse and the rectangular pulse are two examples of this phenomenon. A signal cannot be confined in both time and frequency, we may thus say. We have trouble defining the signal's bandwidth, however, when the signal is not exactly band restricted, which is usually the case. The issue stems from the mathematical ambiguity of the definition of "significant" as it relates to the spectral composition of the signal. As a result, there is no agreed-upon definition of bandwidth [7], [8].

However, there are a few definitions of bandwidth that are often used. In this part, we'll take a closer look at three of these definitions. How each term is put together depends on whether the signal is low-pass or band-pass. If a signal's considerable spectral content is concentrated near the origin, it is said to be low-pass. If a signal's substantial spectral content is concentrated around a consistent frequency, it is referred to as being band-pass.

We may utilise the main lobe as the foundation for determining the signal's bandwidth when a signal's spectrum is symmetric and has a main lobe that is bordered by clearly defined nulls i.e., frequencies at which the spectrum is zero. This is justified since the majority of the signal energy is found in the primary spectral lobe. The bandwidth of a low-pass signal is equal to half the width of the primary spectral lobe, since only half of this lobe is located within the positive frequency range. As a result, we may describe this rectangular pulse's bandwidth in hertz. The bandwidth is determined by the width of the major lobe for positive frequencies if, on the other

hand, the signal is band-pass with the main spectral lobes centred around where is big. The null-to-null bandwidth is the name given to this concept of bandwidth. For instance, we may thus use hertz to denote the null-to-null bandwidth of this RF pulse. We may conclude from the definitions given here that a low-pass signal's bandwidth is effectively doubled when its spectral content is shifted by a sufficiently big frequency.

The 3-dB bandwidth is another widely used measure of bandwidth. The 3-dB bandwidth is specifically defined as the distance between the positive frequency at which the amplitude spectrum reaches its highest value and the zero frequency at which it reaches its peak value if the signal is low-pass. For instance, the rising and decaying exponential pulses shown in have a 3-dB hertz bandwidth. On the other hand, if the signal is band-pass, the 3-dB bandwidth is defined as the distance between the two frequencies where the amplitude spectrum of the signal reaches its highest value along the positive frequency axis.

The 3-dB bandwidth has the benefit of being easily read from an amplitude spectrum display. Its drawback is that it could be deceptive if the amplitude spectrum contains progressively fading tails. The root-mean-square (rms) bandwidth is yet another metric for signal bandwidth and is calculated as the square root of the second moment of the signal's squared amplitude spectrum around a suitable point. To allow for the second instant to be measured around the origin, we assume that the signal is low-pass. To normalise the squared amplitude spectrum, we need a nonnegative function with the denominator that performs the right normalisation in the sense that the integral value of this ratio throughout the whole frequency axis is 1. Although it is more difficult to measure in the lab, the rms bandwidth has the advantage of being more amenable to quantitative assessment than the other two definitions of bandwidth.

The product of the signal's duration and bandwidth is always a constant for any family of pulse signals that vary by a time-scaling factor, as shown by. The product is also known as the bandwidth-duration product or time-bandwidth product. Another example of the inverse connection between the time-domain and frequency-domain representations of a signal is the consistency of the time-bandwidth product. In particular, if the time scale of a pulse signal is compressed by a factor, let's say, a frequency scale of the signal's spectrum is extended by the same factor, and as a result, the signal's bandwidth, by Property 2 (dilation), is preserved constantly. For instance, the time-bandwidth product of a rectangular pulse with a duration T seconds and bandwidth defined as the positive frequency component of the main lobe is equal to hertz. What's crucial to remember is that, regardless of how we define a signal's bandwidth, the time-bandwidth product holds for certain classes of pulse signals. The specification of bandwidth that is chosen only affects the constant's value.

1. The theory of the Fourier transform, as outlined in, is strictly speaking only relevant to time functions that meet the Dirichlet requirements. Energy signals that is, signals for which the condition is true are examples of such functions. The hypothesis should be expanded in two ways, however, as follows:
2. To provide a unified framework that combines the theories of the Fourier series and Fourier transform, allowing the Fourier series to be considered as a specific instance of the Fourier transform.

3. To broaden the Fourier transform's range of applications to power signals, or signals for which the condition is true.

It turns out that the "correct usage" of the Dirac delta function or unit impulse achieves both of these goals. The Dirac delta function, indicated by $\delta(t)$, is said to have zero amplitude everywhere save when it is infinitely huge and has a single region under its curve. It fulfills the relationship between the Dirac delta function and the delta function must be an even function of time t , according to this set of relations.

The delta function, however, must strictly only occur as a factor in the integrand of an integral about time and then only when the other element in the integrand is a continuous function of time for it to have any significance. Consider the product of a function $f(t)$ and the time-shifted delta function $\delta(t - t_0)$ given that $f(t)$ is such a function. This equation's left-hand side operation separates the value of the function at that particular moment. This leads to the term "sifting property of the delta function". This property combines. In other words, any time function that is convolutional with the delta function does not affect whatsoever on the original function. The replication property of the delta function is what we call this claim. Using the sifting feature of the delta function and observing that $\int_{-\infty}^{\infty} \delta(t) dt = 1$ we derive the Fourier transform of the delta function, which by definition is provided by the Fourier-transform pair for the Dirac delta function so as follows:

It's crucial to understand that the Fourier-transform pair only makes sense in a restricted sense. The key argument is that none of the two qualities of equations nor the corresponding filtering feature of the equation exists for any function in common sense. The value of the function tends to zero at every point except where it approaches infinity, but we may envisage a succession of functions with gradually higher and thinner peaks with the area under the curve staying equal to unity. In other words, when the pulse's duration approaches 0, we may think of the delta function as the limiting form of a pulse with a unit area. What kind of pulse shape is employed is irrelevant [9], [10].

The Dirac delta function is formally a member of the group of functions known as generalised functions or distributions. There are times when using it calls for extreme caution. However, the Dirac delta function has a certain beauty in that the right answer is often obtained by treating the function like the one presented here. Two beneficial characteristics of the Gaussian function are that its derivatives are all continuous, and it decays more quickly than any power of t . The limit is taken to get the delta function. When this happens, the Gaussian pulse's area stays finite and fixed at unity, but its duration and amplitude become indefinitely long and narrow, respectively. Except for the fact that it has now been scaled in duration by the factor σ and in amplitude by the factor $1/\sigma$, the Gaussian pulse described here is the same as the unit Gaussian pulse generated. Therefore, using the Fourier transform pair and the linearity and dilation features.

The equation states that a dc signal is transformed in the frequency domain into a delta function occurring at zero frequency, as shown in and noting that the delta function is an even function. This outcome makes intuitive sense, of course. Using the Fourier transform formulation, we can easily get the relevant conclusion. Given that the delta function has real values, the following

simplified version of the connection possibly offers a different definition of the delta function, this time one that is in the frequency domain.

Then, and the frequency-shifting characteristic, we arrive at the Fourier transform pair, which represents a complex exponential function of frequency. Next, consider the issue of determining the cosine function's Fourier transform. Consequently, we discover that the Fourier-transform pair represents the cosine function using Eq.

In other words, the cosine function spectrum consists of two delta functions that occur at each and are each weighted. Similarly, we can demonstrate that the Fourier transform pair, which is shown represents the sine function demonstrates that the signum function equals both positive and negative time. The signum function was previously defined in Eq, and for the sake of exposition, this definition is repeated here: Since the signum function does not meet the Dirichlet requirements, it does not technically possess a Fourier transform. However, when the parameter a gets closer to zero, we may construct a Fourier transform for the signum function by considering it to be the limiting form of the odd-symmetric double-exponential pulse.

The continuous curve represents the amplitude spectrum of the signum function (b). We can observe that, for tiny a , the approximation is excellent, except for the region close to the frequency axis origin. While the spectrum of the signum function extends to infinity at the origin, the spectrum of the approximation function is zero. For positive time and zero for negative time, the unit step function $u(t)$ equals. It is repeated here for convenience even though it was already. The unit step function and signum function are connected by this defining equation and that of the signum function, or by the waveforms of Figs. This indicates that a delta function with a weight of a and occurring at zero frequency may be found in the spectrum of the unit step function, as illustrated.

The relationship assuming that a is zero, explains the impact of integration on a signal's Fourier transform. We will now analyse the more general scenario without making this assumption. As shown by where the time-shifted unit step function is defined, the integrated signal may be thought of as the convolution of the original signal with the unit step function. Using the Fourier-transform pair for the unit step function, we discover that the Fourier transform is where is the Fourier transform of convolution in the time domain and is multiplication in the frequency domain in line with Property. We have a sifting property for a delta function expressed in the frequency domain.

REFERENCES:

- [1] L. Lamata, A. Parra-Rodriguez, M. Sanz, and E. Solano, "Digital-analog quantum simulations with superconducting circuits," *Advances in Physics: X*, 2018. doi: 10.1080/23746149.2018.1457981.
- [2] M. Mubarak and M. D. Adnjani, "STRATEGI SOSIALISASI MIGRASI SISTEM PENYIARAN ANALOG KE DIGITAL DI JAWA TENGAH," *J. ASPIKOM*, 2018, doi: 10.24329/aspikom.v3i4.215.
- [3] C. Schmidt, C. Kottke, R. Freund, F. Gerfers, and V. Jungnickel, "Digital-to-analog

- converters for high-speed optical communications using frequency interleaving: impairments and characteristics,” *Opt. Express*, 2018, doi: 10.1364/oe.26.006758.
- [4] P. Del Hougne and G. Lerosey, “Leveraging Chaos for Wave-Based Analog Computation: Demonstration with Indoor Wireless Communication Signals,” *Phys. Rev. X*, 2018, doi: 10.1103/PhysRevX.8.041037.
- [5] M. Lim, “Roots, Routes, and Routers: Communications and Media of Contemporary Social Movements,” *Journal. Commun. Monogr.*, 2018, doi: 10.1177/1522637918770419.
- [6] D. DARLIS, A. R. DARLIS, and M. H. ABIBI, “Implementasi Sistem Penyiaran Musik Digital di Kafe menggunakan Visible Light Communication,” *ELKOMIKA J. Tek. Energi Elektr. Tek. Telekomun. Tek. Elektron.*, 2018, doi: 10.26760/elkomika.v5i1.60.
- [7] J. Zhang, Y. Huang, T. Yu, J. Wang, and M. Xiao, “Hybrid Precoding for Multi-Subarray Millimeter-Wave Communication Systems,” *IEEE Wirel. Commun. Lett.*, 2018, doi: 10.1109/LWC.2017.2782811.
- [8] A. H. Naqvi and S. Lim, “Review of recent phased arrays for millimeter-wave wireless communication,” *Sensors (Switzerland)*. 2018. doi: 10.3390/s18103194.
- [9] W. Utschick, C. Stockle, M. Joham, and J. Luo, “Hybrid LISA Precoding for Multiuser Millimeter-Wave Communications,” *IEEE Trans. Wirel. Commun.*, 2018, doi: 10.1109/TWC.2017.2770125.
- [10] C. Xu, R. Ye, Y. Huang, S. He, and C. Zhang, “Hybrid Precoding for Broadband Millimeter-Wave Communication Systems with Partial CSI,” *IEEE Access*, 2018, doi: 10.1109/ACCESS.2018.2862432.

CHAPTER 3

TRANSMISSION OF SIGNALS THROUGH LINEAR SYSTEMS: CONVOLUTION REVISITED

Dr. Abhirup Bhawal, Assistant Professor

Department of Electronics and Communication Engineering, Presidency University, Bangalore, India

Email Id- abhirup.bhawal@presidencyuniversity.in

Now that we have the Fourier transform theory at our disposal from the earlier parts, it is time to focus on the investigation of a particular type of system known as linear systems. Any physical object or phenomena that generate an output signal in response to an input signal is referred to as a system. The output signal is often referred to as the response, while the input signal is commonly referred to as the excitation. The concept of superposition applies to linear systems, meaning that the total of a system's reactions to several excitations delivered concurrently is equivalent to the system's responses to each excitation applied separately. Convolution in Signal Transmission through Linear Systems 53 linear region revisited. A filter is a frequency-selective device used to confine a signal's spectrum to a certain range of frequencies. A communication system's physical material used to link the transmitter and receiver is referred to as a channel. We want to assess the results of sending signals via communication channels and linear filters. Depending on the description used for the filter or channel, there are two methods to do this assessment. In other words, as explained below, we may use time-domain or frequency-domain concepts.

A linear system is characterized in terms of its impulse response in the time domain, which is the reaction of the system with zero starting conditions to an applied unit impulse or delta function. This feature indicates that if the system is time-invariant, a time-shifted unit impulse at the input of the system generates an impulse response at the output of the system that is time-shifted by the same amount. In other words, regardless of when the unit impulse is administered to the system, the impulse response of a linear time-invariant system will always have the same form. As a result, we can represent the impulse response of a linear time-invariant system, assuming that.

Without a doubt, the approximation improves with smaller Each pulse approaches a delta function weighted by a factor equal to the pulse's height as it gets closer to zero in the limit. Think of a typical pulse. The convolution integral refers to this relationship. Three separate time scales are involved in system-memory time, reaction time, and excitation time the linear time-invariant systems time-domain analysis is based on this connection. It claims that a weighted integral over the prior history of the input signal, weighted following the system's impulse response, represents the current value of a linear time-invariant system's response. As a result, the system's impulse response serves as a memory function.

The dc component becomes the dominating output and the form of the input square wave is entirely obliterated by the filter when the fundamental frequency of the input square wave is raised further to the high value that corresponds to a time-bandwidth product. These findings lead us to a crucial conclusion: We need to employ a time-bandwidth product when applying an ideal low-pass filter to make sure that the output waveform can be distinguished from the input waveform. The rise time and decay time of the filter pulse response tend to decrease with increasing BT values.

You may describe a filter by giving details about its impulse response or transfer function. Nevertheless, the use of a filter often entails the separation of signals based on their spectra (i.e., frequency contents). In turn, this implies that the frequency domain is often used in the construction of filters. The design of a filter involves two fundamental steps:

1. A realizable transfer function's approximation of specified frequency response (i.e., amplitude response, phase response, or both).
2. The physical manifestation of the approximate transfer function.

An approximate transfer function must represent a stable system to be physically realizable. The conventional method is to replace with s and recast the transfer function in terms of s to provide the associated stability condition in terms of the transfer function. Both a real and an imaginary portion may exist in the new variable s . Therefore, s is referred to as the complex frequency. Let be the system's transfer function, defined in the way outlined. The approximate transfer function is often rational, therefore it may be represented in the factored form where K is a scaling factor. These points are known as the transfer function's zeros and poles, respectively. The quantity of zeros, m , for a low-pass transfer function is fewer than the number of poles, n . Note that the condition for stability only applies to the poles of the transfer function; the zeros may be located anywhere in the s -plane if the system is causal. If the system is causal, then the bounded input-bounded output condition for the stability of the system is satisfied by limiting all of the transfer function's poles to be inside the left half of the s -plane. Depending on where the m zeros are located in the s -plane, two kinds of systems may be distinguished. Systems with a minimum phase are identified by a transfer function whose poles and zeros must all fit within the left hand of the s -plane [1], [2].

Nonminimum-phase systems are allowed to have zeros in their transfer functions on both the right half of the s -plane and the imaginary axis. The phase response of this family of linear time-invariant systems, known as minimum-phase systems, is uniquely correlated with the gain response. We may note two common families of filters in the case of low-pass filters, where the main criterion is to approach the ideal amplitude response.

The origin serves as the center and radius of a circle with the poles of the transfer function in a Butterworth filter, where B is the filter's 3-dB bandwidth. On the other hand, with a Chebyshev filter, the poles are on an ellipse. Naturally, the poles are limited to the left side of the s -plane in both scenarios. When it comes to the actual manifestation of the filter, there are essentially two ways to go about it, one analogue and the other digital either inductors and capacitors or

capacitors, resistors, and operational amplifiers are used to construct analogue filters. The ease of implementation is a benefit of analogue filters.

Digital filters, where the signals are quantized and sampled in time along with their amplitude. The name of these filters comes from their use of digital electronics. A crucial component of a digital filter is its programmability, which provides a great level of design freedom. In essence, flexibility is sacrificed for complexity. The characterization of signals and systems is continued in this part by concentrating on the concept of energy while taking into account the class of energy signals, where we analyse the second kind of signals, power signals, and completes the categorization of signals and systems. The amplitude spectrum of the signal of interest squared is what we refer to as the spectral density, a new quantity that we specifically add. Consider an energy signal that is considered to have complex values for the sake of generality. Following the information provided in the discussion of the correlation theorem, we explicitly define the autocorrelation function of the energy signal for a lag.

The autocorrelation function offers a measure of the similarity between the signal and its delayed counterpart, according to this formula. As a result, it may be calculated using the configuration in. The time lag functions as a variable for scanning or searching. If is complex-valued, then take note that is complex-valued. The Rayleigh energy theorem is significant because it not only identifies the squared amplitude spectrum as the distribution of the signal's energy measured in the frequency domain but also offers a practical method for calculating the energy of a pulse signal. We formally define the energy spectral density or energy density spectrum of an energy signal as where is the amplitude spectrum of. This definition is based on the theorem mentioned before. Despite the possibility that the signal itself may have a complex value, it is obvious that the energy spectral density is a nonnegative real-valued number for all. Let where following the correlation theory outlined as an energy signal that is Fourier transformable. The autocorrelation function of the signal is defined by the left-hand side as a consequence of this circumstance. As a result, the right-hand side of the equation in the frequency domain determines the energy spectral density. As a result, we may say that, given an energy signal, the autocorrelation function and energy spectral density make up a pair of Fourier transforms[3], [4].

The entire area under the curve of the complex-valued autocorrelation function of a complex-valued energy signal is equal to the real-valued energy spectrum at zero frequency, according to the whole area under the curve of the real-valued energy spectral density of an energy signal is equal to the total energy of the signal. The Rayleigh energy theorem is simply introduced differently by this second finding. Squaring does not affect the rectangular function hence the energy spectral density is by using the inverse Fourier transform, we can determine that the autocorrelation function of the sinc pulse is provided by, which has a waveform that is identical to the sinc pulse itself when displayed as a function of the lag.

This example demonstrates that, in certain cases, it is simpler to compute the autocorrelation function of an energy signal indirectly, based on the energy spectral density, as opposed to directly, by using the autocorrelation function formula. Let's say that the energy signal is now processed by a linear, time-invariant transfer function system to produce the output signal shown indicates that when an energy signal is passed via a linear time-invariant filter, the energy

spectral density of the resultant output equals the energy spectral density of the input multiplied by the squared amplitude of both sides of the equation by the filter's squared amplitude response. The straightforwardness of this assertion highlights the significance of spectral density as a variable for describing the energy distribution of a Fourier transformable signal in the frequency domain.

Additionally, based on the link between the Wiener-Khintchine equations we may define an indirect technique for assessing the impact of linear time-invariant filtering on the autocorrelation function of an energy signal:

1. To get and, respectively, find the Fourier transforms of and.
2. Use to calculate the output's energy spectral density.
3. Calculate by using the inverse Fourier transform on the results from point 2 to determine.

This chapter's content amply demonstrates the significance of the Fourier transform as a theoretical tool for the representation of deterministic signals and linear time-invariant systems. The existence of a family of algorithms known as fast Fourier transform algorithms for the very effective numerical computation of the Fourier transform serves to further emphasize the significance of the Fourier transform. The discrete Fourier transform, as its name suggests, represents both time and frequency in discrete form. This is where the rapid Fourier transform technique derives from. An approximate representation of the Fourier transform is given by the discrete Fourier transform.

We must use extreme caution while carrying out the sampling procedures necessary to define the discrete Fourier transform to correctly reflect the information content of the original signal, the sampling procedure will be treated in full. For now, it is sufficient to state that, given a band-limited signal, the sampling rate must be more than twice the input signal's highest frequency component. Additionally, the signal's spectrum repeats per Hz if the samples are equally spaced apart by seconds. Let N represent the number of frequency samples in an interval.

Sequences of integers specified at evenly spaced points in time and frequency make up the input and output of the discrete Fourier transform (DFT), respectively. The DFT is well suited for direct numerical assessment on a digital computer because of this property. Additionally, the fastest way to do the calculation is to use a family of algorithms known as fast Fourier transform (FFT) techniques. Because they use far fewer arithmetic operations than the DFT's brute-force processing, FFT techniques are computationally efficient. In essence, a divide-and-conquer method is used by an FFT algorithm to achieve its computing efficiency, where the initial DFT calculation is broken down into smaller DFT computations one at a time. In this part, we provide an overview of a popular FFT method that was created using a similar approach [5], [6].

Twisted pair is the primary transmission method used to link residences to telephone central switching offices. A twisted pair typically consists of two solid copper wires covered with polyethylene. The American Wire Gauge, or 26 AWG, the designation for this cable size is if the copper strand has a diameter of 0.4 mm. A transmission line is an illustration of a twisted pair. Two conductors make up a transmission line, and each one has its intrinsic resistance and inductance. Since the two conductors are often close to one another, there is also a potential

conductance via the material that is employed to insulate the two wires. The lumped circuit is a common representation of such a transmission line. Although the impedances are shown as discrete components, it would be more accurate to think of them as spread throughout the transmission line's length.

A transmission line will have a distorting impact on the transmitted signal based on the circuit element values. The frequency response of the transmission line will also increase with line length since the overall impedance does, too. We demonstrate the usual behaviour of a twisted pair with lengths ranging from 2 to 8 kilometres. Twisted pairs with one pair devoted to each phone line go straight from the central office to the residence. As a result, the transmission cables may be quite lengthy. The outcomes presumptively include a continuous cable. In actual use, the cable may have several splices, different gauge cables running along various stretches of the course, and so on. The frequency response of the cable will be further impacted by these discontinuities in the transmission medium.

Amplitude Modulation: Benefits, Drawbacks, and Modifications

The first kind of modulation is amplitude modulation. Its main advantage is how simple it is to produce and reverse, as was previously mentioned. The end consequence is that it is reasonably cheap to construct an amplitude modulation system. But as we know from our two main communication resources transmitted power and channel bandwidth should be utilised wisely. We discover that the amplitude modulation described has two significant practical constraints in this context:

Transmission power is wasted by amplitude modulation. The information-carrying signal is not at all reliant on the carrier wave $c(t)$. Since only a small portion of the total transmitted power is changed by amplitude modulation, the transmission of the carrier wave constitutes a waste of power. Amplitude modulation also wastes channel capacity. Due to the symmetry that exists between the upper and lower sidebands of an AM wave concerning the carrier frequency, we may uniquely identify one sideband by knowing its amplitude and phase spectrum. This implies that only one sideband is required for information transmission, and as a result, the communication channel only has to provide the same bandwidth as the message signal. As a result of this finding, amplitude modulation wastes channel capacity since it needs twice as much transmission bandwidth as message bandwidth.

We need to make certain adjustments that make the amplitude modulation process more complicated to get beyond these two constraints of AM. In essence, we compromise system complexity for better communication resource use. We can differentiate three variations of amplitude modulation, starting with amplitude modulation:

1. Double sideband-suppressed carrier (DSB-SC) modulation, in which only the top and lower sidebands are broadcast as a wave. Here, the carrier wave is suppressed to reduce transmitted power, but the channel bandwidth need remains the same (i.e., twice the message bandwidth).
2. Single sideband modulation (SSB), in which the modulated wave is made up only of the upper or lower sideband. Therefore, translating the spectrum of the modulating signal

(with or without inversion) $m(t) \cos(\omega_c t)$. The primary purpose of SSB modulation is to shift the spectrum of a message signal to a new point in the frequency domain. Due to the energy difference between zero and a few hundred hertz in the spectrum of speech transmissions, single-sideband modulation is especially well suited for the transmission of voice communications. Concerning transmitted power and channel bandwidth requirements, SSB is the ideal continuous-wave modulation method. Its main drawbacks are higher complexity and a narrow range of applications.

3. Vestigial sideband (VSB) modulation, in which only a faint remnant of the other sideband is kept when one sideband has nearly fully passed. Because of this, the needed channel bandwidth is somewhat more than the message bandwidth by a factor of the width of the vestigial sideband. The transmission of wideband signals, like television broadcasts, which include major components at very low frequencies, is ideally suited for this kind of modulation. In commercial television transmission, a significant carrier is delivered in addition to the modulated wave, allowing the arriving modulated signal to be demodulated [7], [8].

Motivation for Vestigial Sideband Modulation

For an information-carrying signal such as a voice signal with an energy gap centred on zero frequency, single-sideband modulation performs adequately. But for the spectrally effective transmission of wideband signals, we must consider a novel modulation technique for two reasons:

1. Wideband transmissions often include large low frequencies in their spectra, as seen in television visual signals and computer data, making SSB modulation impracticable.
2. Wideband data's spectral properties are appropriate for DSB-SC application. The bandwidth conservation condition is broken by DSB-SC, which needs a transmission bandwidth twice as large as the message bandwidth.

We need a compromise modulation technique that, in terms of spectrum features, falls midway between SSB and DSB-SC to get over these two practical constraints. This section's last modulation scheme to be taken into account is called the vestigial sideband. In two practical ways, vestigial sideband (VSB) modulation differs from SSB modulation:

1. A remnant or trace of a sideband rather than its total removal is conveyed; therefore, the term "vestigial sideband."
2. Almost the whole second band is also transmitted, as opposed to only the opposite sideband.

Therefore, where B is the vestige bandwidth and W is the message bandwidth, the transmission bandwidth of a VSB-modulated signal is determined which consists of a product modulator followed by a band-pass filter, which may be used to provide VSB modulation. The band pass filter is referred to as a sideband shaping filter for VSB modulation. The VSB spectrum at the modulator output is structured in the manner shown in assuming that the remnant of the VSB is located in the bottom sideband of the DSB-SC modulated wave. The transfer function of the filter, which is represented by the symbol, determines the spectrum shaping. The transmitted

remnant must make up for the spectral component that the other sideband lacks for the sideband shaping to be successful. This criterion makes sure that, except for amplitude scaling, coherent detection of the VSB-modulated wave recovers a copy of the message signal.

Hardware and software developments in info-communication technologies are connected. Fractal and multiracial analysis of data streams, converged network service architecture, parametric synthesis of networks with self-similar traffic, and managing the process of servicing hybrid telecommunications services are some examples of the areas of software info-communication systems that are currently undergoing rapid development. The most recent advancements in semiconductor device engineering are largely responsible for the status of hardware today. This strategy suggests that the physical implementation of semiconductor devices will eventually hit its technical limit. As a result, characteristics of transistor architectures with negative differential resistance have lately received increasing attention.

The development and study of devices on transistor structures with negative differential resistance that is compatible with microelectronic technology for producing and forming signals with regular and chaotic dynamics for information communication systems is a promising area of engineering. Since the early 1980s, devices using transistor architectures with negative differential resistance have been developed and used to generate and shape signals. Applications of devices with chaotic signal dynamics in information communication systems have been established on both a theoretical and practical level. An essential scientific and technological problem at the moment is the development and use of devices for the generation and formation of signals with regular and chaotic dynamics based on transistor architectures with negative differential resistance.

Modern oscillators for info communication system facilities need to have a broad operational frequency spectrum and enough power. Additionally, energy-efficient equipment for creating and forming signals for info-communication systems is required. Such oscillators must be designed to produce signals in a certain frequency range with both regular and chaotic dynamics and little out-of-band radiation. Additionally, silicon or silicon-germanium integrated circuits must be used to build the electric oscillators.

The need for high-performance, reasonably priced, and energy-efficient radio-frequency integrated circuits have surged in response to the contemporary information market's explosive expansion. Voltage-controlled oscillators are the heart of such radio frequency integrated circuits that are energy-efficient. Microwave oscillators have historically been constructed using two-transistor cross-connected designs, particularly those using CMOS or HEMT technology. As components for regulating the frequency change voltage, reactors or MOS transistors are used. The high sensitivity of the oscillator and the tuning nonlinearity, however, make this solution unsuitable for monolithic integration of the oscillator with the radio receiver. As a result, in real-world applications, a voltage-controlled oscillator with sub band division is employed. One of two methods adding or subtracting a specific amount of capacitance or inductance from the oscillator's oscillating circuit can be used to do this or switching between oscillating circuits that have been separately adapted and adjusted for various frequency ranges.

The authors of this paper suggest a method for building negative differential resistance transistor architectures with nonlinear and reactive features to create voltage-controlled microwave oscillators. Electric oscillations with both regular and chaotic dynamics may be produced by these oscillators. The regular dynamics of electric oscillations in voltage-controlled oscillators on transistor architectures with negative differential resistance are studied theoretically and experimentally in this study [9], [10].

This article is a continuation of research that was first presented at the conference under the title "Synthesis of Ambiguity Functions for Complex Radar Signal Processing" and published in the 2019 IEEE International Scientific-Practical Conference Problems of Info-communications, Science and Technology (PIC S&T). The proposed paper in addition outlines the potential for furthering the investigation by accounting for multipath signal propagation through the communication channel, using multiple position types of modulation to speed up the transmission of information, and channel coding to increase noise immunity.

Clock synchronization between the transmitter and receiver is required in contemporary information transmission systems. The sample frequencies of the transmitter and receiver vary as a result of the usage of separate reference generators. The beginning and finish of each character must be known by the recipient. To determine the proper integration interval for determining a character's meaning, this information is necessary. The creation of a component of the broadcast signal in the receiver is necessary for symbol synchronization. These coordinated rectangular oscillations occur at the same rate as character transmission.

More and more tasks that were formerly carried out by analogue devices are now being accomplished based on digital signal processors as digital communication networks are built (DSP). The line between the analogue and digital components of communication systems which are now divided by an analogue to digital converter, or ADC moves relentlessly to the antenna with the advent of DSP. Antennas, prefilters, switches, preamplifiers, and power amplifiers are examples of analogue components in software-defined radio (SDR). General-purpose processors, digital signal processors, field-programmable gate arrays, and ASIC (Specialized Integrated Circuit). These combined computation and control nodes may perform a wide range of diverse tasks, including modulation, demodulation, filtering, and coding. Instead of being coded, each application-specific ASIC method is created. Low manufacturing costs, little power usage, and great productivity are its defining characteristics.

A software radio cannot function without an FPGA because of its tremendous productivity and programmability. Compared to DSP or GPP, their computation productivity is much greater. This is because quasi-parallel data processing is a possibility. Data processing is only performed successively, though sometimes iteratively, by DSP and GPP methods. DSP and GPP's programmability and configuration rearrangement are their key benefits. Generally speaking, the following key elements that affect how a signal behaves as it propagates via a communication channel must be taken into consideration when developing a communication system:

1. The effect of thermal noise;
2. Frequency and phase signal offsets that may be brought on by the mutual movement of the transmitter and receiver antennas or their heterodyne mismatch brought on by the instability of the reference frequency sources;
3. Signal delay in the communication channel brought on by propagation from the transmitter antenna to the receiver antenna and in the feeder systems;
4. Fading brought on by multipath signal propagation
5. Signal delay in the communication channel should be taken into consideration while simulating communication networks on a personal computer.
6. To effectively investigate the receiver of synchronization systems, a fractional delay in the communication channel must be included since computer simulations can only be discrete in time.
7. Development of Digital Signal Processing Schematic Solutions

The accuracy of the radar signals' conversion into digital form is the determining factor of efficiency when using the algorithm for estimating radar signals in the whole receiver bandwidth while taking into account angular and amplitude changes. All signal elements outside of the known values are lost at this processing level with a maximum allowable deviation of frequency, amplitude, and phase. Analog to digital conversion takes place after the detector in the majority of contemporary radar systems.

In the design of radar structures with digital signal processing, it is required to use a different strategy when applying the autocorrelation estimation technique, namely the use of ADC in the intermediate frequency path-to-the-detector. In this instance, the carrier frequency is amplified and reduced to a value that is practical for further processing before the received signal is sampled immediately after spatial selection in a suitably broad frequency range. This implementation allows for the execution of all digital processing activities, including frequency-time signal processing that may be carried out in a single sounding, namely: Preliminary identification of relevant signals by the results of one sounding; coordinates measurement according to the discovered signals; optimum one- and multi-channel frequency-time filtering of signals.

The operation of the signal processing device for digital processing must be organized to ensure the completion of the tasks listed above, as well as additional ones, such as the selection of echo-signals by the correlation, features properties of their complex bypass, and therefore only quadratic ADC implementation or detection. This strategy offers a clear system benefit:

The ability to adapt to changing working conditions;

1. the ability to upgrade a device by changing the software without changing the hardware;
2. a reduction in weight and size, which results in a significant increase in reliability;
3. ease of equipment configuration;
4. A lower price compared to the analogue variant due to the greater process ability and low component prices in the wide production of a signal processing device built around a

programmable processor consisting of two interconnected components: a gain and signal conversion device and the actual programmable signal processor.

Controlled amplification, digital signal processing, and analogue-to-digital signal conversion are the primary responsibilities of the first unit. The initial block is a crucial node that determines several crucial aspects of the whole device, including sensitivity, dynamic range, and the maximum bandwidth of radar signals, even though all fundamental processing is done in the processor.

The Noise Automatic Gain Control-NAGC, the first adjustment shown, operates on the following principles. The radar's timing diagram occasionally, for instance, every few minutes emphasizes the specific clock for the modification under consideration. At this time, no radar is released, and the signal processing route runs at its noise. In this instance, the signal processor assesses the ratio \ln/h (in rms input noise; h —quantization step of the ADC source codes and determines the required gain adjustment.

The second adjustment is necessary because the signal must fall inside the linear portion of the amplitude characteristic within the noise dynamic range for the device to function normally. Gain tuning may be done for quasi-continuous signals at the start of the sounding cycle. In this scenario, the source code analyses for the pulse repetition period dictate that the gain reduction instruction be issued using a particular technique at the ADC's output. During the first repetition periods instantaneous automatic gain control—IAGC), this operation is done cyclically. Finally, the limiter before the pre-selection filter may be substantially improved by the location. The restriction level and the ADC restriction level must match. The selection of the generated harmonics enables the filter to greatly lessen its negative influence by transferring the limitation to the point of the route to the filter.

The second adjustment is necessary because the signal must fall inside the linear portion of the amplitude characteristic within the noise dynamic range for the device to function normally. Gain tuning may be done for quasi-continuous signals at the start of the sounding cycle. In this scenario, the source code analyses for the pulse repetition period dictate that the gain reduction instruction be issued using a particular technique at the ADC's output. During the first repetition period of Instantaneous Automatic Gain Control (IAGC), this operation is done cyclically. Finally, the limiter before the pre-selection filter may be substantially improved by the location. The restriction level and the ADC restriction level must match. The selection of the generated harmonics enables the filter to greatly lessen its negative influence by transferring the limitation to the point of the route to the filter.

The ADC is the most important node in the device's signal amplification and conversion chain since it controls the device's overall frequency and dynamic properties. Table 1 presents the current status of ADC technology and lists the qualities of the top integrated ADC circuits on the global market. The table displays the dynamic range for its noises and the dynamic range for the stray spectra or harmonics, which are the key ADC parameters for the applications under consideration, in addition to the bit rate and the maximum sampling rate demonstrates that commercially available twelve-bit ADCs can be employed in the appropriate range of sampling

frequencies and intermediate frequencies. ADC A06640, for instance, may be used for $FD = 40$ MHz, $f_{IF} = 30$ MHz. Roughly 70 dB is the range of dynamic noise, while about 80 dB is the range of harmonic noise. With common filter coefficients for the digital section (20–30 dB), it is feasible to get a dynamic noises range of the whole device of roughly 90 dB, which is suitable for the scenario under discussion.

REFERENCES:

- [1] J. W. Larkin *et al.*, “Signal Percolation within a Bacterial Community,” *Cell Syst.*, 2018, doi: 10.1016/j.cels.2018.06.005.
- [2] D. M. Waldner, N. T. Bech-Hansen, and W. K. Stell, “Channeling Vision: CaV1.4 - A Critical Link in Retinal Signal Transmission,” *BioMed Research International*. 2018. doi: 10.1155/2018/7272630.
- [3] A. Ghita, P. Matousek, and N. Stone, “Sensitivity of Transmission Raman Spectroscopy Signals to Temperature of Biological Tissues,” *Sci. Rep.*, 2018, doi: 10.1038/s41598-018-25465-x.
- [4] Z. Jin *et al.*, “All-Fiber Raman Biosensor by Combining Reflection and Transmission Mode,” *IEEE Photonics Technol. Lett.*, 2018, doi: 10.1109/LPT.2018.2792489.
- [5] A. Sakai, “Admittance of atomic and molecular junctions and their signal transmission,” *Micromachines*. 2018. doi: 10.3390/mi9070320.
- [6] I. Grothe *et al.*, “Attention selectively gates afferent signal transmission to area V4,” *J. Neurosci.*, 2018, doi: 10.1523/JNEUROSCI.2221-17.2018.
- [7] C. Brauchli, S. Elmer, L. Rogenmoser, A. Burkhard, and L. Jäncke, “Top-down signal transmission and global hyperconnectivity in auditory-visual synesthesia: Evidence from a functional EEG resting-state study,” *Hum. Brain Mapp.*, 2018, doi: 10.1002/hbm.23861.
- [8] F. G. Woodhouse, J. B. Fawcett, and J. Dunkel, “Information transmission and signal permutation in active flow networks,” *New J. Phys.*, 2018, doi: 10.1088/1367-2630/aab680.
- [9] T. Jiang and X. Chen, “Transmission of Signal Nonsmoothness and Transient Improvement in Add-On Servo Control,” *IEEE Trans. Control Syst. Technol.*, 2018, doi: 10.1109/TCST.2017.2672399.
- [10] M. R. Joglekar, J. F. Mejias, G. R. Yang, and X. J. Wang, “Inter-areal Balanced Amplification Enhances Signal Propagation in a Large-Scale Circuit Model of the Primate Cortex,” *Neuron*, 2018, doi: 10.1016/j.neuron.2018.02.031.

CHAPTER 4

NEXT-GENERATION MOBILE NETWORKS

Dr. Saurav Ganguly, Assistant Professor

Department of Electronics and Communication Engineering, Presidency University, Bangalore, India

Email Id- saurav.ganguly@presidencyuniversity.in

Electronic and communications systems are now extensively employed in many facets of society's daily life. The provision of high-quality service and traffic management and control is a crucial problem in the operation of such systems. Additionally, high-tech information transmission devices used in current mobile and telecommunication networks need innovative and advanced signal-generating circuits. The production of electrical oscillations is the process of transforming various forms of energy into electrical oscillation energy. Electrical oscillation generators are independent sources that operate in self-excitation mode.

Electrical oscillation generators can be categorized into two main categories based on the source of the converted electrical energy. If primary electrical oscillations need to be transformed into oscillations with the desired frequency and shape, generators with external excitation and parametric generators are used. If DC voltage sources need to be converted, reference generators auto generators are used. Electrical oscillation generators are used in many different technologies and communication systems as functional components. Such generators are grouped into two primary categories based on the shape of the unmodified signals they produce: harmonic and pulse oscillations.

The electrical oscillation generator is a closed system with positive feedback that includes a power source, a frequency-selective system (resonator), which establishes the frequency of generated oscillations, an active element covered by a positive feedback circuit, which accounts for energy losses in a frequency-selective system, and a nonlinear element, which restricts the generated oscillation amplitude. Utilizing devices with negative differential resistance to make up for energy losses in the oscillating system and passive tuning circuits of the generator is a promising method for building electric oscillation generators. This method will enhance the energy characteristics of these generators.

Researchers have looked into harmonic oscillators that use the negative differential resistance effect. Rectangular oscillator oscillators have the leading position among non-sinusoidal signal sources. The most common method for obtaining rectangular-shaped voltage or current pulses is to employ multivibrators, which are functional components of more complicated communication devices. Application of new technologies and materials that permit the developing pulse generators that use pulse and multifrequency Van der Pol generators based on pulse technology is one of the potential areas of pulse technology research previously undiscovered effects and fundamentally new options for controlling output pulse parameters are offered.

A combination of a feedback two-pole and a nonlinear active two-pole is used in pulse generators based on transistor architectures with negative differential resistance (NDR), which produces negative differential resistance under certain circumstances. By adding this resistance to a circuit, one may make up for losses and produce oscillations that are undamped over time if the negative resistance of the oscillating circuit is larger than the positive resistance [1], [2].

Devices with negative differential resistance may lead to either full or degenerate self-oscillating systems. Depending on the completeness of the set of reactive components in an oscillating generating circuit, self-oscillating systems are classified as complete or degenerated. Generators of the relaxation type often degenerate self-oscillating systems. However, the resulting oscillations may be harmonic depending on the magnitude of the reactive component of the impedance of a transistor structure with negative differential active resistance. The major drawback of such generators is their low output power, which is decreased as a result of more output voltage spectrum components being filtered.

1. This study's objective is to create and evaluate pulse and multifrequency Van der Pol generators based on transistor architectures with negative differential resistance for use in info-communication system infrastructure.
2. Van der Pol Oscillator-Based Relaxation Type Generators on Transistor Structures with Negative Differential Resistance
3. A large class of pulse signal generators are built using the relaxation mode of Van der Pol generators' functioning. Electrical oscillations with saw tooth, triangular, and rectangular geometries are common kinds of pulse signals. A quick rise in oscillating circuit losses caused by the inductive component distinguishes the relaxation mode of the generator constructed using the Van der Pol oscillator approach.

As a result, the Van der Pol oscillator technique will provide the following equivalent circuit for the relaxation type generator on the transistor structure with NDR. Transistor architectures with NDR and S-type I-V curves are employed as the active component when building pulse generators with saw tooth, triangular, and linear AC voltage. Transistor architectures with NDR and N-type I-V curves are employed as the active component in rectangular voltage pulse generators. Let's build a generator that produces linearly alternating voltage. A combined static I-V curve for the transistor structure with NDR and the operating point trajectory for one oscillation period is shown. Van der Pol generator equivalent circuit based on transistor structure with NDR (TSNDR) in relaxation mode the transistor structure's static I-V curve, NDR, and operating point trajectory throughout one oscillation period depict the equivalent circuit of the linearly alternating voltage Van der Pol pulse generator for slow movements. The equation that follows Kirchhoff's first law describes dynamic processes in the electrical circuit. Generator of linear alternating voltage's equivalent circuit for slow motion.

The operating point movement along the lower branch of the static I-V curve of the bipolar transistor structure corresponds to the formation of the section of linearly alternating voltage. The bottom portion of the static I-V curve of the transistor structure with NDR must be estimated to integrate the right part. The linear AC voltage generator's forward time in this instance is $t = 2C A$.

The combined static I-V curve of the transistor structure with NDR and the operating point trajectory throughout a period is shown in Figure 4 together with the I-V curve displays the produced current pulses showing the electric circuit for the authors' construction of a linearly alternating voltage Van der Pol generator. The Van der Pol oscillator method's linear alternating voltage generator functions as follows. When the transistor structure's approximate I-V curve is combined with the operating point trajectory throughout one period, shows the electrical circuits of the bipolar transistor-based linearly alternating voltage generator with NDR: Without negative feedback or with global negative voltage feedback, the supply voltage U rises to a level that causes the collector-collector electrodes of the bipolar transistors $VT1$ and $VT2$ to exhibit a negative differential resistance. At this point, relaxation oscillations appear as a result of the capacitor $C2$'s cyclic charging and discharging processes. The oscillating circuit of LC1 elements corrects for the transistor structure's impedance reactive component at the produced pulse frequency [3], [4].

In a bipolar transistor arrangement with NDR, resistor $R1$ restricts the supply current value, and together with resistor $R2$ it creates a voltage divider. Together with the inductor, capacitor $C2$ creates a series oscillating circuit that modifies the generator's output resistance to match the load. Bipolar transistors have a reactive, capacitive impedance at the collector-collector electrodes that are dependent on the supply voltage value. Inducing negative voltage feedback via the resistor $R2$ improves the frequency stability of the pulses that are created. A change in the supply voltage value. Semenov et al. results in changes to the repetition frequency and rate of the produced voltage's linearly variable pulses.

In the fundamental linearly alternating voltage generating circuit (Fig. 6a), the global negative voltage feedback (NF) reduces the return time and increases the forward voltage linearity. Figure 6b depicts the generator's circuit. Sawtooth-shaped pulses of linearly alternating voltage are produced. By applying the control voltage U_c , one may adjust the parameters of the linearly alternating voltage pulses that are created, which enhances the generator's energy efficiency.

The duration of the leading and trailing fronts must be ensured in rectangular voltage pulse generators built using the Van der Pol oscillator technique, and the pulse or pause form must be obtained. Given that the equivalent loss resistance R_{eq} is compensated by the negative differential resistance of the transistor structure with NDR in relaxation mode, we can formulate the following system of differential equations for the equivalent circuit using Kirchhoff's principles.

It is necessary to separate the pulse production process into the area of rapid and slow movements when building rectangular voltage pulse generators using the Van der Pol oscillator technique because it gives the duration of the fronts or a certain pulse shape. Capacitance C_{eq} of the transistor structure with NDR may be disregarded for the slow-motion area. The Van der Pol relaxer equivalent circuit. The analogous circuit of the Van der Pol relaxer takes the shape seen in because the current is assumed to be $i_0 = I_0 = \text{const}$ for the area of rapid movements displays equivalent circuits for the Van der Pol generator of rectangular voltage pulses in the domains of a slow motion and b rapid motion.

According to the findings of research on dynamic processes in Van der Pol generators on transistor structures with NDR in relaxation mode, utilising an inductor as a source of electrical energy deforms the vertex and front shapes of rectangular voltage pulses that are formed. A transistor inductor may be used to enhance its form. The electrical circuit of the Van der Pol generator of rectangular voltage pulses on the field-effect transistor structure has been created by the authors using NDR.

By altering the resistor R_1 's resistance in a variety of ways, one may regulate the frequency of rectangular voltage pulses. An oscillogram of the voltage rectangle pulses produced is shown in It was shown via experimentation that the supply voltage $U_{p.s.}$ Has an impact on the rectangular form of the produced voltage. This is explained by the fact that, during one period of oscillations, the operating point moves twice through the static I-V curve of the transistor structure with NDR, which controls the relationship between the rectangular voltage pulses' shape, period, and duration, and the shape and duration of the fronts. In light of this, the Van der Pols technique of building rectangular voltage pulse generators based on transistor structure with NDR enables its formation following the desired pulse shape and front duration.

In, an estimated static-type I-V curve was used to determine the connection between the field-effect parameters and the form of voltage pulse oscillations $u(t)$ shows the electrical circuit for a rectangular Van der Pol voltage pulse generator using a field-effect transistor construction and NDR. Oscillograms of rectangular voltage pulses produced by the active element of the Van der Pol generator suggested in 's generator transistor structure with NDR are shown. We will obtain if we choose field-effect transistors with identical cut-off voltage levels but varied drain current parameters [5], [6].

By using field-effect transistors with drain currents $ID_{03} > ID_{04}$ that varied by 1.5–2.0 times, with precision of order 2, the current equation for the field-effect transistor structure with NDR was determined. The authors have created novel circuits of generators on transistor structures with NDR that operate in oscillatory and relaxation modes as a component of radio-measuring transducers of physical quantities by using the Van der Pol oscillator technique. Using the Van der Pol oscillator method, a Multifrequency Generator of Quasi-Periodic Oscillations on the Field-Effect Transistor Structure with Negative Differential Resistance was developed.

A pertinent problem in contemporary electronics is the analysis and synthesis of multifrequency signal generators with the necessary spectral characteristics and noise-like signals. Chaotic generators are a different class of oscillators that produce unique shape-signals. A weird non-chaotic attractor appears on their phase plane as a collection of them are generators of quasi-periodic oscillations. The traditional Van der Pol multifrequency generators are made up of linked linear and nonlinear oscillating circuits as well as a nonlinear amplifier that controls the amplitude of the produced stationary oscillations and provides self-excitation for the self-oscillating system. The self-oscillating system uses the barrier capacitance of the p-n junction as a 140 A technique for building a multifrequency Van der Pol generator using the capacitive effect of a field-effect transistor structure with NDR has been suggested by the authors. The authors examined the generator's oscillation dynamics in multifrequency mode while taking into account the following simplifications The circuit with a current source connected in parallel with

the nonlinear resistance and the parallel connection of Leq and Req is the equivalent circuit of the multifrequency generator; The amplitude and frequency of harmonic oscillations of the current source correspond to the amplitude and frequency of the single-frequency stationary mode of the generator; and The occurrence of other harmonic components of the multifrequency mode is due to both n and n 's interaction.

The single-frequency, dual-frequency, three-frequency, and multi-frequency modes of operation for the Van der Pol multi-frequency generator are all available. The operating point location on the falling I-V curve of the transistor structure with NDR active component of the transistor structure with NDR's impedance and the volt-farad characteristic of the transistor structure with NDR is altered to modify the operation modes of the electrically reactive component of the impedance of the transistor structure with NDR. The beat of quasi-harmonic sounds near in frequency may be seen beginning with the two-frequency mode. The ratio (36) $p = \frac{E_m}{3hU_2} \frac{S}{g} + 3.4 \frac{hU_2}{CT} \frac{UCT}{UCT}$ is used to calculate a crucial detune in the transition from single-frequency to multi-frequency mode. (37) The operational band's lower and higher cutoff frequencies are, respectively, equal to $H = 0.1 \frac{E_m}{2QUCT}$ and (38) $B = 0.1 + \frac{E_m}{2QUCT}$. (39) $\frac{E_m}{UCT}$ is the reason $B \approx H \approx 0$ when the oscillating circuit of the multifrequency generator has a high-quality factor. The electrical circuit of the authors' multifrequency Van der Pol generator. The nonlinear oscillating circuit is made up of the reactive component of the impedance of the transistor structure with NDR at the drain-drain electrodes of the field-effect transistors VT1 and VT2, as well as inductance L1. The linear oscillating circuit is made up of the ones of parts L1 and C3. The equivalent capacitance of the field-effect transistor is the variable resistor R2 slider's minimum value at the position.

The electrical setup for a multi-frequency Van der Pol generator using a field-effect transistor structure with NDR. The natural resonant frequencies of linear and nonlinear oscillating circuits are the same because the transistor structure with NDR is equal to the capacitance of capacitor C3, which causes quasiharmonic oscillation. The equivalent capacitance of the field-effect transistor structure with NDR changes as the value of resistance R2 changes, changing the resonant frequency of the nonlinear circuit. The excitation frequency is where k is a harmonic number with amplitude U_k and is normalized to the average frequency of the operating range. The outcomes of the mathematical modelling performed by the authors in with the circumstances and 21, and time and frequency are normalized about the frequency of stationary oscillations of the single-frequency mode 0 in these figures.

In this part, signal generators with regular relaxation dynamics and quasiperiodic types were built for info communication system facilities using the Van der Pol oscillator technique on transistor architectures with NDR. The built-in generators' electric circuits were shown, along with a description of their operating principles and a study of their dynamic processes. The following results both theoretical and practical were attained. Based on the nonlinear and reactive characteristics of transistor structures with NDR, Van der Pol pulse signal generators have been developed. These devices operate in relaxation and quasi-periodic modes with electrical control over a broad range of the parameters of their self-oscillating systems.

Based on the nonlinear and reactive characteristics of transistor architectures with NDR, new circuits for Van der Pol pulse signal generators were built. These generators were the subject of theoretical and experimental research. The development of mathematical models of the Van der Pol generators with intricate dynamics of produced oscillations. Results of experimental research and numerical modelling are presented. The accuracy of the generated mathematical models is confirmed by the convergence of the findings.

New analytical ratios that represented the characteristics of rectangular and sawtooth voltage pulses produced by Van der Pol generators on bipolar and field-effect transistor architectures with NDR were found. The electric oscillations of the Van der Pol generators in relaxation and quasi-periodic modes were captured in phase portraits, time diagrams, and amplitude spectra. A mathematical model for the multifrequency Van der Pol generator of quasi-periodic electric oscillations based on the field-effect transistor structure with NDR was put forward. The stationary oscillation amplitude in single-frequency and multi-frequency modes, the essential frequency detuning in switching from single-frequency to multi-frequency mode, and the lower and higher operating frequency limitations were all calculated using new analytical ratios[7], [8].

At the turn of the 21st century, Ukraine's mobile networks are actively deploying 4G and 5G technology. The current data support the notion that development trend predictions were inaccurate. When all voice traffic is supplied by 2G and 3G networks for an extended period, the problem is made worse. The utilization of the current network segment also generates financial and commercial benefits for the Operators. As a result, methods for enhancing the performance of current networks are required. A hybrid telecommunication service combines elements of telephony and cloud services, according to. Computer systems play a crucial role in how the telecommunications network operates. Local area networks, radio access networks, and a provider's core networks make up a mobile network.

The options for maintaining telecommunications networks have increased with the development of cloud computing. The number of services and transmitted traffic is gradually increasing, which opens the door to a steady rise in the resources needed to support a wide range of application types in operator systems. Radio frequency planning, which also defines the electrical compatibility of network objects and the calibre of services offered, is the first step in the deployment process of a mobile operator network. The amount of the incoming load necessitates an upgrade to the network architecture to adjust the cell's subscriber count. Service area forecasting and location range coverage analysis are two methodologies that are differentiated in mobile network operation.

Our results suggest that past radio coverage proposals were developed using mobile networks in planning contexts RPLS ONEGA, Enterprise Asset, which may be roughly translated. The procedure for estimating radio coverage was used following the BS's technical specifications. Technical, geographic, BS coordinates, transmitter power, type, suspension height, elevation angles, azimuths of a sector antenna, frequency resource distribution, etc. are a few examples of these features.

With the introduction of the UMTS technology stack and subsequent next-generation mobile networks (not 5G), the number of calls has reduced as a result of increased data transmission. The radio coverage of the data network is the main area of attention for mobile network carriers. The subscriber's voice loads not increasing is the major cause. This is accomplished by choosing the base station's ideal parameters using an empirical method. The 3GPP standards are only suggestions for improvement lower quality limit and customer satisfaction with the level of communication quality upper-quality limit. The advice could be to pay attention to those operators who have their criteria for an ideal setup.

There have been other complaints regarding this kind of radio coverage. As a consequence, the provision receives a substantial fraction of such complaints. Voice service network process planning is common across GSM and CDMA networks. The quality of speech transmission degrades due to an increase in mistakes caused by ineffective radio scheduling, which is seen from the perspective of the ultimate subscriber. The radio planning was outstanding in terms of EMC, interference level, and hysteresis all at once.

It is suggested in this study that the data supplied, taking into consideration the data from the Billing System, be used to enhance the current planning methods. It is thus required to do the first calculation of the load associated with the BS sectors and use them to evaluate the efficacy of radio planning, as indicated in general, to increase network efficiency and service quality. Suggest describing the planning process in this article using the model. The conventional concept of access to a mobile communication network's radio resources is predicated on the subscriber's conditional placement within the network at the time of connecting the BS with the maximum radiation signal harm.

There is no subscriber-created projection of load distribution in such a communication system. In anticipation of anomalous phenomena in the form of a sudden shift in the concentration of subscribers within the provided cell, the operator's network runs round-the-clock in the peak power mode of the emitters and receivers. Additionally, blocking and denial of service take place in the case of a peak load rise brought on by a high volume of calls to the telecom operator's base stations in a single cell.

The operator's network's control objective is to evenly distribute all radio resources while considering abnormal events. The addition of new functions for billing data analysis, clustering, and channel resource management sets the proposed conceptual method for analysis of subscriber access to radio resources and traffic distribution in cellular communication systems apart from existing ones and enables cellular communication systems to be more effective while still meeting QoS requirements. The technique enables forecasting in the mobile communication systems under consideration. Consequently, the best traffic distribution method serving the changeable load of the operator of billing systems based on the sectorial method of a loading network element is a critical job. The fact that the computation of payment for services necessitates multi-stage processes is the cause of the increased burden on the tariff system. To assess their worth, these processes are required, which results in poor call service efficiency; decreasing flexibility and efficiency of tariff methods; failure to guarantee owing to service quality[9], [10].

The primary goal of GSM networks has always been to provide enough radio frequency coverage and a strong enough BS signal in the consumer region. In UMTS networks, the strength of the radio resource made available to the subscriber (virtual channel) continues to be advantageous. Based on information about how the channel resource has been used thus far during operation, the network is changed. However, the study does not account for the type of the data, such as a direct call or a manual call, and does not account for the subscriber profile's features. Although the information is continually accumulating in the billing system and is used to anticipate the delivery of services, this data is virtually ever utilised in network planning.

Mathematical models for computation and forecasting the network are utilised during the planning phase to calculate metrics like coverage and subscriber load. One of the most often used models is the Okumura-Hata signal strength calculation model. As a result, claims that while utilizing this strategy, manual motion adjustments were taken into consideration in terms of shared electromagnetic impact. The method put out in this article suggests taking into consideration the fact that manual (handheld) traffic results from poor planning on the part of BS sectors. In the CIS nations, using UMTS and GSM networks differently is the most typical approach. Transfer of confidence to networks Shortly, LTE operators in the CIS nations will not give dual network usage significant consideration.

Therefore, it may be argued that the majority of network operations are handled by data centres and that the network only serves as a channel for the transmission of information illustrates how a mobile subscriber interacts in a GSM/CDMA network that combines radio and optical signals before sending the signal to the core network, which is also housed in the data centre. The technology then states that the flow is transferred to the operator's core for further processing. Data channels continue in a path that is mostly controlled by the service: the flow enters the home network, must leave the operator's internal network, and is then routed to the margin router before entering the external network.

These issues lead to the fact that operators encounter a variety of issues in such circumstances. Operators in industrialiser nations were able to stop this at the same time by moving to "pure" UMTS and, therefore, to Lethe article's major emphasis is on how the UMTS and GSM cells are situated concerning one another. The major objective of such placement is to consider how their interactions affect the load distribution. These scenarios apply to locations with a modest amount of population. The quality of communication in hybrid networks will also increase concurrently with better UMTS zones. First and foremost, lowering the frequency of connection failures is the primary requirement for enhancing communication quality. The key to doing this is achieving ideal load distribution inside the cells. The best coverage may be graphically described, and the research suggests estimating the optimal coverage using indications from the Payment System, a crucial component of the Operator's network. The mechanism for estimating network load will be useful in determining how accurate the approach is. Figure 1 discloses the Mobile Terminal and the subnet.

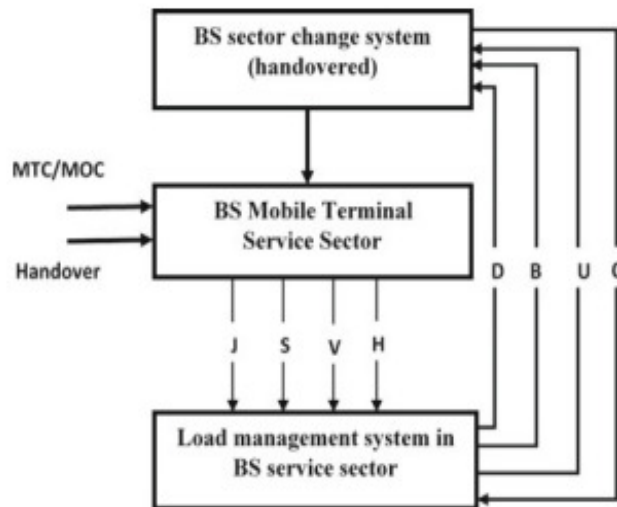


Figure 1: Discloses the Mobile Terminal and the subnet.

The generalized method's analysis revealed that a variety of elements had a significant impact on how the service load operation was carried out. Due to these elements, we were able to benefit from our flexibility in responding to developments in the load services industry. It will be possible to increase the effectiveness of load distribution in the network with this design of coverage regions depending on the anticipated degree of handover. Sector Analysis Method for Net Load Distributional mobile communications subsystems are managed by the controller located in the data Centre. Only at the data center do controller interactions in control subsystems take place. The tasks of controlling service processes include searching for subscribers, looking for physical components involved in the transfer process, and transferring instructions. The base station-trolled in the data Centre is linked to the recording equipment. The system controller connects to the central data Centre and sends the finished hardware solution to actual physical devices to start the data transfer procedures, depending on the protocols.

Locally is where the network is designed and where the greatest quality control is applied. Systems for that LTE network often carry out several activities following the specifications and standards. The article aims to distinguish between the responsibilities of the data transmission system directly to the LTE network and tasks related to subsystem management. When compared to previous generations of networks, the structure increases system efficiency. More than half of the subsystem's functions have to do with managing the communication system rather than the service. There is service type control in a few places in Node, SGSN, and PCRF.

The interactive games in the system and the sion-sion of the operations management and data transmission capabilities. This physical node has been requested for protection during method analysis for the GSM and UMTS net schema. The volume of requests indicates how heavily loaded a certain service node is. We can identify four elements of this approach to evaluating the ideal traffic distribution using performance analysis tools for load control in mobile systems.

1. Mobile Sector BS service terminal.
2. Sector BS modifies the system.
3. The BS sector's load management system; Elements that influence them.
4. The control object, or load, in the BS service sector is a collection of components that are functionally tied to one another and interact with subscribers.
5. The operation system consists of elements that control objects and controls, has communicated information, and is defined by variables for various data kinds.
6. The ability of a mobile network to process incoming applications with the necessary probabilistic temporal features is referred to as the network's quality of service.

REFERENCES:

- [1] A. Mirzaei Somarin, M. Barari, and H. Zarrabi, "Big Data Based Self-Optimization Networking in Next Generation Mobile Networks," *Wirel. Pers. Commun.*, 2018, doi: 10.1007/s11277-018-5774-6.
- [2] H. Fall, O. Zytoune, and M. Yahyai, "Theory of algorithm suitability on managing radio resources in next generation mobile networks," *J. Commun. Softw. Syst.*, 2018, doi: 10.24138/jcomss.v14i2.406.
- [3] H. Chen, D. Zhao, K. Liu, W. Wu, and L. Wang, "Improving reliability of cloud computing services for next generation mobile communication networks," *Int. J. Comput. Appl.*, 2018, doi: 10.1080/1206212X.2017.1413626.
- [4] C. Bouras and N. Kanakis, "Evolving AI-FEC application on 5G NGMN-edge computing systems," *Adv. Sci. Technol. Eng. Syst.*, 2018, doi: 10.25046/aj030519.
- [5] B. Kim, D. Calin, J. Ling, and H. Viswanathan, "Dynamic IP tunneling for next generation mobile networks," in *IEEE International Symposium on Personal, Indoor and Mobile Radio Communications, PIMRC*, 2018. doi: 10.1109/PIMRC.2017.8292391.
- [6] M. Pozza, A. Rao, H. Flinck, and S. Tarkoma, "Network-in-a-box: A survey about on-demand flexible networks," *IEEE Commun. Surv. Tutorials*, 2018, doi: 10.1109/COMST.2018.2807125.
- [7] C. Liang, Y. He, F. R. Yu, and N. Zhao, "Enhancing video rate adaptation with mobile edge computing and caching in software-defined mobile networks," *IEEE Trans. Wirel. Commun.*, 2018, doi: 10.1109/TWC.2018.2865354.
- [8] M. R. Kanagarathinam, S. Singh, I. Sandeep, A. Roy, and N. Saxena, "D-TCP: Dynamic TCP congestion control algorithm for next generation mobile networks," in *CCNC 2018 - 2018 15th IEEE Annual Consumer Communications and Networking Conference*, 2018. doi: 10.1109/CCNC.2018.8319185.
- [9] R. Ricart-Sanchez, P. Malagon, P. Salva-Garcia, E. C. Perez, Q. Wang, and J. M. Alcaraz Calero, "Towards an FPGA-Accelerated programmable data path for edge-to-core communications in 5G networks," *J. Netw. Comput. Appl.*, 2018, doi: 10.1016/j.jnca.2018.09.012.

- [10] P. Mandl, P. Pezzeri, and E. Leitgeb, "Selected Health and Law Issues Regarding Mobile Communications with Respect to 5G," in *Proceedings - 2018 International Conference on Broadband Communications for Next Generation Networks and Multimedia Applications, CoBCom 2018*, 2018. doi: 10.1109/COBCOM.2018.8443980.

CHAPTER 5

DEVELOPMENT OF A SYSTEM FOR REGISTRATION AND MONITORING OF UAVS USING 5G CELLULAR NETWORKS

Dr. Prabhu T, Assistant Professor

Department of Electronics and Communication Engineering, Presidency University, Bangalore, India

Email Id- prabhu@presidencyuniversity.in

A UAV registration and monitoring system must be established due to the unregulated distribution and use of unmanned aerial vehicles (UAVs) across the globe, as well as dangers to aircraft, other property, people's lives, privacy, and safe areas. The purpose of this study was to evaluate the UAV registry's existing situation in Ukraine, pinpoint its primary weaknesses, and create an architecture for the UAV registration and monitoring system. To accomplish the objective, the following tasks were completed: Analyzing the state of the Ukrainian UAV registry at the moment; identifying the main issues with UAV registration and monitoring in Ukraine and figuring out how to address them; developing a system for registering and monitoring UAVs; creating a model for registering and monitoring UAVs using 5G cellular networks; and developing software for registering and monitoring UAVs. The effort led to the creation of a system that enables the registration of UAVs when they are switched on and the monitoring of the current coordinates of the UAVs using the system.

Dynamics of UAV utilization analysis. The first UAV was developed in 1849, more than 150 years ago, but active UAV development didn't start until the start of World War I, and most UAVs were developed for military use up to the turn of the twenty-first century. The following are the major turning points in the history of UAV development: The Chinese Corporation DJI has been the undisputed industry leader for the last several years, controlling more than 70% of the global market and more than 80% of the Ukrainian market. Recent information indicates that Ukraine's UAV market has grown to a value of \$1 million each month. The value will reach \$185 billion globally in 2019 the market price of all UAVs is rising by around 15% annually. According to analysts, if this trend continues, the USD will reach 2.8 trillion in 2030. Ukraine is ranked 27th in the world in terms of the variety of UAVs manufactured, although the majority of these UAVs are relatively obsolete and ineffective. In contrast, domestically produced UAVs only account for 7% of all UAVs in Ukraine.

Purchases in the USA, China, Israel, and Russia account for over 90% of the entire amount. Unmanned aerial vehicles (UAVs, sometimes known as drones), which have a variety of uses ranging from military to commercial, have grown significantly in popularity in recent years. Surveillance, reconnaissance, remote sensing, search and rescue, aerial photography, crop surveys, on-demand emergency communications, traffic control, monitoring of natural resources like oil or gas exploration, and more are a few of the successful uses of drones that are already available on the market.

The safe usage of UAVs is one of the most crucial issues that have to be addressed as unmanned aerial vehicles (UAVs) become more prevalent in both business and people's everyday lives. The development of prospective information technology is very important at this time. The establishment of a single registry and the direct registration of each UAV is a top priority in Ukraine for the growth of UAVs. Information about the owner, the location, the date, and the time of registration for each of them. Additionally, the full monitoring of UAV movements is envisaged, allowing for the constant tracking of all UAVs. Since the airspace of Ukraine is now comparatively vacant but will progressively fill up with the growth of UAVs, this will provide inhabitants with a guarantee of safety. M2M (machine-to-machine) communication technology may avoid in-flight mishaps that might cause a crash and further fatalities. The use of 5G cellular networks offers new possibilities for this technology's advancements, including inter-UAV communication [1], [2].

The coordination of UAV surveillance is complicated by the communication needs of many objects. It is still necessary to send data as quickly as possible, that is, with little lag time and a high data transmission speed. Widespread use of contemporary cellular networks should be made possible in Ukraine to adequately support radio access technologies. The quality of the fundamental requirements for UAV monitoring should greatly increase thanks to mobile communication technology.

The Convention on International Civil Aviation, popularly known as the Chicago Convention, has undergone nine editions, the most recent of which is the ICAO Statute. An aeroplane is defined as any machine that may acquire support in the atmosphere via air reactions other than air interactions against the surface of the planet. A pilotless aircraft known as an unmanned aerial vehicle (UAV) is flown without a pilot-in-command on board and is either remotely and completely controlled from a different location on the ground, another aircraft, or space or programmed and entirely autonomous. Remotely piloted aircraft, or RPA for short, is an unmanned aircraft that is flown from a distance. All unmanned aircraft are subject to the requirements of Article 8 of the Chicago Convention for getting special authorization, regardless of whether they are remotely piloted, totally autonomous, or mixed.

Every aircraft engaged in international navigation is required to have a certificate of airworthiness that has been granted or made valid by the state's authority in which it is registered. The RPAS remotely piloted aircraft system does not have to be self-sufficient; it consists of UAVs and a control system on the surface of the planet. Only the RPA is included in the aircraft registration, according to ICAO documents, out of all the parts that make up the RPAS. The introduction of new equipment, methods, or the redesign of the airspace must be done, as well as the identification and mitigation of these concerns for safety risks. All nations that are ICAO members must put the relevant legislation into effect to do this. Except for situations specified by the Air Codes, permission to use the airspace of European nations and the conditions for its use are given by a combined civil-military air traffic management system based on an application for the use of airspace. Regarding Ukraine, at the moment there isn't a registration made expressly for UAVs; in other words, the Air Code of Ukraine legislation doesn't specify the usage of

UAVs. Determining the ideal guidelines for UAV registration and monitoring initially is crucial, followed by the creation of creative architectural solutions.

Wireless communication is one of the enabling technologies for UAV registration and monitoring and has attracted much more attention recently. The standards organisations are already looking into options for using cellular networks to connect commercial UAVs. While academics are actively investigating mathematical and algorithmic answers to exciting new challenges originating from flying nodes in cellular networks, industries are starting to test early prototypes of flying base stations or consumer devices. A thorough overview of all of these advancements supporting the seamless integration of UAVs into cellular networks. In addition, a significant amount of scientific work has been devoted to the analysis of wireless technologies, as well as to the new opportunities and difficulties presented by their application to drone communications, the development of LTE network upgrades to support aerial vehicles, and other unresolved issues.

Therefore, it is necessary to develop strategies that will enhance cellular communication networks' performance to meet several criteria in modern urban areas, including ensuring the introduction of new mobile systems and supporting existing savings on investments that were made); meeting the requirements of next-generation network-generation network-generation networks; and supporting remote registration and monitoring processes. The efficiency of data transmission should therefore be increased while lowering the cost of delivering each megabyte of traffic and providing the quality of service (QoS) required by each type of traffic to properly support new broadband radio access technologies in today's 5G cellular networks. With the growth of cellular networks, new, more advanced network designs for data storage and transmission are also developing[3], [4].

The 5G network designs for various UAV use cases should be analysed in this chapter. To determine whether needs are not satisfied by alternative wireless technologies, a gap analysis should be carried out. The architecture for the 5G network will then be created. Therefore, the procedure of unmanned aerial vehicle registration and monitoring via cellular networks is the subject of the study. The methodology, architectural designs, and technologies for recording and monitoring unmanned aerial vehicles utilising 5G cellular networks are the focus of the study. The task is to make sure that unmanned aerial vehicles are registered and monitored. To do this, the following scientific challenges were resolved:

1. A 5G network architecture for UAV registration and monitoring was built, and the analysis of the present level of UAV use regulation in European and Ukrainian nations.
2. The development of a tracking model for UAV motions.
3. The development of a network-centric solution for UAV registration and monitoring.
4. The development of UAV registration and monitoring procedures.

Focus on binary and quaternary signalling in phase-shift keying (PSK). Quaternary communication uses pairs of bits; binary signalling, naturally, uses single bits. We covered quadrature phase-shift keying (QPSK) and an off-set version of it known as offset quadrature phase-shift keying under quaternary signalling (OQPSK). OQPSK has one benefit over QPSK: it is less

susceptible to nonlinearities. Binary signaling with a focus on frequency-shift keying (FSK). Additionally, we covered minimum-shift keying (MSK), a continuous-phase frequency-shift keying variant of binary FSK (CPFSK). A key characteristic of MSK is the use of minimum frequency spacing, which enables the two FSK signals that correspond to the symbols 0 and 1 to be coherently orthogonal and prevent interference during coherent detection in the receiver. When it comes to extracting the multiplexed-offset streams from the incoming binary data stream for its creation, MSK adheres to a process similar to OQPSK. In OQPSK, these two auxiliary binary waves are weighted by a rectangular function on a bit-by-bit basis, but in MSK, the weighting is carried out by the positive half cycle of a sinusoid. This difference between them is both straightforward and significant.

Coherent detection requires that the receiver and transmitter being in sync concerning both carrier phase and bit timing, irrespective of the modulation scheme of interest. Noncoherent detection is a technique where the receiver disregards the knowledge of the carrier phase between its operation and that of the transmitter. Both amplitude-shift keying and frequency-shift keying allow for the simple implementation of no coherent detection. However, a closer look is needed for phase-shift keying that is no coherent. In particular, differential phase-shift keying, which combines differential encoding with phase-shift keying, is developed as a pseudo-form of no coherent detection (DPSK). However, keep in mind that no coherent receivers, regardless of where they came from, need to be aware of bit timing information.

Spectral analysis, which was shown by studies on sample band-pass signals illustrating various digital modulation techniques. Because the bit rate was a negligible portion of the carrier frequency, the tests had some instructive value. But in reality, we often discover that the bit rate is a great deal lower than the carrier frequency. In these circumstances, it is advised to do the spectrum analysis at the baseband, where the carrier wave is eliminated without losing crucial information by expressing the modulated signal in terms of its in-phase and quadrature components. The place where the reader may redo the spectrum analysis, but this time using the baseband method.

M-ary signaling techniques, which are used instead of binary modulation schemes for digital data transmission across band-pass channels where channel bandwidth preservation is of paramount significance. The transmitted signal envelope is constant in M-ary PSK and M-ary FSK signaling systems, allowing for their application across nonlinear channels. In contrast, M-ary QAM's changing transmitted signal envelope restricts its use of linear band-pass channels.

We looked at three widely used digital systems from different angles as topic examples: Using twisted pairs to link households to telephone central switching offices, high-speed data transmission is made possible by orthogonal frequency-division multiplexing (OFDM). Gaussian-filtered minimum shift-keying, a kind of MSK used in the Global System for Mobile (GSM) communication (GMSK). Digital television has the same channel specifications as analogue television and aims to provide high-quality video and audio.

Observed signal fluctuations that are chaotic and seem to be unexpected are referred to be "random." Every realistic communication system encounters random signals in one way or

another. Consider voice communication, where the speech is often amplified by a microphone and turned to an electrical signal before being processed for transmission.

When looking at this electrical signal on an oscilloscope, we would be inclined to comment that it looks to be highly random, meaning that it would be challenging to anticipate or duplicate. The stream of 0s and 1s that are sent over the Internet is an example of digital communications that behave similarly. Although they are always 0 or 1, their placement and order are very unpredictable. Information's underlying quality of randomness or unpredictability. Communication wouldn't be necessary if the information could be predicted since the other end could do so before getting it. Contrarily, noise is the scourge of the majority of communication systems. The range and/or quality with which information-bearing signals may be sent through a channel is limited by noise. Any unwanted signal that obstructs or distorts the signal being sent is referred to as noise. Another example of a random signal is noise; if the noise were predictable, we could anticipate it at the receiver and eliminate it, which would negate its impact.

As a result, due to its random nature, noise and information are identical in certain aspects. The goal of the communications engineer is to separate the two as much as possible from one another. The risk assessment of a direct lightning strike or distant voltage surges determines the requirement of choosing the kind of protective device and the installation plan for them. The intensity of lightning flashes at site N average yearly number of lightning strikes per km² per year determines the demand for lightning surge protection. An automated lightning strike detection system in Europe can quickly gather these facts. These systems are made up of several single-control network sensors dispersed across Europe [5], [6].

Except for thunderstorm activity maps by region, information from sensors is sent in real-time to monitoring servers that are accessible via the Internet with a special password; risk assessments of the electrical installation's vulnerability, for example, underground power supply systems are for obvious reasons thought to be less vulnerable than aerial ones; the cost of connecting to the protected electrical infrastructure; and

1. It's important to consider these factors while selecting protection devices for arresters or oxide-zinc visitors:
2. The recommended operating voltage (UN). This is the network's rated voltage for which the protection device is designed.
3. The protection device's maximum permitted operating voltage maximum operating voltage U_c . For the full lifespan of the protection device, this is the maximum AC voltage that may be used.
4. Voltage classification parameter for varistor surge suppressors. This is the amount of industrial frequency voltage that is used to restrict the varistor. A valid classification current is obtained by Integer current (I_{imp}). A charge Q and a test impulse peak of 10/350 microseconds determine this current. Used for evaluating Class I protective device applications (category B).
5. Maximum discharge impulse current. (I_n) The test current pulse of 8/20 s current flowing through the protective device had a peak value of this. The safety device can repeatedly sustain the current of this value. Used for Class II SPD testing (Category C and D). The

- device's degree of protection is determined by how this impulse reacts. This parameter also coordinates the SPD's other features, as well as the standards and testing procedures.
6. The highest impulsive discharge current (IMAX). The protective device may miss this peak value once and fail the 8/20 s test current pulse.
 7. Used for Class II SPD testing (Category C and D).
 7. Complementing existing if the parameter for SPD based on arresters. This current, which is sustained by the current source itself, which is the power system, passes through the arrester after the surge pulse has ended. The amount of this current contributes to the estimated short-circuit current at the spot where the arrester is located for this specific electrical system. Install "L-N; L-PE" gas-filled and other arresters with an I_f value of 300-400 A in the circle. Do not use them since they will be damaged and perhaps catch fire if the accompanying current is operated for an extended period. Arresters with values greater than the estimated short-circuit current, i.e., values between 2 and 3 kA and higher, must be installed in this circuit.
 8. Protection level (Up). When an impulse discharge current passes through the protective device, the voltage drop that results reaches this maximum value. The parameter describes how well the system can control surges that emerge on its terminals. Typically, the rated impulse discharge current is used to determine it (I_n).
 8. Trigger duration value for zinc oxide varistors is no more than 25 ns. The working period for dischargers of different designs might vary from 100 nanoseconds to several microseconds.

Current settings for contact clamps and SPD are assessed in each situation separately. The permitted voltage of the internal system is coordinated with the maximum pulse overvoltage at the border of each zone. Energy performance also coordinates the SPD at various zones. Due to the requirements of insulating impulse resistance coordination in power plants and the resistance of the equipment to damage, it is important to choose the SPD level at a voltage lower than the maximum value. Because of this, the impact on the equipment will never exceed the permitted voltage. When determining the amount of damage resistance, a test or suggestive level should be employed. In this scenario, using a measuring device to establish and regulate the degree of impulse overvoltage for this objective, suggested methods were created [7], [8].

When selecting an SPD, other factors are also taken into consideration, including leakage current, the maximum energy released on the visitor, and fuse current for protective devices with built-in fuses. It is advised to start with the building's grounding system configuration, equipotential bonding, communications supplied to it, and the value of the current passing through the limiter of the first level of protection in the event of a direct lightning strike into a building protected by an external BZS Facilities with strategically positioned structural parts and open-air locations must implement the most complicated protective system plan. These structures include houses in rural locations, industrial buildings with high pipes, communication towers, and other structures where lightning is likely to hit. The choice is a little easier to make when, for instance, a building within an urban area has to be protected. In urban settings.

Characteristics at Risky Working Scenario for SPD Balancing. The equalization of potentials between two conductors, one of which is often a phase conductor and the other a zero working or zero protective conductors, is the fundamental tenet of the protection techniques discussed above. However, if the limiter fails, a short circuit might develop between these conductors, leading to the breakdown of the electrical system and perhaps even a fire. When the varistor ages, leakage currents grow, or the actual discharge current through the limiter exceeds the maximum, the varistor overheating mechanism thermal protection, which is included in varistor limiters, typically functions.

The discharge of a significant quantity of thermal energy will cause the varistor to be removed from the protected circuit even if it may not even fail throughout the latter process' brief length. When the network is constantly overvoltage over the maximum permitted working voltage for the SPD, a slightly different scenario occurs. The result of this circumstance can be the burning off of the zero functional conductors when it enters the electrical system. As is well known, a phase voltage of 380 V may be delivered to the load in this situation. The varistor opens, allowing a sustained current to pass through it. This current may be several hundred amps in value and is similar to the short circuit current. The practice has shown that the heat protection system does not always function in certain circumstances [9], [10].

Additionally, it should be noted that arresters based on arresters lack a thermal shutdown component in their design. The protective device is often destroyed by the action of a significant quantity of heat energy as a consequence of the indicated action. When the body plastic melts, it is also possible for an arc to form and the terminals of the device to the cabinet or DIN rail to melt. Therefore, it is necessary to provide additional protection in the form of high-speed fuses with the characteristic of gG or gL (classification according to VDE 0636 (Germany)), which are installed in series with each limiter, to protect electrical installations and limiters of all types from short circuits possess a rather sophisticated internal structure and is intended to safeguard wires and switching equipment against overloads and short circuits.

It is important to remember that in this case, automated switches may not provide the intended outcome. Experience has shown us that a lightning current surge may harm circuit breakers themselves. As a consequence, there may be welding between the coupler's contacts, which increases the likelihood that a load short circuit won't cause the machine to malfunction. This issue is eliminated by the fuse. In addition, the proper nominal selection substantially reduces the chance that the fuse will blow when the impulse current passes through the lightning protection mechanism.

Additionally, it must be recognised that if the fuses are not present, the input automatic switch will be activated in the case of a short circuit in at least one of the SPDs, cutting off the consumer's power supply until the issue is fixed. The chance of such an event occurring far less often when fuses are used in each SPD's circuit. The manufacturer's guidelines for surge protection devices should be followed while deciding on their denominations. The selectivity of a protective device's action and its capacity to resist the estimated short-circuit currents for a certain electrical system are what decide the values of common and individual fuses.

The correct protective device type and installation plan will augment the precautions against the direct lightning strike or voltage guiding by distant discharge that is already in place. Installation of lightning arresters, capable of passing through themselves 10/350 s impulse currents with an amplitude value of 50-100 kA and providing a level of protection (U_p) less than 6 kV (SPD A), is advised as the first level of protection when:

1. Air power supply is introduced regardless of the presence of an external LPS, when lightning can directly penetrate the power lines immediately adjacent to the facility; with an underground power supply and in the presence of an external LPS.
2. The second protection level uses modules with a maximum impulse current of 20–40 kA of 8–20 s form and a protection level (U_p) of less than 2.5 kV (SPD C).

The third level of protection (SPD D) uses modules with a maximum impulse current of 6–10 kA of 8–20 s form and a protection level of less than 1.5 kV. It is possible to employ combined devices, together with an extra noise-bandwidth filter in the 0.15–30 MHz range. At the border between zones 0 and 1, following the introduction panel, Class I protection devices must be fitted in an inboard panel or special box. The following switchgear includes Class II protective devices such as floor or other panels. It is best to group them. These devices may be found anywhere between zones 1 and 2. Installation of Class III protection is also possible in distribution boards or proximity to customer protection zone 3. Installing a second Class III device right next to the protected equipment is preferable when the SPD installation location is more than 10-15 metres from the customer, as this will ensure that the required cable lengths may be removed.

REFERENCES:

- [1] F. Sharevski, "Towards 5G cellular network forensics," *Eurasip Journal on Information Security*. 2018. doi: 10.1186/s13635-018-0078-7.
- [2] U. N. Kar and D. K. Sanyal, "An overview of device-to-device communication in cellular networks," *ICT Express*. 2018. doi: 10.1016/j.icte.2017.08.002.
- [3] C. M. Huang, M. S. Chiang, D. T. Dao, W. L. Su, S. Xu, and H. Zhou, "V2V Data Offloading for Cellular Network Based on the Software Defined Network (SDN) Inside Mobile Edge Computing (MEC) Architecture," *IEEE Access*, 2018, doi: 10.1109/ACCESS.2018.2820679.
- [4] S. R. Samal, "Interference management techniques in small cells overlaid heterogeneous cellular networks," *Journal of Mobile Multimedia*. 2018. doi: 10.13052/jmm1550-4646.1432.
- [5] M. Alenezi, K. Almustafa, and M. Hussein, "On virtualization and security-awareness performance analysis in 5G cellular networks," *J. Eng. Sci. Technol. Rev.*, 2018, doi: 10.25103/jestr.111.24.
- [6] M. A. Ferrag, L. Maglaras, A. Argyriou, D. Kosmanos, and H. Janicke, "Security for 4G and 5G cellular networks: A survey of existing authentication and privacy-preserving schemes," *Journal of Network and Computer Applications*. 2018. doi: 10.1016/j.jnca.2017.10.017.

- [7] P. Ziyu, H. Han, and Y. Jie, "Modeling and analysis of downlink heterogeneous cellular networks," in *Procedia Computer Science*, 2018. doi: 10.1016/j.procs.2018.04.245.
- [8] H. C. Nguyen, R. Amorim, J. Wigard, I. Z. Kovacs, T. B. Sorensen, and P. E. Mogensen, "How to Ensure Reliable Connectivity for Aerial Vehicles over Cellular Networks," *IEEE Access*, 2018, doi: 10.1109/ACCESS.2018.2808998.
- [9] O. Onireti, A. Imran, and M. A. Imran, "Coverage and rate analysis in the uplink of millimeter wave cellular networks with fractional power control," *Eurasip J. Wirel. Commun. Netw.*, 2018, doi: 10.1186/s13638-018-1208-0.
- [10] U. Habiba and E. Hossain, "Auction mechanisms for virtualization in 5g cellular networks: Basics, trends, and open challenges," *IEEE Commun. Surv. Tutorials*, 2018, doi: 10.1109/COMST.2018.2811395.

CHAPTER 6

WIRELESS SENSOR NETWORK PROTECTION SYSTEM

Dr. K Gowri, Assistant Professor

Department of Electronics and Communication Engineering, Presidency University, Bangalore, India

Email Id- gowri.k@presidencyuniversity.in

Creation of Evaluation Templates for the Wireless Sensor Network Protection System. Without a plethora of information systems, including sophisticated automation systems for managing robotic systems, modern civilization is unimaginable. Of course, without a wireless sensor network (WSN), which enables the gathering and processing of significant amounts of important data. Enterprise and organizational performance are directly impacted by WSN quality, and one of the WSN quality indicators is security. Because it is hard to officially explain and anticipate an attacker's behavior, providing defense is difficult. Another aspect influencing WSN security is its ongoing growth and rising complexity. The issue of developing templates for evaluating the present security of WSN, taking into consideration both known and brand-new threats and weaknesses, becomes crucial. Such security patterns might be used to create new systems as well as to evaluate the security of systems that are currently in use. The issue of establishing such standards is inadequately codified, and its resolution requires a thorough examination of several system factors.

One of the most promising fields of artificial intelligence development today (AI). AI research is now being actively carried out, and the outcomes are successfully being utilized in several human activity domains. Therefore, using techniques from AI systems to WSN security control issues seems to be a potential field of study. The wireless sensor network is implemented based on the defined wireless sensor nodes and is used to collect, analyse, and send strain gauge data as well as to track outcomes under various static test loads. The network coordinator may autonomously manage the source of gas emission using the wireless actuator and alerts an operator when an emergency is identified through the GSM/GPRS or Ethernet networks.

We do not yet propose their usage for fire monitoring and mitigation since the authors also demonstrate that measurement precision acquired from wired systems cannot be attained with current wireless technologies. Creating a low-cost detection system that could recognize shipboard damage control circumstances and give real-time danger information was the goal of the enhanced volume sensor job. The modelling and analytical findings are supported by the performance assessment of this actual test-bed scenario, which shows the viability of the platform proposed. The authors first develop adequate access-point density parameters that assure the statistical assurance that the data loss rates are less than a specified threshold.

To effectively manipulate nodes, a novel method for determining nodes' relevance in the network has been developed. For both the square and hexagonal access point deployment patterns, authors determine theoretical constraints on the predicted hitting time between two successive visits of a mobile node to access points. The system is built around a server that can make requests for data from several nodes, gather that data, and store it in a database (DB). In the

document, which may be used as a foundation for the deployment of Internet Protocol (IP) based IWSNs needing IoT connection, several potential reasons for the delay in IWSNs are identified [1], [2].

The paper presents the state-of-the-art research in sensor-based M2M communication networks for monitoring agriculture, several existing agricultural monitoring systems and compares them on different design factors, the technical framework of some recent deployments of agriculture monitoring systems in developing countries, and identifies their design challenges, as well as significant design and implementation differences of these monitoring systems in developed and developing countries. The effectiveness of the Development of Evaluation Templates was tested using the NS2 simulation tool. When using the proposed 231 detection mechanism, the experimental findings demonstrate that the IDM can increase the detecting rate and decrease the false detecting rate with appropriately chosen detection mechanism parameters, and every node-link can achieve a relatively fair throughput to enhance the performance of overall networks.

A technique for creating an electronic digital message signature based on encryption utilising elliptic curves was taken into consideration in prior research. The transport layer security protocol's primary methods for information protection are fully covered. The report gives an examination of the primary traffic decryption techniques. The issue of intrusion detection by categorization of network traffic realizations was taken into consideration. The findings of our calculations are presented numerically by other writers, who also calculate the predicted waiting time and time in the system, assess them, and offer matching curves for them. New converged network applications and services will be quickly configured and tested using a modelling framework defined in the paper.

Applying the variation-gradient technique to the control tasks in the study will enable a wider variety of tasks to be taken into account. The article comes to the recommendation that such a model be used when developing scanners to look for unauthorized transmitters and bugs. Ontologies may be formally defined in several languages. Their biggest issue is that they don't provide users with the chance to explain both the data and the metadata. Machines can better account for the condition of objects in the actual world when interpreting data based on metadata. This makes machine learning and data processing simpler. Languages based on Web standards have recently gained popularity. Most of them are based on the XML format and are used for data exchange via networks. Semantics are included in languages used to describe ontologies, unlike XML, however.

The lack of the necessary number of circuits is the biggest obstacle to creating a perspective for wireless sensor networks (WSN) analysis and acquiring a static template. We'll use one of the languages based on Web standards to make their production and dissemination to explain the related ontology easier. The majority of IT workers are acquainted with these very expressive languages. Furthermore, these languages are intended to describe resources, and from our perspective, the WSN is a collection of resource components.

Properties are required for the later insertion of people who belong to classes. Characteristic properties and communication properties are the two sorts of properties available in the OWL

language. The former associate classes with certain sorts of data, whereas the later do the opposite. Property limitations may take the form of a domain and ranges. Classes that may have the given attributes are defined by domains.

Additionally, ranges define classes whose members may represent values for the listed characteristics. Add "Data Characteristic" with the "Data" domain and a range of positive numbers, as well as "Impact" with the "Vulnerability" domain and a range of positive integers. Explain the "Data Characteristic" property with three sub-properties to describe the data that needs accessibility (Data Availability), confidentiality Data Confidentiality, and integrity (Data Integrity); and "Damage" by sub-properties to determine the impact on these data characteristics: damage to accessibility (Impact Availability), confidentiality (Impact Confidentiality), and/or integrity [3], [4]

We'll use the following properties to connect classes:

1. "Implements" and "Realizes" for the relationship between prototypes and their implementations.
2. "Contains" and "to associate elements with children" are transitive properties. Along with drop-down domains, ranges, and inverse properties, the sub-properties "Contains a prototype" and "Contains an implementation" are also included.
3. The terms "Data transfer" and the opposite of the property "Receive data from" are used to denote the transmission of data between elements.
4. "Directed towards" to make the threat's objective clear.
5. "Has a vulnerability" for implementation connections and vulnerability.

Because property A is the inverse of property B, if an (x, y) is true, then $B(y, x)$ is likewise true. If $A(x, y)$ and $A(y, z)$ are true, then $A(x, z)$ is likewise true, according to the transitivity assumption. The characteristic property introduced by object Property has two sub-properties, `rdfs: domain` and `rdfs: range`, which specifies their respective domains and ranges. To clarify properties in the ontology, restrictions are imposed on them, such as a domain and a range. In the study, the "Contains" property is introduced with the domain and ranges the data element inverse to "Contained in," the property "Data Characteristic," and the child "Characteristic of accessibility." These are properties' general qualities. Other regional traits, limitations on cardinality, and a range within a subclass exist. Several essential features of an ontology cannot be established in Enterprise Architect, thus Protégé was used to further construct the ontology. Protégé not only enables you to add several extra limitations but also considers them when characterizing people. Additionally, Protégé has SPARQL, allowing you to do ontology queries.

The first of them is meant to provide information assistance for the majority of business operations connected to the higher education system's system for training experts. The SZ system supports the centralized administration of directories, the search for any information objects by any criteria, the flexible mode of power differentiation between users depending on their job duties and administrative affiliation, supports the maintenance of an ordered archive, an archive of reporting forms, and storage of the history of changes of all information objects. The system involves programmers moving around projects. By enforcing the order, any modifications to a

programmer's characteristics may be made. To allow for the customization of order templates and routes for transferring draught orders, a flexible method is offered. The created solution offers strong capabilities for OLAP cube-based statistical report generation.

In terms of curriculum creation, calendar schedules for the educational process, theoretical education plans, and semester curricula, the WSN system encompasses the complete educational process. The module offers practical tools for developing lesson plans, curricula, including theoretical training plans, semester curricula, and educational process schedules. Operational control is used throughout the whole planning phase of the educational process to ensure compliance with state criteria. The technology allows users to export documents in Excel or Word formats. Several reports are offered by way of comparison with the "protection system" (PS), however, they are not constructed using the OLAP cube.

On the Microsoft Dynamics CRM platform, PS is put into use. This platform consists of a "wrapper" around MS SQL Server that allows users to see and alter data in the database. On top of HTTP, a Web interface is used for interaction. The MS Internet Information Services process HTTP queries. Analysis Services, a feature of MS SQL Server, was used to create the OLAP cube. The reports themselves are created with the help of MS SQL Server's Reporting Services technology. Three servers running Windows Server 2008 R2 are used to run the system. The first one handles HTTP requests, the second one helps with DBMS, and the third one handles OLAP cube processing. The most important data is kept in the database and may be temporarily cached by the website. Statistics that have been anonymised are stored in OLAP cubes. Figure 4 shows the schemes that go along with such a design. Five first-tier plans and two second-tier schemes were successful. The "Contains" connection is shown by dashed lines, while the "Implements" relationship is denoted by tiny dashed lines. The WSN system was implemented using the same technology, except the MS CRM Dynamics 2011 platform. The Web interface is also used to arrange data processing, although this process is entirely self-written.

To simulate the MAC, we will employ streamlined versions of WSN agents and components. The study uses PA, counteraction agents, and agents that represent the behavior of the typical user, the attacker, and the component, referred to as agent-user, agent-attacker, and agent-component, respectively. Let's first think about the reasoning behind each agent's actions. The user agents are the model's most basic component. They act in a very rudimentary manner. They send requests to components that must be handled, imitating the typical WSN behavior. Each agent instance's parameter renders the return with a certain probability, which is depicted by sending a message to the related resources. The model level specifies every relationship. When a request is answered, the user agent enters the intermediate state of "Successful Response" and then immediately moves into the "Waiting" state, from which the request may be resent. The user enters the "No Response" state through timeout and subsequently the "Standby" state (1 step) in the absence of a response from the component. A transition is indicated by an arrow with a "timer" after a certain amount of time, an "envelope" when receiving messages from other agents, a rhombus to verify that the condition is satisfied, and a label when a specific condition is met. It is noteworthy that the agents' design included both drawing a state diagram and outlining

the Java transition operations. As a result, it is feasible to transition between two states using two separate processes but using two different actions.

Before the attacker started the attack, user agents had already overloaded the attacked components. In this instance, the attacker's attempt eventually succeeded since some of his requests were fulfilled. User agents operated silently and without overtaxing the components that were under assault. Depending on the intensity chosen, the attack agent increased the load of the attacked component following the assault. Similar to the previous instance, the attacker eventually "broke" the barrier whether the component was overloaded or not[5], [6].

In the actual world, the design, capabilities, and amount of the components are chosen so that users can interact with the system correctly and promptly get all of their requests. In light of the initial parameter choices, the first batch of findings may be regarded as inaccurate. It is evident that the burden on the component IIS1 grows beginning with the third hundredth step, as would be anticipated by the attacker. However, IIS2's entirely comparable component's load does not alter. As a result, in this model, the characteristic that is suited for determining DC is the load. In other words, security personnel want to reach a high DC before an intruder may access important information.

To determine the DC load of the components, several PA techniques were evaluated throughout the simulation. There have been efforts to ascertain the typical load and take into account any deviations from it. In this instance, the average load was calculated for both the full work day and a brief, recent period. A percentage of the average load was used to compute the variance. This strategy came up empty-handed. Calculating the root mean square load variance is a different approach that likewise didn't provide encouraging results. Similar techniques for calculating DC were used to determine the extent of the readings' discontinuities after failures in the examination of load data. There were several false positives in this instance.

The discrepancy between the total number of assaults and the total number of PA warnings was used to establish false triggers. Since the counter-attack agent could take out several attackers on a single detected attack beginning with attackers, this technique started to provide inaccurate results. The goals of attack agents may conflict. Only a tiny percentage of attacks no more than 2% were effective, according to the findings. This most likely occurred when the attackers' intentions coincided, attacking both the defense and one or more components at once. This theory underwent more testing to support it. They demonstrated that at least two attackers must assault the same target to boost the chance of a successful attack by up to 5%. PA's strike is useless since it swiftly resumes operations.

In this instance, the attack durations need to be associated for the PA to repeatedly locate the first attacker while missing the second and be carefully chosen so that the component doesn't have time to decrease the load from the assaults. The PA will repeatedly identify the attackers before the assault is effective. In this situation, the success of the assault will be decreased to 2% if the counter-attack agent implements increasingly rigorous protective measures, each time raising MinWaitTime by 5%. Thus, it may be inferred that careful preparation and the collaboration of the attacker agents are necessary for a successful assault. The PA must be "tricked" for the

assault to go undetected. Due to the attacker's ignorance of both his existence and the work's algorithm, this is challenging.

Gas monitoring systems are used in a variety of settings, including commercial and residential settings, especially when it comes to the detection of dangerous or environmental gases. The popularity of the Internet of Things (IoT) in recent years has made tiny, portable gas-monitoring devices more popular. Due to their compact design and great sensitivity, semiconductor-type resistive gas sensors are particularly appealing at this moment. Additionally, they are inexpensive and simple to create.

These benefits demonstrate that the semiconductor-type gas sensor is a strong contender for the Internet of Things. The use of gas-detecting systems based on these sensors is currently hindered by several obstacles, including heaters' excessive power consumption for battery-powered systems and the poor selectivity of resistive-type sensors. We have previously proposed a highly integrated platform that allows micro-scale multi-sensing while using very little power, approximately, to address this issue. Writing partner.

Additionally, numerous resistive sensor-based selectivity-enhancing approaches are being explored. Circuit concerns must read out resistance over a broad range (i.e., fluctuation over many decades), and heater drivers must provide consistent power to sensors to maintain a regulated and ideal temperature. A lot of research on interface circuits suggests adopting stable DC-excitation or pulse-width-modulation (PWM) schemes techniques to solve the aforementioned problems. Resistance readout circuits utilizing a current-driving mechanism were also suggested as a means of interfacing multichannel MEMS type sensors. Despite these efforts, the development of an on-board multiple gas sensing module suitable for the Internet of Things is still challenging due to sensor and circuit difficulties[7], [8].

This study recommends a portable gas sensing module with an ultra-compact MEMS gas sensor device for Internet of Things (IoT) applications that include wireless connection, analog/digital signal processing, heating control, and multiple gas sensor readout and data analysis. For more stable operation, eliminating sensor lifespan issues and AC-affecting parasitic effects, trans-impedance amplifiers (TIA) are utilised instead of PWM techniques. A simplified overview of the proposed system shows that it consists of three main components: an AFE to drive heaters and readout sensor signals, a microcontroller-RF combined SoC to regulate the AFE components, and wireless sensor data transmission. A picture of the sensor module's front and rear highly adaptable power injection for heaters is made possible by the heater driver's tance and digital control. The complete module may be made smaller by using a system-on-chip (SoC) chipset that combines a CPU and two wireless communication protocols (Bluetooth Low Energy and Wi-Fi). This greatly expands the module's potential applications for both stationary and portable purposes. Additionally, multiplexing a sensor array and doing a principal component analysis show how to overcome the poor selectivity problem caused by utilising a single metal-oxide gas sensor (PCA).

In comparison to other research, our system is more precise, size-efficient, and has the potential to interface several sensors with a greater sensing range simultaneously. Our study is focused on

creating a directly applicable end-to-end system towards IoT that those ICs have not yet supported, despite the integrated circuit (IC) design methodologies showing improved performance, lower size, and more adaptability. While maintaining the module's mobility, we were able to outperform or provide outcomes that were equivalent to those of the IC techniques in terms of sensing range, precision, and heating control capabilities.

The analogue front-end (AFE), which drives heaters and reads out sensor signals, the microcontroller-RF integrated SoC, which regulates the AFE components, and the suggested gas-detecting system are the three key components. Let's start with the power management aspect. This system may be powered by a lithium-polymer battery with a nominal output voltage of 3.7V or a 5V USB power source. While the system's supply voltage is 3.3V, the lithium-polymer batteries' output typically ranges from 4.2V to 2.7V during use. A buck-boost converter is used to guarantee that the system will still function even if the battery output drops below 3.3V. This sort of power converter is more suited for this system in terms of conversion efficiency than other converters like low-drop out (LDO) regulators. The charge controller IC (LM3658, TI, USA) controls battery charging when a battery is inserted. The charge controller runs in LDO mode, which produces continuous 4.2V, when the system is charged via USB. The buck-boost converter subsequently converts this voltage to 3.3V.

Resistive gas sensors (R_{sens}) are activated by the AFE, which also regulates power to the heaters (R_{heat}). For R_{sens} to produce a current that matches the resistance, a constant voltage is provided. The R_{heat} uses a digital-to-analogue converter (DAC)-AD5314, Analog Devices, USA- enabling flexible power regulation via the microcontroller, and the power monitoring is made easier by the use of a current monitoring chip to track the current flowing through the R_{heat} .

Data from the sensors is received by the microcontroller-RF combined SoC (ESP32, Espressif Systems, China) via an external analogue-to-digital converter (ADC)-AD7091R-8, Analog Devices, USA. Depending on the device, Bluetooth Low Energy (BLE) or Wi-Fi is used to communicate this sensor data. Additionally, software-based algorithms are used to adjust the heater power and TIA gain. Implementation of the variable R_f and the R_{sens} interface circuit. A DC voltage excites the resistance, and the resistance data is transformed into the current. To protect TIAs from the MUX switching impact, current mirrors are used. Current monitoring through a shunt resistor in DAC-based heater driving and power monitoring circuits

To get around the DAC output power restrictions, high-output buffers are used simplified diagram of the microprocessor's algorithm (ESP32). The first procedure generates a ramp voltage to initialise the circuit components in the AFE and sets each heating power to the target value (V_{DAC}). By monitoring I_{heat} and subsequently changing V_{DAC} , the heater control keeps the heating power at the desired level. To prevent the TIA output from being saturated, the proper R_f is automatically chosen for the R_{sens} readout control ability gained by R_f , which changes it to the voltage so that the ADC can read it. One variable-gain TIA is shared by several R_{sens} due to the circuit's high module capacity requirements. Here, an ADL5315 from Analog Devices in the USA, a widerange (3 nA-3 mA) logarithmic current mirror IC, is used. It enables user-definable voltage application (VSET) at the highest level possible to increase the sensitivity of the

resulting current to the multiplexer and to prevent the multiplexer from unnecessarily switching the receiver so that the receiver maintains a stable DC-excitation condition even when the multiplexer switches. The reference voltage for TIA is selected to be the same as VSET because the accuracy of the current mirror is at its greatest when the output node voltage is the same as VSET (2.3V) (positive terminal of the op-amp). R_f , which is pre-set to accommodate a broad range of R_{sens} fluctuation, controls the conversion gain from the current to the voltage. This is because resistive gas sensors often have extremely significant resistance changes and they need to cover diverse resistance across many input channels. As a result, the component of the variable R_f is a group of resistors with switches attached to each of them. The resistors are a variety of commercial chip resistors, with resistance values ranging from 1 k to 10 M over a period of little over half a decade.

Giving up our aim is another good alternative for us to function as an attack agent. The model assumes that the load on the component will allow the attacker to be identified. However, it is possible for it to remain undetected and not affect load. Therefore, selecting the appropriate set of attributes for DC computation is crucial. PAs were altered to identify DCs using the altered barrier size and pheromone signals messages left by PA invaders pretending to be themselves. The results of these tests were consistent with those of the earlier ones and showed that the DC each PA uses has a significant role in the MAC's ability to operate successfully.

The processing time of a user request component was calculated experimentally while designing a MAC based on the processing time of actual answers. The server that would be the first to "fail" in an attack was found when simulating the behaviours of attackers among the servers handling requests for the PS. Using the HULK programme, a DDoS assault was launched against the frontend servers to verify the potential issues. There were 3000 virtual users in the assault. The simulated findings and the consequences of the assault were identical.

For many years, adaptive antenna arrays (AAA) have been recognised to enhance the performance of many complex systems. The most significant uses of these materials are in radars and telecommunications. The field's scientists and engineers have created a wide variety of very simple, but efficient, methods for AAA convergence to the ideal weight vector. The production of the reference signal is required by several of these algorithms, which places restrictions on their practical uses. In the realm of communications, this issue manifests as particularly severe. Since only fresh information-containing signals are delivered in telecommunications, some of the benefits of deploying AAA are lost since engineers must make do with substitute reference signals.

Modern IoT and automotive systems need dependability at a low cost, thus their high-quality and affordable testing procedures are crucial. Although digital and memory circuits predominate in many SoCs, analogue and mixed-signal circuits are often their problematic components, and their testing methodologies are crucial. This article highlights the research efforts of the latter in the authors' lab. In the mature semiconductor industry, the circuit designer should be capable of both advanced circuit design and low-cost and high-quality testing design.

The operational amplifier is a crucial part of sensor interface circuits, but its testing procedure is secret, thus we have created several techniques to test it. We looked at the NULL approach to use for the operational amplifier's mass production testing. Although it takes a while, it is often employed to evaluate the operational amplifier properties properly at the laboratory level. We have discovered that using the correct compensating capacitor values in the NULL approach may result in quick and reliable testing, allowing for its use in mass production testing. We have developed a precise and quick testing method for assessing a high-precision operational amplifier's tiny DC offset voltage. Accurate DC voltage measurement on the order of μV is thus possible by combining methods for DC-AC conversion and FFT spectrum analysis, as well as by reducing thermo-electromotive force effects. It is also feasible to extend it to multi-channel realisation.

We have suggested a quick test technique for the integral nonlinearity (INL) of a high-resolution, low-sampling-rate ADC. We take into account a polynomial model of the input-output characteristics of an AD modulator, estimate its coefficient values from the fundamental and harmonic power, apply a cosine input, and derive the 1-bit data stream power spectrum of the modulator's output. To effectively assess the linearity of ADCs using the histogram approach, we have created an algorithm for generating test signals. For ADCs with low sample rates and high resolution, the linearity testing is time-consuming for numerous sine waves, to carefully verify the linearity for certain significant codes using an arbitrary waveform generator (AWG) and an analogue filter.

To solve this issue, the authors created a simple but effective gradient method that eliminates the existence of the reference signal. The method has shown strong performance in a difficult interference environment in computer simulation and is seen as a feasible choice for use in the area of telecommunications, namely mobile telecommunications. There are still some undiscovered research topics, particularly those that deal with how the continuous usable signal affects the algorithm's convergence. The issue is that one presupposition made before testing the algorithm was that the useful signal does not affect how well it performs. This assumption often holds for radar applications, when the valuable signal is only a brief pulse and the interfering sounds are continuous. However, in a telecommunications setting, valuable signals are also continuous and may affect how effectively the algorithm performs.

Therefore, the purpose of this research is to investigate how the continuous useful signal affects the functionality of the previously developed algorithm and, if required, to identify strategies for reducing such impacts to maintain the earlier achieved high convergence characteristics. IFF systems are the primary source of air traffic data in the airspace control system. The IFF system enables independent airspace monitoring, which entails locating an air object (AO) utilizing ground-based infrastructure. The examined information tools' membership in cooperative surveillance systems is established by the employment of an aircraft responder to provide response signals required for determining the position of AO in a ground requester.

Identification systems' informative job is to ascertain the owner of a detected AO using the "friend or foe" characteristic. IFF systems are a subset of asynchronous two-way data transmission systems and are made up of a number of transmitters and receivers that operate in

several frequency bands. This enables us to draw the conclusion that IFF systems constitute a non-synchronous information network by virtue of their design. A request channel and a response channel make up an IFF system's two data transmission channels. The aircraft responder (AR), an open single-channel queuing system with rejects, is the most susceptible and has major security flaws[7], [9].

This shows that despite the use of contemporary IFF technology and even though much research effort has previously been made in this field, aircraft identification remains a challenge. The construction of AR based on the idea of an open single-channel queuing system with rejects offers numerous opportunities for the interested party, including the suppression of them by establishing intentional interference at the necessary level of intensity as well as unauthorized use of AR information. In this instance, the condition $t_i \geq T_p$, where t_i is the signal duration and $s_i(t)$ is the repetition period of request signals, is often met. The functioning of such systems under the effect of deliberate as well as intra-system interference is hampered by the use of a single channel for sending request signals and the development of a full monitoring system based on the theory of an open queue system with rejects. However, it should be noted that the operation of IFF systems in the frequency band of data transmission of cooperative monitoring systems 1030 MHz channel for transmitting request signals; 1090 MHz channel for transmitting an information packet results in significant challenges, which is noted, in particular.

The system's architecture results in a considerable density of intra-system interference in the request and answer channels, which significantly reduces the noise immunity of the IFF systems under consideration in terms of Interference Immunity Assessment Identification Friend or Foe... 289. The papers presented demonstrate that there are significant spectrum overloads in the frequency band 1030-1090 MHz that is designated for air traffic surveillance and that are used by cooperative surveillance systems, collision avoidance systems, and ADS-B systems. Alternative techniques for using variable query powers concerning azimuth sectors and tracking data are presented aircraft to lessen spectrum overload. It is demonstrated that a high probability of overlap prevents the 1090ES signal from being properly decoded and that the use of the 1090 MHz aerial surveillance frequency band with an expanding number of aircraft, applications, and equipment types can cause intra-system interference to reach critical levels. All protocols allow for some amount of data loss owing to overlapping messages or message distortion, but there is fear that as message density rises, this performance loss may eventually become intolerable.

According to the construction principle, the networks of IFF systems are non-synchronous, which means, firstly, there is no time synchronization between the radiation of individual requesters by aircraft responders and, secondly, there is no time synchronization between various Identification friend or foe systems. Airborne responders of IFF systems make use of single-channel queuing systems (QS) with servicing of the first properly received request signal in line with the concept of service of request signals. Therefore, following the construction idea, IFF system responders link to QS with rejects. The fundamental feature of these systems is that AR shuts for a predetermined period, known as the paralysis time t_p , while serving a successfully received request signal. The period is determined by the IFF system's paralysis mode. The existence of AR paralysis time restricts the throughput of both the identification friend or foe

system as a whole and the aircraft responder specifically. As a result, the chance of an air object being detected by the requester P_s , which is defined as the probability of obtaining the necessary number of answer signals to reply to requests from this requester, may be used as a characteristic of the noise immunity of the IFF system. The availability factor of the aircraft responder P_0 , which is the likelihood that the aircraft responder would emit a response signal in response to a certain request signal from the requester, serves to determine the capacity of the aircraft responder IFF system.

The responders are a component of open queuing systems since they service any validly received request signal, even those supplied by interested parties. The aircraft responder may be categorised as a single-channel open queuing system with rejects due to the availability of just one channel for service request signals and the potential for paralysing an aircraft responder when servicing request signals are present.

As a result, the concepts are used to construct IFF systems, and these principles heavily influence the latter's poor noise immunity. Using the justification presented above, it can be concluded that identification friend or foe systems transmit data in a query-response fashion. They have a channel for signal transmissions that request, as well as a channel for signal transmissions that are responses. The considered information systems' construction methodology, which is based on the idea of an open single-channel queuing system with faults, permits both allowed and illegal usage of airborne IFF systems.

The IFF system's guiding principles include creating responders to gather data and disabling the latter by establishing correlated in the request channel interference at the required level of intensity. The low information security of the systems under consideration is caused by such a construction philosophy and a service signal request principle. Additionally, the signals used for information encoding in IFF systems were not effective. The information capacity of data transmission channels and the noise immunity in generally thought-of IFF systems were both severely lowered by the adoption of primitive time-interval and location codes.

Conversations may significantly affect how people and communities recall the past, as the contributions to this special issue demonstrate. Notably, communication has rapidly changed during the last 25 years to encompass digital forms of communication, particularly social media. And although if more "analogue" kinds of communication, including face-to-face interactions, are still crucial in daily life, it is now more critical than ever to comprehend how social media affects how people communicate and recall the past [10], [11].

According to Perrin, 65% of American adults and 90% of American teenagers actively use social media, making it one of the most effective and widespread ways for people to curate, share, and communicate information with their friends, family, and the rest of the world. Users of social media have increased significantly in number over the last several years as well. For instance, there were 600 million Instagram users in 2016 as opposed to 90 million in 2013. According to research, the surge in social media use may be because information sharing generates benefits for people in and of itself. Nevertheless, psychologists are only now beginning to understand how social media may affect how people and groups remember the past despite the prevalence and

intrinsic value associated with sharing and consuming information via social media. As a result, the purpose of this work was to give a critical evaluation of the existing studies on the mnemonic effects of social media usage.

To do this, we will emphasise two main elements: the nature of the information that is shared on social media and the actions that users do in response to that information. Some of this material tends to be more autobiographical or personal, while others are more public or communal. People may play one of two roles: "producers" those who upload material on social media or start the content-sharing process or "consumers" those viewing or interacting with what a producer has posted or shared on social media. When one obtains knowledge and then shares it, the roles of producers and consumers might mix. We concentrate on two crucial areas of study in our distillation of the literature on the mnemonic effects of social media use: induced forgetting of personal information and false memories/truthiness for public information. We'll wrap up with some last observations on the significance of these elements in comprehending how and when social media affects how people and communities recall the past and a discussion of research directions. We will first create a connection between social media usage and the extensive body of research on selective remembering to make sense of the mnemonic effects related to social media use.

Social media interaction is a selected activity: From the quantity and variety of photos a producer posts from her last Oktoberfest excursion to the tweets she reads from different political experts a consumers. Social media will never be able to fully convey a person's experience: It is naturally picky. How may this selective usage of social media affect how individuals recall their pasts, both private and public? Psychologists have not extensively researched this subject. However, they have researched a variety of different subjects, including personal content, to understand selective memory. We apply this research to the current situation remembering through social media.

Although it has not been specifically investigated, there are grounds to think that the literature on selective remembering also applies to cases of creating and receiving content on social media. For instance, Conway and Pleydell-Pearce (2000) said that selective memory is facilitated by the goal-directed nature of memory. They asserted that each act of remembering has a self-goal that serves the present "functioning self": People may recall earlier occasions that confirm their perception of themselves as shy if they hold that belief. Similar to a "working virtual self," which represents the person's online persona, when it comes to posting on social media. People's social media posts will be selective to the degree that their sharing and consumption align with their "working virtual persona" at any given moment. It's important to note that one's "working virtual self" need not completely match their "non-virtual" life.

Due to the public, interactive, and multimedia nature of online conversations, what is selectively recalled online may vary systematically from what may be selectively remembered offline? For instance, social media users often offer idealised versions of their "non-virtual" selves as their "reality" to the world. Additionally, different people may exhibit this "functioning virtual self" in different ways. For instance, extraversion has been favourably linked to social media usage, whereas emotional stability in males has been linked to social media use in a negative one. In

other words, those who are more extroverted and guys who have lower emotional stability are more prone to utilise social media. Additionally, extraverts are more likely than introverts to post private, self-revealing material online. Thus, the "working virtual self" may exhibit personality characteristics and self-goals, which may influence how often and how much information is created, shared and consumed online.

In addition, social media is used by individuals for a wide range of activities. According to studies on memory function, humans use memory to understand themselves (self), connect with significant others (social), soothe emotional wounds (therapeutic), and absorb lessons to guide their present and future conduct directive. Similar functional memory uses may also be seen in online conversations. A person may then choose to generate, distribute, or consume content on social media based on their communication goals at any given moment.

Audience tuning may also result in selective memory. According to Marsh and other researchers, individuals adjust what they recall to the audience they are speaking to. As a result, for instance, individuals often post images and/or articles on Facebook that support the views or interests of their friends. Wang adds that online posting is a dialogical process in which individuals deliberately publish information with a targeted audience, and the readers subsequently selectively confirm or refute the uploaded information by their likes/responses or by staying silent. Such filtering of information during processing might influence how social media usage affects mnemonics.

The research that is now available demonstrates that selective remembering may boost memory of the material that was selectively recalled, causing the forgetting of related information. It is uncertain whether these mnemonic effects also reflect the social media users' natural tendency towards selectivity. Regardless, the study on selective remembering offers a useful theoretical and empirical framework from which to start comprehending the mnemonic effects connected to social media usage.

The role, information type, and truthfulness distinctions. Three differences are relevant for analyzing and comprehending how selective social media usage affects how people recall the past: Three factors come into play while using social media the function that person plays; the kind of information processed on social media; and the accuracy of the information processed on social media. We'll go through each one's importance in quick order.

First, depending on the role played by the user, the memory effects of selective social media usage may vary. Researchers in the area of social memory, particularly those working on the conversational study, distinguish between the speaker and the listener. The speaker must perform the retrieval operations almost by definition. However, listeners do not. Thus, we would anticipate mnemonic disparities to the degree that processes between the speaker and listener vary. Similar distinctions may be seen between social media content producers and consumers. The consumer may or may not participate in processes of selective encoding as well as other socio-cognitive processes like commenting while the producer, presumably, is doing selective retrieval when she uploads social media messages. Moreover, in contrast to a typical

discourse, the four producers and consumer through social media may lack that immediacy in terms of reaction and counter-response.

In addressing the effects of social media on memory, the present research shows a significant difference between public and private information. Here, we define public information as data regarding societal or communal activities that may be viewed outside of a social media platform. Alternatively, personal information is information about a person's private affairs that are typically not publicly available outside of the social media platform, or at least not without direct communication with the person who created the information. Finally, the accuracy of the information shared on social media has a direct bearing on the outcomes of the campaign. For this article, we define true information as being "objectively" true and false information as being "objectively" false, regardless of whether or not a person has access to or is oblivious to the true information.

Therefore, in the sections that follow, we look at the mnemonic effects of selective media use in terms of the role an individual plays on social media at any given time, such as a producer or a consumer, as well as whether the information produced or consumed is of a private or public nature and whether it is true or false. The relevant data shows that social media improves recognition of the material when it is consumed as actual, personal information. For instance, observed in two studies that people were better able to recognize information whether it originated from a Facebook post than when it originated from human faces or a book. In a third trial, the researchers assessed how well-breaking news and entertainment news were recognized in terms of web article headlines, comments on the news, and phrases.

They discovered that participants recalled more comments than headlines or random paragraphs from the post and that participants identified more entertainment news than breaking news. According to the authors, one explanation for why Facebook posts are so memorable is that they are "gossipy" like entertainment news and contain complete thoughts like the comments. Or, to put it another way, Facebook posts may simply be more "mind-ready" and, consequently, more cognitively sticky. Whatever the mechanism, this line of the study indicates that taking in information, at least in the style that Facebook users are used to, improves people's capacity to identify the information.

There are grounds to think that, similar to the selective remembering literature described earlier, the selective sharing of personal information may improve recollection of the posted material. According to several studies, selectively retrieving and sharing information has been shown to strengthen the recall of that information in the future. Simply recalling an event promotes later memories of that "same" experience, and the impact is amplified when it occurs in the context of social sharing. Consider becoming the first person to traverse a trail through a forest. The trail may be first overgrown and difficult to navigate. However, the trail grows clearer and simpler to follow with each consecutive visit. Sharing and retrieving memories are comparable. Any given event's memory becomes easier and simpler to recall with each successive retrieval and sharing.

Sharing personal information on social media also seems to fall under this mnemonic advantage of selective production looked at the effects of posting autobiographical experiences on social

media on mnemonic devices. Participants in their research were asked to keep a journal of their life experiences, and the events were categorized as either being shared online or not. They discovered that 98% of the events that were posted had higher ratings for importance and intensity than those that were not reported, indicating that online posting is extremely selective. More importantly, regardless of the details of the experiences, individuals remembered more memories of those that were put online than those that weren't. Online sharing of personal tales improved memory recall. Social media and the Internet provide a forum for people to practice memories and give meaning to externalized memories. IN other words, social media may provide a mechanism for a person to consider the personal significance of the events shared and, as a result, have a better memory of them.

It is important to point out that the research had the drawback of allowing participants to choose what they shared online. Therefore, the events that were uploaded could have been "inherently" remarkable rather than necessarily being more remembered because they were shared online. The precise processes behind this improved recollection need more investigation.

Selectively creating personal information on social media may improve memory of the information posted, but it may also cause forgetting of related but unproduced information. In what they named the retrieval practice paradigm, Anderson and his colleagues first investigated this sort of amnesia using word-paired associations. The research phase, retrieval-practice phase, and final recall phase were the three sequential stages of this paradigm. Participants in the study phase saw several category-exemplar paired associations. The participants were told to research their partnered partners. Participants only recover half of the exemplars from half of the categories during the retrieval practice phase. The category containing the first two letters of the example was given to the participants to limit the things they may recollect. After a short pause, the participants completed a final recall in which they had to recollect all the examples from the study phase after being given a list of all the categories.

Over 15 days, the experiment was conducted. Participants maintained a journal throughout the first week of the research, noting distinct occurrences, four in each of the following four categories: cheerful, humorous, thrilling, and entertaining. The researcher told the subjects to snap a photo of each occurrence that occurred. Participants were contacted by the experimenter at the end of the week and given the option to upload images from half of the categories on Instagram at random. The researcher gave individuals instructions to respond to their postings normally throughout the next week. The participants returned to the lab after the second week to perform a counterbalanced, recognition, and cued recall test. The cued memory test assessed their recollection of the real memories linked with the photographs, while the recognition task measured their response speed and accuracy when presented with their pictures. Although there were no RIF effects for recognizing the images, early findings imply that RIF took place for the memories that surrounded the shared images. That is, selectively publishing photos on Instagram caused people to lose memories linked to the corresponding, private photos. This shows that carefully organizing one's life on social media may improve recollection of shared events but potentially cause forgetting of associated memories. These impacts were unaffected by how many people "loved" or commented on the image.

REFERENCES:

- [1] L. Alonso, J. Barbarán, J. Chen, M. Díaz, L. Llopis, and B. Rubio, "Middleware and communication technologies for structural health monitoring of critical infrastructures: A survey," *Comput. Stand. Interfaces*, 2018, doi: 10.1016/j.csi.2017.09.007.
- [2] M. S. Arshad Malik, M. Ahmed, T. Abdullah, N. Kousar, M. N. Shumaila, and M. Awais, "Wireless body area network security and privacy issue in E-healthcare," *Int. J. Adv. Comput. Sci. Appl.*, 2018, doi: 10.14569/IJACSA.2018.090433.
- [3] E. Molina and E. Jacob, "Software-defined networking in cyber-physical systems: A survey," *Comput. Electr. Eng.*, 2018, doi: 10.1016/j.compeleceng.2017.05.013.
- [4] S. Khairunniza-Bejo, N. H. Ramli, and F. M. Muharam, "Wireless sensor network (WSN) applications in plantation canopy areas: A review," *Asian Journal of Scientific Research*. 2018. doi: 10.3923/ajsr.2018.151.161.
- [5] J. Wang *et al.*, "A software defined radio evaluation platform for WBAN systems," *Sensors (Switzerland)*, 2018, doi: 10.3390/s18124494.
- [6] G. Barile, A. Leoni, L. Pantoli, and V. Stornelli, "Real-time autonomous system for structural and environmental monitoring of dynamic events," *Electron.*, 2018, doi: 10.3390/electronics7120420.
- [7] A. H. Mohsin *et al.*, "Real-Time Remote Health Monitoring Systems Using Body Sensor Information and Finger Vein Biometric Verification: A Multi-Layer Systematic Review," *Journal of Medical Systems*. 2018. doi: 10.1007/s10916-018-1104-5.
- [8] Y. Xue, W. Jia, X. Zhao, and W. Pang, "An Evolutionary Computation Based Feature Selection Method for Intrusion Detection," *Secur. Commun. Networks*, 2018, doi: 10.1155/2018/2492956.
- [9] M. Yaseen *et al.*, "Secure sensors data acquisition and communication protection in eHealthcare: Review on the state of the art," *Telematics and Informatics*. 2018. doi: 10.1016/j.tele.2017.08.005.
- [10] V. Romashchenko, M. Brutscheck, and I. Chmielewski, "Investigation and Implementation of Robust Wireless Zigbee Based Security System," in *29th Irish Signals and Systems Conference, ISSC 2018*, 2018. doi: 10.1109/ISSC.2018.8585286.
- [11] A. T. Sasongko, G. Jati, and W. Jatmiko, "Multipath Routing Protocols in Vehicular Ad hoc Networks (VANETs): Performance Evaluation in Various Conditions," in *ISSIMM 2018 - 3rd International Seminar on Sensors, Instrumentation, Measurement and Metrology, Proceeding*, 2018. doi: 10.1109/ISSIMM.2018.8727733.

CHAPTER 7

MASSIVE MIMO SYSTEMS: A FAMILY OF HYBRID ANALOG-DIGITAL BEAM FORMING METHODS

Dr. Ajit Kumar, Assistant Professor

Department of Electronics and Communication Engineering, Presidency University, Bangalore, India

Email Id- ajitkumar@presidencyuniversity.in

As a top contender for 5G wireless connectivity, massive MIMO wireless systems have developed. It provides better data rates and capacities than conventional MIMO systems and incorporates mm Wave technologies, which have lately been acknowledged as crucial for addressing the spectrum crisis. Higher array gain than previously may be possible with the utilisation of large antenna arrays at the transmitter and receiver. Precoding and combining methods are used to capitalize on this benefit. These techniques, which are often used in Baseband (BB), call for a specific piece of RF hardware for each antenna. Unfortunately, when you factor in a huge number of antennas, the cost is high since RF components, particularly for mm.Wave technology is costly and has significant power consumption. As a result, it is preferable to build affordable hardware that will make use of the potential gain from a lot of inexpensive antenna components while only employing a few costly RF chains.

Several hybrid analogue-digital systems have been put forward to accomplish this aim. In hybrid precoding and combining, the processes are divided between the digital and analogue domains: at the transmitter side, a low-dimensional digital precoder works on the transmitted signal at BB. The modest number of digital outputs are then mapped to a large number of antennas by an analogue precoder; the receiver side goes through a similar process. Analog switches and phase shifters are the foundation of most analogue topologies. According to the budget for both electricity and space, the particular systems may change. The fully-connected and partially-connected structures are the two primary categories of architecture. Maximizing precoding and combining gain is possible in fully linked networks because they provide a mapping from each antenna to each RF chain. There are fewer analogue components utilised in the partly linked design. Despite lowering power consumption and device complexity, the resulting gain is reduced as a result.

Precoding methods are used by the transmitter to provide numerous data streams to the receiver across a continuous and well-known channel during the data phase of each coherence interval during MIMO communication. To estimate the data vector from the signal received at the antennas, a combiner is utilised at the receiver side. A desired performance metric, such as estimate error or system spectral efficiency, is optimised by selecting the precoder and combiner. The precoder and combiner matrices of a hybrid beam former, in contrast to the fully-digital scenario, are bound by the particular hardware selection and are unable to include any arbitrary entries. Only unimodular matrices, for instance, are taken into account when utilizing a phase shifter network on the analogue side. The objective is to maximize the performance measure across all pairings of digital and analogue precoder matrices, leading to a challenging non-convex optimization issue.

The fully-connected phase shifter network was taken into consideration in earlier efforts on hybrid beam forming. The combined precoder and combiner design issue was divided into two sub-problems, and each was advised to be solved separately. The challenging joint optimization issue is significantly simplified by this method, even though it is not ideal. It was shown that the precoder's spectral efficiency may be maximised by roughly decreasing the difference between the hybrid precoder and the best digital one across all hybrid precoders. On the combiner side, it was shown that reducing the mean squared error (MSE) across all hybrid combiners is comparable to reducing the weighted approximation gap between the fully-digital combiner and the hybrid one [1], [2].

The authors took into account a fully-connected phase shifter scheme and demonstrated that for flat-fading channels, a hybrid beamformer can perform as well as a fully-digital one if the number of RF chains is double that of the number of data streams. They then provide a heuristic technique for precoder design that first determines the best baseband precoder for a given analogue precoder and then uses an iterative process to get the local best analogue precoder. The studies, and took into account precoder design and sought to maximise the spectral efficiency of the system. The best fully-digital precoder, according to their analysis of the mmWave sparse multipath channel topology, is made up of a minimal number of guiding vectors. Then, using a dictionary of steering vectors, they propose a modification of the orthogonal matching pursuit (OMP) technique to build a workable precoder that approximates the ideal one. By limiting the set of potential precoder vectors to steering vectors, this technique significantly decreases the problem's complexity but leaves a significant performance gap with the best precoder.

Similar methods for combiner design, under an MSE or spectral efficiency aim, were used. The authors took into account both rich and sparse scattering channels and demonstrated that the channel singular vectors are unimodular for the asymptotic case when the number of antennas reaches infinity. By setting the phase shifters to the phases of these vectors, the authors were able to create the ideal hybrid beamformer. Two strategies were proposed to substitute a workable fully-digital precoder for the ideal one. Manifold optimization is the foundation of the first, MO-AltMin.

The approach builds a conjugate gradient method for each iteration to discover an analogue precoder that is a local minimizer of the approximation gap from the fully-digital one. Each iteration assumes a specified digital precoder. Next, a least squares solution is used to calculate the digital precoder. This approach only works for fully-connected phase shifter networks and has a high level of complexity and runtime while producing excellent performance. In the second method, a low complexity technique is used to generate an upper limit on the approximation gap, which is then reduced over all analogue precoders. This algorithm assumes that the digital precoder is a scaled unitary matrix. Performance is lost when the combiner is restricted to such a structure, however.

The majority of the prior research focused on fixed sub-arrays for the partly linked design, where each RF chain is connected to a certain sub-array in advance. The authors proposed a low-complexity codebook architecture that would result in a tiny dictionary of workable precoding vectors, selected according to the intensity of the transmitted signal. To optimise the mutual

information between the receiver and transmitter, they next thoroughly search through all conceivable combinations from the limited vocabulary. When the channel is not sparse, this last step might result in a significant computing burden.

The authors take into account discontinuous sub-arrays and propose an iterative technique to approach the best fully-digital precoder, which alternatively optimises across the analogue and digital combiners. It is shown that the analogue precoder issue is separable in the antennas and has a closed-form solution for discontinuous arrays. A proposed semidefinite relaxation applies to the digital precoder. However, a closed-form solution for the digital combiner is already available, making this computationally demanding and unneeded. This method of alternating reduction still leaves a significant performance difference. In, a few less restricted plans were taken into consideration. A twin-phase shifter with dynamic mapping is taken into consideration. The prior solutions' unit modulo restriction is relaxed by using two-phase shifters per antenna, but the cost, complexity, and area are doubled. Orthogonal frequency division multiplexing (OFDM) is addressed using a dynamic sub-array technique, and it is recommended to use a greedy algorithm to optimise the array partition based on the long-term channel characteristics. This approach, meanwhile, only applies to OFDM broadcasts[3], [4].

The majority of the studies mentioned above employ spectral efficiency as a performance criterion. The MSE of the transmitted data serves as our primary performance criteria in this study. We provide a basic framework for hybrid beamforming that works with a variety of hardware configurations and channels, including whole and partial networks with varied numbers of phase shifters and switches. In a single-user massive MIMO system with huge antenna arrays on both the receiver and transmitter and fewer RF chains than antennas, the data estimation issue is taken into consideration. With a given number of RF chains and a Bayesian model in which the data and interference are both random, we want to minimise the MSE of the transmitted data from the low-dimensional received digital signal at the receiver. In line with earlier research, we divide challenging joint optimization into two distinct issues in the precoder and combiner.

We provide a methodology for designing the precoder that approximates the ideal fully-digital precoder with a workable hybrid precoder. Our alternating minimization of approximation gap (AltMaG) technique takes use of the unlimited number of best precoders that vary from one another by a unitary matrix. To discover the fully-digital solution that yields the least approximation gap from its hybrid decomposition, we advise optimising over this matrix and the hybrid precoder alternatively. Depending on the hardware restrictions, any of the previously recommended approaches may be utilised for the hybrid precoder optimization stage. With no appreciable increase in complexity, Alt-Mag reduces MSE even further as compared to state-of-the-art methods by optimising over the unitary matrix as well.

We then provide a straightforward alternative to the hybrid precoder optimization problem, leading to the minimum gap iterative quantization approach, a low complexity technique (MaGiQ). The completely digital solution is approximated using just the analogue precoder in each iteration of MaGiQ. This leads to a closed-form solution, which is provided by a straightforward quantization function that is dependent on the hardware architecture. Although

personal use is allowed, republication and redistribution need IEEE approval. Figure 1 discloses the Mobile Terminal and the subnet of the system.

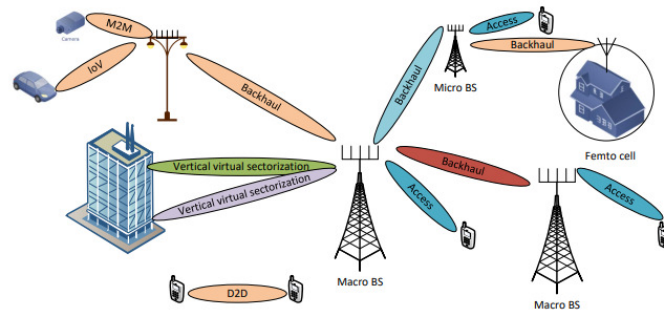


Figure 1: Discloses the Mobile Terminal and the subnet of the system.

Although it hasn't been completely edited, this paper has been accepted for publication in a future edition of this magazine. Before the final publishing, the content may change. Additionally, it is the best entirely digital option in certain particular instances. We illustrate the performance of the algorithm using this aim and show that the Alt-Mag framework and the MaGiQ algorithm can also be employed when taking the spectral efficiency measure into account. Next, we use MaGiQ to create a combiner after making minor modifications. Next, we recommend the greedy ratio trace maximisation (GRTM) approach, which uses an appropriate dictionary selected following the hardware design to directly reduce the estimated error. We show via simulations that GRTM performs well and runs quickly, particularly as the number of RF chains rises.

A new framework called Alt-MaG for designing hybrid beamformers that takes use of the unitary matrix's degree of freedom in the best-unconstrained beamformer. Alt-Mag improves hybrid beamformers' performance and may be utilised with a variety of performance metrics, including MSE and spectral efficiency. MaGiQ, a straightforward low-complexity algorithm that adheres to the Alt-MaG framework, produces lower MSE than other low-complexity algorithms while employing a minimal number of RF chains. Figure 2 discloses the Mobile Terminal and the subnet of the system and CMOS.

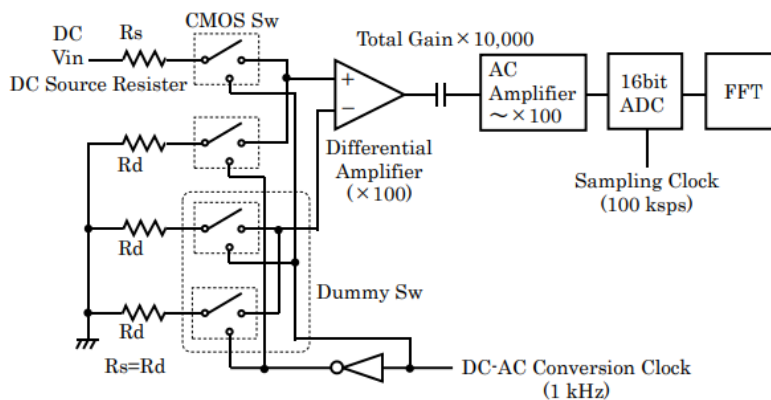


Figure 2: Discloses the Mobile Terminal and the subnet of the system and CMOS.

A greedy framework for combiner design that, by solving a straightforward ratio-of-scalars issue for each combiner vector individually in a greedy manner, directly reduces the estimated error. GRTM, a straightforward method, is used to solve the ratio-of-scalar issue using a dictionary that is appropriate for the hardware design. Each of our methods works with different hardware configurations and channel topologies. Recently, there has been a lot of focus on research into fifth-generation (5G) wireless networks, which intends to satisfy and address a variety of technological needs and obstacles from both academics and businesses. According to a study by Wireless World Research, mobile data traffic is growing (at least) twice as fast as cable data traffic and will overtake it by 2018.

The emergence of a wide variety of bandwidth-hungry applications, such as three-dimensional video games, Car2X communications, and high-resolution augmented reality video streams not only for gaming but also in factories of the future, has also resulted in a significant increase in users' traffic demand over time. Additionally, it is anticipated that by 2020, there will be around 50 billion gadgets supporting the community and that each individual will own more than six devices, which will support both human and machine connections. The goal is to create a space where sensors, appliances, automobiles, and drones can interact with one another through cellular networks. The capacity of the cellular network must be considerably increased to support such communications. In this aspect, it is predicted that the 5G network would need to provide 1000 times more capacity than the existing system to support such huge communications. Energy-related issues will inevitably arise as a result of this ambitious ambition, thus it is crucial to provide energy-efficient solutions while upholding the technical specifications. The radio component accounts for more than 70% of the mobile operator's electrical costs. Additionally, the expanded use of mobile networks greatly increases the emission of carbon dioxide, which is a current important issue.

The need for wireless communication is rising steadily system is strongly reliant on bandwidth and spectral efficiency (SE). Currently, the 300 MHz to 3 GHz spectrum is where all wireless technologies operate. The only untapped possibility is the system bandwidth since Shanon capacity has already been reached using physical layer technology. The key to 5G wireless networks is thus the research of the high-frequency mm Wave spectrum, which spans from 3 GHz to 300 GHz. On the other hand, MIMO technology, which employs multiple antennas at the transmitter (TX) and receiver (RX), is seen to be one of the most promising ways to enhance SE. SE differs from MIMO in two ways:

- 1) Multiple user equipment (UEs) may connect with a base station (BS) using the same time, frequency, and space resources, and
- 2) Multiple data streams can be sent between the BS and each UE. Massive MIMO, where there are hundreds of thousands of antenna elements at BS, is the next step in the evolution of the MIMO idea from multi-user (MU)-MIMO.

Due to beamforming gain, massive MIMO may aid in reducing small-scale fading and necessary transmission energy. Massive MIMO is also necessary for mmWave frequencies since it uses beamforming gain to counteract significant pathlosses and get a satisfactory signal-to-noise ratio

(SNR). As a result, mmWave and massive multiple-input multiple-output (MIMO) communications provide for increased access to the 30 GHz to 300 GHz bands and enhance SE. Machine to machine (M2M), Internet of vehicles (IoV), device to device (D2D), backhaul, access, femto cell (often referred to as a tiny cell), vertical virtual sectorization, etc. These technologies put a lot of strain on cellular networks to satisfy communication needs, and massive MIMO has the possibility of improving capacity, SE, and energy efficiency in this context (EE). On the other hand, larger route losses affect the target frequencies. By offering potential lines of sight or fewer multi-paths to the goal, a multi-tier system may help to solve the path losses issue.

A large antenna array is used in beamforming in mmWave massive MIMO systems to make up for route losses with directed broadcasts. Traditional baseband digital beamforming (DB) in huge MIMO systems needs a unique radio frequency (RF) chain for each antenna. The choice to use hybrid beamforming, which operates in the baseband and analogue domains, was made due to the high power consumption and high cost of mixed-signal and RF chains (analogue-to-digital converters (ADC)/digital-to-analogue converters (DAC), data converters, mixers, etc. To decrease the number of RF chains, much research has developed various designs known as hybrid forming approaches, which combine an analogue RF beamformer with a baseband digital beamformer. To increase the attainable rate, hybrid beamforming techniques are created to jointly optimise the analogue and digital beamformers. Since beamforming is done in the analogue domain at RF and many sets of beamformers may be coupled to a limited number of ADCs or DACs, the hybrid beamforming design seems to be more suited to mmWave than the typical microwave architecture.

The majority of signals produced by a spread of transmit antennas are guided in the desired angular direction by a process called beamforming. Beamforming specifically delivers the same symbol with a weighted scale factor across each transmit antenna. To increase the received SNR, all received signals are coherently merged at the RX using a distinct scale factor. Beamforming gain is the name for this increase in SNR in antenna array systems.

The diversity gain is the shift in the slope of the error probability brought on by the beamforming gain. The sole lower limit on the number of RF chains is the number of transmitted data streams, but the number of antenna components determines the beamforming gain and diversity order, which is why hybrid beamforming is attractive. A digital signal processor is used to process beamforming in pure digital beamforming, which offers more flexibility and degrees of freedom to construct effective beamforming algorithms. The pure digital beamforming approach results in a complicated design and significant power consumption since each antenna element has its own RF chain. The antenna weights may be applied in analogue beamforming either by utilising time delay elements or by phase shifting the signal either before or after the RF up-conversion step [5], [6].

Hybrid beamforming is a suitable architecture that can take use of a big mmWave antenna array with reduced architecture, according to rising interest in both digital beamforming and hybrid beamforming. Each RF chain in fully linked hybrid beamforming systems is connected to every antenna, whereas sub-connected or partly connected hybrid beamforming structures only connect each RF chain to a subset of the antenna components. The two designs pay off complexity for

benefit in different ways. The number of signal processing paths is $N_t N_r$ for a fully linked design with N_t transmit antennas and N_r RF chains, compared to N_t for a sub-connected system. The completely linked design's beamforming gain, however, is N_r times larger than the sub-connected approach.

All hybrid beamforming designs seek to provide near-optimal performance or performance that is comparable to pure digital beamforming, while minimising hardware and signal processing complexity. We outline application examples, products, and standards that demonstrate the development of hybrid beamforming in this section. The following areas are the focus of 5G wireless systems: The terms "urban micro" and "suburban micro" are used. The cell radii are maintained under 100m in the UMi environment, and the BSs are positioned below the roofs. In contrast, the cell radius in a SMi environment is around 200 m, and the BSs are installed at a height of 6 to 8 m. Hybrid beam forming makes it possible to package mmWave huge MIMO transceivers in a tiny form factor that may be installed in a variety of locations, such as lampposts, power line towers, building corners, etc. Due to the expense and energy consumption of a high number of ADCs/DACs, this was not conceivable with the digital precoding and beamforming designs employed in MIMO systems in the past.

In order to counteract the significant route losses, diffraction, limited penetration, and blockages at mmWave frequencies, the tiny sized BS has envisioned the idea of a cluster network, in which a number of coordinated BSs give ubiquity coverage via BS diversity. A cluster of BSs will be used to secure the quasi line of sight, such that in the case of a blockage brought on by shadowing, one BS will quickly pass over the UE to another BS in the cluster. When moving about, these handoffs may happen rather often. A dual connection between Long Term Evaluation (LTE)-Pro and 5G New Radio (NR) could be offered during the transition from fourth generation (4G) to fifth generation (5G), allowing users to connect to both systems at the same time and maintaining radio link connectivity even if the mm .Wave system is blocked. In Barcelona, Spain, during the Mobile World Congress (MWC) 2017, Ericsson displayed several creative applications for 5G networks. Inside MWC, they demonstrated remote automobile driving using visual and haptic input to the driver's seat. They followed the moving automobiles on a test track blanketed with 5G using antenna beamforming, antenna beam tracking, and a 15 GHz radio. Another demonstration by Ericsson Research demonstrated how 5G may be used to merge several technologies including radio and fixed access, distributed cloud, machine learning, and orchestration into one integrated platform. This demonstration featured a 5G radio running at 15 GHz.

They divided the robot's motor and control components. Advanced tasks like pattern recognition and machine learning were employed in the control element's decision-making for the robots' motions, allowing it to complete the cooperative tasks for the robots. The control part was shifted to the cloud. The use-upper case's limit on latency from the robot via 5G radio to the cloud execution environment and back to the robot was 3.5 milliseconds. The next generation of huge M2M will allow devices with a lot of antennae to connect in a small space. Each device may utilise the same time-frequency resource to connect with other devices by using precise beamforming to remove inter-device interference.

Products: Products for MmWave large MIMO indoor use have been developed and marketed successfully. The 60GHz unlicensed spectrum is used by IEEE802.11ad/WiGig (6.76Gbps) and WirelessHD (3.8Gbps) to target Gbps WLAN and HD video streaming, respectively. The Dell Alienware Gaming Laptop M17x, the Epson Powerlite Home Cinema Projector, the Sony Personal 3D Viewer, the ZyXel AeroBeam WirelessHD A/V Kit, and the Sharp Wireless TX/RX Unit are examples of devices that comply with WirelessHD. On the other hand, 802.11ad compatible devices include the Qualcomm Technologies 802.11ad WiFi client and router solution, Intel Tri-Band Wireless, and Dell Latitude E7450/70. The two main manufacturers of tri-band chipsets, which operate in the 2.4, 5, and 60 GHz bands, are Qualcomm and Intel.

Standards: For easy integration with the present 4G LTE system, the 3GPP began standardising huge MIMO systems in Release 13 under the moniker full-dimensional MIMO (FDMIMO, 16 antenna ports). It supports 8-, 12-, and 16 antenna ports with 2D codebooks and beamforming reference signal improvements. Although the 3GPP standard does not specify any specific beamforming topologies, the sub-connected hybrid beamforming structure is strongly tied to the design of the channel state information (CSI) acquisition methods in Release 13 of LTE-Advanced Pro. The beamformed pilots are transmitted using a sub-connected-like structure using the FD-MIMO. The FD-MIMO proof-of-concept systems' potential for improvement in terms of coverage and capacity has been shown in field tests. Rel-14 has suggested further improvements to multiuser massive MIMO systems, supporting up to 32 antennas with an enhanced codebook architecture for high-resolution beam forming. With these advancements, the mmWave massive MIMO architecture of 5G networks will get closer to 3D hybrid beamforming.

Following 3GPP Rel-14, Qualcomm has launched the first Cellular Vehicle-to-Everything (C-V2X) testing with Audi and others. Recently, the 3GPP Rel-15 working item for the 5G New Radio (NR), which is anticipated to be implemented in 2019 or later, added hybrid beamforming is a suitable architecture that can take use of big mmWave antenna array with reduced architecture, according to rising interest in both digital beamforming and hybrid beamforming. Each RF chain in fully linked hybrid beamforming systems is connected to every antenna, whereas sub-connected or partly connected hybrid beamforming structures only connect each RF chain to a subset of the antenna components. The two designs pay off complexity for benefit in different ways. The number of signal processing paths is $N_t N_{RF}$ for a fully linked design with N_t transmit antennas and N_{RF} RF chains, compared to $N_t N_{RF}$ for a sub-connected system. The completely linked design's beamforming gain, however, is N_{RF} times larger than the sub-connected approach.

Usecases: The usefulness of hybrid beamforming in a range of difficult use cases, including autonomous driving automobiles, M2M, etc., has been shown in a variety of use scenarios. The following areas are the focus of 5G wireless systems: The terms "urban micro" and "suburban micro" are used. The cell radii are maintained under 100m in the UMi environment, and the BSs are positioned below the roofs. In contrast, the cell radius in a SMi environment is around 200 m, and the BSs are installed at a height of 6 to 8 m. Figure 3 discloses the Mobile Terminal and the subnet of the system and CMOS with AWG.

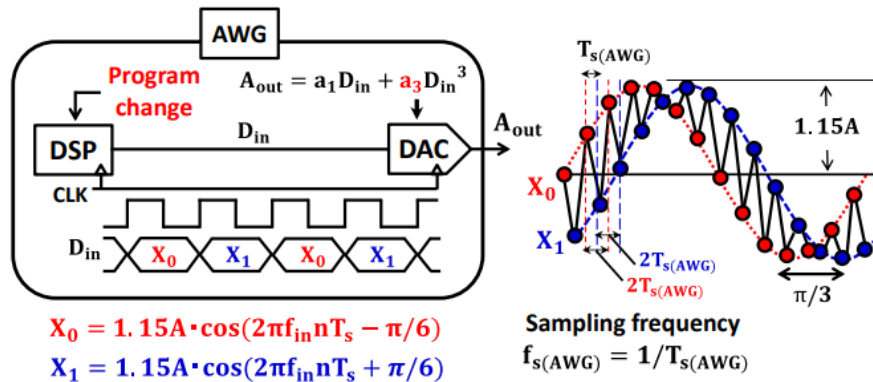


Figure 3:Discloses the Mobile Terminal and the subnet of the system and CMOS with AWG.

Hybrid beamforming makes it possible to package mmWave huge MIMO transceivers in a tiny form factor that may be installed in a variety of locations, such as lampposts, power line towers, building corners, etc. Due to the expense and energy consumption of a high number of ADCs/DACs, this was not conceivable with the digital precoding and beamforming designs employed in MIMO systems in the past.

To counteract the significant route losses, diffraction, limited penetration, and blockages at mmWave frequencies, the tiny-sized BS has envisioned the idea of a cluster network, in which several coordinated BSs give ubiquity coverage via BS diversity. A cluster of BSs will be used to secure the quasi-line of sight, such that in the case of a blockage brought on by shadowing, one BS will quickly pass over the UE to another BS in the cluster. When moving about, these handoffs may happen rather often. A dual connection between Long Term Evaluation (LTE)-Pro and 5G New Radio (NR) could be offered during the transition from fourth generation (4G) to fifth generation (5G), allowing users to connect to both systems at the same time and maintaining radio link connectivity even if the mm Wave system is blocked. In Barcelona, Spain, during the Mobile World Congress (MWC) 2017, Ericsson displayed several creative applications for 5G networks. In this part, we look at three common uses for filtering, including the processing of electrocardiogram (EKG) signals, the processing of stock exchange data, and the sequences of proteins and DNA. Although there might be considerable differences between individuals, much as with fingerprints, the EKG of a healthy person takes on a pretty well-defined structure. However, a cardiologist can detect certain heart diseases or illnesses using particular telltale EKG patterns.

The electrocardiogram, often known as an EKG, is a graph that represents a low-level electrical signal that was detected by a pair of electrodes affixed to certain, well-defined sites on the body and linked to an electrical device. These devices are employed in clinics and hospitals where a wide range of other electrical devices, including x-ray machines and electrical motors, are also present. All of these devices create electrical 60-Hz noise, which might contaminate an EKG waveform, along with the power lines and transformers that provide them with energy. Fig. 1.13a displays a typical, noise-free EKG signal shows an EKG signal that has electrical 60-Hz noise

contaminating it. As can be observed, the distinctive EKG characteristics are almost lost in the tainted signal and are consequently difficult, if not impossible, to identify. Such an EKG is unreliable for making a diagnosis.

One may create a band stop filter that will reject the electrical noise since the electrical noise coming from the power source has a well-defined frequency of 60 Hz. A filter of this kind was created using the techniques that will be covered in subsequent chapters, and it was then applied to the tainted EKG data. As can be observed, the filtered signal is an accurate representation of the original noise-free signal, except for a few transient artefacts spanning the range $n = 0$ to 100. The filtered signal is shown in. A band pass filter that was intended to pick the 60-Hz noise component was applied to the tainted EKG data in a different experiment to demonstrate the nature of filtering. A continuous noise component is separated by the band pass filter after initial transience spanning the range $n = 0$ to 150.

For a variety of reasons, we are all concerned about the state of the market. Everybody wants to save money for a rainy day, for instance, and naturally wants to invest that money in safe, low-risk equities, bonds, or mutual funds that provide good returns. We study the business section of our daily newspaper or scan the Internet for quantitative stock-exchange statistics when making judgments like these about our finances. Figure 4 discloses the Mobile Terminal and the Hilbert Filter.

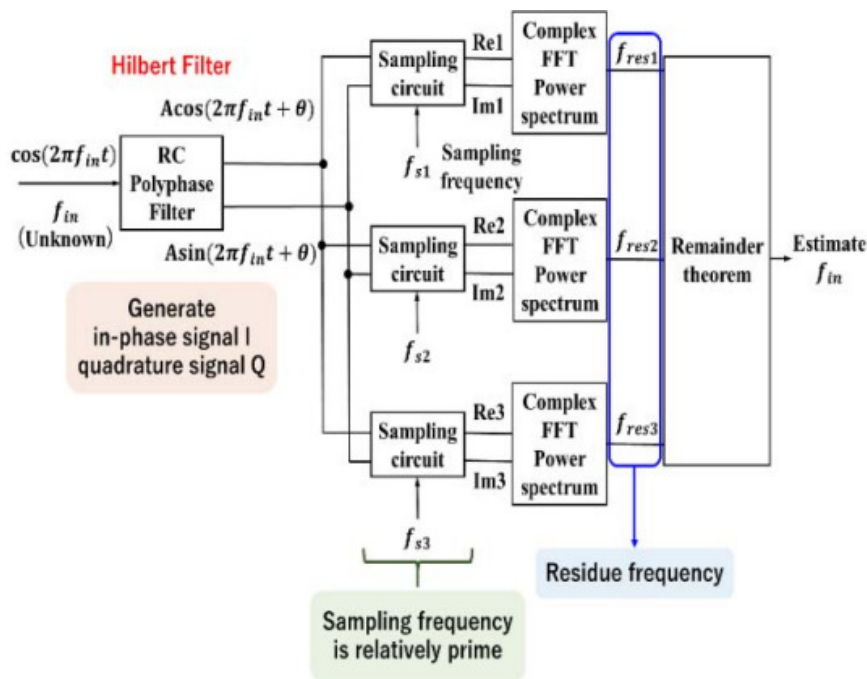


Figure 4: Discloses the Mobile Terminal and the Hilbert Filter.

Of course, we'd like to invest in things that increase consistently over time at a reasonable rate and never lose value at; a constant pace. But in reality, things don't work out that way. Since

stock prices fluctuate quickly over time, they sometimes lose a significant amount of their value during market downturns, for instance. The value of stock often changes as a result of several economic factors. Some of these causes are transitory, while others are a reflection of enduring economic constraints. As long-term investors, we may choose to disregard daily fluctuations and concentrate as much as we can on the fundamental shifts in stock price. An astute trader could be able to make deductions by only comparing the accessible stock exchange data of two rival companies. Most of us find this to be a difficult chore. However, using DSP may significantly simplify the work, as will be seen in the example that follows.

A signal's spectrum may be altered by filtering, and the price of a company's shares is one such signal. The high-frequency portion of a stock's spectrum represents day-to-day fluctuations, while the low-frequency portion of the spectrum represents the stock's underlying trend. Perhaps we should filter out the high-frequency portion of the spectrum if we are interested in the long-term performance of a company. On the other hand, if we find that we cannot accept significant daily fluctuations, maybe we might try to check the stock's volatility. There are several easily accessible volatility indicators, such as a stock's standard deviation.

Processing of data from the stock market, Unit values of high-tech and bond mutual funds, as well as data that has been lowpass filtered. A highpass filter is used to filter out the low-frequency material of a stock while keeping the high-frequency components.

Two real mutual funds were processed to demonstrate these concepts: a bond fund and a high-tech fund. The data for one year were selected for processing, and to make comparisons easier, the scaled share prices of the two funds were normalised to one at the beginning of the year. As can be observed, whereas the high-tech fund had significant fluctuations during the year, the bond fund exhibited rather constant annual performance. Daily fluctuations, or high-frequency content, in the two mutual. To get the smooth curves shown, money may be removed by using a lowpass filter. On the other hand, the mutual fund's underlying trend or the low-frequency spectrum may be eliminated by using a highpass filter to produce the high-frequency material seen. The filter output is shown as a percentage of the unit value in this graph.

During the first 50 or so sample values in the plots collected, certain oddities are seen. These are a result of certain initial transient circumstances that are present in all sorts of systems, including filters, although they may be avoided in practise by employing appropriate initialization. Ignoring this early stage, we see that the lowpass-filtered representation of the data offers a less crowded perspective of the funds while showing their relative volatilities more clearly. In this regard, see how the two funds' y-axis scales vary by a ratio of 5 to 1.

Plots like those may be used to calculate quantitative measures of volatility that are comparable to a stock's standard deviation. For instance, one may calculate the mean-square average (MSA) of $y(n)$, which is given by $MSA = \frac{1}{N} \sum_{n=1}^N [y(n)]^2$, or the average of $|y(n)|$, or any other norm. It is simple to calculate the MSA values for the bond and high-tech funds for values of $50 \leq n \leq 250$ as 0.0214 and 1.2367, respectively, giving the bond fund a ratio of 1 to 57.7. The message is extremely clear on the sort of investment that should be purchased to prevent restless nights. Figure 5 discloses the Mobile Terminal and the Hilbert Filter and Wave form.

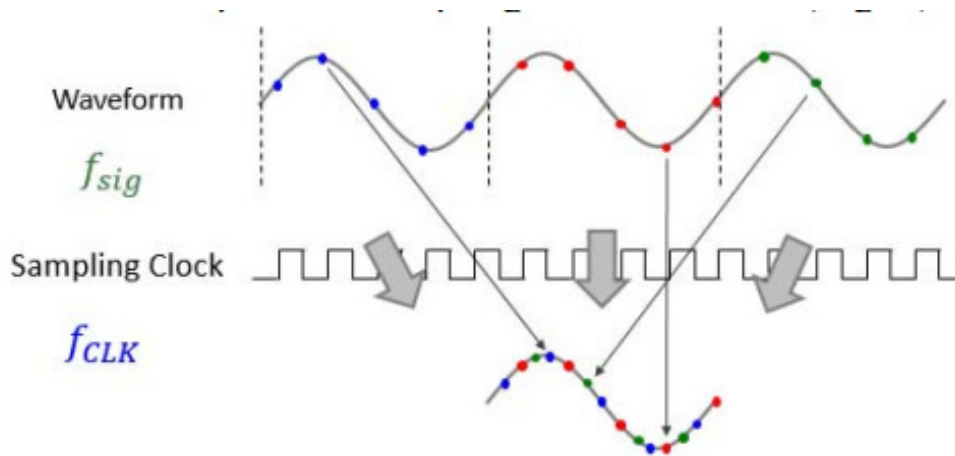


Figure 5: Discloses the Mobile Terminal and the Hilbert Filter and Wave form.

Extrapolating filters are a fascinating alternative that should be mentioned. These kinds of filters may be used to forecast stock values for the future, but if we go into the matter more, we'll enter the realm of technical analysis, which is a term used in the business world. Since DNA and protein sequences are discrete biological entities that resemble lengthy strings, significant progress has been made in this area recently. It did not take long for these sequences to be susceptible to numerical and computational approaches due to their discrete character. The DNA double helix is widely known to be kept together in a form like a ladder by simpler molecules called nucleotides acting as rungs. Adenine, guanine, thymine, and cytosine commonly denoted by the letters A, G, T, and C are the four different kinds of nucleotides that may be found in DNA sequences. A series of numbers is produced as soon as a DNA sequence is given a numerical value, and they are not dissimilar to the series of numbers produced by sampling an electrical signal.

In addition to being a string-like chain of many other chemical molecules known as amino acids, proteins are the basic building blocks of life. Although there are theoretically a large number of distinct amino acids that may exist, just 20 of them are typically present in the proteins of living things. A protein may be uniquely represented by its amino acid sequence, and by somehow allocating numbers to a protein sequence, a discrete-time signal can be produced.

The features, traits, and physical properties of DNA and protein sequences are many. Hot spots and so-called exons are two of them. These are areas of the DNA and protein sequences, respectively, that are essential to how the molecules of DNA and proteins work. The majority of the binding energy for protein-target interactions comes from hot spots, while exons carry the DNA instructions for protein synthesis. Because of this, precisely identifying and pinpointing exons and hot spots in DNA and protein sequences is a vital task that may help us better understand how DNA and protein sequences work and how they are interdependent.

In the past, experimental methods were used in wet labs to locate exons and hot spots in DNA and protein sequences, which added time and expense to the process. Different computational algorithms for the identification of exons and hot spots started to be developed in recent years to

lower costs, increase efficiency, and enable large-scale use. One such strategy is created by making use of a filter-based system, like the one shown in, in which a bandpass digital filter is utilised to extract the necessary data from a protein or DNA sequence.

Hot Spots' location

The input block transforms the sequence of amino acids that make up a protein, denoted as $p(n)$, into a sequence of numbers $x(n)$, using the known numerical values of the so-called electron-ion interaction potential (EIIP) [30] associated with amino acids. This is done in the case of determining the location of hot spots in protein sequences. The series of numbers thus shows a filter-based method for processing DNA and protein sequences. Exons in DNA sequences are located using (a) a method for the identification of hot spots in protein sequences, and (b) a technique for the placement of exons obtained is quite similar to a sampled electrical signal, and just like that signal, it has a frequency spectrum like the one shown. As a result, filtering is possible for $x(n)$. A bandpass filter that has been specifically created to pass a very restricted range of frequencies processes the sequence $x(n)$ in the filtering system shown. The square of the filtered sequence, $y^2(n)$, which is referred to as the power associated with the sequence by analogy to the power associated with an electrical signal, is computed by the output block. The mechanism effectively determines the power as a function of the length of the protein sequence for those frequency components of $x(n)$ that have gone through the band pass filter.

Recent research has shown that a strong component at a clearly defined frequency known as the characteristic frequency, such as char is present in the frequency spectrum linked to a group of functionally related proteins. This component's amplitude is significantly increased at hotspot locations. The presence of hot spots along the length of the protein sequence can be detected as well-defined peaks in the power output of the system by filtering a protein sequence using the system in with the passband of the bandpass filter tuned to select the characteristic frequency of a protein sequence of interest that belongs to the same functional group. As a result, a power profile of the hot spots can be built [6], [7].

DNA sequences' exon locations

It is possible to locate exons in DNA sequences using the filter-based technique. Four binary sequences, one for each nucleotide, known as locator sequences, may be used to describe DNA sequences. In each locator sequence, the presence or absence of a letter is denoted by a 1 or 0, respectively. A sampling frequency of 2 Hz may be connected with a locator sequence even if the independent variable is more like distance than time, which shows the typical waveform at the output of the band pass filter. This similarity allows for the association of an amplitude or power spectrum with a locator sequence, which can then be assessed very similarly to an electrical signal's spectrum.

Another recent finding in this field of study is the presence of a strong frequency $2/3$ in rad/s component in the power spectra of locator sequences as well as a linear combination of the locator sequences, such as that. This component is equivalent to a frequency of $1/3$ Hz or a period of 3 s in the case of an electrical signal. Because of this, the term "period-3 property" is often used to describe this extremely basic physical trait. The inclusion of exons significantly

increases the amplitude of the period-3 component. A period-3 sequence, similar to that in whose amplitude is controlled by the presence of exons in the DNA sequence under test, will be produced by filtering sequence $x(n)$ using a bandpass filter with its passband adjusted at frequency $2/3$ rad/s. As with hot spots in protein sequences, a power profile for exons in a DNA sequence may be built using the square of the filtered output.

Exon power profile samples for two genes; the greyed bars indicate exons that are well-known and are simple to find using the approach outlined. quantity of interest in the sequence is its amplitude. Similar to the carrier in an amplitude-modulated electrical signal, the period-3 component may be removed by filtering it out with a proper low pass filter. The exon power profile may often be seen more easily as a result displays typical exon power profiles. The known exons are shown by greyed bars, and their locations may also be determined using the filter-based approach previously discussed.

Inside MWC, they demonstrated remote automobile driving using visual and haptic input to the driver's seat. They followed the moving automobiles on a test track blanketed with 5G using antenna beam forming, antenna beam tracking, and a 15 GHz radio. Another demonstration by Ericsson Research demonstrated how 5G may be used to merge several technologies including radio and fixed access, distributed cloud, machine learning, and orchestration into one integrated platform. This demonstration featured a 5G radio running at 15 GHz. They divided the robot's motor and control components. Advanced tasks like pattern recognition and machine learning were employed in the control element's decision-making for the robots' motions, allowing it to complete the cooperative tasks for the robots. The control part was shifted to the cloud. The use-upper case's limit on latency from the robot via 5G radio to the cloud execution environment and back to the robot was 3.5 milliseconds. The next generation of huge M2M will allow devices with a lot of antennae to connect in a small space. Each device may utilise the same time-frequency resource to connect with other devices by using precise beam forming to remove inter-device interference.

Standards: For easy integration with the present 4G LTE system, the 3GPP began standardising huge MIMO systems in Release 13 under the moniker full-dimensional MIMO FDMIMO, with 16 antenna ports. It supports 8-, 12-, and 16 antenna ports with 2D codebooks and beamforming reference signal improvements. Although the 3GPP standard does not specify any specific beamforming topologies, the sub-connected hybrid beamforming structure is strongly tied to the design of the channel state information (CSI) acquisition methods in Release 13 of LTE-Advanced Pro. The beamformed pilots are transmitted using a sub-connected-like structure using the FD-MIMO. The FD-MIMO proof-of-concept systems' potential for improvement in terms of coverage and capacity has been shown in field tests and has suggested further improvements to multiuser massive MIMO systems, supporting up to 32 antennas with an enhanced codebook architecture for high-resolution beamforming. With these advancements, the mmWave massive MIMO architecture of 5G networks will get closer to 3D hybrid beamforming. Following 3GPP Rel-14, Qualcomm has launched the first Cellular Vehicle-to-Everything (C-V2X) testing with Audi and others. Recently, the 3GPP Rel-15 working item for the 5G New Radio (NR), which is anticipated to be implemented in 2019 or later, was added[8], [9].

IBER-optic communications have historically emphasised fast connectivity over great distances throughout the world. Demand for short-reach networks in data centres has increased recently due to new applications including the Internet of Things (IoT), Augmented/Virtual Reality, Cloud Computing, storage, and other software-as-a-service (SaaS) models (DCs). Short-reach communications refer to all optical communication lines from servers inside a DC to inter-DC linkages that are between tens of kilometres in length, as depicted in It should be noted that these ER inter-DC connections have length scales that are similar to those of ordinary Metro and Access lines. On-board chip-to-chip optical interconnects are linkages with an even shorter distance at the opposite end of the spectrum. The emphasis of this review article is not on their design concepts and concerns, which are more Application Specific Integrated circuits (ASIC) development-related and include things like electronic packaging, power, thermal management, and other mechanical factors. Interested readers are directed to a thorough explanation of the subject.

According to a recent Cisco research, by 2020, 77% of all Internet traffic will be DC-related and 86% of it will be inside a DC. The likes of Facebook, Google, Amazon, and other content providers are responsible for the DC traffic's tremendous expansion. They have made significant investments in their infrastructure over the last several years and surpassed conventional telecommunications providers as market leaders for optical transceivers, particularly for short-reach lines. The greatest important progress in optical transceiver technology over the last ten years may have been made by digital coherent systems, which use all three degrees of freedom of the optical carrier amplitude, phase, and polarization to encode data. The whole field information in both polarisations is recovered by the digital signal processing (DSP) of the receiver.

Chromatic dispersion (CD) and polarization-mode dispersion (PMD), two transmission defects, become linear and are simple to adjust adaptively. Transmission bit rates per channel may now reach 100Gbit/s and 200Gbit/s, respectively, thanks to high-order modulation schemes such as polarization-division multiplexing -quadrature phase shift keying (PDM-QPSK) and polarization-division multiplexing -16 quadrature amplitude modulation (PDM-16QAM). Recently, single-channel 1Tbit/s transmission was demonstrated, and further advancements towards commercial transceivers are anticipated shortly.

The research community has worked very hard in recent years to create DSP solutions for short-reach systems that mimic the successes of long-haul systems. The sheer magnitude of the short-reach transceiver market, however, makes cost the top priority and prevents the straightforward implementation of the digital coherent system theory into short-reach connections. Additionally, transceiver form factors are crucial because port density the total number of physical connections and data rate per area is a crucial elements in determining the overall size and energy consumption of DC. The realization of next-generation DC for the aforementioned applications requires novel signalling, sensing, and DSP methodologies due to the limitations' unprecedented demands on physical layer devices.

We expand on our discussion from our OFC contribution to this work and provide a more thorough overview of this crucial subject of DSP for short-reach communication systems. The

remainder of the essay is structured as follows: Section II discusses the history of DSP and signalling strategies for coherent systems and identifies particular difficulties for short-reach systems. The primary distinction between analogue and digital communication is the use of digital signals for data transmission and reception in contrast to analogue communication's use of analogue signals. Digital signals are made up of discrete values, while analogue signals are continuously changing temporal signals.

Digital communication has a number of benefits, including a higher signal-to-noise ratio and immunity to noise and distortion. The SNR (Signal to Noise Ratio) is further improved when repeaters are used in digital communication. Additionally, analogue communication uses more power than digital communication. In analogue communication, analogue signals are used to communicate data between the transmitter and receiver. The amplitude of an analogue signal is continuously changing throughout time. Any kind of data, including speech, sound, and so on, may be sent via an analogue signal dig in analogue

The data must first be transformed into an electrical form. With the use of a transducer, speech and sound, which are inherently non-electric, may be transformed into an electric form. The communication channel is then used to transmit this signal. Short-distance communication is best done with analogue technology. However, with the aid of analogue modulation techniques like amplitude modulation and angle modulation, we may also utilise it for long-distance communication anatomical structure of analogue communication

The process of modulation involves combining a high-frequency carrier signal with a low-frequency information stream. Following that, this signal is sent across the channel. One modulator is thus needed at the transmitter end, and one demodulator is attached at the receiving end to recover the original signal. The main disadvantage of analogue communication is that as the signal travels further, its intensity begins to deteriorate. As a result, the signal-to-noise ratio begins to decline. Additionally, since analogue signals are continuous time-varying signals, noise has a greater impact on them than on digital signals.

Digital Communication Definition

Digital communication is the process of sending information between a source and a destination using digital signals. A square wave is used to represent digital signals. Rather than having continuous values, this signal has discontinuous values. The analogue signal is sampled to create the digital signal. Analog signal samples are collected, and then they are quantized. Digital signals typically have two states, ON or OFF, i.e., 0 and 1. The digital signal that has been produced after sampling and quantization is modulated using digital modulation methods. Digital modulation methods include PCM (Pulse Coded Modulation) and DPCM. The digital communication system also includes repeaters to amplify the signal that weakens as it travels over a certain distance. The noise signal is reduced and the information signal is amplified by the repeaters. As a result, repeaters efficiently maintain the SNR [10], [11].

Communication Block Diagram for Digital

Utilizing digital communication has the important benefit of not being affected by channel noise. This is so because the digital signal is not constantly changing. Therefore, the original signal may be recovered from the distorted signal if noise effects are mixed with the digital data. This is because digital signals consist of discrete values, thus if noise affects one of the signal amplitude points, we can determine the range in which that point sits.

Key Disparities in Communication Bandwidth between Analog and Digital: The primary distinction between analogue and digital communication is brought about by this element. The transmission of an analogue signal needs less bandwidth than that of a digital signal, which needs more. **Power Requirement:** When compared to analogue communication, digital communication requires less power. Digital systems need a greater amount of bandwidth, thus they use less power. And analogue communication systems use more electricity since they need less bandwidth.

Fidelity: A significant distinction between analogue and digital communication is made by fidelity. The capacity of the receiver to receive the output precisely in coherence with that of the input is known as fidelity. Compared to analogue communication, digital communication provides higher levels of fidelity. **Hardware Flexibility:** Compared to digital communication, analogue communication systems' hardware is less versatile. Digital technology is characterized by small, power-efficient devices. **Error Rate:** Another important distinction between analogue and digital communication is the error rate. There is a parallax or other kind of observational technique mistake with analogue devices. **Synchronization:** Digital communication systems provide synchronization, whereas analogue systems do not. So, another important distinction between analogue and digital communication is created by synchronisation. **Cost:** Digital communication equipment is expensive, and transmitting digital signals requires more bandwidth.

Information is sent from the transmitter to the receiver through a continuous, time-varying signal in analogue communication. Digital communication, on the other hand, uses digital technology to transmit information via a channel. Modern society is moving away from analogue communication as digital technology is developed. The disadvantage of employing digital communication is that it is more expensive and takes more bandwidth for transmission. Therefore, we may utilise digital communication for our purposes if cost is not a concern; but, if we want an affordable system, we should use analogue.

REFERENCES:

- [1] F. Wang, J. Fang, H. Li, Z. Chen, and S. Li, "One-Bit Quantization Design and Channel Estimation for Massive MIMO Systems," *IEEE Trans. Veh. Technol.*, 2018, doi: 10.1109/TVT.2018.2870580.
- [2] K. Ghavami and M. Naraghi-Pour, "Blind Channel Estimation and Symbol Detection for Multi-Cell Massive MIMO Systems by Expectation Propagation," *IEEE Trans. Wirel. Commun.*, 2018, doi: 10.1109/TWC.2017.2772837.

- [3] W. Tan, G. Xu, E. De Carvalho, M. Zhou, L. Fan, and C. Li, "Low Cost and High Efficiency Hybrid Architecture Massive MIMO Systems Based on DFT Processing," *Wirel. Commun. Mob. Comput.*, 2018, doi: 10.1155/2018/7597290.
- [4] W. Shen, L. Dai, B. Shim, Z. Wang, and R. W. Heath, "Channel feedback based on AoD-adaptive subspace codebook in FDD massive MIMO systems," *IEEE Trans. Commun.*, 2018, doi: 10.1109/TCOMM.2018.2849755.
- [5] D. Neumann, T. Wiese, M. Joham, and W. Utschick, "A Bilinear Equalizer for Massive MIMO Systems," *IEEE Trans. Signal Process.*, 2018, doi: 10.1109/TSP.2018.2838577.
- [6] S. A. Busari, K. M. S. Huq, S. Mumtaz, L. Dai, and J. Rodriguez, "Millimeter-Wave Massive MIMO Communication for Future Wireless Systems: A Survey," *IEEE Communications Surveys and Tutorials*. 2018. doi: 10.1109/COMST.2017.2787460.
- [7] K. Kim, J. Lee, and J. Choi, "Deep Learning Based Pilot Allocation Scheme (DL-PAS) for 5G Massive MIMO System," *IEEE Commun. Lett.*, 2018, doi: 10.1109/LCOMM.2018.2803054.
- [8] R. Chopra, C. R. Murthy, H. A. Suraweera, and E. G. Larsson, "Performance Analysis of FDD Massive MIMO Systems under Channel Aging," *IEEE Trans. Wirel. Commun.*, 2018, doi: 10.1109/TWC.2017.2775629.
- [9] M. Hanif, H. C. Yang, G. Boudreau, E. Sich, and H. Seyedmehdi, "Antenna subset selection for massive MIMO systems: A trace-based sequential approach for sum rate maximization," *J. Commun. Networks*, 2018, doi: 10.1109/JCN.2018.000022.
- [10] K. Xu, Z. Shen, Y. Wang, X. Xia, and D. Zhang, "Hybrid Time-Switching and Power Splitting SWIPT for Full-Duplex Massive MIMO Systems: A Beam-Domain Approach," *IEEE Trans. Veh. Technol.*, 2018, doi: 10.1109/TVT.2018.2831790.
- [11] S. Kim and B. Shim, "FDD-Based Cell-Free Massive MIMO Systems," in *IEEE Workshop on Signal Processing Advances in Wireless Communications, SPAWC*, 2018. doi: 10.1109/SPAWC.2018.8446023.

CHAPTER 8

TIME-TO-DIGITAL CONVERTER (TDC)

Dr. Vipin Solanki, Assistant Professor

Department of Applied Science, Sanskriti University, Mathura, Uttar Pradesh, India

Email id- hodmaths@sanskriti.edu.in

An electromagnetic or electrical current known as a signal is used to transfer data from one system or network to another. Although it may sometimes take other forms, such as current, a signal in electronics is often a time-varying voltage that is also an electromagnetic wave conveying information. Analog and digital signals are the two primary forms of signals used in electronics. This article compares analogue and digital signals and explains their related properties, functions, benefits, drawbacks, and common usage. Digital Signal An analogue signal has a restricted number of possible values within a continuous range that is time-varying and often limited to a certain range (for example, +12V to -12V).

An analogue signal, such as electricity flowing over a wire, exploits a specific feature of the medium to transmit the signal's information. To represent the information in an electrical signal, the signal's voltage, current, or frequency may be changed. In reaction to changes in light, sound, temperature, location, pressure, or other physical phenomena, analogue signals are often computed responses. An analogue signal ought should result in a smooth, continuous curve when plotted on a voltage vs. time graph. Electronic Signal Any signal that encodes data as a series of discrete numbers is referred to as a digital signal. A digital signal can only have one value at a time, chosen from a limited range of potential values. The physical quantity that corresponds to the information in digital signals might be any of the following:

1. electric current or voltage that is variable
2. polarization or phase of an electromagnetic field
3. Acoustic force
4. a magnetic storage medium's magnetization

All digital electronics, including computer hardware and data transfer devices, employ digital signals. Digital signals have one of two values and are typically between 0V and VCC (often 1.8V, 3.3V, or 5V) when plotted on a voltage vs. time graph. Digital electronics Resistors, capacitors, inductors, diodes, transistors, and operational amplifiers (op amps) make up the majority of the basic electrical components.

Analog circuits may be made up of many different components or they can be as basic as two resistors working together to create a voltage divider. Generally speaking, analogue circuits that provide the same function are more challenging to design than digital circuits. Since digital components have been utilised to simplify such designs, analogue designs for radio receivers and battery chargers would need the expertise of a designer who is conversant with analogue circuits. Typically, analogue circuits are more prone to noise, which is defined as any minute, unwanted voltage changes. Small variations in an analogue signal's voltage level might result in substantial processing mistakes. Communication systems that employ a continuous signal to transmit

speech, data, image, signal, or video information often use analogue signals. Analog transmission may be divided into two categories that are both dependent on how data is adjusted to combine an input signal with a carrier signal. Amplitude modulation and frequency modulation are the two methods. Amplitude modulation (AM) modifies the carrier signal's amplitude. FM (frequency modulation) modifies the carrier signal's frequency. There are many ways to produce analogue transmission:

1. via a coaxial or twisted pair of wire
2. via a fibre optic wire
3. using radio
4. across water

Analog circuits employ these techniques to interact with the outside world and to precisely record and process these signals in electronics, just as the human body uses its eyes and ears to collect sensory information. The MP2322, a low IQ synchronous step-down converter in a compact 1.5mmx2mm QFN packaging, is one of the many analogue ICs and components that MPS manufactures. Digitized electronics Logic gates and other more sophisticated digital ICs are implemented in digital circuits. These ICs are shown as rectangles with pins jutting out of them.

We have created a technique for employing an AWG to create low-distortion sinusoidal waves, where the third-order harmonics of the signal produced are simply suppressed by altering the waveform memory contents of the AWG — AWG nonlinearity detection is not necessary. It is also feasible to extend it to the creation of two-tone signals for the reduction of intermodulation distortion. We have looked at using a complex band-pass (BP) DAC to generate I-Q signals for ATE system use and I-Q balancing testing of communication ICs [9]. We demonstrate that, in terms of noise-shaping properties, the complex BP DAC is better than two genuine BP DACs.

Then, we looked at the characteristics of the complicated BP phase-switching method for the creation of low-distortion signals. Every clock, two sine wave signals with a $\pi/3$ phase shift are interleaved. DAC, its extension, a sophisticated multi-BP DAC, and its recently developed Data Weighted Averaging (DWA) algorithm for its linearity increase. We also provide a method for digital self-calibrating. To evaluate communication application ADCs, we have developed multi-tone curve-fitting methods for precise identification of intermodulation distortion products. We discovered that these techniques provide more accuracy than traditional curve-fitting algorithms, particularly for incoherent sampling when the input frequency is uncertain [1], [2].

For the speed-up of the SAR ADC linearity test, we created a design-for-test. Assume that a staircase ramp is provided in a 12-bit SAR ADC linearity test such that the value of the ramp input is regulated at each sampling period. We don't need to require a 12-step algorithm since we are aware of the input value at each test point. Instead, a final 4-step procedure may be sufficient if we pre-adjust the respective comparator reference voltages to values that are near the input voltages.

With the use of several low-frequency sampling circuits, an analogue Hilbert filter, and analogue-to-digital converters (ADCs), we have developed a signal high-frequency estimating

circuit. In this case, the sample frequencies are comparatively prime. Our suggested approach is based on the residue number theory and frequency domain aliasing problems in waveform sampling. The sampling-induced spectrum folding is proactively used. In an equivalent-time sampling system for a periodic waveform under measurement, we have identified the ideal waveform acquisition condition between the observed waveform repetitive frequency (f_{sig}) and the sampling clock frequency. A waveform missing phenomena for the equivalent-time sampling may be avoided in the case of the golden ratio, and very effective waveform acquisition sampling can be achieved.

The analysis is done on the effects of sampling circuit non-idealities such jitter, finite time, and input-dependent sampling. Additionally, the basic tradeoff of the sampling circuit is elucidated, and additional findings from related research are given. In ATE systems, the time-to-digital converter (TDC) is often employed for timing measurement. We have created a variety of designs, including the Gray code TDC, Residue number TDC, SAR TDC, integral-type TDC, and TDC. To measure the one-shot timing, we additionally used the trigger circuit to save the timing difference data.

A method for assessing a clock's phase noise using a TDC has been put forward. Due to the following, it may be constructed using very simple circuitry. The clock being tested (CUT) is a signal that repeats itself. A longer measuring period may improve the temporal resolution. (iii) The delta-sigma TDC output data may be used to determine the phase noise power spectrum using FFT. There is no need for expensive, high-performance spectrum analyzers with lengthy measurement times. Using a self-referenced clock and a cascaded, we have created a reference-clock-free, high-time resolution on-chip timing jitter measuring circuit. The suggested new architecture offers fine-time-resolution measurement capabilities for all-digital timing jitter measurements without the need for a reference clock.

The time-interleaved ADC system is capable of realizing a high sampling rate ADC, however timing skews across channel ADCs are problematic, particularly for high-frequency input signals. Using the correlation between collected data, we created their digital compensation circuit and algorithm. Communication circuits require complex signal processing circuits, and a technique for assessing their I-Q balance has been established. We have suggested a technique to calculate the loop gain in a DC-DC buck converter with voltage and current mode controls from the open-loop and closed-loop output impedances. This makes it possible to measure the loop gain without sending a signal into the feedback loop. An analogue filter is crucial for ATE systems and evaluating one might be difficult.

The study findings for the analogue/mixed-signal circuit testing methodologies at the authors' lab have been discussed in this work. For further improvement, we also think about using all technological elements, including circuit method, built-in self-test (BIST), built-out self-test (BOST), and ATE [40], as well as signal processing and measurement/control algorithms and SOC resources like the P core, memory, and ADC/DAC. It would be most beneficial to include robust digital hardware and software in the SOC, which is why this test should be referred to as a digitally-assisted analog/mixed-signal circuit test. There is no royal way to analogue testing, which makes this study topic both intriguing and difficult, as we mention in this work.

A binary system is often used in digital circuits. Although just two states (0s and 1) may be used to represent data values, groupings of binary bits can be used to represent bigger values. A 0 represents a data value of 0, while a 1 represents a data value of 1, for instance, in a 1-bit system. A 00 denotes a 0 in a 2-bit system, a 01 denotes a 1, a 10 denotes a 2, and an 11 denotes a 3. The maximum number that can be represented in a 16-bit machine is 216, or 65,536. These bit groups may be recorded as a parallel bus or as a series of succeeding bits. This makes it simple to handle huge data streams. The majority of practical digital circuits are synchronous, which means that a reference clock is used to synchronise the functioning of the circuit blocks, making them more predictable than analogue circuits. Because analogue electronics function asynchronously, they process the incoming signal as it comes in. The majority of digital circuits manipulate data using a digital processor.

This may take the shape of a simple microcontroller (MCU) or a more sophisticated digital signal processor (DSP), which can filter and handle huge data streams like video. In communication systems, digital signals are often used to transmit data across point-to-point or point-to-multipoint channels, such as copper wires, optical fibres, wireless communication media, storage media, or computer buses. The electromagnetic signal that conveys the transferable data might take the form of a microwave, radio wave, electrical voltage, or infrared signal. Though they are more often more expensive than analogue circuits meant for the same functions, digital circuits are typically simpler to construct. The MP2886A, a digital multi-phase PWM controller with a PWM-VID interface compatible with NVIDIA's Open VReg standard, is one of the digital components offered by MPS. Digital-to-Analog (DtA) and Analog-to-Digital (ADC) (DAC) Conversion of Signals Analog and digital signals must be processed by many different systems. The employment of an analogue signal, which serves as an interface for the transmission medium to send and receive information, is typical in many communications systems[3], [4].

The information is filtered, processed, and stored using digital signals that are created from these analogue impulses. The RF analogue front-end (AFE) depicts a typical design in which all analogue blocks are used to amplify, filter, and gain the analogue signal. The information is filtered and processed by the digital signal processor (DSP) portion. An analogue-to-digital converter (ADC) is used in the received route (RX) to transfer signals from the analogue subsystem to the digital subsystem. A digital-to-analogue converter (DAC) is used in the transmitted route (TX) to transform signals from the digital subsystem to the analogue subsystem showing an analogue and digital communication system. A microprocessor chip designed specifically to handle digital signal processing is known as a digital signal processor (DSP). DSPs are built on MOSFET integrated circuit chips and are extensively utilised in high-definition television goods, telecommunications, digital image processing, common consumer electronics like mobile phones, and many other important applications.

Continuous real-world analogue signals are utilised to measure, filter, or compress data using a DSP. Due to its restrictions on power usage, dedicated DSPs often offer superior power efficiency, making them appropriate for portable devices. Most general-purpose microprocessors can also run algorithms for digital signal processing. Operation of ADC Figure 6 depicts how the

ADC works. The analogue signal is used as the input and is processed using a sample-and-hold (S/H) circuit to approximate its digital version. Depending on the ADC's resolution, the amplitude has been "quantized" that is, reduced from having infinite values to discrete ones. Finer step sizes and a more accurate representation of the input analogue signal are characteristics of an ADC with a greater resolution. The digitised signal is encoded into a binary stream of bits that represents the amplitude of the analogue signal at the last step of the ADC. Now that the output is digital, it may be processed digitally.

Operation of DAC The reverse action is provided by a DAC. The digital-to-analogue converter (DAC) receives a binary stream of data from the digital subsystem as input, and it generates a discrete value that is roughly analogue. The output signal becomes closer to a truly smooth and continuous analogue signal as the DAC's resolution rises. The analogue signal chain often includes a post filter to further smooth the waveform.

As was previously established, many modern systems are "mixed signal," which means they depend on both analogue and digital subsystems. To convert data between the two domains, these systems need ADCs and DACs. **Advantages and Drawbacks of Digital and Analog Signals** There are advantages and disadvantages for both analogue and digital signals, as with most technical problems. Analog or digital signalling (or a mix of the two) may be appropriate depending on the particular application, performance requirements, transmission medium, and operational environment. **Advantages and Drawbacks of Digital Signals** The following are the benefits of employing digital signals, including digital signal processing (DSP) and communication systems:

1. Less noise, distortion, and interference may be used to transmit information via digital signals.
2. Digital circuits are simply and inexpensively reproducible in large numbers.
3. As a result of the ability to change DSP processes utilising digitally programmable devices, digital signal processing is more versatile.
4. Digital information may be readily encrypted and compressed, making digital signal processing more secure.
5. Digital systems are more accurate, and by using error detection and correction codes, the likelihood of a mistake occurring may be decreased.
6. Using semiconductor chips, digital signals may be readily stored on any magnetic or optical medium.
7. Long distances may be covered through digital signal transmission.
8. The following are drawbacks of employing digital signals, including digital signal processing (DSP) and communication systems:
9. When comparing analogue and digital transmission of the same information, greater bandwidth is needed for digital communication.

DSP utilises more top internal hardware resources and processes the signal quickly. Compared to analogue signal processing, which uses passive components and uses less energy, this causes larger power dissipation. The complexity of digital systems and processing is usually higher.

Advantages and disadvantages of analogue signals. The following are the benefits of employing analogue signals, including analogue signal processing (ASP) and communication systems:

1. Processing analogue signals is simpler.
2. The finest signals for transmitting audio and video are analogue ones.
3. Analog signals have a far greater information density and may convey finer details.
4. Digital transmissions use more bandwidth than analogue ones.
5. Changes in physical phenomena, such as sound, light, temperature, location, or pressure, are better represented by analogue signals.
6. Systems for analogue communication are less electrically sensitive.
7. The following are drawbacks of utilising analogue signals, including analogue signal processing (ASP) and communication systems:
8. Unwanted signal disruptions may emerge from long-distance data transfer.
9. Generation loss may happen to analogue signals.
10. Unlike digital transmissions, which have far better resilience to noise and distortion, analogue signals are susceptible to these problems.

In comparison to digital signals, analogue signals are often of inferior quality. Systems and Applications for Analog and Digital Signals Analog signals were employed in conventional audio and communication systems. However, many of these systems have transitioned to digital due to improvements in silicon process technologies, digital signal processing capability, encoding techniques, and encryption requirements as well as gains in bandwidth efficiency. Analog signals continue to have certain applications where they are advantageous or have historical uses [5], [6]. The majority of systems that interface to real-world signals including sound, light, temperature, and pressure record or transfer the data via an analogue interface. Here are a few examples of uses for analogue signals:

1. audio reproduction and recording
2. temperature gauges
3. imaging devices
4. radio broadcasts
5. Control systems for telephones

Among the many analogue components offered by MPS are the MP2322, MP8714, MP2145, and MP8712. Modern technologies employ digital signals due to their benefits in terms of noise immunity, encryption, bandwidth efficiency, and the ability to use repeaters for long-distance transmission, even though many early communication methods used analogue signalling (telephones). Below is a list of a few uses for digital signals:

1. telephony systems (broadband, cellular)
2. collaborating online and exchanging data
3. digital interfaces that allow for programming

Learn more about digital MPS components like the MP2886A, MP8847, MP8868, MP8869S, and MP5416 by visiting our website. Conclusion the essential ideas behind analogue and digital signals, as well as how they are used in electronics, are introduced in this article. Each

technology has distinct benefits and drawbacks, thus choosing the right signal or signals will depend on your application's goals and performance requirements.

The analogue signal is utilised for information transmission in analogue communication, while the digital signal is used for information transmission in digital communication. While digital communication employs digital signals whose amplitude is of two levels, either low level 0 or high level 1, analogue communication communications use analogue signals whose amplitude fluctuates continuously from time from 0 to 100. While digital communication is completely unaffected by noise during transmission across a communication channel, analogue communication is significantly impacted by noise during the same transmission.

1. Only a small number of channels may be transmitted concurrently in analogue transmission. While digital communication may concurrently transmit a lot of channels.
2. Digital communication has superior noise immunity compared to analogue communication's weak noise immunity.
3. Digital communication coding is feasible while analogue communication coding is not. Certain mistakes may be found and fixed using various coding strategies.
4. The likelihood of an analogue communication mistake is considerable, compared to a low likelihood of a digital communication error.
5. Analog communication does have some synchronisation issues, however, digital communication synchronisation issues are simpler.
6. Systems for analogue communication have complicated hardware and are less adaptable than those for digital communication, which has simpler hardware and is more versatile.
7. In contrast to digital communication, where it is feasible to separate noise and signal, analogue transmission cannot distinguish between noise and signal.
8. Digital communication is more portable than analogue communication, which is less portable.
9. The cost of an analogue communication system is inexpensive compared to the cost of a digital communication system.
10. While digital communication is utilised for multiplexing, analogue communication is used for frequency division multiplexing and both digital and analogue communications are used for time-division multiplexing.
11. Analog communication requires little bandwidth, but digital communication systems need huge bandwidth, and analogue communication uses a lot of electricity, whereas digital communication uses very little.
12. Digital communication offers a high level of privacy whereas analogue communication has less privacy and is thus less safe.
13. While digital communication guarantees a more precise data transfer than analogue communication, the former does not.

Over the last 60 years, there have been enormous advances in the production of microchips and their use in the construction of effective digital systems, which has sparked the development of a brand-new field known as digital signal processing, or DSP. DSP has enabled the development of complex communication systems, the emergence of the Internet, the distillation of valuable

information about the cosmos from astronomical signals, the analysis of seismic signals to gauge earthquake intensity or predict the stability of volcanoes, the enhancement of computer images or photographs, and many other applications.

Using a common class of devices known as digital filters, a significant portion of DSP involves the altering of the signal spectra. The study, creation, and use of digital filters in DSP are all topics covered in this book. The fundamental ideas of digital filtering and DSP are introduced in this chapter. The sampling process, which is how analogue signals are transformed into matching digital signals, is introduced after a look at the many signal types found in nature, science, and engineering. The forms of processing that can be done to a signal and the various digital filters that can be used for this are then looked at. Three introductory applications that highlight the diversity of DSP for the benefit of beginners make up the chapter's conclusion.

Many scientific and technical disciplines, including astronomy, acoustics, biology, communications, seismology, telemetry, and economics, to mention a few, produce signals. Signals may be created artificially or spontaneously via certain physical processes. Seismic signals are the results of upcoming earthquakes or volcanic eruptions, whilst astronomical signals might be produced by massive cosmic explosions called supernovas or by fast-spinning neutron stars. Biology is also rife with signals, such as those created by the brain or heart, the acoustic signals used by dolphins and whales to communicate, or the signals produced by bats to help them navigate or capture prey. Contrarily, man-made signals appear in modern systems like computers, telephones, radar, and the Internet, as would be anticipated. Even the market is a source of many important signals, such as the Dow Jones Industrial Average or the pricing of commodities on a stock exchange.

Natural signals are of great interest to us for a variety of reasons. Astronomers may analyse the nature of a supernova explosion, measure the magnitude of a neutron star from the periodicity of the signal received, or extract critical information from optical signals received from the stars, such as their chemical makeup. While volcanologists can often foretell if a volcano is poised to blow its top, seismologists can pinpoint the size and location of an earthquake. By scanning electrocardiograms for certain telltale patterns or aberrations, cardiologists may identify a variety of cardiac diseases.

We are very interested in man-made signals for a variety of reasons, including the fact that they allow us to communicate over great distances, enable the Internet to spread vast amounts of information, allow computer components to communicate with one another, teach robots how to quickly perform extremely complex tasks, assist aircraft in landing in adverse weather and low visibility, or alert pilots about the loss of separation between aircraft. The market indexes, on the other hand, may assist us in deciding if it is the proper moment to invest and, if so, whether to choose bonds or shares.

We've implied in the sentences above that a signal is some amount, quality, or variable that changes over time, such as the brightness of a star or the potency of a seismic signal. Although this is often the case, there are signals in which the independent parameter is a different amount than time, and on occasion, there may be more than one independent variable. A picture or

radiograph, for instance, may be thought of as a two-dimensional signal in which the light intensity is determined by the x and y coordinates, which are lengths. On the other hand, a time-varying TV picture may be thought of as a three-dimensional signal, where time is one of the independent factors and two lengths are the other independent variables.

Signals may be categorised as discrete or continuous time signals. Continuous-time signals include, for example, an auditory wave made by a dolphin or an electromagnetic wave coming from a far-off galaxy. Continuous-time signals are characterised at every moment from beginning to end. Discrete-time signals, on the other hand, are specified at certain points in time, potentially every millisecond, second, or day. The closing price of a certain commodity on a stock exchange and the daily precipitation as a function of time are two examples of this sort of signal.

The signs of nature are often constant in time. There are several significant exceptions to the norm, however. For instance, in the world of quantum physics, electrons receive or lose energy at discrete times and in distinct quantities. Contrarily, the DNA of all living organisms is built of a ladder-like structure, the rungs of which are composed of four fundamentally different chemical components. Any live organism's genome may be represented by a discrete-time signal by giving these fundamental molecules unique numbers and considering the length of the ladder-like structure as it is time[7], [8].

A continuous-time signal may be represented mathematically by a function $x(t)$ whose domain is a set of integers (t_1, t_2), where t_1 and t_2 are equal, as shown in a discrete-time signal may also be represented by the function $x(nT)$, where n is an integer in the range (n_1, n_2) and T is the time interval between consecutive discrete signal values. T is referred to as the sampling period because discrete-time signals are often created by sampling from matching continuous-time signals. The sampling frequency, or $f_s = 1/T$, is reciprocal.

Additionally, nonquantized and quantized signals may be categorised. A quantized signal can only assume discrete values, which are typically uniformly spaced, whereas a nonquantized signal may take on any value within a certain range. In the literature, signals are sometimes referred to as analogue or digital. Generally speaking, a continuous-time signal is thought to be an analogue signal and vice versa. Similar to how a discrete-time signal is thought to be a digital signal, and vice versa. If the emphasis were on a pulse waveform's two-level idealised representation, it would be viewed as a digital signal, similar to the many waveforms contained in a normal digital system. The pulse waveform would, however, be handled as a continuous-time signal since the signal level may take on an unlimited range of values if the precise real level of the waveform were of interest.

An analog-to-digital (A/D) interface is often used to create discrete-time signals from matching continuous-time signals, while a digital-to-analog (D/A) interface is frequently used to receive continuous-time signals. As shown, an A/D interface normally consists of three parts: a sampler, a quantizer, and an encoder. The sampler is essentially just a switch operated by a clock signal that shuts briefly every T s when the input signal is in the form of a continuous-time voltage or current waveform, sending the level of the input signal $x(t)$ at instant nT , or $x(nT)$, to the output.

A quantizer is an analogue device that senses the level of its input and outputs, from a range of permitted levels, the closest possible level, say, $x_q(nT)$, i.e., a quantized continuous-time signal like that in An encoder is essentially a digital device that will sense the voltage or current level of its input and produce a corresponding number at the output, i.e., it will convert a quantized continuous-time signal of the type shown into a corresponding discrete-time signal of the type shown in A discrete-time signal will be transformed by the decoder into a matching quantized voltage waveform, as shown in The smoothing device's goal is to remove the inherent discontinuities by smoothing out the quantized waveform. A/D and D/A converters, which come in a variety of varieties including high-speed, low-cost, and high-precision, are commonly accessible as off-the-shelf components.

This book primarily focuses on discrete-time systems that can perform digital filtering or DSP. A quick summary of the historical growth and uses of analogue filters is valuable since digital filters developed as a logical extension of analogue filters and are often created using analogue-filter approaches.

Analog filters are still essential parts of many kinds of communication systems today since they were first developed for use in radio receivers and long-distance telephone networks. Based on their components and the technology they use, the many families of analogue filters that have developed throughout time may be divided into the following categories.

1. Switched-capacitor filters
2. Discrete active RC filters
3. Integrated active RC filters
4. Passive RLC3 filters

In the early 1920s, widespread usage of passive RLC filters started. They are described as passive because they do not need an energy source, such as a power supply, to function. They are constructed of linked resistors, inductors, and capacitors. Through the feature of electrical resonance⁴, which happens when an inductor and a capacitor are coupled in series or parallel, filtering action is accomplished. Between the 1930s and 1950s, engineers and mathematicians developed some very potent and complex techniques for the construction of passive RLC filters, driven by the significance of filtering in communications.

Discrete active RC filters first appeared in the middle of the 1950s and were a popular area of study in the 1960s. They include electronic amplifier circuits, discrete resistors, and capacitors. Active RC filters are appealing because they lack inductors, which is a benefit. Particularly for low-frequency applications, inductors have long been big, costly, and less desirable than resistors and capacitors. Unfortunately, electrical resonance cannot be accomplished without inductors, and simple filters can only be created with resistors and capacitors. However, it is feasible to replicate resonance-like phenomena that may be used to generate high-quality filtering by cleverly using amplifying electrical circuits in RC circuits. The amplifying electronic circuits need a power supply as an energy source, which is why these filters are considered active.

Active RC filters that are built directly into integrated circuits follow the same fundamental operating principles as their discrete counterparts. Filters that can work at frequencies as high as

15 GHz may be created using high-frequency amplifying circuits and the appropriate integrated circuit parts. During the 1980s and 1990s, there was significant interest in these filters, and research is still ongoing. In the 1970s and 1980s, switched-capacitor filters underwent significant development. Except the use of switches and amplifiers, they are active RC filters. Switches are employed in this family of filters to imitate high resistance values that are challenging to achieve in integrated circuit form. Switched-capacitor filters are compatible with integrated-circuit technology, much as integrated active RC filters. Transverse electromagnetic (TEM) transmission lines, waveguides, dielectric resonators, and surface acoustic devices are only a few examples of the many microwave parts and gadgets that go into making microwave filters. They are used in applications with frequencies ranging from 0.5 to 500 GHz. Over time, analogue filters have been used in a variety of settings. The following is a brief list that is not all-inclusive:

- a. TVs and radios
- b. Telephone systems; communication and radar apparatus; sampling apparatus; audio apparatus

We must first choose our preferred radio station or TV channel each time we wish to listen to the radio or watch television. By lining up the frequency of a bandpass filter inside the receiver with the broadcasting frequency of the radio station or TV channel, we tune the radio or TV receiver when we turn the radio knob or press the channel button on the remote control to the radio station's or TV channel's broadcasting frequency. We choose the frequency of a desired signal, i.e., our preferred radio station when we tune a radio receiver. All of the other stations' broadcasts are undesired and are ignored. The same idea may be used to stop communication signals from interfering with radar signals, for example, or communication signals from interfering with radar signals at an airport.

Noise, a collective term for erroneous signals, often corrupts transmissions. Such signals may come from a variety of places, including power lines, transformers, electrical motors, and lightning. Frequency spectrums that cover a broad variety of frequencies are a defining characteristic of noise signals. They may be removed by using bandpass filters, similar to those used in radio receivers, which would pass the intended signal but reject everything else, including the noise content.

We all communicate regularly over the phone with our friends and family. They often reside in a different city or nation, necessitating the need for pricey communication methods to talk with them. Even the extremely wealthy would never be able to afford a phone call if these channels were only able to convey a single voice, as they were in Alexander Graham Bell's day. Our capacity to transmit hundreds of talks across a single communications channel is what makes long-distance calls economical. And to do this, a communications method known as a frequency-division multiplex (FDM) is used. A basic representation of this kind of system is shown. An FDM communications system functions as follows:

1. Using a technique called modulation, the various speech signals are overlaid on various carrier frequencies at the transmit end.
2. An adder circuit is used to mix the various carrier frequencies.

3. Bandpass filters are used at the receiving end to isolate the carrier frequencies.
4. Demodulation is then used to separate the voice signals from the carrier frequencies.
5. The voice signals are sent to the proper individuals through local phone connections.

The transmit part of the aforementioned system shifts each voice signal's frequency spectrum by the frequency of the carrier by adding the frequency of a specific carrier to the frequencies of each voice signal. This creates the composite signal $g(t)$, also known as a group by telephone engineers, by contiguously arranging the frequency spectra of the several speech signals one after the other. Shows the frequency spectrum of the function $g(t)$. The translated speech signals are separated and their native spectrums are restored in the receive portion, on the other hand.

The foregoing system needs as many bandpass filters as there are voice signals, as shown in additionally, the system has an equal number of modulators and demodulators, each of which requires a specific amount of filtering to function properly. In other words, filters are a need for communications networks. In addition, several groups may be further modulated independently and combined to create a supergroup, as shown in to enhance the number of speech signals sent via, for instance, an interstate cable or microwave connection. A bank of bandpass filters at the receiving end divides a supergroup into separate groups, which are subsequently split into individual voice signals by the proper banks of bandpass filters. Similarly, a master group may be created by combining many supergroups and so on, until the cable or microwave link's bandwidth is fully used.

Due to the sampling theorem, it is crucial to remember that the sampling frequency must be at least twice the highest frequency present in the signal spectrum when developing a sampling system like the one shown. It is essential to bandlimit the signal to be sampled in cases where the sampling frequency is fixed and the highest frequency contained in the signal might exceed half of the sampling frequency to avoid aliasing-related signal distortion. A lowpass filter may be used to perform this bandlimiting procedure, which entails deleting signal elements whose frequencies are higher than half the sampling frequency.

Continuous-time signals are often transformed back to discrete-time signals. As an example, the signal stored on a CD is a discrete-time signal. A CD player's job is to perform the sampling process in reverse, as shown in, which requires it to read the discrete-time signal, decode it, and then replicate the original continuous-time audio signal. A lowpass filter may be used to rebuild the continuous-time signal, as will be shown. The behaviour of loudspeaker systems is extremely similar to that of filters, and as a result, they often alter the spectrum of an audio signal. This is because the audio signal might often experience mechanical resonances that are overlaid on the enclosure's or cabinet's usage.

This is also one of the reasons why various loudspeaker system brands often generate their distinctive sound, which is different from the sound captured on the CD. Sound reproduction devices like CD players and stereos often come with equalisers that may be used to alter the audio signal's spectrum to correct for these flaws. These subsystems often have a variety of sliders that may be changed to alter the sound reproduction quality. For instance, the audio signal's low-frequency or high-frequency (bass or treble) content may be made stronger or

weaker. Equalizers are filters in the sense of the larger term used before since they are devices that can alter the spectrum of a signal. The sliders work by changing the filter's settings, which equalises the sound [9], [10].

The acoustics of the space might also be taken into account. For instance, if the room has a thick carpet, it could be necessary to slightly increase the treble since the carpet would likely absorb a lot of the high-frequency information. The spectrums of the signals conveyed across transmission lines, phone wires, and communication channels often act very much like filters as a consequence of this behaviour. Local telephone lines are renowned for this in particular. Only because the signal's spectrum has been greatly changed do we often not identify the other person's speech. The quality of transmission over communication channels may be enhanced, much as with loudspeaker systems, by utilising the right equalisers. In reality, high data transfer rates over local telephone lines are only conceivable with the usage of equalisers. The modems at each end of a phone line have sophisticated equalisers built into them to do this. Figure 1 discloses the Mobile Terminal and the LO laser and Wave form.

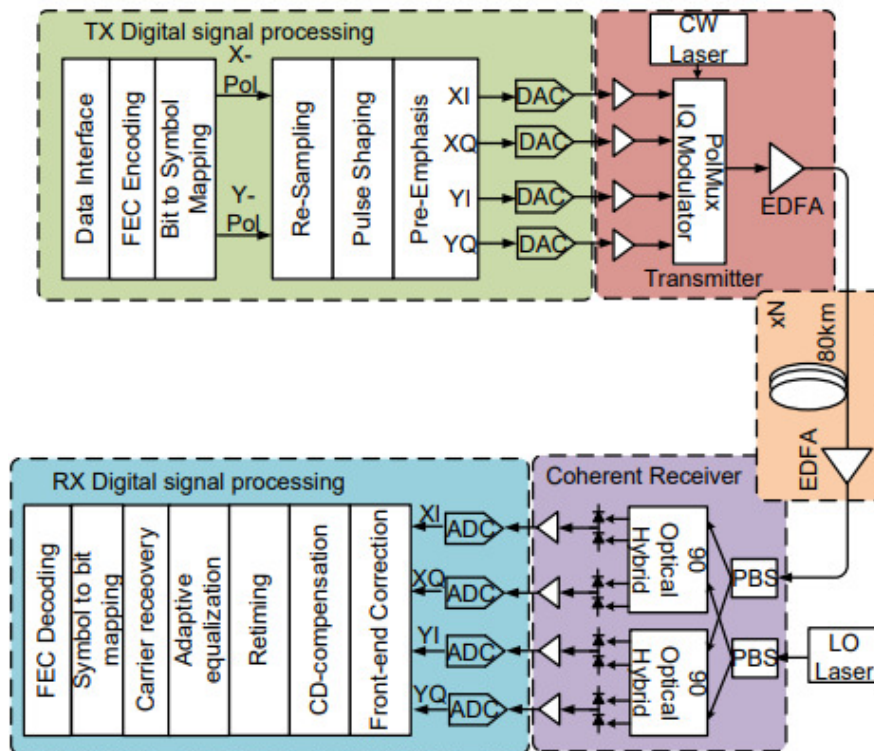


Figure 1: Discloses the Mobile Terminal and the LO laser and Wave form.

A digital filter is, in its most basic form, a device that, as shown in, will accept input in the form of a discrete-time signal and will output another discrete-time signal. This category includes a wide variety of discrete-time systems, including encoders, decoders, and digital control systems. The kind of processing done distinguishes digital filters from other digital systems. The output signal's spectrum must follow some law of correspondence with the input signal, much as in analogue filters. Digital filters have their earliest historical origins in the 1600s when

mathematicians were working to derive formulae for the areas of various geometric forms and astronomers were working to explain and interpret their observations of planetary orbits. In those days, there was a need for a method that could be applied to interpolate a function represented by numerical data. Formulae that conduct numerical differentiation or integration on a function represented by numerical data may be created using interpolation formulas. During the seventeenth and eighteenth centuries, these formulae were effectively used to build mathematical, scientific, nautical, and it is based on numerical formulas that his machines were supposed to perform their computations. Babbage was motivated by the great need for accurate numerical. If a numerical procedure is used to determine the derivative of a signal at $t = t_1, t_2, \dots, t_K$, and suppose that the signal is represented by its numerical values $x(t_1), x(t_2), \dots, x(t_K)$. In this case, the algorithm accepts a discrete-time signal as input and outputs a discrete-time signal that differs from the original signal. As was previously shown, differentiation is a filtering process, hence an algorithm that does numerical differentiation is a digital filtering process.

The current digital computer is the ideal environment for numerical approaches, and during the 1950s and 1960s, significant progress was made in the creation of algorithms that may be used to analyse signals that are represented as numerical data. By the late 1950s, pioneers like Blackman, Bode, Shannon, Tukey and others had contributed to the development of a coherent group of methods known as data smoothing and prediction. The term "digital filter" first appeared in the literature in the early 1960s to designate a group of algorithms that might be used for spectrum analysis and data processing. In his foundational book on the topic

Blackman detailed the state-of-the-art in the field of data smoothing and prediction and included a few methods he referred to as numerical filtering. In less than a year, in 1966, Kuo and Kaiser co-wrote the seminal chapter "Digital Filters" in which he described a range of signal processing methods that could be used for the modelling of dynamic systems and analogue filters. Digital signal processing, which started to gain traction in the late 1960s, is the analysis and processing of signals that take the form of numerical data, and it includes techniques, computer programmes, and systems that may be utilised to do so. With the explosive development of integrated circuit technology in the 1960s, a movement towards digital technologies emerged to benefit from the traditional advantages of digital systems generally, which are as follows:

- a. Tolerances for components are not important.
- b. High accuracy.

Component drift is comparatively insignificant, reliability is excellent, physical size is minimal, and electrical ambient noise has a low impact. Digital technology may be utilised to develop systems that are trustworthy, adaptable, and economical because of these crucial characteristics. As a result, starting in the early 1960s, there was a continual evolution or maybe a better term would be a revolution where analogue systems were constantly replaced by comparable digital systems.

Pulse-code modulation was used to digitise the telephone system first, followed by long-distance digital communications, and subsequently, digital audio cassettes and compact discs were used in

the music business. High-definition digital TV and digital radio have only just started to enter the market. Even the film business has started a massive automation of the filmmaking process.

As digital filter research progressed over time, a wide range of filter families emerged, including the following: Nonrecursive, recursive, fan, two-dimensional, adaptive, multidimensional, and multi-rate filters are only a few examples of filters. Digital filters are used for a variety of things, including but not limited to instrumentation, image processing, image enhancement, processing of seismic and other geophysical data, processing of biological signals, artificial cochleas, speech synthesis, audio systems, including CD players, and communications systems

Nowadays, it is simple to think of computer programmes and digital hardware that are capable of digital filtering as two separate digital filter implementations, i.e., software and hardware. Software digital filters may be developed using a low-level language on a general-purpose digital signal-processing device or a high-level language on a personal computer or workstation, such as C++ or MATLAB. At the opposite end of the spectrum, hardware digital filters may be created utilising a variety of intricately coupled VLSI processors. Real-time or nonreal-time (recorded) signals can be processed by both hardware and software digital filters, however, the former is often quicker and can handle real-time signals whose frequency spectrums reach far higher frequencies. Digital filters are sometimes employed in so-called quasi-real-time applications, where the processing seems to a human to be in real-time but is really done by collecting and storing samples of the signal in digital memory, retrieving them in blocks, and then processing them. Radio signal transmission via the Internet is a well-known, quasi-real-time application. These signals are sporadically sent by data packets. However, the only reason the music seems to be playing continuously is that the data packets were correctly saved before being sequenced. This explains why the transmission starts a bit slowly.

In addition to the traditional advantages of digital systems in general, hardware digital filters provide a significant advantage over analogue filters. A digital filter's settings may be quickly modified in real time since they are stored in computer memory. This indicates that applications requiring programmable, time-variable, or adaptive filters are better suited for digital filters. They do, however, have some significant limits. A digital filter computes a sequence of values using some of the input signal values and maybe some of the output signal values to produce the value of the output signal at any instant, let's say $t = nT$. Once the sampling frequency, f_s , and sample period, $T = 1/f_s$, are determined, a fundamental restriction is placed on the amount of computation that the digital filter may carry out during period T . As a result, T decreases as the sampling frequency rises, which in turn reduces the amount of computing that can be done per period T . Eventually, a digital filter will experience computation boundness and malfunction at a sufficiently high sampling frequency. In practise, digital filters are appropriate for low-frequency applications with operating frequencies that fall within a certain range, such as 0 to \max . The maximum frequency of application, \max , is challenging to define since it relies on a variety of variables, including the speed and competence of the digital hardware for number-crunching and the difficulty of the associated filtering jobs. Figure 2 discloses the Mobile Terminal and the TX Digital Signal Processing.

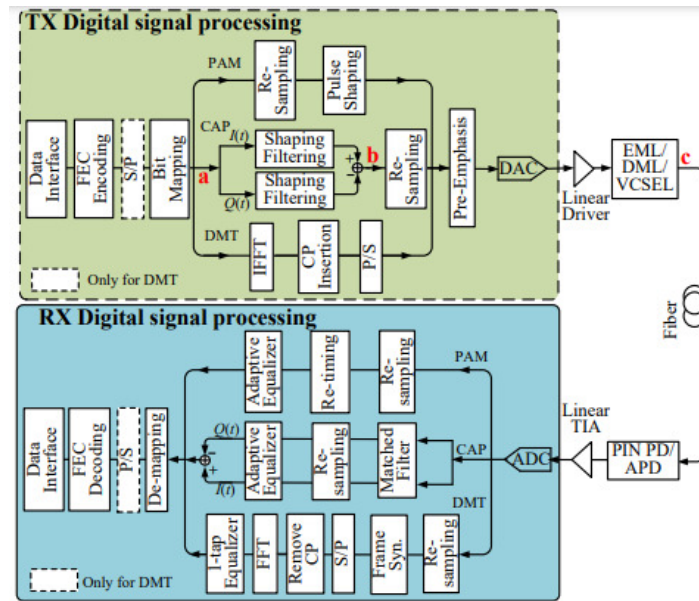


Figure 2: Discloses the Mobile Terminal and the TX Digital Signal Processing.

When the signal is in continuous-time form and a processed version of the signal is needed, also in continuous-time form, this is when a fundamental restriction of digital filters comes into play. The signal has to be transformed into a discrete-time form in this case, processed by a digital filter, and then transformed back into a continuous-time form. Due to the two conversions needed, different interface devices, such as A/D and D/A converters, would be required, and a digital filter solution may become prohibitively expensive when compared to an analogue filter solution. Naturally, if we begin with a digital system in which the signals to be processed are already in discrete-time form, this restriction is not present.

The frequency range for which the different kinds of filters are applicable is summarised. As can be shown, digital filters are most likely to provide the optimum engineering solution for frequencies under, say, 20 kHz, but microwave filters are a clear option for frequencies beyond 0.5 GHz. The selection of filter technology for frequencies between 20 kHz and 0.5 GHz relies on a variety of variables and trade-offs, and it also heavily depends on the kind of application.

To wrap up this section, it should be noted that software digital filters are the sole option for non-real-time applications since there is no analogue to them. The processing of electrocardiogram (EKG) signals, the processing of stock exchange data, and the processing of DNA and protein sequences are three common applications of filtering that are covered in this section. The EKG of a healthy person takes on a pretty well-defined shape, however, considerable variances might exist between individuals, much like fingerprints. However, certain telltale EKG patterns allow a cardiologist to identify particular heart diseases or disorders.

A pair of electrodes linked to specific, well-defined sites on the body and coupled to an electrical device called an electrocardiograph to produce a low-level electrical output that is represented by an EKG as a graph. These devices are employed in clinics and hospitals together with a wide

variety of other electrical devices including x-ray equipment and electric motors. The electrical 60-Hz noise produced by all of this equipment, coupled with the power cables and transformers that provide them with energy, might taint an EKG signal. A typical EKG signal without any noise is seen. As can be observed, the distinctive characteristics of the EKG are almost completely lost in the tainted signal, making them difficult, if not impossible, to distinguish. Such an EKG would be unreliable for a diagnosis.

Since the power supply's electrical noise has a well-defined frequency, namely 60 Hz, one may construct a bandstop filter to reject the electrical noise. Using the techniques that will be covered in subsequent chapters, such a filter was created and then applied to the tainted EKG data. As can be seen, the filtered signal is an accurate representation of the original noise-free signal except for a few transient artefacts across the range $n = 0$ to 100. In a different experiment, the tainted EKG data was sent through a bandpass filter that was intended to pick out the 60-Hz noise component to demonstrate the nature of filtering. The bandpass filter's output is shown. The bandpass filter isolates a continuous noise component after initial transience across the range $n = 0$ to 150. This is a sinusoidal waveform. There are only six samples every cycle with approximate values of 0, 1.7, 1.7, 0, 1.7, and 1.9, so it doesn't seem to be the case.

For a variety of reasons, the state of the market interests us all. For instance, we would all want to save away some money for a rainy day, and we would all naturally prefer to invest any such money in safe, low-risk equities, bonds, or mutual funds that provide good returns. We study the business section of our daily newspaper or search the Internet for numerical stock-exchange statistics before making judgements of this kind of constant pace, never losing value. In reality, though, things don't work out that way. Stock prices fluctuate quickly over time, and sometimes, such as during a market slump, they may even lose a significant amount of their worth. Figure 3 discloses the Mobile Terminal and the TX Digital Signal Processing with Electrical Spectrum.

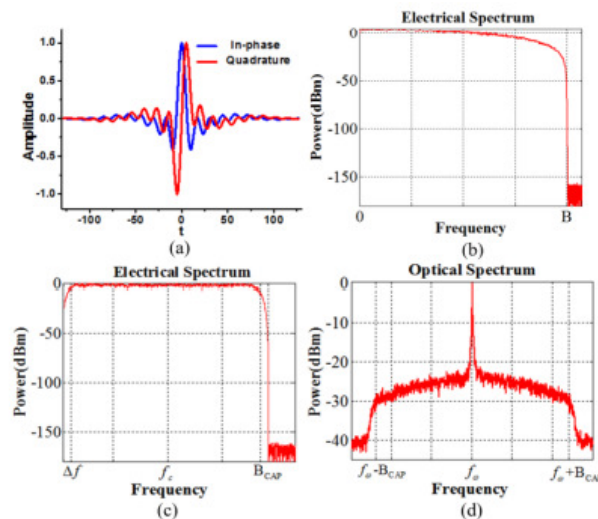


Figure 3: Discloses the Mobile Terminal and the TX Digital Signal Processing with Electrical Spectrum.

The value of stock often fluctuates due to a variety of economic factors. While some of these causes are transient, others are the result of enduring economic pressures. As long-term investors, we may choose to disregard daily fluctuations and concentrate as much as we can on the fundamental shifts in stock price. Simply analysing the accessible stock exchange data of two competing stocks may allow an astute investor to reach a judgement. This is not a simple process for the majority of us. However, as will be seen in the example that follows, the work may be much reduced by using DSP.

Since the price of a company's stock is a signal, filtering may be used to change its spectrum. The high-frequency portion of the spectrum represents the daily fluctuations in stock, whilst the low-frequency portion represents the stock's underlying trend. Maybe we should filter away the high-frequency portion of the spectrum if we are interested in a stock's long-term performance. On the other hand, if we are unable to accept significant daily fluctuations, we could want to evaluate the stock's volatility. Volatility indicators are easily accessible, such as a stock's standard deviation. To analyse the volatility might be another method. Data processing for stock exchanges: Bond and high-tech mutual fund unit values, as well as data that has been lowpass filtered. Using a highpass filter, a stock's low-frequency material is eliminated while its high-frequency content is kept.

Two real mutual funds, a bond fund and a high-tech fund were arbitrarily selected for processing to serve as examples for these concepts. The scaled share prices of the two funds were normalised to one at the beginning of the year to make the comparison easier. One year's worth of data was picked for processing a display of the normalised share prices for the two funds. As can be seen, the high-tech fund had significant fluctuations during the year, in contrast to the bond fund, which has stayed rather constant throughout the year as planned. The high-frequency composition of the daily changes in the two mutual

A lowpass filter may be used to exclude money and produce slick curves. On the other hand, the low-frequency spectrum or the mutual fund's underlying trend may be eliminated using a highpass filter to produce the high-frequency material. The filter output is shown in this figure as a percentage of the unit value. Some oddities are seen in the charts within the first 50 or so sample values. These are brought on by certain initial transient circumstances that are present in all sorts of systems, including filters, although they may be avoided in practise by employing appropriate initialization. Ignoring this first stage, lowpass-filtered representation of the data offers a less crowded perspective of the funds and provides a much clearer representation of their relative volatilities. In this regard, see how the size of the y-axis differs between the two funds by a ratio of 5 to 1.

It also is used to derive quantitative measures of volatility that are comparable to the standard deviation of a stock. For instance, the average of $|y(n)|$ or any other norm might be obtained. The mean-square average (MSA) of $y(n)$ is defined as $MSA = \frac{1}{N} \sum_{n=1}^N [y(n)]^2$. For values of $50 \leq n \leq 250$, it is simple to calculate the MSA values for the bond and high-tech funds as 0.0214 and 1.2367, respectively. This results in a ratio of 1 to 57.7 in favour of the bond fund. The message on the kind of fund one should purchase to prevent restless nights is pretty apparent. Figure 4

discloses the Mobile Terminal and the TX Digital Signal Processing with Electrical Spectrum frequency.

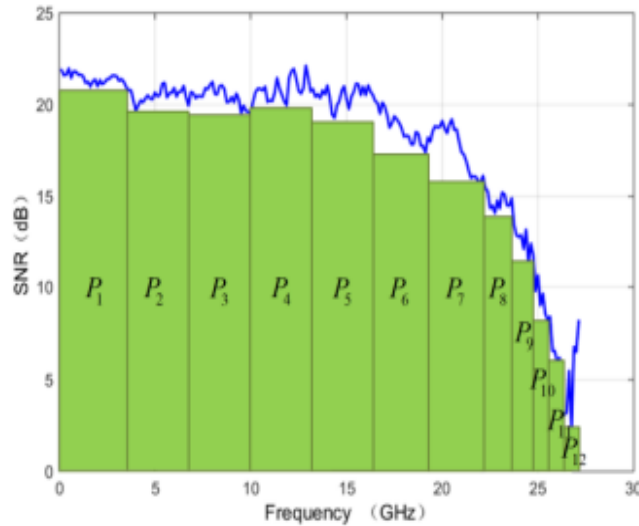


Figure 4: Discloses the Mobile Terminal and the TX Digital Signal Processing with Electrical Spectrum frequency.

The usage of extrapolation filters is another fascinating approach that ought to be mentioned. These kinds of filters may be used to forecast stock values for the future, but if we go deeper into the topic, we enter the territory of what is known as technical analysis in the business world. Processing of DNA and Protein Sequences, significant progress has been made in the study of these long string-like biological molecules in recent years. It did not take long for these sequences to become amenable to numerical and computational methods. It is commonly known that the smaller molecules known as nucleotides act as rungs to hold the DNA double helix together in a configuration resembling a ladder. DNA sequences include four different kinds of nucleotides, namely adenine, guanine, thymine, and cytosine, which are often denoted by letters.

Directed Energy Weapon Systems

High-energy lasers (HEL), charged particle beams (CPB), neutral particle beams (NPB), and high-power microwaves are four examples of directed energy weapons (HPM). These weapons often attack at the speed of light, which is their most prominent feature. This aids in taking down targets like theatres and ballistic missiles before they can use submunitions that overwhelm defences. Such weapons also have the benefit of being able to simultaneously engage many targets. HEL systems, out of all four weapon types, offer the most possibilities for military technological advancement to be used in tactical and strategic warfare applications. Although HPM technology, which would serve as the foundation for the planned e-bomb in this research, has comparable potential, its development seems to be lagging behind that of lasers since it has

not received as much funding. Particle beam weapons, however, remain the stuff of science fiction since they are too heavy and expensive to be weaponized [11]–[13].

Since pilots may increase their survivability on the battleground, where the warplanes are weak and vulnerable to warhead threats, by shielding themselves with electromagnetic fields, DEWs offer significant promise for aviation operations. By limiting the enemy's ability to identify and target the aircraft in such a circumstance, DEW systems may shield the aircraft from danger. By deflecting, blinding, or causing the approaching missile to lose lock, they may also assist in hit avoidance. If required, they may even end up destroying the missile itself before it approaches its target. Destroying the approaching missile's fusing mechanism can be another strategy. Directed energy weapons still have two key issues in common [14], [15]. The term "getting the projectile to effectively travel a functional distance and reach the target" and the phrase "create meaningful damaging effects" are used to describe these issues.

Electronic weapons

High Altitude Electromagnetic Pulse (HEMP), High Power Microwave (HPM) Weapons, and Electromagnetic Bombs are the three electromagnetic weapons that will be defined in this research (e-bomb). Although the technology behind e-bombs and HPM weapons may be deemed to be similar, this research will proceed on the assumption that the two weapons' modes of delivery make them distinct. HEMP isn't a weapon that uses focused energy. Due to its comparable effects on the electromagnetic spectrum and potential effects on electrical equipment, HEMP is classified as an electromagnetic weapon.

A nuclear explosion's radiation causes an immediate electromagnetic energy field known as a high-altitude electromagnetic pulse (HEMP) to be created in the upper atmosphere. The detonated altitude and framework used to evaluate the nuclear bomb determine the possible impact of HEMP on electrical equipment across a very large region. As stated in the description of HEMP, HEMP can only be created by a nuclear weapon explosion that occurs far above the Earth's surface. Gamma radiation is produced in this way, interacting with the atmosphere to create an instantaneous, intense electromagnetic energy field that can overload computer equipment with effects similar to, but much more quickly causing damage than, a lightning strike. This electromagnetic energy field does not harm people as it radiates outward from the burst.

E-bomb usefulness will be assessed in contrast to HPM and HEMP in subsequent sections the e-bomb is referred to as a kind of electromagnetic pulse weapon in this research. Even though the e-technical bomb's characteristics are based on HPM technology, its distribution method is different from HPM's. After HPM and High Altitude Electromagnetic Pulse, the e-bomb will be considered the third electromagnetic weapon to better comprehend its military value and demonstrate its benefits and drawbacks (HEMP). The justification is provided by apparent parallels between these technologies and by the lack of any open-literature e-bomb data.

A series of numbers that are instantaneously created by somehow assigning numbers to a DNA sequence is not all that dissimilar from the series of numbers produced by sampling an electrical signal. The primary constituents of life, proteins, are composed of chains of other organic

molecules known as amino acids. Only 20 of the theoretically potential many different amino acids are typically present in the proteins of living things. An amino acid sequence may serve as a unique representation of a protein, and by somehow allocating numbers to a protein sequence, a discrete-time signal can be produced.

Sequences of DNA and proteins exhibit a wide range of traits, attributes, and physical properties. Exons and hot spots are a few of them. These are areas of the DNA and protein sequences, respectively, that are very important to how DNA and protein molecules work. While exons carry the DNA instructions for generating proteins, hot spots give the majority of the binding energy for protein-target interactions. As a result, precisely identifying and pinpointing exons and hot spots in DNA and protein sequences is an essential task that may help us better understand how DNA and protein sequences work and how they are interdependent. Figure 5 discloses the Mobile Terminal and the TX Digital Signal Processing with Electrical Spectrum frequency receiver sensitivity.

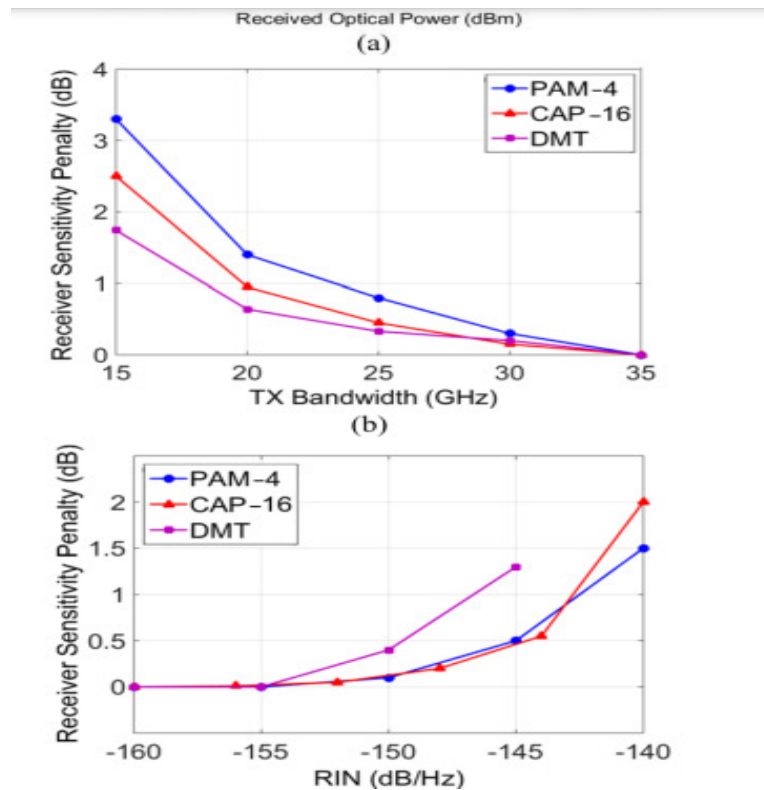


Figure 5: Discloses the Mobile Terminal and the TX Digital Signal Processing with Electrical Spectrum frequency receiver sensitivity.

Experimentation was used in wet labs in the past to pinpoint the positions of exons and hot spots in DNA and protein sequences, which added time and expense to the process. In recent years, a variety of computational algorithms have been developed for the identification of exons and hot spots to lower costs, increase efficiency, and enable the large-scale application. The usage of a

filter-based method. Using known numerical values of the so-called electron-ion interaction potential (EIP) associated with amino acids, the input block converts a sequence of amino acids that make up a protein, designated as $p(n)$, into a sequence of numbers $x(n)$. This is done in the case of the location of hot spots in protein sequences.

REFERENCES:

- [1] T. Al Abbas, N. A. W. Dutton, O. Almer, N. Finlayson, F. M. Della Rocca, and R. Henderson, "A CMOS SPAD Sensor with a Multi-Event Folded Flash Time-to-Digital Converter for Ultra-Fast Optical Transient Capture," *IEEE Sens. J.*, 2018, doi: 10.1109/JSEN.2018.2803087.
- [2] Y. Wang, Q. Cao, and C. Liu, "A multi-chain merged tapped delay line for high precision time-to-digital converters in FPGAs," *IEEE Trans. Circuits Syst. II Express Briefs*, 2018, doi: 10.1109/TCSII.2017.2698479.
- [3] Y. H. Chen, "Time resolution improvement using dual delay lines for field-programmable-gate-array-based time-to-digital converters with real-time calibration," *Appl. Sci.*, 2018, doi: 10.3390/app9010020.
- [4] T. Polzer, F. Huemer, and A. Steininger, "Refined metastability characterization using a time-to-digital converter," *Microelectron. Reliab.*, 2018, doi: 10.1016/j.microrel.2017.11.017.
- [5] J. P. Caram, J. Galloway, and J. S. Kenney, "Time-to-Digital Converter with Sample-and-Hold and Quantization Noise Scrambling Using Harmonics in Ring Oscillators," *IEEE Trans. Circuits Syst. I Regul. Pap.*, 2018, doi: 10.1109/TCSI.2017.2712518.
- [6] B. Wu, S. Zhu, Y. Zhou, and Y. Chiu, "A 9-bit 215 MS/s Folding-Flash Time-to-Digital Converter Based on Redundant Remainder Number System in 45-nm CMOS," *IEEE J. Solid-State Circuits*, 2018, doi: 10.1109/JSSC.2017.2782766.
- [7] J. Zhang *et al.*, "A Time-to-Digital Converter-Based Correction Method for Charge Measurement Through Area Integration," *IEEE Trans. Nucl. Sci.*, 2018, doi: 10.1109/TNS.2018.2878721.
- [8] P. Chen, X. Huang, Y. Chen, L. Wu, and R. B. Staszewski, "An on-chip self-characterization of a digital-to-time converter by embedding it in a first-order $\Delta\Sigma$ Loop," *IEEE Trans. Circuits Syst. I Regul. Pap.*, 2018, doi: 10.1109/TCSI.2018.2857999.
- [9] H. Wang, F. F. Dai, and H. Wang, "A Reconfigurable Vernier Time-to-Digital Converter with 2-D Spiral Comparator Array and Second-Order $\Delta\Sigma$ Linearization," *IEEE J. Solid-State Circuits*, 2018, doi: 10.1109/JSSC.2017.2788872.
- [10] A. I. Hussein, S. Vasadi, and J. Paramesh, "A 450 fs 65-nm CMOS Millimeter-Wave Time-to-Digital Converter Using Statistical Element Selection for All-Digital PLLs," *IEEE J. Solid-State Circuits*, 2018, doi: 10.1109/JSSC.2017.2762698.
- [11] O. S. Oladejo, A. O. Abiola, A. A. Olanipekun, O. E. Ajayi, and A. O. Onokwai, "Energy Potential of Solid Waste Generated in Landmark University, Omu- Aran, Kwara State Nigeria," *LAUTECH J. Civ. Environ. Stud.*, 2020, doi: 10.36108/laujoces/0202/50(0150).

- [12] S. E. Mace and A. Sharma, "Hospital evacuations due to disasters in the United States in the twenty-first century," *Am. J. Disaster Med.*, 2020, doi: 10.5055/ajdm.2020.0351.
- [13] R. L. Murray and K. E. Holbert, "The History of Nuclear Energy," in *Nuclear Energy*, 2020. doi: 10.1016/b978-0-12-812881-7.00008-3.
- [14] C. F. Waythomas, M. Loewen, K. L. Wallace, C. E. Cameron, and J. F. Larsen, "Geology and eruptive history of Bogoslof volcano," *Bull. Volcanol.*, 2020, doi: 10.1007/s00445-019-1352-3.
- [15] E. E. Lower-Spies, N. M. Whitney, A. D. Wanamaker, S. M. Griffin, D. S. Introne, and K. J. Kreutz, "A 250-Year, Decadally Resolved, Radiocarbon Time History in the Gulf of Maine Reveals a Hydrographic Regime Shift at the End of the Little Ice Age," *J. Geophys. Res. Ocean.*, 2020, doi: 10.1029/2020JC016579.

CHAPTER 9

HIGH-POWER MICROWAVE WEAPONS

Dr. Rahul Kumar, Assistant Professor

Department of Mechanical Engineering, Sanskriti University, Mathura, Uttar Pradesh, India

Email id- rahulk.oeit@sanskriti.edu.in

Numerous societies researching the creation of coherent electromagnetic radiation with frequencies between 1 GHz and above 100 GHz utilise the ambiguous term "high power microwave" (HPM). High-average-power microwaves, which denote lengthy pulse duration, high repetition rate, or continuous beam source, are one way to interpret the word. High-peakpower microwaves are another interpretation, which denotes a source with a single, brief pulse with a low repetition rate. The characteristics of HEMP and lightning are included in HPM in this thesis. This is done on purpose to take advantage of the wealth of information on these two powerful electromagnetic hazards. The different electromagnetic hazards will be compared as relevant to highlight their inherent distinctions.

High-power microwaves (HPM) that operate in a single shot or with tens or hundreds of Hz repetition rates are being developed in several nations. Along with their frequency flexibility, they have also attained a power level in the GW range. The use of HPM technology as a weapon for defence has piqued military attention since the power levels of HPM sources were increased to GW levels. The potential for such applications to interfere with or even destroy the electrical systems of offensive weapons like missiles was recognised. Unlike linear-beam tubes like the klystron, the magnetron is a self-contained microwave oscillator that functions differently. The magnetron uses crossed electron and magnetic fields to provide the high output necessary for radar and communications devices. Since the magnetron tube was developed earlier than the klystron, it is more often employed in power oscillator applications. 100-MW pulsed magnetrons and klystrons were made commercially accessible in the late 1970s [1]–[3].

However, a commercially viable relativistic magnetron source in the L band with a peak output of 1.8 GW is currently available. Gyrotrons a novel form of millimeter-wavelength microwave device is the gyrotron. The electron beam used in these devices is typically formed into a thin, hollow cylinder and directed into a high axial magnetic field inside of a circular cylindrical cavity. Gyrotron oscillators have been claimed to produce output outputs of up to 800 MW at 7.5 GHz, 350 MW at 15 GHz, and 8 MW at 37.5 GHz while operating in pulse mode [4], [5].

The virtual cathode oscillator, also known as the vircator, is a powerful source that can operate at frequencies between a few hundred megahertz and tens of gigahertz. Up to 20 GW of output from the vircator have been recorded. One may create pulses with lengths ranging from 10 to several hundred nanoseconds. Although there are other elements at play, the electrical pulse driving the anode typically controls the pulse duration. In terms of utilisation in munition applications, the Vircator is the best suitable HPM source. Due to its straightforward construction, low cost of manufacture, and ability to produce tens of Gigawatts of power, electromagnetic weapon researchers are very interested in this technology.

Up to the 1980s, several HPM technology experts have contemplated utilising microwave radiation both as a weapon and for communications and detection. The deployment of HPM technology as a weapon was not in the analysts' best interests since the damage thresholds of typical electronic equipment were high in comparison to the available microwave output power (kilowatts) at the time. Then, this view was altered by two new technical developments. First, there was a real danger to military equipment from the source growth of microwave power in the gigawatt range. Second, the military became more and more reliant on microelectronics, which were far more sensitive to big voltage transients than their predecessors at much lower power levels. Due to these two events, observers started to think that HPM would be crucial for the battlefield of the future given the fast advancement of pulsed power technology. These tools might be useful in conventional Electronic Warfare (EW) operations. They may be used as a jammer against enemy command and control systems and radar.

Hypothetical Electromagnetic Bomb

The idea behind HPM technology is first explained. The propagating pattern of the produced electromagnetic field is then defined and utilised to determine how well it can be approximated as a relation of range. The connection methods between the target system and the output of the HPM device are then specified. The effect on electronic systems is taken into account when the yield for the conception e-bomb from an HPM source is defined. Based on the well-known, publicly available threshold values for electronic systems, considerations are made. The prospective outcomes are examined, and a range of lethality for various targets is calculated. A model is utilised to simulate e-bomb impacts using HPM theory to help the interaction assessment. The model is then validated using published data for relevant systems. Finally, defense against e-bombs is taken into account, and the benefits and drawbacks of various e-bomb design elements are assessed in terms of their military value.

Particulars

A frequency range of 0.5 GHz to 3 GHz is used for our concept. Because radars, television broadcasts, and mobile communications involving aero planes and surface vehicles are heavily concentrated in the ultrahigh-frequency (UHF) zone between 300 MHz and 3 GHz, this range was chosen. Collateral impacts on critical civilian systems are undesirable in the majority of military operations contexts and should be avoided.

A suitable rectangular waveguide is selected for the required frequency range. If more than one waveguide is available that is suitable for the requested frequency range, the larger waveguide is selected since it offers a stronger field in the distant field. Additionally, the waveguide's field intensity is kept relatively low, preventing it from exceeding the atmospheric breakdown limit and causing ionisation rather than propagation [4]–[6].

The user will choose the frequency (f) and pulse width (τ) of the microwave signal for the simulation model. To compare the various classes of e-bombs in a pertinent yet meaningful way, the default pulse width for the research is 100 nanoseconds (ns). From the perspective of interactions, 100 cycles should be sufficient to ring up the majority of system resonances at

frequencies at or above 1 GHz. This will lead to a steady-state maximum signal (voltage or current) at the failure port.

The moderately e-bomb, as described in this thesis, calls for considerably more complex parts, such as commercial radar systems that can be converted into weapon systems like e-bombs, as well as the expertise of a skilled electrical engineer. For the simulations, it will be considered that systems with moderately protected defences will be targeted by medium-tech moderate e-bombs. For moderately protected systems, a 30 dB shielding efficacy is taken into consideration. An excellent example of a moderately insulated system, one that could have around 30 dB of shielding, is a civil aviation aeroplane.

It is well known that electromagnetic pulses with enough power between 200 MHz and 5 GHz may harm many different systems' electronic components. Due to their widespread application to common radar and telecommunication technology that are comparable in form, 1.2 GHz and 1.7 GHz were selected as the operating frequencies for the modelling of medium-tech e-bombs [1]–[3].

The range of moderate power levels is between 1 and 20 MW. To determine the best charging station and operating frequency, a range of 1 to 20 MW for the average power will be examined. Additionally, there are commercially available radar installations that operate in the frequency bands of 1.2 GHz and 1.7 GHz and emit radiation with an average output of up to 20 MW, the matching rectangular waveguides for the medium-tech e-bomb are designated as WR770 for 1.2 GHz frequency and WR650 for 1.7 GHz frequency. The greatest output from the two will be designated as the medium-tech (moderate) e-bomb for the examination of the possibly fatal impact on various systems after considering the discharges of each frequency choice of the moderate e-bomb.

High-Tech (Powerful) E-Bomb

More advanced high-tech electromagnetic devices would undoubtedly need specialised and advanced technology, maybe even output that was specially calibrated to do catastrophic harm to a particular target. It will be assumed for the e-bomb simulation that highly sophisticated (potent) e-bombs will be employed against completely insulated systems. For completely protected systems, a shielding efficacy of 40–50 dB is expected. An excellent example of a completely protected system is a military system, which is purchased with shielding specifications to carry out intended duties.

Following Giri's pioneering work, 2 GHz is selected as the operating frequency for high-tech (powerful) e-bombs. High power levels may vary from a few hundred megawatts (MW) to gigawatts (GW). To evaluate the impact of a potent e-bomb on the target systems, a 20 GW source will be employed for the average power. Benford reported a 20 GW vircator emitter in 1987. Technology has advanced over the last 20 years, and more power can now be produced in an acceptable, small footprint. One may simply consider the consequences of a potential lethality level achieved by present technology after the lethality produced by 20 GW sources has been evaluated [1]–[3].

Estimates Coupled

Under electromagnetic irradiation of sufficient intensity, all electronic equipment is prone to faults and long-term damage. The connection of external fields to electrical circuits and the accompanying sensitivity properties determine the intensity level for system vulnerability.

When an illuminating electromagnetic field produces current and charges in the network resources and services required computer chips at levels that are equivalent to the typical operating signals, a transient malfunction (or upset) might happen. When these produced stresses reach levels that cause thermal damage to the point of joule heating, permanent damage may result often ranging from 600 to 800 degrees Kelvin. When determining how much power is done in conjunction into target systems, two primary coupling patterns are acknowledged in the literature regardless of the kind of e-bomb utilised or the power/frequency/mode applied:

- Front Door Connector
- Back Door Connector

Although both coupling processes are described here, only the back door interfacing will be used in the computer to determine the lethality of three hypothetical classes of e-bombs. It may be anticipated that, in practice, higher susceptibility can be attained than the susceptibility revealed in this work since front door coupling naturally delivers more energy into the operating system than the energy given by rear door coupling. The target system will be considered to be in the primary lobe of the e-bomb antenna in all coupling estimations. The coupling efficiency will drop and the target will receive less power if it is in the multipath propagation or at random angles.

Front Door Coupling

When the power emitted from the e-bomb is directly linked to the electronic systems, which entail an antenna like radars, electronic warfare, or communications devices, front door coupling is commonly seen. The antenna subsystem is made to couple electricity into and out of the apparatus, creating an effective pathway for the electromagnetic weapon's power flow to enter the apparatus and do damage. Operating the e-bomb at the target system's in-band frequency may be useful if front door coupling needs to obtain admission via an antenna [4], [5], [7].

Back Door Connector

Back Door Coupling occurs when the electromagnetic field from bombs produces large transient currents through cracks, small apertures, and on fixed electrical wiring and cables interconnecting equipment, or providing connections to power mains or the telephone network also known as spikes when produced by a transient source or electrical standing waves when produced by an HPM weapon. Equipment linked to exposed cables or cabling may suffer either high voltage transient spikes or standing waves, which, if not insulated or fundamentally resilient, can harm power supplies and communications interfaces. Additionally, if the transient enters the equipment, other components within may suffer harm due to reciprocal interaction. Regardless of the reference images of the e-bomb, every cable may consist of many linear segments, which are often at nearly right angles. As a result, one or much more segments can

have extremely strong coupling efficiency. Network cables are highly effective in the propagation of such transients with little loss because they employ quick, low-loss dielectrics. Although back door coupling is often thought of as wideband, resonance effects may lead it to exhibit narrow-band properties.

Effects on Targets

The four degrees of damaging effects associated with e-bomb interactions with system electronics upset, lock-up, latch-up, and burnout and their corresponding conditions are as follows. These four possible outcomes of e-bombs on targets may be arranged into a hierarchy of lethality, each of which necessitates increased microwave emission on the target explained in the next paragraphs.

Soft-Kill

When a weapon's effects momentarily interrupt the functioning of the target system or equipment, it results in a soft kill. A computer system that resets or enters an unrecoverable or stuck state is an excellent illustration. The end effect is a brief interruption in function, which may drastically jeopardise the performance of any system that is very reliant on the in-issue computer system.

Soft death may have two different forms:

Anger

One or more nodes may get temporarily upset, which results in a change in their electrical state and the loss of their regular functionality. Upset refers to a specific interaction between a weapon and the target system's operational state at the moment; if the neural impulses, upsets may disappear. As long as the imposed radiation is there, the upset persists in the operational state. It is simple to return the afflicted system to its original state after the 54 signal has been eliminated. Lightning and equipment jamming are two instances of this kind of denial effect.

Arrest

Similar to upset, lock-up causes temporary changes to the electrochemical states of the afflicted nodes, but the functional changes persist even after the radiation has been eliminated. Lock-up causes a momentary modification similar to upset, but once the radiation is removed, functioning must be restored by an electrical reset, shut down, and restart. Degrading is an example that requires the involvement of an outside operator or unique safety precautions to reload the target system [4]–[6].

Hard-Kill

A hard kill occurs when a weapon's effects permanently electrically harm the target system or piece of equipment, making repair or replacement of that system or piece of equipment necessary. An example is a personal computer that sustains damage to its memory, peripheral ports, and power supply. Depending on the extent of the damage, the apparatus may or may not

be repairable; in this case, any system that is very reliant on this computer system may become unusable for a lengthy period. Hard kill comes in two varieties:

Latch-up

A severe kind of lockup known as latch-up occurs when parasitic elements get excited and address these concerns in relatively high levels until the node either self-destructs permanently or the power is cut off to the node. This impact may draw down completely supply voltages or deplete the batteries powering the afflicted nodes. Two latch-up instances are semiconductor devices failing to react to inputs or transistors malfunctioning on a circuit board as a result of radiation overloads [8], [9].

Damage or Burnout

A node is said to be damaged or burned out if it is electrically destroyed by a process like latch-up, metallization exhaustion, or junction burnout. Damage is often categorised according to its performance level because electrical overstress may lead to charge buildups in formation of a protective layers and dielectric layers that deteriorate over time. The most severe types of damage are often referred to as "permanent damage" or "electrical burnout."

When the high-power thermal processing melts conductors, capacitors, or resistors, damage or burnout results. Burnout often includes electrical arcing and happens at the junction area where many wires or a transistor's base collector or transmitter meet. As a result, the junction area alone experiences the warmth. An illustration of burnout is the result of a lightning strike on electronic equipment.

Potential Lethality of Hypothetical E-Bomb

Depending on the target hit, several types of interest e-bombs may be deadly. There are many types of targets:

1. Unshielded Systems
2. Systems with Moderate Shields
3. System Shielding in Full

In the interest of the low-tech (small) e-bomb, unshielded systems will be taken into consideration since they are completely exposed to the electric fields generated by radiating sources. Systems with 30 dB shielding are considered to be moderately protected systems. The interest of the medium-tech (moderate) e-bomb is civil aviation. Following the data and HIRF requirements, civil aviation may also be regarded as a system that is substantially insulated. Systems that are fully protected have a shielding efficacy of 40–50 dB.

Military systems are included in this category and serve the high-tech (potent) e-bomb. It is possible to use topological shielding, terminal protection devices, and filter isolation to guard against high-power microwave radiation. It may be used to provide any degree of exposure suitable hardening. However, when the incident fluence rises, it becomes harder to attain the necessary level of shielding [5], [6], [10].

If the e-bomb is successful, it will undoubtedly be a crucial component of electronic warfare (EW). One of the three EW divisions, Electronic Target, uses electromagnetic or directed radiation to attack people, places of business, or infrastructure to deteriorate their quality. The preceding sections have shown that even if electronic equipment is protected, such a weapon may most likely achieve power outputs that are greater than its estimated sensitivities levels. E-bombs can permanently harm an opponent's electronic equipment if they are deployed as intended on the battlefield. A successful e-bomb strike may also disrupt the adversary's systems, giving time for other capabilities to engage the opposing troops. An e-bomb strike may impair network operation if the opponent relies heavily on a network to sustain C4ISR (command, control, communication, computation, intelligence, surveillance, and reconnaissance). One can predict with certainty that an e-bomb will pose a significant danger to C4ISR on the future battlefield since the next generation of battlefields focuses on network-centric combat [11], [12].

As was seen in the preceding sections, even while a 50 dB shielding efficacy is attained, electronic equipment may still be at risk from e-bombs. Stronger protection will be offered by shielding efficacy that is 60 or 70 dB or higher. On the other hand, retrofitting outdated systems to this degree of hardening may not be feasible. They may need to be completely replaced. Simply put, it would be simpler, cheaper, and more effective to harden by design during the system acquisition phase than to try to harden the existing equipment. Even in this situation, the topological shielding idea as a whole may not always be the most economical choice. If hardening is included in the initial design, it would cost between 3% and 10% more to harden most military systems and mass-produced commercial equipment, such as PCs and communications equipment, against HPM. Hardening would increase the cost of current military electrical equipment by around 10%. Using passive electronic countermeasures like the low probability of intercept (LPI) methods might be a useful alternative to shielding for securing the systems. A notable illustration of these precautions is the new LPI radar technology. The opponent would have no visible target to fire an e-bomb against if it were possible to conceal the radar emissions from them.

DEFENSE AGAINST E-BOMB

Electronic equipment only within the lethality range may be permanently damaged or disturbed as a result of an e-bomb. Even when the electronic item is off, there is still a significant chance that it might because harm affected-bombs also fall under the general rule that the greatest defense against any armament is the destruction of the platform from which the projectile is delivered. However, this technique isn't always feasible or even readily implementable. Hardening seems to be the most effective defense against e-bombs in this situation the protection of electronic devices against microwave radiation.

E-bombs might be the first kind of weapon deployed against communication and air defence systems in the event of a conflict, according to the defense viewpoint. In such a situation, it is essential to be ready by strengthening all defensive countermeasures in advance of the assault. The best way to shield electronic equipment is to completely enclose it in a Faraday cage, an electrically conductive container that blocks the electromagnetic field from reaching the shielded equipment. However, even in this situation, as the majority of such equipment must be powered

by external sources, penetrations, cracks, scams, etc. lead to a vulnerability at the entrance points against an electromagnetic environment, such as that posed by e-bombs [13]–[15].

If the shielding efficiency rises to a point where the lethality range of an e-bomb is no longer justified, the opponent would no longer be wise to deploy one. The e-bomb source's strength is being increased as a counterattack for the shielding. The disintegration of the atmosphere, however, will eventually become a limiting issue for the construction of such a large capacity source-e-bomb. It is possible to use topological shielding, terminal protection devices, and filter isolation to guard against high-power microwave radiation. It could be utilized to provide a certain degree of exposure to suitable hardening. However, when the incident fluence rises, it becomes harder to attain the necessary level of shielding [3], [16], [17].

As was seen in the preceding sections, even while a 50 dB screening efficacy is attained, electronic equipment may still be at risk from e-bombs. Stronger protection will be offered by shielding efficacy that is 60 or 70 dB or higher. On the other hand, retrofitting outdated systems to this degree of hardening may not be feasible. They may need to be completely replaced. Simply put, it would be simpler, cheaper, and more effective to harden by design during the system maturation period than to try to adapt the existing facilities. Even in this situation, the topological shielding idea as a whole may not always be the most economical choice. If hardening is included in the initial design, it would cost between 3% and 10% more to harden most weapon satellites and mass-produced commercial equipment, such as PCs and communications equipment, against HPM. Hardening would increase the cost of current military electrical equipment by around 10%. Three different sorts of fictitious e-bombs have been suggested for this investigation.

Such a crude weapon idea would undoubtedly have drawbacks throughout the design and implementation stages. However, it is appealing to invest more time in investigating the military usefulness of such a firearm due to the anticipated benefits, as evidenced in the simulation findings. If the e-bomb is successful, it will undoubtedly be a crucial component of electronic warfare (EW). One of the three EW divisions, Electronic Target, uses electromagnetic or directed radiation to attack people, places of business, or equipment to deteriorate their quality. The preceding sections have shown that even if electronic equipment is protected, such a weapon may most likely achieve power outputs that are greater than its known susceptibility levels. E-bombs can permanently harm an opponent's electronic equipment if they are deployed as intended on the battlefield. A successful e-bomb strike may also disrupt the adversary's systems, giving time for many other assets to engage the opposing troops.

An e-bomb strike may impair network operation if the opponent relies heavily on a network to sustain C4ISR command, control, telecommunications, computer, intelligence, surveillance, and reconnaissance. One can predict with certainty that an e-bomb will pose a significant danger to C4ISR on the future battlefield since the next generation of battlefields focuses on network-centric combat.

Comparison of Weapons by Using Multiple Objective Decision Making

This chapter provides a formulation for the comparison of the three kinds of weapons (the HEMP, the HPM, and the e-bomb) using the data from the preceding chapters. To achieve this, the three different kinds of weaponry are evaluated using multi-objective decision analysis. Here's how this chapter moves along, A model is suggested to compare electromagnetic weapons, certain fundamental rules are outlined to incorporate multi-objective decision-making, and the results are analysed [3], [18], [19].

Making decisions involves choosing a potential course of action from a variety of accessible options. There are many different criteria for evaluating the options in practically all of these issues. In many cases, the decision-maker seeks to achieve many objectives or goals while adhering to the limitations imposed by the environment, business procedures, and available resources. The goals usually seem to be incommensurable, which is another trait of these issues.

To address the multiple-objective choice issues that arise due to the complexity of various circumstances and the multitude of contributing elements, a significant and diversified body of literature has been created since the early 1960s. Based on a variety of various viewpoints, theoretical and methodological advancements have been made, reflecting the diversity of fields involved. Problem solving as a whole is involved in multi-objective decision-making. A crucial component of a multi-objective decision issue is a clear explanation of the choice scenario that corresponds to it, defining the problem's structure and decision environment. By defining the problem's limits and fundamental elements, this description may be completed. There's going to be some input data and a method that the decision maker defines if the non-linear and non-planning phase and the choice circumstance are structurally seen as a black box. As a consequence, an outcome a decision will be generated [4], [5].

Estimating the total efficacy of each choice is one method for making a multi-objective decision. The decision maker, a collection of alternative courses of action, the ecosystem in which the alternatives are molded, a set of goals, and a set of choosing rules make up the method of measuring the efficacy of any system and display the process flow diagram. Depending on the decision-tastes, maker's possibilities seem better than others as a result of this process [8], [20].

The crucial stage in assessing each option is to specify the goals that will be examined after identifying the alternative solutions and the fighting scenario environment. The additive value model is the most popular way to establish the goals and associated sub-objectives. The "additive value model" may be used to provide a general measure of effectiveness. The goals in this model are laid out in a hierarchical structure, with each relevant objective being combined with others to form a collection of objectives. In a hierarchical system, lower-level objectives are more definite and practical than higher-level objectives. In other words, the goals at the bottom of the hierarchy are the general goals that are most practical and concrete. The most crucial phase in nonlinear objective planning process is establishing the objective hierarchy. You may go from a variety of objectives to a solitary measure of effectiveness thanks to objective hierarchy.

If the degree of attaining a given aim can be evaluated in a useful manner, the objective as described in the structure becomes operational. Each aim is described in terms of a specific set of

qualities at the lowest level to make it operational. An attribute is a quantifiable number whose measured value indicates how well a certain aim has been accomplished. Even when success is stated in qualitative terms, a characteristic may be quantified.

E-Bomb in Military Rivalry

Throughout military history, the laws of war have evolved. Weapons, technology, strategy, and tactics have been the main factors in defining what sort of rules are applicable on the battlefield. The guidelines for future combat are so listed here. Maintaining leadership in military affairs heavily relies on foreseeing future battles and predicting the technologies that underpin future systems. The nation, together with its regular army, must accurately forecast the future and be more prepared than its competitors.

The Further Future Battlefield

The ability to defeat other nations militarily rests on proactive future planning. The operational relevance of e-bombs is largely responsible for the military advantage they may provide. The Joint Chiefs of Staff's blueprint for the future battlefield and the current state of armed services technical developments are both available in open literature. The Joint Chiefs of Staff published a paper titled Joint Vision 2010 to help with future combat planning. This research provides a thorough foundation for comprehending future combined combat. Additionally, it instructs US military acquisition programmers to acquire the skills necessary to conduct military operations using dominating movements, full-dimensional force protection, and precise engagement. JV2010 reflects the fundamental conviction that there is a revolution taking place in military affairs and it presupposes that new skills are required to deal with that Military Technical Revolution (MTR) [4], [5], [7].

Since the thirteenth century, there have been around a dozen revolutions in siege warfare. One started when the US exploded its first atomic weapon in the Trinity test at the beginning of 1945. The August 1945 bombings of Hiroshima and Nagasaki contributed to the conclusion of World War II. The Japanese used germ warfare during that conflict by using bombing operations to infect Chinese population centers with bubonic plague pathogens. Sarin and Inherited predisposition nerve gases were produced by the Germans during World War II, although they were not used. These new "trinity" weapons of mass destruction nuclear, biological, and chemical threaten to make combat in the twenty-first century costlier than ever before.

These principles will govern the conflict regardless of the period. The future battlefield is most likely to be governed by one of these factors, mass. The spread of mass-killing weapons impact may likely herald a new age of conflict. These provide the benefits of simultaneous and deep assault, information supremacy, and precise targeting, all of which are described differently in JV2010. For instance, the revolution in precision means that destroying a single target no longer requires hundreds of planes to deliver thousands of bombs. Instead, one aircraft may deliver a precise weapon to kill targets and achieve the same objectives as hundreds of flights were required. To alter the way battles are fought, "information warfare" research and development are now being conducted. In a nutshell, it is a technique for employing information technology to transform the battlefield of the future. Given that microprocessor speeds have doubled every 18

months, it is logical to infer that media manipulation will have a significant impact on how the battlefield develops in the future.

The need for quick information flow is growing every day. Without quick information flow, massive institutions like governments, the armed services, and businesses cannot operate. The systems utilized in these industries have the feature of being constructed using contemporary, high-density semiconductor components. The dependence on these microelectronics makes systems more and more dangerous as technology advances so quickly. That is, for the foreseeable future, data and communication infrastructure will continue to be a soft electromagnetic target. This is because no one wants to pay to harden these systems yet. Consequently, there is a basic and expanding electromagnetic infrastructure vulnerability that may be used shortly by terrorists and others [8], [9].

The rise of information warfare would unquestionably bring new strategies for eliminating adversary targets and sabotaging operations. Since they include a clandestine assault using time-phased, adaptive computer viruses, autonomous information warfare operations might be the initial stage of the conflict in this new kind of warfare. After the first phase, overt strikes utilizing HPM weapon attacks, conventional electrostatic pulse weapons for area effects, anti-satellite and media override operations, and conventional electro-magnetic pulse weapons would disable particular targets. Integrated information warfare tactics might deceive an opposing force about the strength, position, and direction of friendly troops in addition to offensive techniques like temporarily or permanently shutting down an adversary's sensor and knowledge management.

Most allied space assets are thought to become inactive when one of the designated electromagnetic weapons, HEMP, is used. The majority of allied wireless signals, computers, televisions, and power grids might have their circuitry destroyed by an electromagnetic pulse emanating from such a weapon, making many of the allies' increased assets harmless. This provides such weapons with a significant place in information warfare on the battlefield of the future.

Directed-energy weapons are regarded as a significant technological revolution of the twenty-first century since they have advanced in many sectors. Future battlefields are predicted to have a significant amount of these weapons, both offensively and defensively. One of the possible directed energy weapons of the future is the e-bomb, which is suggested in this paper. Instead of being employed as a defensive weapon, the suggested e-bomb is designed to be an aggressive weapon.

Three classes of hypothetical e-bombs were put forward in this thesis, and a theoretical simulation was created to illustrate the characteristics of each class. To model such a weapon, the switching frequencies theory was used. The findings of the simulation demonstrated that, when employed against the right targets, such weapons are capable of producing power levels greater than those known to permanently disrupt or destroy electronic equipment and systems.

More variables are involved than are described in this work in the coupling of the produced field strength with the target. A simple coupling calculation, however, revealed that the hypothetical

e-potential bomb's lethality range depends on the targets' efficiency as shields. The fact that such a weapon's commercially accessible technology is sufficiently developed to pose a danger in many contexts is another intriguing outcome of the simulation. Low-tech and medium-tech e-bombs, in particular, use readily available gadgets and don't need in-depth technical skills. Because of this, everyone finds these weapons to be incredibly intriguing. Future asymmetric threats will likely take on new dimensions as terrorists investigate these weapons and their simplicity [8], [9].

Engineering research must endeavour to find solutions to the problems that still need to be solved in the development and use of such weapons. Such study includes reducing the size, boosting the power, and finding the best delivery system that offers the greatest range, in addition to streamlining the complexity of a hypothetical e-bomb. However, it is anticipated that e-bomb research for military applications will continue, and that nations will adopt this weapon in smaller forms and create new defensive strategies against such weapons shortly[4]–[6].

This research evaluated the efficacy and function of a hypothetical e-bomb in military competition as well as its technological aspects. A methodology for measuring efficacy was created to compare electromagnetic weapons. According to the model's findings, the suggested e-bomb might be just as effective as HEMP, sometimes referred to as the nuclear bomb for electronic gadgets. The suggested measure of efficacy model mostly focuses on the qualitative measurements established by the study's author since there are no officially documented e-bombs in the open literature and insufficient secondary information to compare such weapons. Even while the model itself serves as a solid benchmark for the efficacy of electromagnetic weapons, additional quantitative data are undoubtedly required for it to be more realistic.

The Turkish Armed Forces may investigate the essential elements that will be crucial on this new battlefield given that future clashes will feature new forms of warfare like Information Warfare and Network Centric Warfare. The Turkish Armed Forces may benefit from investing in the study and development of a proposed e-bomb because it poses a significant threat to the main sensors and systems used in cyber warfare and network-centred warfare, such as command and control systems, computer systems, communication devices, etc.

The Turkish Armed Forces might create a combined organisation to study the e-bomb with involvement from public universities and national organizations research institutions with the most cost-effective investments. The creation and manufacture of these weapons may fall under the overall control of such an entity, which would hasten the development of e-bomb technology. This may also assist civilian contractors in contributing to the military industry and leading comparable applications in several fields. It is increasingly probable that in the future, the rising cost of standard weapons will be a significant issue. Although such armaments provide a significant tactical advantage, their long-term maintenance will be challenging because of the anticipated rising costs of development, operation, and support. The suggested e-bomb may be a superior alternative with comparable efficacy to conventional weapons for the Turkish Armed Forces due to its cheaper cost and multiplier impact.

REFERENCES:

- [1] P. Poveda, "Urânio Exaurido: Origem, aplicações e suas consequências," *Acad. Soc. J.*, 2020, doi: 10.32640/tasj.2020.4.219.
- [2] C. F. Waythomas, M. Loewen, K. L. Wallace, C. E. Cameron, and J. F. Larsen, "Geology and eruptive history of Bogoslof volcano," *Bull. Volcanol.*, 2020, doi: 10.1007/s00445-019-1352-3.
- [3] E. E. Lower-Spies, N. M. Whitney, A. D. Wanamaker, S. M. Griffin, D. S. Introne, and K. J. Kreutz, "A 250-Year, Decadally Resolved, Radiocarbon Time History in the Gulf of Maine Reveals a Hydrographic Regime Shift at the End of the Little Ice Age," *J. Geophys. Res. Ocean.*, 2020, doi: 10.1029/2020JC016579.
- [4] E. G. Pfenninger, W. Klingler, T. Keiloweit, M. Eble, V. Wenzel, and W. A. Krüger, "Terrorismusabwehrübung – Was können wir daraus lernen?," *Anaesthetist*, 2020, doi: 10.1007/s00101-020-00797-4.
- [5] G. Taino, C. Buonocore, A. Stanga, and M. Imbriani, "Gammopatia monoclonale di incerto significato (MGUS) e radiazioni ionizzanti," *G. Ital. Med. Lav. Ergon.*, 2020.
- [6] C. L. Quinan and H. Pezzack, "A Biometric Logic of Revelation: Zach Blas's *SANCTUM* (2018)," *M/C J.*, 2020, doi: 10.5204/mcj.1664.
- [7] E. S. Dremicheva, "Energetic properties of peat saturated with petroleum products," *Saf. Reliab. Power Ind.*, 2020, doi: 10.24223/1999-5555-2020-13-2-105-109.
- [8] A. Arimuko, E. Sujarwanto, and A. Marsono, "Measurements of Earthquake Moment Magnitude (Mw) to Estimate Detonation Energy of a Nuclear Bomb as Plutonium-240," in *Journal of Physics: Conference Series*, 2020. doi: 10.1088/1742-6596/1491/1/012034.
- [9] Y. Zhang, M. Jia, and W. Gao, "Synthetic biology of active compounds," in *Molecular Pharmacognosy*, 2020. doi: 10.1007/978-981-32-9034-1_9.
- [10] A. A. Ivanov *et al.*, "Modeling of laboratory animals exposure conditions behind local concrete shielding bomb arded by 650-mev protons," *Med. Radiol. Radiat. Saf.*, 2020, doi: 10.12737/1024-6177-2020-65-5-77-86.
- [11] E. A. Camarillo, H. Flores, and J. Carvente, "Gas-phase standard enthalpy of formation of 3,5-dimethyl-4-nitroisoxazole determined by semi-micro-combustion calorimetry and thermal analysis," *J. Therm. Anal. Calorim.*, 2020, doi: 10.1007/s10973-019-08548-3.
- [12] D. Zuercher, G. Nakano, J. Anjain, and I. Yeung, "STEM EDUCATION IN THE PACIFIC ISLANDS," in *INTED2020 Proceedings*, 2020. doi: 10.21125/inted.2020.2014.
- [13] J. Kaizer, Y. Kumamoto, M. Molnár, L. Palcsu, and P. P. Povinec, "Temporal changes in tritium and radiocarbon concentrations in the western North Pacific Ocean (1993–2012)," *J. Environ. Radioact.*, 2020, doi: 10.1016/j.jenvrad.2020.106238.
- [14] S. Rhim, C. Kim, J. Y. Kim, and J. W. Yoon, "Optimum design and vibration analysis of a naval piercing bomb for impact assessment on a fuze structure," *Trans. Korean Soc. Mech. Eng. A*, 2020, doi: 10.3795/KSME-A.2020.44.1.021.

- [15] M. Dirgantara, K. Karelius, and M. D. Ariyanti, Sry Ayu K. Tamba, "Evaluasi Prediksi Higher Heating Value (HHV) Biomassa Berdasarkan Analisis Proksimat," *Risal. Fis.*, 2020, doi: 10.35895/rf.v4i1.166.
- [16] A. G. Korotkikh, I. V. Sorokin, E. A. Selikhova, and V. A. Arkhipov, "Ignition and Combustion of Composite Solid Propellants Based on a Double Oxidizer and Boron-Based Additives," *Russ. J. Phys. Chem. B*, 2020, doi: 10.1134/S1990793120040089.
- [17] P. E. TETLOCK and A. BELKIN, "Counterfactual Thought Experiments in World Politics:," in *Counterfactual Thought Experiments in World Politics*, 2020. doi: 10.2307/j.ctv10vm1bn.5.
- [18] S. Rizal, M. Faisal, and E. Yuliwati, "Uji perfoma tungku gasifikasi untuk pirolisis gas metan dari ampas tebu," *J. Inov.*, 2020, doi: 10.37338/ji.v3i1.108.
- [19] F. Cheng, M. Dehghanizadeh, M. A. Audu, J. M. Jarvis, F. O. Holguin, and C. E. Brewer, "Characterization and evaluation of guayule processing residues as potential feedstock for biofuel and chemical production," *Ind. Crops Prod.*, 2020, doi: 10.1016/j.indcrop.2020.112311.
- [20] P. Tiwari, P. . M.N Bandyopadhyay, S. Chatterjee, and P. S. N. Bandyopadhyay, "Expansion of the universe and its correlation with dark energy," *Int. J. Adv. Astron.*, 2020, doi: 10.14419/ijaa.v8i1.30599.

CHAPTER 10

DIGITAL SIGNAL PROCESSING

Dr. Vikram Singh, Associate Professor

Department of Computer Science and Engineering, Sanskriti University, Mathura, Uttar Pradesh, India

Email id- vikrams.oeit@sanskriti.edu.in

Since each kind of gas sensor has a certain operating temperature and since external factors, such as cooling, may alter the temperature, it is essential to continuously monitor and regulate the heating power. Real-time heating control is put in place to meet this need. The heater driving and power monitoring circuits together with a current monitoring method via a shunt resistor. It is not necessary to monitor the heater voltage when using DAC since it makes it simple to manage power using a microcontroller. The DAC uses a 10-bit, 4-channel DAC. Here, a high-output power op-amp is required since the DAC is unable to drive a significant amount of current. As a result, an op-amp of the accuracy, rail-to-rail, and high output type (LM7332, TI, USA) are used. Rheat draws a pretty large current (about 10 mA), hence the gain for the current monitoring IC is set to as little as 100V/V. It is impossible to prevent a load voltage across Rshunt; in this system, it is 1 mV/mA. The software has been adjusted to account for this impact in power calculations. Theoretically, 12 A is the present readout resolution when the current monitor gain (100V/V) and 12-bit ADC with 2.5V reference are taken into account. The power is continuously computed based on the DAC value and the measured current after the output of the current monitoring is received via the ADC.

As a result, the heaters may receive individualised and consistent power input, and maintaining a steady temperature for the gas sensors shows a simplified schematic of the microprocessor's algorithm (ESP32). The system initially performs several initializations for the AFE circuit components, and the heater power is increased until it achieves its goal power by creating a ramp voltage (VDAC). The current flowing through the heater (I_{heat}) is monitored by the heater control algorithm so that the CPU can compute the power and keep it at the goal by changing VDAC. To prevent the saturation of the TIA output voltage, R_f should be automatically chosen to read R_{sens} in real-time ($V_{out\ sens}$). A lower R_f is used if the $V_{out\ sens}$ get close to 0V. As an upper limit to adjust R_f in the opposite situation, 2.1V is used. This is because even a very slight noise on $V_{out\ sens}$ may result in a significant inaccuracy in the computation of R_{sens} if $V_{out\ sens}$ approaches the TIA reference (i.e. 2.3V). In the ideal lines, a little difference in observed $V_{out\ sens}$ may result in a significant mistake in R_{sens} as the lines approach 2.3V.

Fabrication and characterization of a low-power MEMS gas sensor array. To reduce the thermal power consumption, each heater in our MEMS-based low-power microheater platform [10–14] is set up as a suspended dual-cantilever structure. The 110 m long, 9 m wide hanging microheater is designed like a beam. The fabrication of microheaters using traditional MEMS techniques such silicon wet etching, electron beam evaporation, chemical vapour deposition (CVD), and UV

photolithography. The heating area's microscale size meant that just 6 mW of electricity was required to raise the temperature to 260 C. A 2 2 array of microheaters was built into a single chip.

The sensing nanoparticles were successfully integrated into a tiny heating patch using a localised hydrothermal synthesis and liquid-phase deposition (LPD) technique. The following four stages make up the fabrication process: (1) Zinc nitrate hydrate, hexamethylenetetramine (HMTA), and polyethyleneimine (PEI) at concentrations of 25 mM each were added to DI water to create an aqueous ZnO precursor. All compounds were obtained from Sigma Aldrich. (2) Substituting SnO₂ nanotubes for produced ZnO nanowires in a SnO₂ LPD solution (3.75 mM SnF₂, 15 mM HF, 7.5 mM H₂O₂, and 37.5 mM H₃BO₃ in DI water) for 20 min. (3) Using the same procedure as step 2, ZnO nanowires were produced on the opposite pair of the naked microheater (1). (4) A shadow mask was placed over a pair of microheaters comprising produced ZnO nanowires and SnO₂ nanotubes, and the other pair was coated with Pt nanoparticles using electron beam evaporation (Pt thickness of 2 nm). As a consequence, it was possible to create a sensor array made up of Pt-coated SnO₂ nanotubes, bare ZnO nanowires, and bare SnO₂ nanotubes[1], [2].

Sensitivity study of the sensor array for improving gas selectivity is shown in Comparison of the sensor array's sensitivity to CO and H₂S gases in (a), and (b) PCA results based on the obtained sensitivity. The sensing system can discriminate between these two gases because of the sufficiently distinct distribution of the sets of points in PCA shows the sensor reactions under pulse-heating conditions. (A) The resulting pulse current produced by a pulse voltage when applied to a heater, and (B) a comparison of the responses of H₂S gas under continuous and pulse heating conditions. The sensor nevertheless provides acceptable gas response and recovery/response in the pulse-heating mode, even if sensitivity and response/recovery speed are slower than in the continuous heating state.

The characterisation of manufactured sensor arrays was done using SEM and SEM-energy dispersive spectroscopy (EDS) analysis. SEM images of uncoated SnO₂ nanotubes, coated SnO₂ nanotubes, uncoated ZnO nanowires, and coated ZnO nanowires are shown in through, respectively. Due to their random growth direction and average diameter and length of 70 nm and 1 μ m, respectively, ZnO nanowires create a complex electrical network. Additionally, ZnO nanowires were disintegrated and a hollow structure of SnO₂ nanotubes was created as a result of the acidic nature of the LPD solution. The EDS spectra of the created nanomaterials. While Pt peaks were not visible in the naked SnO₂ nanotubes/ZnO nanowires that were shadowed by the shadow mask during the e-beam evaporation process, they were visible in the Pt-coated SnO₂ nanotubes/ZnO nanowires.

The output voltages of the TIA for each R_f throughout a broad input range of R_{sens} are shown in. Since R_f and R_{sens} ratio mostly affect output voltage as shown by bigger R_f allows for broader R_{sens} fluctuation coverage. The measured points closely resemble the ideal curves shown by the solid lines produced using Equation. The microcontroller calculates R_{sens} based on the observed V_{out sens}, and relative error from the ideal values is illustrated in. Because R_{sens} grows, it becomes more vulnerable to noise and leakage, yet even so, the relative inaccuracy is still less than 1%. Regardless of changes in R_{heat}, heating power must be

maintained to keep sensors at the proper temperatures demonstrates that the control algorithm within the microcontroller permits the application of the target power and keeps the power constant regardless of changes in R_{heat} for three randomly selected instances of target power applied for the heaters. This experiment demonstrates the power control abilities of pure circuits and algorithms. Therefore, we used commercially available fixed carbon film resistors, whose resistances are temperature insensitive (100 ppm/C), instead of fabricating microheaters for R_{heat} .

With heating power maintained at 6 mW for each heater, we saw that the broad range of resistances was covered for all channels (current from nA-order to the hundreds of A at VSET), generating temperatures approximately 260 C. H₂S concentration varied from 1 to 16 ppm, and its cyclic on-off period was 500 s. The sensors' sensitivity to and reaction times in response to H₂S varied, but SnO₂ nanotubes performed better. Multiple sensor raw data transfer via ESP32 over Wi-Fi and BLE: (A) Data transfer over a Wi-Fi access point that is linked to the internet.

In this instance, the sensor data is recorded in a Google Spreadsheet file and shown as graphs. (b) Data transfer over a BLE to an Android application that shows graphs of the sensor data in real-time is equal to 3.0 at 1 ppm, 5.5 at 5 ppm, 7.0 at 7 ppm, and 8.7 at 16 ppm for positivity to H₂S gas. Fast reaction and recovery are shown by both SnO₂-based sensing materials (80% response and recovery time 20 s). Because the module is specifically made for multiplexed gas sensors, it is feasible to provide further analysis, such as principal component analysis (PCA), an efficient solution to the poor selectivity issue with semiconductor metal oxide-based gas sensors. Because they are both reducing gases that enhance the conductance of n-type semiconductor metal oxides, making it difficult to discriminate between them, the sensing of H₂S and CO gases was examined for this investigation.

In addition, H₂S and CO are among the most important target gases when it comes to the environmental monitoring application of this module. When exposed to the human body, these gases may cause headaches, nausea, paralysis, dyspnea, or harm to the nervous system. We obtained the sensitivity values for four sensors using the module. Different sensitivity values to these two gases, and a PCA result derived from the sensitivity shown in H₂S and CO are reducing gases, however, if the PCA points' distribution is sufficiently dissimilar, it may be possible to distinguish between various gases. The ESP32 (32-bit dual core and 80-240 MHz clock frequency)-designed multichannel sensing module has a significant computational capacity that permits reasonably intensive calculation. The software solution for PCA will improve the selectivity of the gas sensing system by using the hardware resources of the module and a remote computer that receives data.

Our module is easily programmable to provide a variety of operating modes, including a power-saving mode. It is advised that the whole system be switched on and off periodically while using a restricted power source, such as battery power. Four-channel heating uses a lot of electricity, thus it should also be switched on and off many times to cut down on use. To save time, the heaters in this situation need to react quickly enough to provide the sensors with the right temperature condition as soon as feasible. We modified the ESP32 to provide a heater with a pulse heating condition by continually adjusting the DAC value. Figure 8(b) depicts the total

reaction to H₂S in the pulse heating condition. The sensor nevertheless provides acceptable gas response and recovery/response rates in the pulse-heating mode, despite having lower sensitivity and response/recovery speeds compared to the continuous heating state. This demonstrates that even with repeated sleep and wakeup cycles, our module and sensor function dependably.

We outline two potential IoT application scenarios that make use of the ESP32's built-in Wi-Fi and BLE technology. A public web application developed in Google Script and the HTTPSRedirect approach allows the ESP32 to record sensor data into Google Spreadsheet, according to an open-source IoT project on the internet. In relation to the project, we obtained our sensor data and entered it into a Google Spreadsheet file; the outcome is shown. Through MIT App Inventor, an open Android programming environment, we created an Android app that shows real-time sensor graphs for the BLE connection. Here, the ESP32 on our module serves as a BLE server that stores sensing data and makes itself known to nearby clients by doing "advertisement." the data stream transfer process. The sent data is correctly processed and shown on four graphs, as seen. Each axis has the same domain as the graphs in, and its size has been fixed such that each line is clearly visible.

Without heating operation, the overall circuit power consumption is 420 mW, of which ESP32's communication component consumes 330 mW (78% of the circuit power). For portable apps where BLE is employed, this is rather high. The high power consumption is attributed to the fact that the ESP32's software framework currently only enables the combined usage of Bluetooth Classic and BLE mode, although still being upgraded. We believe that there is space for significant power reduction for BLE-only mode in the future framework/chip releases given that other commercially marketed UART-supported BLE-only devices use tens of mW[3], [4].

The current study has presented a very portable multiple gas sensing module using semiconductor-type chemiresistive sensors. A compact platform with many integrated gas sensors was attached to the module. Real-time gas responses, PCA, pulse-heating, and data transfer via Wi-Fi/BLE are only a few of the system demonstrations that were carried out employing electronics and sensors. AFE was made to maintain high sensing precision throughout a broad range of resistance (R_{sens}) changes and to regulate heating power to desired levels despite variations in R_{heat} . The microcontroller-RF integrated SoC made it possible to use the IoT for a variety of fixed and mobile applications. Although the present system has a problem with power consumption for communication, it is anticipated that it can be fixed by future ESP32 versions. This system may be immediately used for Internet of Things (IoT) applications since it completely incorporates sensors, AFE, digital signal processing, and RF. This system may be used for many different applications because of its compact size and great functionality, including air quality monitoring in industrial sites, homes, vehicles, etc.

Wireless sensor networks (WSN) have been attracting growing attention in the past few years due to their involvement in new technologies such as the Internet of things (IoT). To fulfil the growing demands of IoT applications, including automated surveillance, environmental monitoring, smart cities, and other applications, advanced sensor networks are required. Sensing nodes should be able to analyse and communicate data with constrained energy harvesting (EH) and consumption budgets to provide a long-lasting autonomous sensor network. There are still

numerous difficulties in adopting these networks despite the large variety of research on WSN/IoT network optimization in the literature. To create self-powered sensing nodes, sensors are expected to save energy and manage their consumption. On the other hand, they also need to collect reliable data and transmit it effectively.

The intricacy of such challenges rests in constructing a mathematical model that accounts for several parameters like measurement precision, observation transmission quality, and EH efficiency. In today's massive sensor networks, managing the available resources, system costs, and data volume while attaining the requisite inference performance represents a significant problem. Therefore, a basic design problem is to position the sensors in the best possible places to collect useful data with fewer sensors while maximising power and spectrum resources.

The issue of selecting the optimal subset of sensors locations from a list of potential sensors is known as sensor selection placement locations. This is a combinatorial issue that may be ideally addressed by doing a thorough search in which all feasible combinations that adhere to a budget limit are evaluated for a performance metric, such as inference accuracy. When there are many selection factors, this procedure becomes computationally infeasible. Instead, by selfishly choosing sensors one at a time, a less-than-ideal outcome may be achieved. If the performance measure can be written as a submodular set function of the selection indicators with cardinal values, then such a greedy method is almost optimum restrictions on it. As an alternative, convex optimization, which uses the convexity of the performance measure and constraint functions to solve the optimization issue may be used to solve the sensor selection problem suboptimally. The discrete selection variables are relaxed to the continuous domain for convex optimization-based solutions, and rounding is used to extract an approximative Boolean answer. For a summary of sensor selection methods for typical statistical signal processing applications. You may also utilise other convex optimization techniques, including the difference between two convex sets and the 0 norm approximation, to arrive at a less-than-ideal result. Online sensor activation/deactivation, where the sensor operation is planned based on real-time readings, is one of two related but distinct significant difficulties in sensor networks.

Additionally, there is offline sensor placement where the goal is to choose the optimal subset of sensors (locations) from a candidate set of sensors (locations). To achieve a desired performance based on past statistics, which do not rely on real-time measurements, offline sensor selection is done at the network design time. The emphasis of this research is on offline sensor selection. By taking into account several practical concerns including measurement accuracy, observation transmission quality, and EH efficiency, the total offline sensor selection is improved. Better overall system performance in terms of lowering the minimal mean squared error (MMSE) at a central fusion centre is ensured by taking into account certain practical challenges (FC). The sensing positions are chosen solely based on measurement accuracy at the sensor level. Addresses the previously stated pragmatic considerations. However, only optimises sensing location, which limits the system's adaptability. Based on the sensor transmission power and assuming that the sensors get feedback upon successful transmission, the authors estimate the uncertainty of successful receipt at a distant estimator. In that work, the sensor selection issue is resolved so that each potential sensing node is equipped with either a low power sensor or a

high-power sensor. However, no spectrum allocation is done and just two different kinds of sensors are taken into consideration.

Based on the measurement model, we carefully built the estimator we suggest. In the case of a linear measurement model for a static source, the maximum a posteriori (MAP) estimator achieves the MMSE. Instead, the Kalman filter is used to achieve MMSE estimate while considering the temporal correlation. The quality of system optimization is improved by modelling the unidentified source while taking into account both the cross-correlation and temporal correlation of the sources. Several greedy techniques were developed to reduce the estimate error for the vector state linear dynamical system subject to a certain number of sensing nodes despite the absence of performance guarantees. The price of transmitting sensor observations to the FC and the calibre of the communication connections between the sensors and the FC have not been taken into account in any of these studies. In this study, we concentrate on two topics: the estimate of static vector source parameters and the estimation of dynamic scalar source parameters.

A static measurement model for an unknown source parameter vector was taken into account such that the distributed parameter estimate is reduced based on the current measurement data. These pieces are regarded as static source material. To estimate the static state, convex relaxation was used to position the sensors in. Digital observation transmission is projected to function better than analogue transmission systems because of their resilience to channel noise. However, due to the complexity of the research, only a small number of studies in the literature take into account digital transmission methods in sensor selection issues. Because of the non-Gaussian nature of the noise created by observation quantization, linear measurement models cannot be used directly. According to, the FC, which receives quantized sensor observations, uses Bayesian Fisher information to online optimise the sensors' overall power usage. The quantity of energy made accessible by EH at each sensor is ignored, however. Figure 1 discloses the Mobile Terminal and the TX Digital Signal Processing with Electrical Spectrum frequency receiver sensitivity IoT devices.

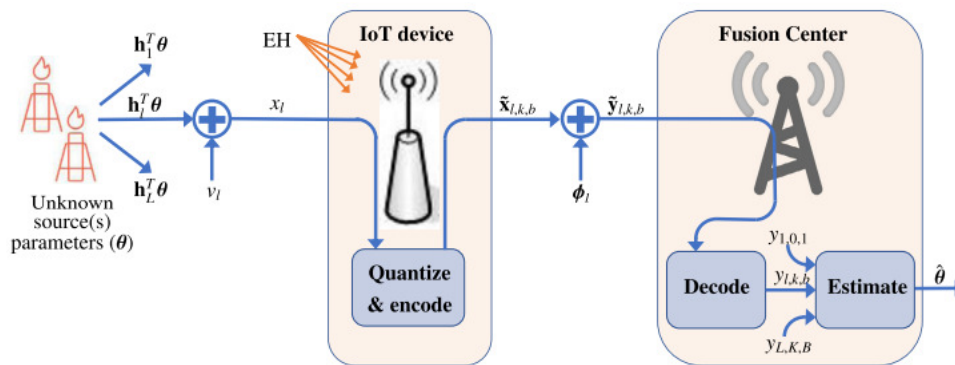


Figure 1: Discloses the Mobile Terminal and the TX Digital Signal Processing with Electrical Spectrum frequency receiver sensitivity IoT devices.

Practical considerations like the EH of the sensor and the observation transmission quality to the FC are made in this study. In order to increase the flexibility of network design, the major objective of this article is to combine optimum sensor placement with innovative and significant selection dimensions, specifically, we allow for transmission power and resource block (i.e., time-frequency channel) allocation.

The transmission power of the sensor is maximised by taking into account the various types of sensors, where more costly sensors are equipped with more EH capabilities and larger battery capacity than less expensive sensors. The method in is extended in this setting by taking K different types of sensors into account. Additionally, we let sensors broadcast their findings across several spectral bandwidths, so limiting the system's overall bandwidth. Despite widespread knowledge of the energy limitations in IoT networks, only a small number of research specifically address the sensor transmission power level for a dynamic estimate. We discuss and contrast sensor selection strategies that take analogue and digital transmission systems into account. We examine observation quantization and encoding in the digital scheme using an information-theoretic framework. Based on the allotted bandwidth and the signal-to-noise ratio between the candidate sensor and the FC, the number of quantization levels is optimised. By relaxing the discrete variables and rounding the resulting solution, we choose a suboptimal sensor using convex optimization. To increase rounding efficiency, a unique rounding method is suggested. This paper's contribution may be summed up as follows:

- a. The sensor transmission power and operational bandwidth are jointly tuned with the sensing site. This offers network designers the freedom to install more costly sensors in key places with a greater power budget and data rate while placing less expensive sensors in less crucial areas.
- b. We simulate a real-world system that accounts for the EH, channel gain, and measurement precision. Similar factors were taken into account but they all assumed that sensors would directly amplify and transfer observations in analogue transmission.
- c. The choice of sensors has been made with the digital transmission of observations to the FC in mind. The quantization and channel error is expressed using an information-theoretic method.
- d. To effectively round the relaxed solutions while taking into consideration the joint power, location, and resource block selection, a generalised randomised rounding technique is suggested.

A comparison of the suggested sensor placement techniques with the current techniques is shown demonstrates that our approaches are superior to others in that the colour of the cell background represents how effectively the trait under consideration is handled. Green indicates that both general and practical examples are taken into account, yellow indicates that there are some constraints, and red indicates that there is a weakness.

A developing paradigm for ultralow-power wireless communication is presented in IEEE Backscatter. It is a competitive core technology for Internet of Things (IoT) applications because of its submilliwatt power consumption. In this article, we provide a signal processing tutorial on

backscatter communication as well as an overview of current research initiatives in this area, with a particular emphasis on bistatic backscatter systems. We also go through the special real-world uses for backscatter communication and point out unanswered issues in this area. We hope that this post will clarify how low-power wireless communication should be designed to construct and deploy IoT services in the real world[5], [6].

Overview of backscatter communication

The Internet of Things (IoT) envisions a future where sensors and actuators are pervasive and networked, enabling us to better comprehend and manage our environment. Building such devices that can be quickly deployed and function independently for a long time is a crucial obstacle towards this objective.

A prominent approach to meet this demand is backscatter communication, a new microwatt-level wireless communication paradigm. Backscatter communication operates on a similar concept. Mirrors have been used for communication purposes by humans for a very long time, and this technique is crucial when there is no energy source present, such as a bonfire or a torch. The sender may use Morse code to communicate with the distant target by flipping the mirror and adjusting the amount of reflected light. The same reflection while the modifying procedure is used on radio-frequency (RF) waves for backscatter communication. The system model of backscatter communication at a high level. The incoming excitation signal produced by a nearby (carrier) transmitter is reflected by a unique gadget known as a backscatter tag. To modulate the signal, it simultaneously adjusts the signal's amplitude, frequency, and/or phase. After being received by a receiver, the backscattered signal is subsequently sent through a signal-processing engine to retrieve information.

The backscatter tag was implanted. A bistatic backscatter system design separates the transmitter and receiver, although they were previously incorporated in conventional or monostatic backscatter systems [such as RF identification (RFID) readers. In particular, the transmitters may be found everywhere as ambient RF sources, such as TV or FM radio towers, cellular base stations, and Wi-Fi access points (APs). The following inherent qualities are introduced by this new modular architecture for improved performance.

The backscatter tag (as a sensor node) must communicate as soon as the sensory data are accessible in various sensing applications. Instead of waiting for protocol-constrained interrogation from a single reader, the tag has additional time slots for data transfer when excitation signals may originate from numerous sources. Spatial adaptability: The effectiveness of backscatter communication depends on the spread of excitation signals.

Being separated from the receiver, the transmitter(s) may be deliberately positioned in appropriate positions to balance the scalability and performance of backscatter tags. Flexibility in technology Different excitation signals and modulation schemes may be employed in situ thanks to the broad and technology-independent communication paradigm that is presented by bistatic backscatter system architecture. Since there are widely available Wi-Fi transmitters (such as APs) and receivers, ambient RF sources, such as Wi-Fi signals, may be employed to make the backscatter technique instantly deployable.

Energy savings is the fundamental benefit of backscatter communication. Backscatter communication uses more than 1,000 times less power than traditional wireless technologies like Wi-Fi (tens of kilowatts), Bluetooth/Bluetooth Low Energy (a few kilowatts), and long-term evolution (LTE), which uses hundreds of milliwatts. The biggest power-consuming process in radio communicators, radio signal production, is offloaded to the powered transmitter to achieve this power reduction and is thus absent from a backscatter tag. The transmitter is also in charge of signal processing and amplification. As a result, the design is asymmetrical, with a thick transmitter/receiver and a narrow backscatter tag. By combining the small form factor (square centimeter of typical IoT devices with today's energy-harvesting technologies, such as solar/light, mechanical motion/vibration, thermoelectric effect, and electromagnetic radiation, it is possible for backscatter tags to operate without batteries. In addition to improving energy efficiency, this asymmetric design results in less complex circuitry, a smaller form factor, and less expensive tags. A more energy-efficient wireless connection may be provided for regular mobile device usage by extending the concept of such an asymmetric architecture. Backscatter is now a viable option for IoT devices thanks to this design, which is also a crucial step towards achieving large-scale IoT application deployment in the real world.

Although there are many different backscatter communication technologies available, they are all based on the same or very similar models and techniques, which allow backscatter tags to reflect an incoming RF signal while also modifying and modulating the signal for backscattering, or secondary transmission. Impedance mismatching is the fundamental concept behind RF signal modification and reflection. A heliograph is a simple yet efficient device that communicates instantly across great distances using flashes of sunlight reflected by a mirror. By briefly turning the mirror or by cutting off the beam using a shutter, the flashes may be modified.

Because each $S_{t \text{ in}}()$ may be seen as a collection of sine waves using Fourier transform, it should be noted that substituting any $S_{t \text{ in}}()$ with a sine wave here does not reduce the generality of the situation. Given the definition of $S_{t \text{ in}}()$ and the reflection coefficient CT , the reflected signal $S_{t \text{ out}}()$ is computed and displayed in: We can see that the backscatter tag controls CT , which is obtained from the impedance of the antenna Z_A and the load Z_L , to control $S_{t \text{ out}}()$. To vary the value of CT for modulating $S_{t \text{ out}}$, we may adjust Z_L (\cdot). In backscatter systems, $S_{t \text{ out}}()$ can only be changed via modifying CT , in contrast to typical radio communication systems, which may directly adjust the amplitude, frequency, and phase of $S_{t \text{ out}}()$ for modulation. The incoming signal $S_{t \text{ in}}()$, where $A_{A \text{ out}} = CT T_{\text{ in}}$ and $I_{I \text{ out}} = I_{I \text{ in}}$ is effectively subjected to a phase shift of iT and an attenuation of CT thanks to CT , as illustrated in The backscatter may switch the reflected signal $S_{t \text{ out}}()$ between a variety of amplitudes and phases by choosing between various CT values. It is implemented on a backscatter tag using an RF switch, a common electrical component. The high-frequency signal may be sent across a variety of transmission lines using an RF switch. The RF switch is used on the backscatter tag to link the antenna to RF loads of various impedances and switch between them. The RF switch is then controlled by a low-power microcontroller unit (MCU) or a field-programmable gate array (FPGA). The backscatter tag is, therefore, able to modify CT and thus manage A_{out} and i_{out} . In addition to these fundamental processes, we provide a taxonomy for backscatter tag designs based on frequency shifting (FS) or not and digital vs analogue modulation.

The capacity of the tag to alter the frequency of the backscattered signal is one of the key variations among backscatter tag systems. The backscatter tag may represent data using a variety of amplitudes, phases, or combinations since it can modify A_{out} and i_{out} by altering $C_T(t)$. $C_T(t)$ applies the function given in (9) to digital data: C_n are discrete numbers that result in distinct S_t outputs in the equation. To adjust A_{out} and i_{out} following the input data value such as voltage, special circuits are created for analogue data. The backscatter tag may then carry out amplitude-shift keying, amplitude modulation (AM), phase-shift keying (PSK), phase modulation (PM), or any combination of these.

$S_{t,in}(t)$ (emitted by the carrier transmitter) and $S_{t,out}(t)$ (emitted by the backscatter tag) may interfere with one another at the receiver, which might lead to issues while receiving $S_{t,out}(t)$. In addition, such a design restricts the utilisation of frequency-related modulation methods, such as FM and FSK.

Many backscatter tag systems employ digital signals like a square wave to resemble a sine wave, even though the sinusoidal $C_T(t)$ may truly be a sine wave signal. To keep things simple, we will define $C_T(t)$ here as a square wave. Note that we may examine various kinds of digital signals using the same methodology we use to evaluate the square wave. With frequency f_T and phase ϕ_T , $C_T(t)$ is here switched back and forth between 0 and A_T . Using the Fourier transform, $C_T(t)$ may be extended into several $c_k(t)$ elements. The following definition of $c_k(t)$ may be found in (10):

The sidebands are phase-shifted from \sin by $\phi_k = \phi_T + k\phi_T/2$, attenuated by (A_T/k) , and frequency-shifted by $k f_T$. Noting that the tag will create many sidebands in $S_{t,out}(t)$, only one of which is utilised for sending data, other unused sidebands may cause interference to nearby wireless devices if $C_T(t)$ is not purely sinusoidal. Although some of those sidebands have been suggested to be removed, a low-power approach to remove the interference has not yet been created. The tag must produce $C_T(t)$ to build an FS backscatter. As was already explained, many tags produce a square wave to simulate a sinusoidal. In this scenario, an RF switch is used to connect multiple RF loads to the antenna, and an FPGA or MCU toggles the RF switch between them. Similar methods may also be used to produce other kinds of $C_T(t)$. We find that in real-world implementations, FPGA is often chosen as the controller instead of an MCU since it uses less energy while operating at the same clock rate. A Freescale Kinetis low-power MCU operating at 50 MHz, e.g., may use up

Digital-to-analog conversion

Backscatter signal modulation may be digital or analogue, much as in traditional communication systems. When using digital modulation, a backscatter tag maps signals to several $S_{t,out}(t)$ waveforms that differ in frequency, amplitude, or phase. To do this, the backscatter tag uses a controller (such as an MCU or FPGA) to transition between the limited set of discrete states, generating $C_T(t)$ that varies with the symbol to be sent.

Digital modulation

The constant variable $S_t \text{ out}()$ is used in analogue modulation. It is accomplished by employing specialised analogue circuits to transform the input data to the frequency, amplitude, and phase of $CT(t)$. The output frequency of a voltage-controlled oscillator (VCO), for instance, and therefore the frequency of a sine wave $CT(t)$ signal, may both be controlled by the input voltage. In this instance, the backscatter tag generates a frequency-modulated $S_t \text{ out}()$. The way that analogue backscatters regulate $CT(t)$ varies depending on the source and the characteristics of the input data. The backscatter tag may directly transform the analogue Antenna Incoming Sine by the use of analogue modulation (t) scattershot South (t)

Input to analogue-modulated $S_t \text{ out}()$ without processing it in the digital domain, which eliminates the need for computational components, such as MCUs or FPGAs, as well as analog-to-digital converters (ADCs) (for purposes of sensing), which are \power hungry especially when processing high-bandwidth data streams, such as audio and video. Even when the input data are already in digital format, analogue modulation cannot handle all types of input data. The data source must be connected to $CT(t)$ using a case-by-case analogue circuit architecture for the input data to modify $S_t \text{ out}()$.

Innovative backscatter systems

Despite the simplicity of backscatter operation in theory, there is a long way to go in delivering a viable (bistatic) backscatter communication system good enough for \real-world IoT applications. Energy efficiency, bit rate, communication range, and deployment cost are the four key difficulties facing backscatter communication, according to the scientific community. The potential benefits of backscatter communication have spurred a flurry of new research initiatives and initiatives to address those issues. The next paragraphs in this section comment on these performance indicators.

Use of less energy

Backscatter communication is ultralow-power, making it possible to operate IoT applications without a battery. In severe circumstances, applications could even need always-on communication, making RF signals (rather than solar, vibration, etc.) the most likely candidate for energy harvesting. As a result, there is strong motivation to create backscatter communication systems that can run solely on RF energy harvested from the environment and the hardware and system design face significant problems with such a tiny energy budget.

Projects investigating the design and execution for this purpose have been active in recent years. The first backscatter communication system that relies exclusively on energy derived from ambient RF signals, including TV and cellphone towers, is presented by ambient backscatter. No specially designed carrier transmitter is used in this system. The key feature of this system is the two-way communication capability and direct communication between backscatter tags. By adjusting the RF switch to reflect or absorb the surrounding RF signal, data injection on the backscatter tag is made possible. While broadcasting 1, for instance, it reflects signals and when transmitting 0, it absorbs them. A nearby backscatter tag may detect a variation in the RF energy

produced by such an activity. However, since the ambient RF signal is already weak and has been modulated to carry other information, like TV, it is difficult to notice such a change on the receiving backscatter tag. A two-step decoding circuit is created to successfully decode the data on backscatter tags. To determine the current RF energy level, an envelope detector and an averaging circuit are first applied to the received RF signal. After that, a threshold comparator determines if the transmitted tag is an RF signal that is reflecting or not. Here, the threshold is calculated by averaging the signal over a lengthy period. In both indoor and outdoor settings, this system can transmit data at a rate of 1 kilobit per second at distances of 0.76 and 0.46 m, respectively.

Another battery-free backscatter device that can recognise and broadcast speech as well as receive and activate audio is presented by the battery-free mobile phone project. In this technology, audio data is sent and received using a battery-free backscatter tag in conjunction with a nearby customised base station that is linked to cellular networks. The design and usage of analogue backscatter, in which analogue data, such as a wave signal, are directly backscattered without being translated and processed in the digital domain, is the major innovation of this technology. Because all of the digital computational components, such as the FPGA and ADC/digital-to-analogue converter (DAC) (for converting sound to and from a digital signal), that could become the bottleneck of battery-free operation are eliminated to save energy, this new design is, even more, energy efficient than the (conventional) digital backscatter design. An electret microphone is a specialised part that is used to translate the input audio to the antenna's impedance. A junction-gate field-effect transistor may be found within the electret microphone (JFET).

In this design, the JFET functions as a voltage-to-impedance converter and is set up to operate in its triode region. As a result, the backscatter tag does away with the requirement for digital circuitry by altering the incoming signal in response to changes in the audio voltage. AM audio is broadcast from the base station to the backscatter tag, travels through an AM demodulator, and is then directly fed into an earphone to receive and activate downlink audio without the requirement for digital components. The backscatter tag also can broadcast and receive digital packets, which allows for the exchange of control orders between the backscatter tag and the base station, however, this feature is only utilised while making and receiving calls, using little total energy.

Other systems exchange energy efficiency for other objectives. For example, to enable data rates of 10+ megabits/s, passive Wi-Fi and backfire use differential quadrature PSK (DQPSK) and 16-PSK, respectively. When compared to situations where the RF switch toggles at a considerably slower speed and the baseband processing is carried out in analogue, such high-speed baseband processing uses a lot of energy. In LoRa backscatter, where chirp spread spectrum (CSS) modulation consumes a significant amount of energy, power consumption is exchanged for communication range. For interoperability with current wireless protocols, HitchHike and FreeRider needs exact synchronisation with Wi-Fi packets in the air. Low-delay RF energy detectors, which utilise more power than passive RF energy detectors used in other systems, are required for this synchronisation.

Byte rate

A smart speaker that continually broadcasts user speech to the cloud, for example, requires a bit rate of more than 70 kilobits per second. Numerous IoT applications demand wireless connectivity faster than several kilobits per second. When in use, vision-based devices like security cameras may easily use more than 1 megabit/s. When taking into account cutting-edge applications like augmented and virtual reality, the bit rate required is considerably greater. To better use the channel bandwidth available, conventional radio technology has adopted sophisticated modulation algorithms including channel bonding and carrier aggregation. However, using comparable techniques to backscatter communication is challenging.

First, a backscatter tag's low capacity for RF signal manipulation and baseband processing makes it difficult to execute particularly complicated modulations on it. To make use of the spectrum more effectively, new methods must be created. Second, high throughput often necessitates quick calculation and high-performance electrical components, which adds to energy usage. Because of this, supporting high-throughput applications on top of backscatter communication systems is difficult, and it is necessary to carefully balance throughput and per-bit energy usage.

Tag to Receiver to Transmitter to Tag to Receiver to Transmitter Receiver BackFi N/A 5.0 Mbps 1 m 7 m 7 m Wi-Fi background and software-defined radio The operational range of a bistatic backscatter system is represented in the "Range" column as the separation between the transmitter and tag and the separation between tag and receiver. The maximum tag-to-receiver distance as well as the equivalent transmitter-to-tag distance are given below. The "Distance" under "Maximum Bit Rate" refers to the tag-to-receiver distance at the maximum bit rate. The value in the "Minimum Power" column is the outcome of an IC design simulation for passive Wi-Fi and all other figures indicated with the "IC" abbreviation. IC stands for integrated circuit; BLE for Bluetooth.

BackFi provides a high-throughput Wi-Fi backscatter architecture that delivers 1,000 times greater throughput than the previous Wi-Fi backscatter system. In this setup, the backscatter transmitter and receiver are shared by a modified Wi-Fi AP that is broadcasting regular Wi-Fi packets to nearby clients. The system's unique backscatter tag, which is intended to provide effective PMs Like 16-PSK, is its standout feature. The specialized Wi-Fi AP may broadcast to nearby Wi-Fi clients while also receiving a reflected signal from backscatter tags thanks to self-interference cancellation technology. Furthermore, a sophisticated decoder is created to decode backscatter on wide-band signals, including Wi-Fi. Figure 7 illustrates a binary tree made of single-pole double-throw (SPDT) RF switches that are used for PM on backscatter tags. To provide the variable phase shifts required to create the PSK constellation, RF delay lines of various lengths are linked at the tree leaves.

Full-duplex radio technology allows for the elimination of self-interference. The self-interference cancellation circuits may utilise this time to estimate the channel between the backscatter tag and the receiver when a backscatter tag detects an incoming Wi-Fi signal before modulating the Wi-Fi signal, preventing the cancellation of real backscattered data. At a distance of 1 m, this system can accomplish 5 megabits/s.

Passive Wi-Fi, where the backscatter tag creates legitimate Wi-Fi 802.11b transmission at all bit rates, including the maximum 11 megabits/s, is another backscatter technology that offers great throughput. As the excitation signal in this system, a single tone is sent at a frequency outside of Wi-Fi channels by a specialised transmitter, and a backscatter tag transforms this signal into legitimate Wi-Fi packets.

All Wi-Fi-capable gadgets can pick up the backscatter tag's broadcast. The development and use of a backscatter tag, which conducts baseband processing and low-power modulation of the incoming single-tone signal into 802.11b packets, is one of the system's significant contributions. The backscatter tag first creates a baseband of Wi-Fi packets that adhere to the 802.11b protocol. It then employs the methods mentioned in the "Tutorial on Backscatter Communication" section to alter the single-tone signal. The two modulations used in 802.11b, differential binary PSK (DBPSK) and DQPSK, are specifically performed via phase modification. The signal is subsequently shifted to the Wi-Fi channel's centre via frequency manipulation. This system's entire network stack, which enables numerous backscatter tags to share the channel and provide acknowledgement and rate adaptation, is another addition. A downlink from the transmitter to the backscatter tag is necessary for this network architecture. On/off keying (OOK) is used to encode the downlink, and a low-power RF energy detector on the backscatter tag is used to decode it [7], [8].

Bit rate may also be exchanged for other things. Legitimate Wi-Fi transmissions are backscattered into other valid Wi-Fi signals via HitchHike and FreeRider. To accomplish so, they need to preserve individual Wi-Fi symbols intact after being backscattered. The size of a Wi-Fi symbol, which is 1 s for HitchHike and much longer for FreeRider due to orthogonal frequency-division multiplexing (OFDM), which essentially restricts the throughput, is the lowest unit of change as a result. Ambient backscatter exchanges power consumption for throughput. The backscatter tag absorbs RF signals while sending 0 s and reflects them when transmitting 1 s in this straightforward modulation technique. To allow for proper decoding on the receiver, the bit rate is constrained.

Figure 6 shows how the LoRa backscatter tag is constructed. In a low-power approach, CSS modulation is carried out using the DAC and VCO. A LoRa backscatter tag may eliminate the majority of sideband interference by switching the SPDT RF switch included in conventional backscatter tags for a single pole multithrow switch.

To precisely phase shift the incoming signal, many SPDT switches are linked into a binary tree, with each leaf of the tree being connected to an RF delay line. IoT services used outdoors often need a communication range of several kilometres. Although practically all wireless technologies currently find it difficult to meet this criterion, backscatter systems find it more difficult, largely due to the increased route loss compared to traditional wireless communication. To be more explicit, there may be substantial loss while the signal is being reflected at the backscatter tag. This attenuation, according to our tests, may reach 30 dB. In addition, radio signals encounter route loss twice, once from the transmitter to the tag and once from the tag to the receiver. This issue may be resolved for traditional wireless systems by either boosting the transmission power or using unique modulation techniques, such as CSS utilised in LoRa. Both strategies, however,

are not easily suited to backscatter. First, to account for the additional attenuation in backscatter systems, the transmission power may need to be raised. It should be noted that when the total distance doubles, the transmission power must at least triple, which may easily overcome the restrictions imposed by the electronic component, circuit design, power budget, and governmental requirements. Second, because of its power budget, a backscatter tag can only carry out a limited amount of signal processing. Therefore, it may be challenging to use particular modulation schemes on common backscatter tags, necessitating the development of unique approaches. The development of a long-range backscatter communication system is difficult due to all of these problems.

It is important to keep in mind that a backscatter communication system involves two distances when thinking about the issue of communication range. The first is the transmitter distance from the transmitter to the backscatter tag, which establishes the range of the region in which the backscatter tag is free to travel while transmitting data. The receiver distance, or backscatter tag-to-receiver distance, establishes the range within which the receiver can safely interpret data. The total attenuation of both pathways results in the overall path loss, which explains how the two distances are connected. The maximum receiver distance for the same backscatter communication method decreases as the transmitter distance rises. However, the two lengths have distinct needs for various purposes. For example, there is no need for a lengthy receiver distance for a wearable health sensor that backscatters data to a user's smartphone since a phone is likely kept nearby at all times. Both the transmitter and the receiver distance are required for a sensor placed on a farm. Applications' various demands give rise to the opportunity to approach the issue of communication range in various ways.

To address the issue of transmitter distance, techniques like FM backscatter make advantage of ambient RF signals that are already strong and have a wide area of coverage. This method makes use of ambient FM radio as the signal source, and the receiver is a standard FM radio gadget. Backscatter tags may now be used in outdoor settings without the need for a separate transmitter thanks to this configuration. The tags are also free to travel throughout a city-sized region without having to worry about going too far away from the transmitter. The backscatter tag's ability to put an FM stream on top of incoming FM-modulated audio is this project's major contribution. It is accomplished by using the frequency modification method described in the section titled "Tutorial on Backscatter Communication." The backscatter tag effectively adds FM to the already-existing FM signal by changing the frequency of incoming signals following the data to be injected. The signal is demodulated as conventional FM by the receiver, which also receives the injected data in addition to the original FM audio. Based on this technique, three operational modes are suggested: overlay, where an audio stream is mixed with an already-playing radio programme; stereo, where the stereo band of an FM radio station is utilised to accommodate reflected signal to remove interference to other radio stations; and cooperative, where two receivers cooperate to remove the original FM audio. This system can reach 3.2 kilobit/s at distances between 1.5 and 18 metres.

To handle both long transmitter and long reception distances, the LoRa backscatter design incorporates sophisticated modulation methods on backscatter tags. It is specifically the first

LoRa-based wide-area backscatter communication system. LoRa was selected because of its outstanding receiver sensitivity of 149 dBm, which is essential to combating both attenuations at the backscatter tag and substantial route loss. The backscatter tag converts the signal into a LoRa signal, which is subsequently picked up by a standard LoRa receiver device. However, creating CSS-modulated LoRa signals using backscatter tags is not simple. The backscatter tag must continually and smoothly adjust the frequency of the reflected signal since CSS employs chirps that linearly increase in frequency. Due to the all-digital control logic of backscatter tags, it could be challenging to accomplish such an operation.

Here, a novel backscatter tag design that blends analogue and digital circuitry to implement CSS is the main innovation that depicts the backscatter tag's layout. A DAC converts the continually rising digital signal produced by a low-power baseband processor into increasing voltage. The voltage is then sent into a VCO, which produces a square wave signal with a steadily rising frequency. The RF switch uses it to produce a CSS-modulated signal after that. To prevent interference between the original signal and the backscattered signal, the backscatter tag employs the frequency modification approach outlined in the "Tutorial on Backscatter Communication" section to transfer the reflected signal off the original channel. Additionally, in order to avoid the backscatter tag from interfering with nearby channels, this study suggests a method to remove harmonics produced while reflecting the signal.

To do this, a single-pole is another backscatter device that accomplishes both long transmitter and receiver distance. To create a single-tone excitation signal at 2.4 GHz or 868 MHz, respectively, in this system, an IEEE 802.15.4 or Wi-Fi chip is placed into a particular test mode. Custom hardware was used to create the receiver and backscatter tag. The system uses ultrasensitive narrow-band receivers by operating at a low data rate of 2.9 kilobits/s. Using OOK or FSK, the backscatter tag modifies data. The backscatter tag moves the reflected signal away from the excitation signal in order to prevent self-interference. One standout feature of the tag design is that the square wave signal used for FS and FSK is produced by an oscillator rather than an MCU or FPGA. Power is conserved, and the tag's design is made simpler. It can attain 3.4 km of receiver range at 868 MHz and 225 m at 2.4 GHz when the transmitter distance is 1 m.

The communication range is often exchanged for bit rate since it is closely related to receiver sensitivity. LoRa backscatter only reaches a data rate of 37.5 kilobit/s since it employs the LoRa modulation method, such as. The majority of alternative backscatter communication technologies sometimes have lower sensitivity while having substantially better throughput when using different modulation techniques.

Cost of deployment

A backscatter tag and (carrier) transmitter and receiver are included as supporting components in a conventional backscatter communication system. While the backscatter tag is often inexpensive and small, the transmitter and receiver are sometimes pricy and big, significantly raising the deployment cost. The market for backscatter communication is presently significantly smaller than that for traditional wireless technologies like Wi-Fi and Bluetooth, therefore manufacturers have less motivation to provide large quantities of low-cost supporting hardware. A typical

ultrahigh-frequency RFID reader, for example, weighs around 0.5 kg and costs more than US\$500, which is often beyond the size and price range of many IoT installations, such as smart home applications. RFID is the most developed backscatter communication technology. The majority of current advancements in backscatter technology rely on specialised hardware, such as software-defined radio devices or even their custom hardware, which may deter users due to the high initial cost, especially given the infrastructure already in place for conventional wireless communication like LTE and Wi-Fi. As a consequence, backscatter communication's practical acceptance is hampered by its high implementation cost.

It is desired to make use of the less expensive and widely available commodity devices and add to them the capability of a backscatter transmitter or receiver since it would be costly to construct specialised transmitter and receiver hardware for backscatter communication from scratch. Commodity wireless devices could include Wi-Fi access points or PCs with Bluetooth capabilities. Utilizing such devices may significantly minimise the deployment overhead since they are often economical and are already present in many situations where backscatter communication is to be implemented. Additionally, common wireless devices often use established technology, and over time, major technical efforts have been made to improve their performance. Many Wi-Fi chips, e.g., give great sensitivity as good as -80 dBm while costing only several dollars. Therefore, using these items has the added benefit of enhancing system performance.

Two major issues must be resolved in order to use commodity hardware as a backscatter transmitter/receiver. In order to properly inject data on an excitation signal delivered by common devices, such Wi-Fi or Bluetooth packets, and the backscatter tag must first be able to do so. Because backscatter tags cannot decipher the signal and must inject data blindly, this might be challenging. Second, a backscatter tag's modification and reflection of the signal need the commodity receiver to be able to interpret and analyse it. The difficulty is that common wireless devices often provide users with little control over the decoding process. Backscatter-tagged packets may be rejected or garbled during decoding, never making it to a user-space application.

Wi-Fi backscatter gives the means to inject data by changing the received signal strength indicator (RSSI) or channel state information (CSI) of the Wi-Fi. Almost all Wi-Fi chips provide RSSI data, and many of them also offer CSI data, which is a collection of complex numbers that shows how each subcarrier's amplitude and phase have changed over time. This system uses an Intel 5300 wireless network interface controller as the receiver and a common Wi-Fi AP as the transmitter. Continuous normal Wi-Fi packet transmission occurs between the transmitter and receiver. An RF switch is often used in backscatter tags to alter the antenna's impedance. The backscatter tag affects the Wi-Fi channel between the transmitter and receiver differently depending on its settings, which causes variations in the RSSI and CSI measurements that are recorded at the receiver and used to represent 0 and 1.

On the receiver, signal processing is employed to consistently identify changes in RSSI and CSI to recover data injected by the backscatter tag. The RF switch maintains the same state over numerous Wi-Fi packets to prevent interfering with packet decoding at the receiver. The system has a range of up to 2.1 metres and a throughput of up to 1 kilobit/s. An alternate strategy is

suggested in FS backscatter when low-level information, like RSSI or CSI, is difficult to acquire. The receiver listens to a neighbouring channel rather than sharing a channel with the transmitter. Incoming Wi-Fi or Bluetooth packets may be redirected by the backscatter tag to the neighbouring channel. The tag may transfer data by switching between shifting and not shifting. A communication range of up to 4.8 m is possible with FS backscatter.

Although Wi-Fi backscatter may utilise common Wi-Fi devices as the receiver, the Wi-Fi protocol itself is incompatible with it. The transmitter and receiver may both be replaced by common devices in projects that are compatible with the main wireless communication protocols. On a backscatter tag, convert a working Bluetooth signal to a working Wi-Fi or Zigbee signal such that a working Bluetooth radio may be used as the transmitter and a working Wi-Fi or Zigbee radio as the receiver. The essential principle behind this system is that, with a properly constructed payload, a commodity Bluetooth radio may emit a single-tone signal. Due to Bluetooth's usage of Gaussian FSK, a continuous stream of 0s or 1s is modulated into a single-frequency tone, making this conceivable. However, the payload has to be carefully planned to fulfil the aim of modulating continuous 0s or 1s. The metadata section of a Bluetooth packet is not a single-tone signal, thus an envelope detector is also employed on the backscatter tag to identify the beginning of a Bluetooth packet and assist in skipping it. The information for a legitimate Wi-Fi packet is created on the backscatter tag. DBPSK and DQPSK, two modulation algorithms utilised by Wi-Fi, are performed using the techniques described in the "Tutorial on Backscatter Communication" section. The tag changes the signal's channel from Bluetooth to Wi-Fi. Backscatter Zigbee signals from Bluetooth may be handled using the same method [9], [10].

Another project that works with a common wireless protocol is packet to another valid one while changing the content to inject data. Two commonly available Wi-Fi radios serve as the backscatter transmitter and receiver in this setup. The main advancement is a technique known as "codeword translation," which enables the backscatter tag to convert a legitimate 802.11b codeword into another one, allowing it to change certain bits in a packet while still enabling the receiver to read the changed packet.

A transformed codeword and an untransformed codeword, respectively, are used to represent the numbers 0 and 1. The receiver then conducts a comparison between the changed and original packets and an exclusive operation to extract the data that the backscatter tag has inserted. With the use of the backscatter tag's RF switch, code word translation is accomplished. There are only two legal code words that represent 0 and 1 in Wi-Fi 802.11b's 1 megabit/s DBPSK modulation, and one code word is the other's flip. The phase of the incoming signal must be reversed by the backscatter tag to convert one code word into the other. This may be done by using the phase modification approach mentioned above. The backscatter also moves the signal to another legitimate Wi-Fi channel so that the original signal and the backscatter signal do not interfere with one another. At 34 meters, the system is capable of 300 kilobits/s of throughput.

Other wireless technologies like Sigsbee and Bluetooth may also benefit from code word translation. They swap deployment costs for other objectives for projects that are incompatible with current technology. For instance, BackFi employs a special transmitter/receiver that enables

simultaneous emission of the transmitter and the backscatter tag. This increases spectrum efficiency, but new hardware is needed. LoRa backscatter needs a specialised transmitter to deliver a single-tone excitation signal. This makes it possible for the backscatter tag to create a CSS-modulated signal, greatly increasing the communication range. Battery-free mobile phones need a specific base station to broadcast an AM speech signal to the backscatter tag and to receive an FM voice signal from the backscatter tag, and it consumes just $3.48 \mu\text{W}$ in operation.

Backscatter communication-powered applications. We believe the widespread use of backscatter tags equipped with extremely low power or even battery-free capabilities will significantly reduce or even completely remove the current deployment barriers for many IoT applications, including universal localization, pervasive surveillance, and intrusive monitoring. The advantages of backscatter communication for these applications and the forthcoming research difficulties are discussed in more detail below.

In mobile/IoT sensing, location is increasingly becoming an essential service. The desire for monitoring is moving beyond wearables and smartphones to include everyday items like wallets, keys, and pill bottles. Prior research may be divided into two categories: active techniques, where the item of interest must emit signals at the milliwatt level and often carry a battery, and passive approaches, such as RFID, where specialised and expensive reader deployment is frequently necessary. It is feasible to use backscatter communication to attach these battery-free tags to any items and make them function with the current network.

The RSSI or CSI received at the receiver (such as an access point, for example) depends on the locations of both the transmitter and the tag, which makes it difficult to localise a backscatter tag. In an office building with common Wi-Fi APs, WiTag provides the first design to accomplish that aim. It calculates the angle of arrival from the tag to several APs and employs triangulation methods to achieve median localization errors of 0.92 and 1.48 m, respectively.

Ubiquitous monitoring

Wireless cameras are becoming more necessary and well-liked for home and workplace security, as well as for public safety. Sadly, they still need external power from outlets to operate, which keeps them from reaching remote locations like fabrication facilities. The deployment scope of wireless cameras might hit a new milestone by disconnecting both the Internet and power cables. Building a workable backscatter communication-based video surveillance system, however, presents several difficulties. The most glaring example is the incompatibility between the occasional kilobits per second that cutting-edge solutions may provide and the megabits per second streaming needed for the application. Additionally very difficult to do traditional codec and compression on backscatter tags with poor design throws open the door in this way. When situated 5 m from a typical RFID reader, its battery-free camera can produce a fresh 176 144 grayscale image that can be collected and sent every 15 minutes. Even 720p full-HD video streaming at 10 frames per second is supported by the most modern analogue video backscatter design up to 4.9 m away from the reader.

Backscatter communication can be particularly helpful in situations where sensor devices need to be instrumented in an invasive way because it may be able to eliminate the need for replacing

batteries and the extra high cost that goes along with it in some applications, like structural health monitoring (SHM) and implantable health-care monitoring (IHM). To be more precise, it is essential for large-scale infrastructure such as trains, pipelines, dams, bridges, and aero planes to undergo regular and effective SHM to ensure their safe and dependable operation. Early detection allows for appropriate action to be done in the event of damage or deteriorations such as corrosion and fatigue. Battery-free IoT systems with backscatter communication may solve the enormous labour costs and possible safety problems caused by human inspection today. IHM has various stringent demands for the design of implanted medical devices in biomedical applications. Rolling related Might reform permanently lay Inter reform Leading lay. Once again, backscatter is the perfect answer to meet all of these demands. Nevertheless, essential tradeoffs existing in power consumption, communication range, bit rate, and form factor need to be completely studied and respected by specialists from diverse areas when creating a backscatter system devoted to each use case.

One of the keys to getting a greater data rate on a backscatter connection is supporting an advanced modulation method. For instance, simulation and implementation have both been used to test the concept of OFDM-based backscatter communication. However, since OFDM employs substantially longer symbols, its throughput is limited. FreeRider's maximum throughput is 60 kilobits per second as opposed to HitchHike's 300 kilobits per second, which employs BPSK and shorter symbols. There is currently no effective backscatter communication architecture that can do that. To produce or alter OFDM signals for backscatter tags in a low-power way and to give a greater data rate, new approaches need to be created.

Full duplex and downlink

The present backscatter downlink design makes advantage of the low-power RF envelope detector and demodulates data that are inherently slow in rate due to the modulation method by looking for and measuring the existence and duration of the excitation signal. The low-power requirement, however, also makes it difficult to execute sophisticated digital signal processing on the tag and, therefore, an effective downlink solution. It would be ideal if the tag's receiver could handle modulation that is both effective and low-power. The tag could broadcast and receive at the same time (i.e., full duplex), which would be more effective and increase throughput overall given the constrained capacity of the present downlink designs. The main issue is that the downlink relies on intermittent patterns whereas the uplink needs a consistent excitation pulse. There is undoubtedly a fundamental trade-off at play here. A full-duplex architecture that achieves 1 kilobits/s downlink and 100 bits/s uplink between two tags has been proven in earlier work, which paved the way for more efforts in this area.

Multiple Inputs and Outputs

Multiple-input, multiple-output (MIMO), a crucial technology that is widely employed in today's wireless systems for performance improvement, is clamouring to be included in the design of the backscatter system from several angles. For instance, beamforming may successfully assist the backscatter tag in receiving a strong excitation signal. Another example is the possibility of using the diversity approach in a dispersed way to increase the bit rate and reliability of the tag-to-

receiver connection. Although the concept of MIMO backscatter has been examined in an analytical model, no real-world application has yet been made to show that it is feasible.

Numerous Access

As the backscatter communication mechanism expands to the network level, it is crucial to effectively handle multiple access. Recent research has shown that the physical layer strategy of parallel decoding is successful. Using parallel decoding, Laissez-faire showed support for up to 16 devices at an aggregate throughput of 100 kilobits/s, while Flip Tracer provides 500 kilobits/s for five tags. A rudimentary media access control layer is used by Free Rider at the connection layer to offer an aggregate throughput of 15 kilobits/s for 20 devices.

There has to be a more effective architecture that can sustain widespread implementation, however alternative means of communication. Visible light communication (VLC), which has enough spectrum and directionality and is sniff-proof, is always viewed as a supplementary alternative, even if the performance of radio communication is sometimes constrained by restricted spectrum resources. Passive VLC offers a cutting-edge design that achieves 1 kilobit/s by manipulating light retro reflection using a commercial liquid-crystal display shutter; nevertheless, it must also handle the difficulties for a greater rate, a larger range, and multiple access.

REFERENCES:

- [1] S. Darvish-Molla, K. Chin, W. V. Prestwich, and S. H. Byun, "Development of a compact and cost effective multi-input digital signal processing system," *Nucl. Instruments Methods Phys. Res. Sect. A Accel. Spectrometers, Detect. Assoc. Equip.*, 2018, doi: 10.1016/j.nima.2017.10.005.
- [2] K. Zhong, X. Zhou, J. Huo, C. Yu, C. Lu, and A. P. T. Lau, "Digital Signal Processing for Short-Reach Optical Communications: A Review of Current Technologies and Future Trends," *Journal of Lightwave Technology*. 2018. doi: 10.1109/JLT.2018.2793881.
- [3] K. B. Kim, Y. Choi, J. Jung, S. Lee, H. jun Choe, and H. T. Leem, "Analog and digital signal processing method using multi-time-over-threshold and FPGA for PET," *Med. Phys.*, 2018, doi: 10.1002/mp.13101.
- [4] Y. Salathé *et al.*, "Low-Latency Digital Signal Processing for Feedback and Feedforward in Quantum Computing and Communication," *Phys. Rev. Appl.*, 2018, doi: 10.1103/PhysRevApplied.9.034011.
- [5] Y. Xi, X. Tang, Z. Li, and X. Zeng, "Application of digital signal processing tools for the detection of voltage sag/swell," *Int. J. Electr. Eng. Educ.*, 2018, doi: 10.1177/0020720918754830.
- [6] K. S. Thyagarajan, *Introduction to digital signal processing using MATLAB with application to digital communications*. 2018. doi: 10.1007/978-3-319-76029-2.
- [7] E. S. Gopi, *Multi-Disciplinary Digital Signal Processing*. 2018. doi: 10.1007/978-3-319-57430-1.

- [8] R. Koma, M. Fujiwara, J. I. Kani, K. I. Suzuki, and A. Otaka, "Burst-mode digital signal processing that pre-calculates FIR filter coefficients for digital coherent pon upstream," *J. Opt. Commun. Netw.*, 2018, doi: 10.1364/JOCN.10.000461.
- [9] B. Baeuerle, A. Josten, M. Eppenberger, D. Hillerkuss, and J. Leuthold, "Low-complexity real-time receiver for coherent nyquist-FDM signals," *J. Light. Technol.*, 2018, doi: 10.1109/JLT.2018.2877479.
- [10] L. Lundberg *et al.*, "Frequency Comb-Based WDM transmission systems enabling joint signal processing," *Appl. Sci.*, 2018, doi: 10.3390/app8050718.

CHAPTER 11

IOT APPLICATION IN ANALOG AND DIGITAL COMMUNICATION

Ravendra Pratap Rana, Professor

Department of SOMFT, IIMT University, Meerut Uttar Pradesh, India

Email id-ravindra.rana777@gmail.com

Agriculture accounts for a large portion of the GDP in emerging countries. Agriculture includes a wide range of operations, such as growing crops (farming), harvesting wood, raising animals for home consumption, or use as raw materials in other industries. It served as the main antecedent in the development of humans. To fulfil the needs of an expanding population and advancing technologies, the agricultural industry is under tremendous pressure from an ever-increasing population. By 2030, there will be 8.5 billion people on the planet, and by 2050, there will be 9.7 billion. With more than 1 billion inhabitants, China and India account for 19% and 18% of the global population, respectively. India's population is anticipated to exceed China's. To provide a living for their expanding populations, many nations rely significantly on agriculture. The following are the main issues facing agriculture in rural and developing areas:

Farmers' poor economic standing. The price difference between farmers and consumers for the same commodity. The difference between what farmers are paid and what buyers pay has grown as a result of third-party involvement. Climatic change has an unanticipated negative impact on agricultural practices and results. The absence of technology in agriculture is either a result of access issues, costly installation and maintenance costs, or a lack of understanding.

IoT is a network of connected computing devices, mechanical and digital machinery, items, animals, or people that may exchange data across a network without needing human-to-human or human-to-computer contact. The usage of WSN identifies the optimum choice since fields are dispersed across a vast region in agriculture for farming or animal viewing. Because of their low power requirements, stationary nodes may run on batteries or solar power. Since they need a lot of power and are less numerous than sensor nodes, actuator nodes are linked to personal area networks (PANs). Using an existing local area network (LAN) and the internet, this system as a whole may be incorporated into an IoT-based system. Cloud-based data analytics software that supports this hardware architecture enables field node monitoring and management from a distance.

Therefore, IoT may significantly improve the roles and functions of every aspect of farming and agricultural. IoT can connect the whole system into a cloud-based system, from livestock raising to horticulture. Each animal and field area may function as a node in an IoT system, and the system can store information about their condition and performance metrics. This data may be utilised to adjust and monitor a variety of performance metrics in real-time, including crop and field temperature, humidity, nutrients, and field moisture. The tags on animals and cattle also aid in tracking their feeding schedules, movement patterns, and health statuses. The field resources may be managed to make the most use of what is available. The major benefits of IoT in agriculture and farming in underdeveloped countries are the cost-effective technology for the

development of agricultural processes and systems. The following are the key benefits of IoT integration in agriculture:

- i. It increases farmers' production, quality, and profit by educating them about agricultural conditions, and it makes effective use of the resources at their disposal.
- ii. Real-time information about the environment, animals, and crops enables quick action to increase productivity
- iii. A suitable cash crop or a suitable crop breed.
- iv. Correct fertilizer dosage and timely application.
- v. Controlled irrigation for the best use of water resources, including drip irrigation when and where necessary.
- vi. Early illness and malfunction detection to help with issue isolation and repair.
- vii. The record of climate change may aid in keeping greenhouses in good shape.
- viii. The recorded data may be reviewed to pick breeds, crops, and animals that will benefit most from the environment and resources that are now accessible. The raw materials and resources utilised may be tracked and audited, allowing for further optimization.

The system may be connected with regional, national, and worldwide organisations that support farmers and agriculture so that they are kept abreast of new developments in agricultural technology, systems, and programmes. The market may be coupled with cloud apps so that farmers can get a fair price for their goods. The integration of farmers and consumers into one system may be beneficial. IoT offers scalable, affordable technology that farmers may implement into their systems based on their financial situation, such as the number of WSNs, the length of drip irrigation, and the number of animal tags. This work examines IoT-based farming and agricultural systems via observation and analysis of published publications.

This study provides a proposal for a scalable Internet of Things system for agriculture and farming that may be deployed in underdeveloped countries while taking into account the existing technological, economic, and utility infrastructure. We examine variables to be monitored and variables to be controlled with their control mechanisms for the monitoring and control of agricultural systems, the Green House, open agriculture, and farming using wireless sensor networks (WSNs). IoT system comprises IoT hardware, communication system, data storage and central control units.

For the measurement and management of agricultural factors, it comprises sensor and actuator nodes. Actuator nodes and WS nodes are programmable and embedded system-based devices. The fundamental component of every wireless sensor network is the WS node (WSN). A wireless sensor network is made up of many sensor nodes that are dispersed around the application area and connect via radio-frequency signals. The following is a list of the WS node's functions.

1. Perceiving
2. Data gathering (Sensor to Signal Conditioner to ADC)
3. Data processing (Logical operation for sending data)

4. Data storage (retention of data before transmission to the base station)
5. Wireless communication (radio frequency) (Signal Transmission Medium)
6. Local and internet data networking

Sensing capabilities, data processing capacity, data storage capacity, unlicensed radio-frequency band communication capability, low power consumption, small size, and low cost are common design criteria for a wireless sensor node. Embedded hardware and software components make up a WS node.

A WS node's front end is made up of sensors. Real-time physical variables are sensed, and they emit analogue electrical signals. Smart sensors are often favoured over traditional sensors because of their built-in signal conditioning circuits, compact size, low power consumption, and excellent operational dependability. DAQ unit is consisting of signal conditioner and an analogue to a digital converter (ADC). To make analogue electrical signals from sensors compatible with the ADC, signal conditioners process or condition the signals. A multi-channel ADC then transforms the conditioned analogue signals into corresponding digital signals. It may not be necessary to do further signal conditioning on a smart sensor (as opposed to a standard sensor) with conditioned analogue output. The usage of a smart sensor with a digital output eliminates the requirement for an ADC for that sensor [1], [2].

A microcontroller, programmable digital signal processor (DSP), field programmable gate array (FPGA), or application-specific integrated circuit (ASIC) are examples of data processing devices. These devices are selected based on their flexibility, performance, cost, and energy efficiency. The incoming input and intermediate results of the calculation are stored in a small (4kB) RAM. An antenna and radio-frequency (RF) transceiver make up the communication unit. With other nodes and the station/gateway node, it is utilised to exchange data. It translates radio waves into bit streams coming from the DPU and vice versa. In most cases, a half-duplex, ISM-RF based, low-cost, low-power, short-range transceiver with energy-saving states is employed with difficulties with the physical and media access. All other components in the node are powered by the PSU (power supply unit). It is an essential part of the WS node since it determines the node's lifespan. Typically, a PSU is made of a battery and a DC-to-DC converter. The battery should have a sufficient capacity, a high energy density, be light in weight, and have a low self-discharge rate. Rechargeable batteries have sometimes been used in conjunction with photovoltaic (PV) solar cells.

The voltage of the power source is controlled by the converter. As it powers the node hardware, software is a crucial component of a WS node's architectural design. The following tasks are performed by the node software: Data capture, signal processing, in-network computing, data compression, error control, encryption, data transfer, and network routing are just a few of the processes that are involved. Numerous modules make up the programme, and they range greatly in complexity. The significant ones are covered below. Because it offers the foundation for creating any programme and frees the developer from the microprocessor's machine-level capabilities, the operating system is a necessary piece of software. All other software modules utilise it as well to provide a variety of purposes. The following list includes desirable operating system characteristics. Because sensor nodes have limited memory, it should:

- a. Be compact in and of itself;
- b. Enable speedy implementation;
- c. Ensure minimal application code size.

The onboard sensors and actuators may perform a variety of tasks thanks to this software module. It makes it easier to establish and configure on-board sensors and actuators. It shields the application programme from these devices' machine-level functions. Each node in the agricultural system has to be linked to a communication network to measure and regulate the system. To monitor and operate systems, data must be exchanged between sensor/actuator nodes and the data storage and processing unit. The sensor nodes are ideally wireless since it is beneficial in required application areas, including:

1. Where sensors are positioned in inaccessible or difficult-to-access locations
2. Where sensors are either mobile or portable
3. Where a sensor network must be deployed quickly. Where sensor nodes must be networked ad hoc.
4. So, for implementation of WSN, we consider unique criteria as. Low latency or minimal end-to-end delay . High data security
5. Superior network safety
6. 4. Efficient energy use or extended battery life
7. Use of the ISM frequency band
8. A low data rate or bandwidth is sufficient

We can use current communication technologies to satisfy WSN's criteria. We take into account the following procedures among the potential technological choices. Zigbee technology meets the measuring and control demands of agriculture (automation). Zigbee complies with the "Low-Rate Wireless PAN Standard" requirement of IEEE 802.15.4. Only the Physical and MAC layers are defined by IEEE 802.15.4. Networking of stationary, mobile, and portable devices is supported by Zigbee (sensor nodes). Wireless sensor and actuator networks have specific needs in terms of low latency, low bandwidth, long battery life, and high data security. Due to the low data rate, it is not appealing for corporate communication networks. Below is a list of Zigbee's primary features [3], [4].

1. It typically starts all network communications.
2. Sends a beacon using a beaconing system for "periodic data transfers"
3. Below is a list of Zigbee's benefits.
4. Low power consumption, low latency, low complexity, low message overhead, and low cost. Small bandwidth.
5. Zigbee's limitations are:
6. Low data rate and limited range
7. A central control unit and data storage unit.

In farming and agriculture, we must track and measure massive, dynamic, geographical, and temporal data that must be processed and stored in databases. The WSN just formats and timestamps data that may be in the form of numbers, photos, text, audio, or video and can be

either organised or unstructured. To prevent the data processor from using additional battery power, this is being done.

In the central control unit, complicated calculations and logical calculations are performed. Time series of data from sensors may be saved in the cloud using Influx Data, which is integrated with cloud-based IoT systems as Google Cloud IoT core. This facilitates real-time decision-making using IoT sensor data and increases operational efficiency for users. For Google Cloud IoT Core, Influx Data offers the data services layer, which enables customers to gather time series data for instrumenting, watching, learning, and automating any system. WSN may either update the cloud database directly or transmit the data to a user application for further processing. Node-red may be utilised in a central control unit or PC as a web service, independent programme, or user interface.

Remote access to the time series data visualisation is made possible through web services. Edge or fog computing at the gateway/ base stations of every WSN offers data-stream acceleration, including real time data processing without latency for critical application. It eliminates lag time and enables smart applications and devices to react to data virtually instantly, as it is being generated. The node-red programme offers data analytics, control logic implementation, and data visualisation.

Therefore, we explore a WSN using the Zigbee protocol, a user application built on Node-RED, and an InfluxData time series database for the implementation of an IoT system in agriculture. The actuator system is built on a low latency PAN with a Master Slave configuration using a simple MAC protocol. This solution took into account the needs of IoT-based agriculture. Battery-operated mobile sensor nodes are small and have minimal power requirements Ad-hoc network with simple sensor node insertion and removal High-level network and data security .We propose RS-485, or the Foundation Field Bus, as the wired network for actuator networks as actuators are high powered and have wired power supply connections. IoT SYSTEM DESIGN The IoT use in agricultural and farming systems may be divided into two categories: monitoring systems and control systems. The main sectors include surveillance, tracking, and tracing, farm equipment, precision farming, and greenhouse farming.

Therefore, the monitoring and control systems are integrated into the Internet using a single workstation. A local and internet-based database (Influx Data) as well as a control system are maintained by the workstation PC (node-red system). A standalone programme may be used for internet-based remote access to the machine. Overall smart phone system the hosting of software as a service in the cloud is possible with cloud computing. The system software application integrates a database for tracking crops and livestock in farms, controls for the appropriate variables in fields and farms, analyses of weather and climate reports, and market status trends to determine which crops are both economically viable and well-suited to the climate and soil conditions. The following programme is a smart app that uses database data. Figure 4 displays the system in its entirety.

1. Data visualisation for plant and soil conditions, greenhouse and outside air temperatures, cow behaviour and health, and other monitoring factors.
2. Remote management of the variables to be managed.
3. Inform farmers of market conditions to keep supply and demand balanced.
4. Alert the weather prediction for backup preparation.
5. Notify farmers if animals on the farm are unwell, unusual movement pattern, feeding schedule, health checkup schedule.

Inform users of the items' availability at the appropriate farmer's depot. Users may request certain crops to be farmed or conduct online transactions with farmers. They include huge analytics, real-time, off-line, memory-level, and business intelligence level. The statistical reading of data via trends, maximum and lowest values, mean, and standard deviation of data from various sensors are all included in the data analysis process. The use of image processing in data analysis involves the collection of data as images using vision systems (camera). In order to identify any irregularities in plants, such as dead leaves, stems, or fruit, fruit quality, weed identification, and irrigation significant image processing is used. The usage of drones has expanded the potential for image processing for early crop failure detection, animal status monitoring, and environmental mapping. Numerous techniques are used in data analysis, including statistical analysis, classification, clustering, and trend analysis. These analyses' findings may assist farmers with insurance, forecasting, decision-making, tool use, store management, and general agricultural operations.

1. IoT enables the analysis of the gathered weather data and allows for the mailing or texting of alerts to farmers about potentially harmful events since the weather is unpredictable. Farmers may then decide whether to implement a backup plan or safeguard their crops against possible damage.
2. Animal footprints may be monitored, allowing researchers to determine if cattle are present and within permitted boundaries. If any unusual animal movement is seen, farms may be contacted.
3. Real-time data is easily accessible on the internet and in the cloud, so if farmers have insured their system, this information may be utilised to create insurance claims and speed up the processing process.
4. Prediction i. Statistical data and data trends may be utilised to gauge the state of the environment.
5. Future situations can be forecast using machine learning methods.
6. Market and environmental data may be used to anticipate the crops that will be grown year after year.
7. The use of dynamic irrigation for efficient water resource management.
8. It is possible to forecast fire, disease, and drought before and during crop production, which will aid farmers in disaster management.

To make decisions, we need precise and appropriate data from sensors that are updated in time series databases. Agriculture decisions may be made on a short-, medium-, or long-term basis. When soil moisture falls below the threshold, using drip irrigation is an instant and short-term

choice. Applying nutrients and using lighting systems are short-term fixes that are dependent on the present scenario and are intended to promptly notify farmers when cattle stray outside of their property lines.

Analysis of patterns in dead leaves and animal movement to assess plant and animal health and determine if they are alive or dead aid in making an accurate action plan. The farm's plants and animals have been evacuated, and the surrounding area has been neutralised to lessen the danger of disease transmission. In a greenhouse, machine learning may be used to determine the best temperature, humidity, and luminosity level for a plant's development, together with the right quantity of nutrients. Demand and supply chain data analysis helps farmers decide which crops to prioritise. Farmers may choose crops and prepare for emergencies by using their knowledge of crops, pests, and diseases. The system is connected with government organisations that support agriculture, enabling the implementation of government programmer and subsidies for crop and animal selection in farms.

Using the right tools and using them effectively are both crucial for increasing production and product quality. If they are not used when necessary, they raise fuel and maintenance costs while decreasing the effective man hour on the field. Data analysis of the soil's moisture and nutrient content in relation to the crop that has to be planted helps to determine which operational equipment and tools should be utilised in the fields. We can also keep track of the machines and tools utilised, as well as the correct and timely maintenance of the tools that are in use. The usage of tools may be maximized by performing selective management of nutrients, moisture, weed, and insect control.

Different agricultural goods need to be kept. This includes beginning raw materials such as seedlings, nutrition containers, medical supplies, animal meals, agricultural equipment and replacement components, as well as completed or harvested goods. In addition to rodents and microorganisms that may contaminate food items, temperature and environmental factors have a significant impact on food quality. Therefore, IoT adoption may enhance store management of all items, particularly completed food products. Using WSN to monitor store and warehouse conditions may assist to keep them in good shape. Depending on the state of the store, the temperature regulators, rodent and microbial control system may all be adjusted. The supply and demand for goods, tools, and replacement parts may be balanced. Farmers may maintain effective and efficient stores with the use of data analysis of work operation in the field, components tracking in the system, market demand, and environmental condition. Security systems coupled with the IoT assist prevent abuse and theft of items.

The monitoring and administration of the farm are part of the overall farm management system. The degree of system integration where operational as well as preventative activities are carried out utilizing software includes the database collection of agricultural data. The programmer includes market trends, consumer e-commerce, and governmental legislation, all of which may be studied together with agricultural factors for the best farm management that maximizes output and profitability. In order to increase productivity, risk management, cost, and productivity yield must be appropriately handled using real-time information. A large number of farms may be incorporated into a farm management system integration at the software level, which supports

the ongoing needs of the farming community. The system may assist the government in revising agricultural policy.

IoT adoption in agriculture is highly positive, however there are obstacles to overcome before the system can be used effectively. The system incorporates market, consumer, and governmental policy integration at the software level as well as internet monitoring and control system integration. The difficulties mostly result from economic and technological problems. These elements have slowed the adoption of IoT-based agricultural systems. The following is a discussion of economic topics.

1. Both capital and operating costs are necessary for the development of an IoT system. The price includes the cost of the hardware (IoT devices, cables, sensors and actuators, base stations, PCs, and power supply systems), the cost of the software (design and implementation of a cloud-based system for monitoring and control), the cost of running spare parts, the cost of using the internet and cloud services, the cost of energy, and the cost of maintenance.
2. Therefore, farmers should be content with the breakeven point, which is the point at which they can start making money from the system they have put in place.
3. According to Turgut and Boloni, the IoT must meet two requirements in order to be successful. Customers must first be convinced that the value provided by IoT devices outweighs their physical and privacy disadvantages. Second, IoT-related firms will profitably turn a profit.
4. Adding additional actuator and sensor nodes will increase the cost.
5. Adding features and services to the programme will raise system costs as well.
6. Despite the free limited subscription model for small systems offered by IoT cloud service providers, bigger systems and data privacy come at a higher cost that is managed by service providers.
7. The necessary internet service may have a low bandwidth or be too expensive for a larger bandwidth.
8. It is not permitted to build an online banking system for quick and simple transactions between farmers and clients or suppliers.
9. The following technical issues are covered, particularly in underdeveloped countries.
10. Internet service is not widely available throughout the nation.
11. Alternative options, such mobile internet services, have capacity restrictions or are too expensive.
12. In poor countries, the governmental software system is not regularly or sufficiently updated with the most recent information.
13. Most farmers in poor countries lack formal education.
14. As a result, they find it challenging to run and integrate IoT-based systems.
15. v. The functioning of the Internet of Things has been hampered by a lack of technical staff since solutions are not readily accessible and all gadgets must be imported.
16. vi. There is a risk that IoT devices may be stolen, damaged, or vandalised.
17. A cyberattack to steal vital agricultural data might target the internet-based system.

18. There are several technologies on the market, but no service providers adhere to a defined system configuration. Thus, system installation, growth, and upgrading may be challenging. Lack of an e-commerce system, an internet-based market system, consumer online payment capabilities, and a mapping system.

This study examines the design and implementation of an IoT-based agricultural system. IoT and data analysis are crucial for successful and productive agricultural methods, as has been shown. The design and presentation of the WSN nodes and their internet connectivity. Also covered is the efficient use of the control system's available systems. This study recommends using cloud-based services, particularly for data databases including information from various sensor and actuator nodes. This study suggests the use of a time series-based database and a node-red-based application for control and visualization on the software side.

It stresses the relevance of data and its analysis for optimal operation of the farming, the importance of customer \and farmer interaction to remove middle man and maximize the profitability for farmers. Its successful implementation in developing countries where agriculture is the mainstay of the economy presents a number of challenges, nevertheless. The agricultural industry has a bright future for the IoT system since it is a natural fit for it. The government must update its policies for improved system utilization and ease of integration. The government should assist farmers by creating a minimum internet infrastructure and making its plans and policies for agriculture available. The two fundamental constraints are price and system expertise.

The government should recognize the value of the data that an IoT system may provide and encourage farmers to do the same by offering more affordable financing and easy access to IoT equipment and services. To make greater use of the system, farmers should be educated, and vocational training programmer should be created. The idea of online payments and e-commerce is spreading quickly in developing countries, which will help with the integration of IoT systems in farming. There is more research being done on IoT systems, and these systems will provide the best IoT solutions for the agricultural industry.

IFF systems are the primary source of air traffic data in the airspace control system. The IFF system enables independent airspace monitoring, which entails locating an air object (AO) utilising ground-based infrastructure. The examined information tools' membership in cooperative surveillance systems is established by the employment of an aircraft responder to provide response signals required for determining the position of AO in a ground requester.

Identification systems' informative job is to ascertain the owner of a detected AO using the "friend or foe" characteristic. IFF systems are a subset of asynchronous two-way data transmission systems and are made up of a number of transmitters and receivers that operate in several frequency bands. This enables us to draw the conclusion that IFF systems constitute a non-synchronous information network by virtue of their design. A request channel and a response channel make up an IFF system's two data transmission channels. The aircraft responder (AR), an open single-channel queuing system with rejects, is the most susceptible and has major security flaws [5], [6].

This shows that despite the use of contemporary IFF technology and despite the fact that much research effort has previously been made in this field, aircraft identification remains a challenge. In fact, the construction of AR based on the idea of an open single-channel queuing system with refuses offers numerous opportunities for the interested party, including the suppression of them by establishing intentional interference at the necessary level of intensity as well as unauthorised use of AR information.

The transmitters of IFF systems produce discrete signals $s_i(t)$, belonging to a finite set—an ensemble $S = \{s_i(t); I = 1, 2, \dots, V\}$ —and transmit them asynchronously, independently of one another, at time intervals set by the signals themselves to the transmission line of request signals and response signals. In this instance, the condition $t_i \leq T_p$, where t_i is the signal duration and $s_i(t)$ is the repetition period of request signals, is often met. The functioning of such systems under the effect of deliberate as well as intra-system interference is hampered by the use of a single channel for sending request signals and the development of a full monitoring system based on the theory of an open queue system with rejects.

However, it should be noted that the operation of IFF systems in the frequency band of data transmission of cooperative monitoring systems (1030 MHz channel for transmitting request signals; 1090 MHz channel for transmitting an information packet) results in significant challenges, which is noted, in particular.

The system's architecture results in a considerable density of intra-system interference in the request and answer channels, which significantly reduces the noise immunity of the IFF systems under consideration in terms of Interference Immunity Assessment Identification Friend or Foe... 289. The papers presented demonstrate that there are significant spectrum overloads in the frequency band 1030-1090 MHz that is designated for air traffic surveillance and that is used by cooperative surveillance systems, collision avoidance systems, and ADS-B systems. Alternative techniques for using variable query powers with respect to azimuth sectors and tracking data are presented aircraft to lessen spectrum overload. It is demonstrated that a high probability of overlap prevents the 1090ES signal from being properly decoded and that the use of the 1090 MHz aerial surveillance frequency band with an expanding number of aircraft, applications, and equipment types can cause intra-system interference to reach critical levels. All protocols allow for some amount of data loss owing to overlapping messages or message distortion, but there is fear that as message density rises, this performance loss may eventually become intolerable.

According to the construction principle, the networks of IFF systems are non-synchronous, which means, firstly, there is no time synchronisation between the radiation of individual requesters by aircraft responders and, secondly, there is no time synchronisation between various Identification friend or foe systems. Airborne responders of IFF systems make use of single-channel queuing systems (QS) with servicing of the first properly received request signal in line with the concept of service of request signals. Therefore, in accordance with the construction idea, IFF system responders link to QS with rejects. The fundamental feature of these systems is that AR shuts for a predetermined period of time, known as the paralysis time t_p , while serving a successfully received request signal. The period of time is determined by the IFF system's paralysis mode (simulation resistant or non-simulation resistant). The existence of AR paralysis

time restricts the throughput of both the identification friend or foe system as a whole and the aircraft responder specifically. As a result, the chance of an air object being detected by the requester P_s , which is defined as the probability of obtaining the necessary number of answer signals to reply to requests from this requester, may be used as a characteristic of the noise immunity of the IFF system. The availability factor of the aircraft responder P_0 , which is the likelihood that the aircraft responder would emit a response signal in response to a certain request signal from the requester, serves to determine the capacity of the aircraft responder IFF system.

The responders are a component of open queuing systems since they service any validly received request signal, even those supplied by interested parties. The aircraft responder may be categorised as a single-channel open queuing system with rejects due to the availability of just one channel for service request signals and the potential for paralysing an aircraft responder when servicing request signals are present.

As a result, the concepts of are used to construct IFF systems, and these principles heavily influence the latter's poor noise immunity. Using the justification presented above, it can be concluded that identification friend or foe systems transmit data in a query-response fashion. Actually, they have a channel for signal transmissions that are requests, as well as a channel for signal transmissions that are responses. The considered information systems' construction methodology, which is based on the idea of an open single-channel queuing system with faults, permits both allowed and illegal usage of airborne IFF systems.

The IFF system's guiding principles include creating responders to gather data and disable the latter by establishing correlated (in the request channel) interference at the required level of intensity. Low information security of the systems under consideration is caused by such a construction philosophy and a service signal request principle. Additionally, the signals used for information encoding in IFF systems were not totally effective. In fact, the information capacity of data transmission channels and the noise immunity in generally thought-of IFF systems were both severely lowered by the adoption of primitive time-interval and location codes.

The IFF system contains the following operating modes, which are separated into non-simulation resistant and simulation resistant. The primary mode while functioning in times of peace is Mode 1, which is intended to ascertain the state affiliation of air objects. The request signal has two pulses of the mode codes P1 and P3, making it the simplest time interval code. To is a 3 s mode code distance. On demand, impulse P2 acts as a side lobe suppressor.

The second mode is intended for the unique identification of aircraft, military installations, or certain numbers of important infrastructure. The request signal's coding distance is $T_k = 5$ s. The primary mode of operation during a conflict is Mode 4, which is created for imitation-resistant identification of military installations. Closed coding provides simulation resistance regarded mode. The request signal consists of a side lobe suppression pulse (SLS), a four-pulse synchrony group (SG), and a 32-bit information code (IC). A crypto computer forms it in the requester and processes it in the responder. An anti-interference pulse (AIP) is introduced if there are no pulses at neighboring places. Passive pause encoding is added to the response's fixed

three-pulse pulse-time code. A cryptographic technique establishes 16 values with a precision of 4 s for response delays.

When a P2 pulse is detected in any operating mode, the aircraft responder is paralysed for 35 s and unable to receive request signals. This is because the P2 pulse indicates that the signal is coming from the requester's side lobes.

Depending on the service of the request signals of simulation-resistant or nonresistant operating modes, the aircraft responder is paralysed for a large amount of time when a request signal is received and the side lobe suppression signal is not recognised.

The Mk-12A next generation identification system, which further employs the simulation resistant mode of operation (Mode 5) [46–50], is now being installed in the aircraft of NATO nations. The characteristics of Mode 5 mode signals include a reference group of pulses (sync groups) with time-pulse modulation, which establishes the identification sub-mode, frequency modulation with a continuous phase (CPFSK, MSK—Minimal Shift Keying) of preamble pulses, and side-lobe suppression by a 16-bit Walsh sequence used in decoding an information group. Analytically, the M5 mode request signal may be stated as follows:

Specifically, $\cos 2\pi f_s t + b_i(k) 2T + I t_0 t t_0 + N T$ time-domain Walsh sequence representation of the RQS impulse that has been frequency-modified; The parameters of the signal are as follows: u_m signal amplitude, t_0 signal start time, $N = 16$ signal elements, T signal element (parcel) duration, f_s signal carrier frequency, $b_i(k) = \text{sgn}(\text{wal}(k, I \text{ sign of the } i\text{th element of the parcel in the time interval } [t_0 + I T, t_0 + I + 1)T])$, $\text{wal}(k,)$ Walsh function under number k , which is defined on the moment values are produced at a dimensionless time. beginning phase of the signal; modulation index = f ; $b_i(k) 1; 1; I = 2 I 1 j=1 b_j (i1) 2 b_i + s$; $s f$ is the frequency spacing; $T = 0.5$. The following is a representation of the preamble pulses:

$g_k(t) = L 1 n=1 a_k(n)p(t nT)$, (2) where $a_k(n)$, $0 n L$; $p(t)$ impulse of time nT coding pattern that establishes the timing of the preamble pulses. Therefore, time-interval codes and position codes which are characterised by simplicity and low noise immunity, respectively are utilised as the request and response signals in IFF systems. In fact, errors such as omissions, false alarms of the first and second kind, or a mess of the request signals are immediately caused by the suppression by interference of at least one pulse of the request signals or by the appearance of false pulses on the code intervals of the request (response) signals.

The request signal for IFF systems looks like this:

$s_i(t) = U_i f_i(t) \cos(\omega t + \phi_i)$, (3) where $f_i(t)$ is a binary coding sequence that may only take values of 1 or 0; "ones" represent impulses and "zeroes" represent pauses in the signal $s_i(t)$ and this sequence; In the typical situation, each pulse in the coding sequence has a distinct carrier frequency and a random beginning phase of high-frequency filling; the amplitude factor U_i remains constant during one complete realisation of this signal. The whole ensemble of signals S consists of K different signals, each with a similar carrier frequency ω and only slight differences in the coding sequence $f_i(t)$, as determined by the number of operational modes of IFF systems. The requirement for the sufficiency of the request signals states that all request signals of the

relevant information systems must have the same pulse length I and pulse count n . Interference Immunity Assessment Identification Friend or Foe... 293 specifications. The code value of the request signal is the quantity of pulses in the code.

Let's assess request signal noise immunity while accounting for the many types of purposeful and accidental interference that might exist in IFF systems.

The interference associated and uncorrelated with the current set of signals is the principal detrimental consequence that reduces the noise immunity of the examined signals and, subsequently, the considered information tools in general. It should be emphasized that such interference may be created by the interested party (deliberate) and happens both inside IFF systems (intra-system). The following primary forms of signal receiving faults may happen when request signals are received asynchronously: Request signal not received; first- and second-kind false alarms; and missing request signal. Thus, P_p , F_1 and F_2 error probabilities must be used to determine the noise immunity of IFF signal systems. Then, based on the uncorrelated interference in the request channel, it is important to evaluate the noise immunity of the request signal in Identification friend or foe systems. We presume that the interference under consideration is stationary. In addition to being statistically and structurally independent of the considered request signal, it has no aftereffect. The detection threshold for the request signal is equal to k , it has an uncertainty function of R , and it consists of n elementary pulses.

$P_p = \sum_{i=k}^n C_i^n P_i^{i-k} (1 - P_i)^k$, (4) where P_{10} is the probability of suppression by the considered interference of at least one pulse of the request signal, which is determined by the type of interference and its intensity. In this case, the probability of missing a signal is the conditional probability that when receiving a request signal will be suppressed by an interference of at least $n - k + 1$ pulses. False alarm probabilities are a bit more intricate. In reality, a fake combination with k or more interference pulses must arrive at the decoder input in order for the first kind of fictional alarm to occur, and the decoder under consideration must also decode this false combination. The likelihood of such an occurrence may thus be calculated as $F_1 = \sum_{i=k}^n C_i^n P_i^{i-k} (1 - P_i)^k P_d$, (5) 294 I. Svyd et al.

Where P_d is the likelihood that the decoder will successfully decode the considered i —pulse combination, and P_{01} is the likelihood that a false pulse will be detected at the decoder's input during the time period. When calculating the likelihood of a second false alarm, we will take into account the likelihood that at least one second false alarm will occur when the signal is being sent through a decoder. Since the arrival time of the received signal will be precisely defined within the pulse length, the reciprocal will in this instance provide the conditional probability of the occurrence. As a result, using this kind of question formulation, $F_2 = 1 - R_{s=1} [1 - F_2(s)]$ may be used to quantify the likelihood of a second sort of false alarm. $M(s)$, (6) where $F_2(s)$ is the probability of forming and decoding a false combination of the second sort made up of interference pulses ($k \leq i \leq n$) and signal pulses that yield one lobe of the uncertainty function equal to s . $F_2(s) = \sum_{i=k}^n C_i^n P_i^{i-k} (1 - P_i)^k P_d (1 + 1)^s$, (7) where $M(s)$ is the quantity indicating how many side lobes there are in the uncertainty function with value s .

Therefore, the aforementioned expressions (4) through (6) create a system of three equations with three unknowns n , k , and R for the provided values of P_{10} , P_{01} , and the specified upper bounds of error probability P_p , F_1 . Once this formula has been solved, it is possible to determine the rational values of these signal parameters, such as the lowest n , maximum R , and corresponding k ($R \leq k \leq n$), where the error probabilities do not go over the specified upper bounds.

Real-world circumstances often involve dealing with random impulse noise and fluctuation, two types of uncorrelated interference. On the basis of feasibility and applicability, it can be shown that chaotic impulse noise is the primary kind of purposeful interference to IFF systems. The sort of intrasystem interference that makes up the majority of this interference is found in the information systems under consideration. Let's calculate the likelihood of the event P_{10} and the occurrence of chaotic pulse interference in the request channel.

The Poisson stream of single pulses is most often used as a model for the chaotic pulsed interference flow. (For fluctuation interference, the Poisson flux of single pulses is the same idealisation as regular noise.) In this instance, $P = 1 - \exp(-\lambda t)$, (8) Interference Immunity Assessment Identification Friend or Foe... 295 where λ is the level of chaotic impulse noise, determines the likelihood of at least one pulse appearing in the time period t .

As a result, $P_{01} = 1 - \exp(-\lambda t_0)$ may be used to determine the probability P_{01} . (9) The relationship $P_{10} = 1 - \exp(-\lambda p) [1 - (1 - \exp(-\lambda p))]^{10}$ can be used to calculate the probability of suppressing one pulse of the interfering request signal. Here, p is the time at which the receiving device becomes paralysed after experiencing an interference impulse, and is a coefficient that determines the likelihood that the received signal pulse will be suppressed by interference when it occurs at the

As a result, the relation (10) considers both the inertial and interferential kinds of suppression that may occur in systems with considering pulse signals. The first suppression results from elements with a non-zero sensitivity restoration time being present in the receiver, and the second suppression is caused by the interaction of the high-frequency fills of the signal pulses and the considered interference when they overlap in time. The ratio of the amplitudes and phases of the interfering oscillations determines the coefficient. It is often believed that is 0.2 when the phase difference has a uniform distribution in the range.

In a packet of served request signals, there are N total response signals; a k -digital threshold is used to decide whether to detect (identify) an AO. The decision to use the quality indicator under consideration is consistent with the general trend to solve the AO identification problem by having both the primary radar and the IFF system detect the AO, which requires the joint processing of data by the under consideration information tools

When two things happen at once, the ground requester will get a response signal from AR: AR will receive the request signal, correctly decode it, and emit a response signal (the probability of this happening is equal to the AR availability factor P_0); The AR response signal will be picked up and detected by the terrestrial radio interrogator. The possibilities of these two occurrences occurring simultaneously will next be examined, along with their probabilities in the presence of interference.

Evaluation of Interference Immunity for Aircraft Responders' Friend or Foe Systems

Assume that the CIN stream, the stream of deliberate correlated interference from the interested party, and the RS stream of nearby IFF systems make up the general interference stream (intentional and unintentional uncorrelated interference). We will do calculations for the "friend or foe" principle-based "friend or foe" operating modes of IFF systems and for the current detection algorithms of AO IFF systems.

Because of the RS stream's effect, AR becomes paralysed for a period of time that depends on the request type mode. We will see that the AR is entirely paralysed for the length of the service while receiving RS on the requester's primary antenna pattern. When RS is received from the requester's side lobes of its antenna pattern, AR is rendered paralysed during the interval between the RS pulse's remembered amplitude and the SLS pulse.

Intentional or intra-systemic CINs have a bilateral impact on how AR works:

- a. First, it blocks individual RS pulses, making it difficult to service the contemplated RS; second, it paralyses AR by forming fake RS (false alarm of types 1 and 2 alert).
- b. Let's assess the AR availability factor when the mentioned interference is present. The responder won't send out a response signal after receiving the RS and CIN streams at the AR input if at least one of the following undesirable circumstances takes place: We denote the probability of this scenario as P_1 .
- c. The RS of the considered requester is suppressed due to the formation of leading false RSs (false alarm of the first kind) from the CIN, which result in the emission of a response signal or the operation of the side lobe suppression circuit.
- d. The request signal of the considered requester is suppressed due to the leading RS of the requester or requester of the interested party (probability P_6).

Assuming that the RS and CIN streams impact the request codes of this requester independently of one another and that there are enough sources contributing to the common RS stream for the stream to be classified as Poisson, let's calculate the probability of these occurrences. We assume that the input AO receives the following streams: CIN stream with intensity 0; RS stream with intensity 1 (consisting of RS streams from nearby requesters and RS streams from intentional interference); and RS flow, which causes the circuit side lobe suppression of the antenna radiation pattern to occur with intensity.

The RS stream's intensity falls as a consequence of the combined action of the CIN and RS stream, which causes high-frequency suppression of the stream's individual pulses at undesirable phase relations. $P_p =$ is the likelihood that at least one CIN pulse will time overlap with the pulse of the RS stream and suppress it. When the pulse of the received request signal coincides in time with the interference pulse, the interference suppression coefficient, $1 - e^{-P_1}$, (13) indicates the likelihood that the interference will be suppressed.

The calculations that follow are performed on the assumption that the strength of the RS stream that is emitted from the requester antenna's side lobes, or 2, is three times greater than that of the

main lobe, or 1, of the requester antenna's radiation pattern. According to $P_1 = 1 - e^{-\rho_1 t_2}$ and (20) $P_2 = 1 - e^{-\rho_2 t_3}$, the probability P_2 that at least one RS falls into the leading interval and suppresses the RS of this IFF systems due to the paralysis time t_2 AR when the side lobe suppression circuit is triggered, from the CIN and from the RS stream is calculated. Interference Immunity Assessment Friend or Foe Identification 299

When receiving RS along the side lobes of the requester antenna radiation pattern, the probability of RS suppression of this IFF requester via paralysis of the responder is $P_2 = 1 - \prod_{i=1}^n P_i$.

The ratio $P_4 = (1 - P_{01})^{n-1} (1 - P_{10})^{n+1}$ determines the likelihood of RS suppression of this requester due to the appearance of leading false request codes generated as a result of the interaction of the first pulse of the request code and leading pulses of the RS stream, and cause the emission of a response signal or triggering of the side lobe suppression circuit. The second component takes into consideration scenarios where false leading request codes might arise, including n request codes that result in the emission of a response code and one suppression signal code that results in the activation of the side-lobes suppression circuit.

The formula for second order false alarm probability P_{01} is $P_{01} = 1 - e^{-\rho_1 t_2}$. The formula $P_5 = (1 - P_{10})^{n-1} P_{n1}$ is used to calculate the probability P_5 of suppressing the request signal of this requester owing to the emergence of a fake suppression pulse that was created via interference. The following relationship 300 is used to calculate the probability P_6 of RS suppression as a consequence of activating the AR time selection circuits. $P_6 = 1 - e^{-\rho_2 t_3}$ according to I. Svyd et al. The probability of a response during the operation of the load restriction circuit of an aircraft responder drops and is $PAR = \rho_2 / 3$, where $3 = 1 + 2$. This occurs if the average number of RSs exceeds the permitted load AR m .

The AR availability factor is thus: When $3 \leq m$ $P_0 = \prod_{i=1}^m (1 - P_i)$, (29) When $3 > m$ $P_0 = PAR \prod_{i=1}^m (1 - P_i)$. (30) Figs. 4 and 5 show calculations based on the aforementioned expressions of non-resistant and simulated resistant operating modes, respectively. In this instance, we took into account that the intensity of the CIN stream $\rho_1 = 0$; $1 \cdot 10^4$; $2 \cdot 10^4$ and the intensity of the RS stream 1, which causes the emission of the response signal, are five times less intense than the intensity of the RS stream 2, which triggers the side lobe suppression circuit.

During both imitation-resistant and non-imitation-resistant working modes, a rise in the RS flux intensity causes a drop in the aircraft responder's availability factor, which indicates a poor noise immunity for the AR. An RS flux intensity of 1600, it lowers the AR availability factor for the non-resistant mode to 0.72 and the resistant mode to 0.65; uncorrelated interference (CIN) has minimal impact on the AR availability factor, and $\rho_1 = 1450$ is sufficient to reach the maximum AR load for the non-resistant mode. The maximum load AR for imitation-resistant mode is reached for $\rho_1 = 0$ at $\rho_2 = 2100$ and for $\rho_1 = 10,000$ at $\rho_2 = 2500$. The maximum load of AR is not at all reached with $\rho_1 = 20,000$. The aforementioned calculations give us an idea of the AR noise immunity, and the evaluation enables us to determine the bandwidth of the current IFF systems. It also shows how poorly IFF systems perform when subjected to purposeful correlated interference.

This issue impacts the power requirements of large data centres, or the Cloud, and can also limit the effective deployment of sensors and actuators for the Internet of Things (IoT) because of limited communication bandwidth and the cost of data transmission. There is no way to transmit and store all the data being gathered now for central analysis, and this challenge is expected to grow with the orders of magnitude more devices expected with the development of the IoT. The result is that the edge of the network will need sufficient intelligence⁴ to pre-process data in place and transmit only the most important information to the Cloud. This edge computation will have to be extremely power efficient, as it may depend only on the energy that it can scavenge from its environment. Thus, new computational devices and approaches are critical, especially those that can interface directly to the analogue output of embedded sensors to filter, analyse, compress, encode and possibly encrypt data before transmittal. Many of these operations can be expressed as a vector-matrix multiplication (VMM), which in principle can be performed in the analogue domain by a memristor crossbar array^{5–10} using Ohm's law for multiplication and Kirchhoff's current law for summation.

Such VMMs are being developed as accelerators for inference on deep neural networks^{31–35}, but may also be used as reconfigurable analogue processors for edge computing. A vector of voltage outputs from a sensor can be applied directly to the rows of a memristor crossbar, in which the values of the appropriate matrix elements have been stored as the conductance of the cells. The currents that appear on the columns of the array in real time represent the output vector of the multiplication if the series resistance of the interconnection wires is negligible compared with the memristor resistances. To read out the results in parallel, the current signal from each column is converted to a voltage signal through a transimpedance amplifier (TIA), which also serves as a virtual ground. So far, demonstrations of this concept have been limited to binary signal input and/or binary matrix weights. Recently, pulse width, instead of amplitude, was used to represent the analogue input signal, but this scheme requires more readout time and more complicated integrated circuits. Previous experimental demonstrations of an analogue-voltage-amplitude-vector by analogue-conductancematrix product, to the best of our knowledge, have been limited to a 1×3 system^{24–26}, which is not strictly a VMM implementation.

Here, we report completely analogue VMMs with adequate accuracy and high speed–energy efficiency that are based on up to 128×64 crossbars of hafnium oxide (HfO₂) memristors³⁶, and experimentally demonstrate the important IoT and network edge applications of signal spectrum analysis, image compression and convolutional filtering. 128×64 memristor crossbars To precisely tune the conductance of each memristor in a crossbar, we monolithically integrated a memristor on top of a metal–oxide–semiconductor (MOS) transistor as an access device in each cell, which is known as the '1T1R' architecture. Compared with passive arrays that use highly nonlinear memristors or discrete selector devices^{40–43} to mitigate the sneak path current problem, the 1T1R scheme has a lower packing density (2.5 times the cell area). However, it allows us to independently access memristors with a linear current–voltage (I–V) relation in an array with the transistor gate control, so each memristor's conductance can be precisely tuned.

Moreover, unlike passive arrays, a 1T1R crossbar enables accurate analogue VMM with linear I–V memristors that yield a good approximation to the scalar product of a vector component and

matrix element crossbars offer reconfigurable non-volatile resistance states and could remove the speed and energy efficiency bottleneck in vector-matrix multiplication, a core computing task in signal and image processing. Using such systems to multiply an analogue-voltage-amplitude-vector by an analogue-conductance-matrix at a reasonably large scale has, however, proved challenging due to difficulties in device engineering and array integration. Here we show that reconfigurable memristor crossbars composed of hafnium oxide memristors on top of metal-oxide-semiconductor transistors are capable of analogue vectormatrix multiplication with array sizes of up to 128×64 cells. Our output precision (5–8 bits, depending on the array size) is the result of high device yield (99.8%) and the multilevel, stable states of the memristors, while the linear device current–voltage characteristics and low wire resistance between cells leads to high accuracy.

With the large memristor crossbars, we demonstrate signal processing, image compression and convolutional filtering, which are expected to be important applications in the development of the Internet of Things (IoT) and edge computing. Nature Electronics | www.nature.com/natureelectronics Macmillan Publishers Limited, part of Springer Nature. All rights reserved. Articles Nature Electronics are attractive for applications in which packing density is not the most critical factor. In principle, depletion-mode transistors that are in the ‘on’ state at zero gate–source voltage can be used so that gate voltages on transistors are only needed for memristor array programming but not for normal VMM operations. We used n-type enhancement-mode transistors in this demonstration. The choice of transistor and its effect on leakage is discussed in Supplementary. Integration was conducted at UMass Amherst by building Ta/HfO₂/Pd (ref. 36) memristors on top of a CMOS chip fabricated by a commercial vendor (see Methods for more details). Figure 1b shows part of the integrated chip consisting of 1T1R arrays with sizes ranging from 4×4 to 128×64 . The detailed structure of some cells and the connection scheme are shown in, demonstrating conductance state linearity, write precision and accuracy, and read stability and reproducibility.

A, Schematic of the VMM operation. Multiplication is performed via Ohm’s law, as the product of the voltage applied to a row and the conductance of a crosspoint cell yields a current injected into the column, while the currents on each column are summed according to Kirchhoff’s current law. The total current from each column is converted to a voltage by a TIA, which also provides a virtual ground for the column wires. b, A $2 \text{ cm} \times 2 \text{ cm}$ detail from a photograph showing two dies of 1T1R memristor crossbars, each of which contains array sizes from 4×4 to 128×64 cells, along with various test devices. Microscope image of four cells in a 1T1R array (scale bar, $10 \mu\text{m}$). Crosses are memristors, and the transistors are ring-shaped. Inset: schematic showing how the memristors and transistors are connected into an array. Photograph of a probe card in contact with an operational 128×64 1T1R array (scale bar, $500 \mu\text{m}$). Quasi-d.c. I–V curves for all the devices with different conductances, showing good I–V linearity over the selected conductance range. f, Histogram of the initial difference between the target and measured conductance written into a 128×64 array. A fit of the peak to a normal distribution yielded a standard deviation of $6 \mu\text{S}$, with the peak maximum located at $-5 \mu\text{S}$. Room-temperature state retention and read disturb of the device states. The d.c. conductance states of all the devices were measured with a 0.2 V bias for 1,000 cycles, or a total of 6.4 h ,

showing no discernible drift in the plots. h, Histogram of the normalized standard deviation (s.d.), defined as the s.d. per conductance range (100–900 μS), for all measured states, which was fitted to a lognormal distribution. This shows that there are fluctuations during the read operation that can occasionally degrade the effective precision of an individual memristor, but 90% of the device states have a normalized s.d. less than 0.39%. The programming and computing were achieved with a custom-built testing system connected to the chip by a probe card [3], [7].

With the 1T1R scheme the array size can be much larger than 128×64, but this array was chosen for the demonstration mainly because of the constraint of the maximum number of probes (388, as shown in Fig. 1d) available on the commercial probe card used for testing. With transistors as the access devices, we were able to program the conductance of nearly all of the memristors to an arbitrary value within a predefined conductance range (Supplementary Video 1). We wrote MATLAB scripts to control the resistance tuning by communicating with the testing system. With the Ta/HfO₂/Pd memristors, the I–V relation of the cells was linear once the conductance was larger than the quantum conductance (77.5 μS) [44,45], as shown in Fig. 1e for conductance ranging from 300 to 900 μS , an important feature for accurate analogue computing. Typical resistance switching curves are plotted in Supplementary Fig. 3. Among the 8,192 devices in the 128×64 array, there were only three stuck ‘on’ and 15 stuck ‘off’ devices after programming, leading to a responsive device yield of 99.8%. A histogram of the writing error, defined as the initial difference between the target conductance value and the measured written value of the responsive memristors, is plotted.

The peak of the writing error conformed to a normal distribution with a standard deviation σ of 6 μS when the writing tolerance was set to ± 10 μS , and could be further reduced by defining a narrower tolerance in the MATLAB script and/or using a larger number of closed-loop programming iterations, at the expense of increased programming time. If, for the moment, we discount the tail of the distribution, which represents a small number of ‘sticky’ cells, and define the interval between states as $\pm\sigma$, we have effectively demonstrated more than 64 levels of conductance or 6 bits of digital precision over the conductance range 100–900 μS , which has been proven to be sufficient for many tasks in machine learning algorithms. The accuracy error δG of the memristor programming operation is taken to be the median value of the writing error, which is -4.7 μS .

To explore the read stability and reproducibility, we measured the conductance of the responsive 8,174 devices in the 128×64 array with 0.2 V read pulses for more than 6 h and did not see any detectable state drift. There were fluctuations in the read operations of individual cells, but these were small enough to have little impact on column current measurements summed over multiple memristors. These fluctuations, however, are a good indicator of the ultimate bit precision of the system. For example, 90% of device states have fluctuations within a 0.39% normalized standard deviation, indicating that the writing precision is 128 states or 7 bits in the conductance range 100–900 μS . The writing error and readout stability are not correlated with the selected conductance range, demonstrating the simplicity of making use of the multilevel conductance

states. The device maintains the stable states at normal working temperatures (room temperature to 85 °C, Supplementary).

The stable multilevel conductance states may be a result of the high migration barrier (measured value 1.55 eV) [36] for the Ta cations and O anions within a Ta-rich conductance channel formed in the HfO₂ matrix for the Ta/HfO₂/Pd memristors that were integrated on the chip. Analogue signal processing and image compression We first configured the array to implement the discrete cosine transformation (DCT) as a typical example of a linear transformation. The DCT is a Fourier-related transform widely used in digital signal processing and image/video compression and processing. Mathematically it can be expressed as $y = M_{DCT}x$, where M_{DCT} is the DCT matrix, and y is the output spectrum vector. One challenge in implementing the DCT with a crossbar is that a memristor conductance value cannot be negative, whereas some of the elements in M_{DCT} have negative values. To address this issue, the first approach used here is to map the matrix values into conductance by the linear transformation $G = \alpha M_{DCT}$ where $\alpha = V_{in}/x$ is the scaling factor to match the voltage range of the input, I_{out} is the vector of output currents, and j is the vector of ones. The second term of the equation includes a summation over all elements of the input voltages, which can be post-processed by either software or hardware.

The second approach we employed was to use the conductance difference of two memristors (a differential pair) to represent one matrix element. The input voltage signals on two neighbouring rows have the same amplitude, but opposite polarity. The differential calculation is performed by direct current summation: G_{ij} is the mapped matrix element in the i th row and j th column and thus can be negative. The differential pair can also mitigate stuck or sticky device issues by setting the conductance of one device in the pair while keeping the other device untouched. This approach provides a level of defect tolerance to the calculation, but at the expense of increasing the number of required memristor cells and thus the chip area. After configuring one 64×64 crossbar with the aforementioned first approach, the linear transform to map DCT matrix values to memristor crossbar conductance, we quantitatively analysed the output accuracy of the memristor DCTs by plotting the experimental measurements versus the expected currents for each. All rights reserved. *Articles Nature Electronics* column for a range of inputs. The readout conductance matrix after programming into the crossbar array is shown in Supplementary.

The raw current is processed in software by a simple scaling, which can be accommodated in hardware with a simple modified design, as the raw column current itself is converted from a voltage output by a TIA. The crossbar output shows an excellent match between the experimental and expected outputs. The high accuracy of the DCT reported here mainly resulted from the high bit yield, the relatively low series resistances (0.35Ω per block for rows, 0.32Ω per block for columns) and the high I–V linearity of the memristors in the crossbar obtained from the back-end process, as summarized in Supplementary. The unresponsive devices, especially those stuck in high conductance, have a significantly adverse effect on the output accuracy as well as the power consumption, based on our simulation results shown in Supplementary it is observed that a larger wire series resistance significantly decreases the output accuracy, especially for larger arrays, and eventually impacts the ability to correct the results with a simple linear correction.

A typical histogram of the estimated output error for a 64×64 memristor crossbar from all the columns, with input vectors representing image pixel intensities multiplied by a fixed DCT matrix (4,096 data points). The results show that the relative output error nearly follows a normal distribution. Similar analyses were performed with different crossbar sizes and the equivalent bit precision was then extracted from the standard deviations of the estimated output errors. The resulting 5–8 bit precision as a function of crossbar size, with larger arrays being systematically less precise. The degradation of bit precision with larger crossbar size could be due to increasing worst-case series wire resistance, leading to significant voltage drops within the array and the presence of increasing sneak currents that cause the conductance states of memristors to influence each other.

This can be remedied by decreasing the wire resistances and/or using lower average device state conductance, at the risk of increasing the device nonlinearity. Additionally, using the defecttolerant approach of differential pairs of devices, described above, also reduces errors. We start with a one-dimensional (1D) DCT for the crossbar array, to be used as a spectrum analyser, where we employ the conductance matrix used in the above accuracy analysis. The input signals are sine waves with different frequencies, the mean values (d.c. components) of which are zero; as a result, they do not require the summation post-processing described above. The experimental crossbar output displays the frequency spectrum, showing good agreement with the software DCT in MATLAB. The realtime crossbar output with changing input frequencies is also shown in Supplementary Video 2. The input to the crossbar can be directly connected to the analogue output of a sensor or other edge device to directly provide spectral analysis of a signal without the need to digitize it first.

We used the same system for image compression, performing a two-dimensional (2D) DCT. The input image pixel intensities were converted to voltage signals and then applied to the DCTprogrammed crossbar, row by row and then column by column. Images with pixel counts larger than the crossbar were divided into sub-images, processed in series, and then tiled together after reconstruction. In this case we used differential pairs of memristors in neighbouring rows to represent DCT matrix elements, and thus the 64×64 DCT matrix was experimentally represented by the full 128×64 memristor crossbar. The 2D cosine transforms of the input images were experimentally acquired from the crossbar, and the amplitudes of the spectra at lower frequencies were much higher than at high frequencies, demonstrating the high energycompaction and noise-filtering capability of the DCT. We retained the frequencies containing the top 15% of the spectral amplitudes that is, compression ratio of 20:3 and reconstructed the image using the 2D inverse DCT function in MATLAB to represent data analysis in the Cloud. The results are compared with those using the MATLAB 2D DCT to compress the image. Different compression ratios ranging from 20:1 to 2:1 were also analysed and compared, showing that even with only 1/20th of the original information we could still reconstruct a reasonable image, even with imperfections, in a memristor crossbar. This demonstration was not optimized for image compression and better results are expected after implementing a quantizer and entropy encoder. Convolutional image filtering we also experimentally demonstrated 2D convolution for image filtering.

We used 10 different convolutional filters: Gaussian, disk and average to smooth out noisy images, Laplacian of Gaussian (LoG) with three different parameters, Sobel (both x and y gradient) to extract the edges and Motion (two directions) to mimic the motion blur effect. Experimental output accuracy and precision for discrete cosine transformation (DCT) using memristor crossbars.

- a. Relation between experimental output and the software DCT result, showing excellent agreement and thus high accuracy.
- b. Histogram of the DCT estimated output error for the 64×64 crossbar, with a fitted standard deviation of $\sigma = 0.46\%$. The estimated percent error is defined as the difference between the corrected experimental output and the expected value divided by the sensing range. The peak of the corrected error distribution is at 0%.
- c. Bit precision estimated from standard deviations of the output error for crossbars of different sizes. In the bit precision estimate, one discrete output level was defined by $\pm\sigma$.

Nature Electronics Articles to the original 128×128 Lena image to show how the convolutions damp out noise and are able to locate edges. The noisy Lena image was used as input, the image intensity of which was converted into voltages applied to the rows of the crossbar. Each pixel in the filtered image was generated by the dot product of the 25-dimensional voltage vector mapped from a 5×5 input sub-image and the 25-dimensional conductance vector mapped from a 5×5 convolution matrix. We scanned the 5×5 sub-image with a stride of one and did not use zero-padding, so the dimension of the filtered images was $124 \times 124 (=128 - 5 + 1)$. The negative values of the convolution matrices were mapped to memristor cell conductance by the differential approach described earlier, but the differential pairs were arranged in neighbouring columns rather than rows.

Thus, the 10 different convolution maps were generated in parallel from 20 columns of current output. 14b for the simple post-processed edges. More results on the original Lena image without noise. The edge extractions described in this step are also a frequent layer of convolutional neural networks (CNNs or ConvNets), which is the most computationally expensive step in the networks. Compared to previously reported convolutions operating with binary inputs, binary weights and series readout¹⁸, our image filtering procedure included both analogue convolution matrices and analogue inputs, as well as parallel readout of 10 feature maps. The key advantages of our hardware VMM approach are reconfigurability of the memristor crossbar, reasonable accuracy and precision of the physical computation and efficiency both in speed and energy consumption. Here we analyse the performance and energy efficiency of the system. Because physical multiplication of a 128-dimensional vector and a 128×64 matrix is accomplished by a single current read process on the column wires, a readout time within 10ns gives 1.64 tera-operations per second (TOPS).

We performed a simulation of the power consumption for the image compression task with our experimental parameters, including conductance measurements after programming, dissipation by the wire resistances and writing the input patterns, and found the power consumed in the 128×64 crossbar array was $\sim 13.7\text{mW}$, or an efficiency of ~ 119.7 effective tera-operations per watt. As an approximate comparison, a highly optimized digital system with an application-

specific integrated circuit (ASIC) fabricated at the 40nm technology node for 4-bit 100-dimensional vector and 4-bit 100×200 matrix multiplication, for which the accuracy is comparable with our solution, has a reported energy efficiency of 7.02×10^{12} operations per second per watt. Although not a direct comparison, our system is 17 times more energy-efficient than the ASIC solution. The energy efficiency could be further improved by using memristors that work in a high resistance range but with linear I–V and stable multilevel states, smaller voltage inputs and/or shorter pulses. | Experimental realization of a memristor crossbar-based spectrum analyser. Input voltage signals (sine waves) with different frequencies. Experimental corrected output and MATLAB calculated output from the array, showing good agreement. Frequencies are represented by column numbers in this demonstration.

Array is a one-step current readout on the column wires, which does not scale up with increased input vector dimension. This is advantageous over a digital system whose latency inevitably increases with the input dimension, because the multiplication and summation have to be calculated step by step. More importantly, our memristor crossbar hardware VMM can process analogue signals acquired from a sensor directly, without the need for extra peripherals such as analogue-to-digital converters (ADCs), which would be required for a digital ASIC solution and consume extra time and energy, but was not considered in the above energy estimation. Additionally, high-bit precision ADCs after crossbar columns are not necessary if only specific features need to be detected within signals, which can be provided with threshold-gate circuits at much lower cost both in latency and energy. This flexibility, along with low latency and high energy efficiency, make analogue crossbar computation ideal for a wide range of edge and IoT computations.

We have demonstrated analogue-vector and analogue-matrix-vector multiplication using crossbars with over 8,000 memristors, with an equivalent 6-bit or 64-level precision and 99.8% device yield. The device conductance states were precisely tuned and the I–V characteristics were linear, ideal for analogue computing. We have successfully implemented some important applications for IoT and edge computing, including signal processing, image compression and convolutional filtering. The energy efficiency of the system was over 119.7 trillion equivalent operations per second per watt using a readout of 10ns, and this is expected to increase significantly with larger vectors and matrices and with improvements in circuitry. Our results are an encouraging advance in the hardware implementation of computing using emerging devices, and provide a promising path towards energy-efficient analogue computing based on memristors.

The transistors arrays were fabricated in a commercial laboratory with minimized wire resistance. For demonstration purpose with reduced cost, the transistors had a feature size of 2 μm and the fabrication did not involve a planarization process. The memristor arrays were fabricated in house using photolithography, thin-film deposition and lifof. Specifically, argon plasma treatment was performed on the as-received CMOS chip to remove native metal oxide layers for better electrical connection, followed by the sputtering of 5nm Ag and 200nm Pd as metal vias. After lifing of in warm acetone, the sample was annealed at 300 °C for half an hour in 20 s.c.c.m. nitrogen flow and processing.

- a. The original image for compression was input into the crossbar for the 2D DCT, block by block. The white arrow shows the block processing sequence. The lower image shows a representative image block to be processed.
- b. The image block was converted to voltages that were applied to the row wires of the crossbar (left), with neighbouring wires having a voltage pair with the same amplitude, representing image pixel intensity, but opposite polarity.

The paired voltages represented by the horizontal arrows were applied to a differential pair of memristor conductance, with the resulting net current representing the product of the absolute voltage value and the conductance difference of the differential pair. Right: differential DCT written into the 128×64 array, with the small number of stuck 'on' or 'off' memristors evident as disruptions in the pattern. Images decoded from the 2D DCT by software and experimentally (d). Before decoding, only the frequencies representing the top 15% of the spectral intensity were preserved (a 20:3 compression ratio). Pd/5nm Ta adhesive layer was then sputtered as the bottom electrode. Te 5nm HfO₂ switching layer was deposited by atomic layer deposition (ALD) using water and tetrakis(dimethylamido)hafnium as precursors at 250 °C. Patterning of the switching layer was carried out by photolithography and reactive ion etch (RIE) using CHF₃/O₂ chemistry.

Finally, a 50-nm-thick Ta layer was sputtered and lifted off to serve as the top electrode, covered with another 10-nm-thick Pd layer as the passivation layer. Electrical characterization. Most electrical characterization was carried out using our custom-built multiboard measurement system⁵¹. A photograph and description of the system are provided in Supplementary Fig. 2. 2D DCT steps for image compression. The 2D spectra of an image could be acquired in two steps of matrix multiplication. In the first step of the 2D DCT of an image, every row of the image intensities was converted to a voltage amplitude vector and applied to the row wires of the crossbar (Supplementary Fig. 12a). It is noteworthy that the voltage amplitude may come from the direct analogue output of an image sensor. In this case, the conductances of the 128×64 memristor array were mapped from a 64×64 DCT matrix with a row differential method (Supplementary Fig. 12b). The image intensities of each row, with 64 pixels, were converted following the differential requirement into a 128-dimensional voltage vector. Specifically, neighbouring voltage vector elements have the same amplitude representing one image pixel intensity, but with different polarity. As a result, the current outputs on the columns of the crossbar array are naturally the VMM result of the input voltages vector and conductance matrix. The output current matrix, in which each row is one VMM result with one row of image intensity as input. Each row of the output matrix is the current vector output when applying one row of voltage vectors and is thus the spectrum of the input image along the horizontal direction after the cosine transform.

The second step DCT calculates the spectrum along the vertical direction, so the output matrix from the first step is transposed and linearly mapped into the voltage input matrix for the second step DCT. The voltages are then applied on the rows of the crossbar, similarly to the first step, without changing the conductance matrix in the crossbar. The output current matrix in this step is the 2D DCT result that represents the 2D spectra of the input image. Data availability. The data

that support the plots within this paper and other findings of this study are available from the corresponding author upon reasonable request.

The input image was a standard Lena image with artificially added Gaussian white noise. Each colour channel of the image is represented by a floating-point number between 0 and 1, and the added noise has a standard deviation of 0.004 and zero mean. Measured conductance after programming 10 convolutional filters into the 25×20 crossbar. The pixel intensities, represented by two voltages with equal amplitude and opposite polarity, were input into the crossbar onto a pair of memristors in adjacent columns. The difference in the conductance of the memristor pair represents one matrix element of a convolution. Ten different filtered images obtained in parallel by the convolution operation: Gaussian, disk and average reduce noise by smoothing the image, Laplacian of Gaussian (LoG) with various parameters and Sobel (x and y gradient) were used to detect edges, and Motion to generate motion blur.

The most prevalent illness in the world, diabetes, may cause death if adequate medical treatment is not provided. Failure to manage the condition has an impact on the patients' lives as well as long-term problems. The patient will be better able to control their health if the glucose level is tracked daily. The patient may take everyday health precautions thanks to the report on their blood sugar level. The system that is intended to track a person's blood pressure, temperature, and glucose level is discussed in this essay. The data is made accessible via the cloud so that physicians may access past data. Better patient care management will result from this. The Raspberry Pi is used to construct this system and read data from the user. The analogue signal is also converted into digital signals using the ADC. In this article, the specifics of the project's execution are addressed.

Everything will change as a result of the Internet of Things (IoT), often known as the Internet of Objects. Education, communication, business, research, governance, and humanity are all impacted by the Internet. The Internet is without a doubt one of the most significant and potent inventions in human history, and with the idea of the internet of things, it is now easier to live a smart life online in every way. People, machines, smart objects, surrounding space, and platforms connected with wireless/wired sensors, M2M devices, and RFID tags will create a highly decentralised resource base that is interconnected by a dynamic network of networks in the near future. This means that storage and communication services will be widely available and distributed. By developing IoT technology and testing and deploying goods, smart environments will be implemented by 2020.

By combining diet, exercise, and insulin, blood glucose monitoring may help a person maintain their glucose levels within a defined target range, lowering the risk of diabetic complications. People may control their diabetes using a variety of testing and monitoring tools. The method described in this study monitors patient glucose levels and stores them in the cloud. For improved medicine and food decisions, both patients and doctors may access historical and current data.

In their discussion of connected health, Prabha Sundaravadivel et al. defined the term as any digital healthcare system that may function remotely and includes extra elements such as continuous health monitoring, emergency detection, and can alert features. They link through the

WBAN network, which is ineffective for readings from mobile sensors. Due to wired network restrictions between the body motions, the WBAN suffers. There are no integrated sensors.

Seniors' remote medical care has been considered by Ahmed Abdelgawad and others. In their descriptions, the ability to seamlessly connect individuals, medical devices, and providers of social and medical services is necessary for health monitoring, rehabilitation, and supported living for the elderly and physically challenged. To help seniors and people with disabilities live independently and enhance their quality of life, they suggest an adaptable, portable Internet of Things solution. The patient's data was read using a Raspberry Pi 2 microcontroller. The Pi 3 features a 1.2GHz Cortex-A53 processor compared to the Pi 2's 900MHz Cortex-A7. The Pi 3 performed the activity across boards to network, scoring 711 on the Whetstone Pi A7 test compared to the Pi 2's 432.

Suhail N. Abood suggested using mobile health to monitor patients. The contacts between patients and doctors serve as a gauge for diabetes patients' self-management. The GSM networks handle communication, sensors are linked to n different mobile nodes, and patient values are uploaded to cloud storage. In a quick overview, the doctor will discuss the patient's lifestyle, including nutrition and activity. To exchange the patient's readings with the device to which they were attached, the authors advise utilising Bluetooth.

However, we suggest using UART to transfer readings to the Raspberry Pi, since this is a simple method of exchanging the data. Additionally, they implemented a GSM network to upload data to the cloud. We are utilising WiFi to upload data since it allows for quick transmission between sender and receiver. A more effective approach has been put out by Ghulam Muhammad et al. for ensuring an ongoing, secure, smooth, and widespread framework for patient IoT monitoring. It makes use of the Internet of Things to record speech, body temperature, electrocardiogram, and environmental humidity. They don't include things like laryngoscopes and stroboscopes since they're hard for patients to use.

The architecture specifies the patient monitoring system's overall design and implementation. A microcontroller called an Arduino Nano is linked to the necessary sensors. The Raspberry Pi 3 is linked to the Arduino microcontroller. WIFI was used to link the Raspberry Pi to the cloud. In our research, we suggest that diabetic patients use IOT-based health monitoring. All individuals can be monitored in the same manner, however some people are going to the online world. So that we could execute this concept in the future. The patient will be under the doctor's daily observation. We gather the sensor-based health values, and the data is then sent to a Raspberry Pi. We upload from there to cloud storage.

An ARDUINO NANO microprocessor is attached to the glucose, pulse, temperature, and blood pressure sensors for the purpose of analogue to digital conversion. Additionally, we use a UART USB connector to send the patient's data reading to the Raspberry Pi 3. All data collects are stored on the Raspberry Pi 3 and sent to ubidots for cloud storage. The arduino readings regarding the patients will be gathered by the transmitter side and sent to the raspberry pi. The visual depiction of the transmitter and receiver sides is illustrated below in Figures 2 and 3,

respectively. The receiver side gathers the read data through WiFi using a Raspberry Pi and stores it in the cloud.

We decided to monitor the blood pressure, temperature, pulse, and blood sugar level for this research. The Arduino Nano ADC is linked to the glucose sensor, blood pressure and temperature sensor, and pulse sensor. Through a USB wire, the raspberry pi and arduino nano were joined. Through WiFi, the Raspberry Pi is linked to the cloud.

Utilizing it is easy. It offers colour and audio warnings in addition to sound alarms. It is a real-time product that we employed in this project to monitor our glucose levels by obtaining its analogue readings. We employ this onetouch real-time device measure the patients' blood glucose levels. We start with an analogue unit and power source, and then we use an Arduino Nano to convert the analogue value to a digital value.

The photo plethysmography theory serves as the foundation for the pulse sensor. It monitors the variation in blood volume through any organ of the body that results in a variation in the amount of light passing through that organ a vascular region. By using infrared lights and centre finger detection, the patient's pulse is read.

A pressure sensor is an apparatus that detects pressure and transforms it into an analogue electric signal, the strength of which is dependent on the amount of pressure being applied. They are also known as pressure transducers since they translate pressure into an electrical signal. Due to the fact that a temperature sensor is an integrated circuit, significant signal processing circuitry may be included in the same package as the sensor. For temperature sensor Ics, additional compensating circuits are not required. The temperature and blood pressure of the patients are measured using this sensor.

RASPBERRY PI 3

An SD card is already included with the Raspberry Pi board. We may put an SD card into this slot and utilise it to operate our gadgets. Similar to the hard drive of a personal computer, the SD card serves as the primary storage device for the Raspberry Pi board. On the card you want to use, the Linux operating system is installed and bootable. Operating systems for ARM, Linux, Qtonpi, and Mac are supported by the Raspberry Pi. You may choose one OS, and you'll need to use a disc management tool to write it on an SD card. Additional storage options include a USB external hard drive or a USB drive. Wi-Fi allowed the raspberry pi 3 to connect. Raspberry Pi. For uploading patient data readings onto the cloud, we are utilising this Raspberry Pi controller.

An Arduino is essentially a microcontroller-based kit that, thanks to its open source hardware feature, may either be produced at home using the components or purchased straight from the seller and used right away. It is mostly used for communications and for running a variety of devices. This Arduino is being used to convert data from analogue to digital. We are programming with the Arduino IDE and running the Raspberry os in a virtual window using MobaXterm.

- **ARDUINO IDE:** The Arduino platform comprises of a physical programmable circuit board (often known as a microcontroller) and a computer application called the IDE

(Integrated Development Environment). This ide is being used in our project to convert analogue values to digital. We use the Arduino IDE to write setup(), loop(), and define certain variables to gather data from the patients.

- **MOBAXTERM:** The X11 server, tabbed SSH client, and other network features for remote computing are all included in this upgraded Windows terminal (VNC, RDP, telnet, rlogin). MobaXterm is a portable executable file that delivers all the necessary UNIX commands to the Windows desktop and is ready to use right out of the box. Using a virtual display and terminal access, we utilise this mobaxterm to connect to the Raspberry Pi 3.

The sensors that we use to gather patient readings from all around the globe and send them to the doctors include glucose, pulse, blood pressure, and temperature sensors. All of this data is sent through an Arduino Nano. The Arduino Nano can receive analogue values and transmit the information to the Raspberry Pi via the UART protocol through a USB wire. The Raspberry Pi will upload the patient readings to cloud storage through wifi. Through the same module, the doctor may access the patient's data on the cloud and provide feedback to the patient. Cloud data storage: The reading values are concurrently uploaded to ubidots cloud storage. Data storage involves three steps:

- a. Send data: Devices are automatically generated when the first data point is received. We pre-configure our properties using device types.
- b. Gather data Obtain information for further processing.
- c. Parse the data: As an alternative, we may create our own API utilising ubiparsers and a few lines of JavaScript, allowing the ingestion and transmission of data in our own format.

Ubidots:

Ubidots focuses on important inputs to offer the appropriate tools promptly and ensure the success of our solution. Despite always occurring failures, they rise to the moment and never accept satisfactory, constantly striving to increase the value of our data. When Ubidot's usability is added, the value-add in terms of development time and cost savings is further improved. Ubidots customers can connect, construct, and deploy cloud IOT apps with ease because to the platform's basic design, which is focused on data efficiency and an engaging UX user experience. This frees Ubidots up to take care of the cloud's end-user UX infrastructure.

The things people do on Ubidots:

- 1) Making a patient's ID unique
- 2) Developing tools for the cure
- 3) Making sensors variables
- 4) The patient and doctor examining the whole data

Patients will get a special ID from the physicians through Ubidots. In order to avoid misunderstanding, the physicians can quickly recognise patient interactions. There are historical events that patients and doctors may attend. The identification photo below. For the patient's

therapy, the doctor wishes to develop a single gadget. In our project, the title is represented by a health monitoring gadget. We have the option to remove or modify the device names if we wish to make a change. The device includes a description, an API label, an API id, the most recent action, and a tag.

Here, we divide the sections where we build the variables for our sensors. Each variable has a unique ID for the Apathy dashboards that we design using graphs and bar charts allow us to examine the aggregate data. Below is a snapshot of the whole data viewing situation. In order to address multidimensional elements of therapy, this research provided an IOT-based health monitoring strategy to diabetic self-management, moving the focus from a conventional clinician-centered approach to a patient-centered one. The creation of a platform and new architecture for a new multidimensional approach to diabetes treatment are the key contributions of this study. The creation of a platform and new architecture for a new multidimensional approach to diabetes treatment are the key contributions of this study.

IOT sensors have the ability to provide information about agricultural areas and subsequently take action depending on user input, making smart agriculture an emerging idea. The development of a smart farm system using benefits of cutting-edge technologies like Arduino, IOT, and wireless sensor networks is suggested in this paper. The goal of the article is to employ IOT and smart agriculture utilising emerging technologies. The key to increasing the production of productive crops is to keep an eye on the environment. This paper's feature entails the creation of a system that can track temperature, humidity, moisture, and even the movement of animals that could destroy crops in agricultural fields using sensors and an Arduino board, and in the event of any discrepancy, send an SMS notification as well as a notification on the application created for the same to the farmer's smartphone using Wi-Fi/3G/4G. Data inspection and irrigation scheduling may be set up using an android application thanks to the system's duplex communication connection, which is based on a cellular Internet interface.

The device has the potential to be helpful in water-scarce, remote places due to its cheap cost and energy independence. Index Terms Sensors for the IOT WSN Smart Agriculture Gateway. India's main line of work is agriculture. IBEF (India Brand Equity Foundation) estimates that 58% of Indians who live in rural regions rely on agriculture. According to the Central Statistics Office's second suggested estimate, agriculture is expected to contribute around 8% of India's Gross Value Addition, which is a fairly large amount. In such a scenario, agriculture would use a significant amount of water, especially fresh water resources. According to recent market surveys, agriculture currently uses 85% of the world's freshwater resources, and this percentage will likely continue to be dominant due to population growth and rising food demand. This necessitates planning and tactics to make wise use of water by applying science and technological improvements. There are several ways, ranging from simple ones to more sophisticated ones, to reduce the amount of water used by different crops.

Thermal imaging is used by one of the current systems to keep track of irrigation schedules and plant water status. By sensing the water level in the soil and controlling actuators to irrigate as and when necessary instead of predefining the irrigation schedule, irrigation systems may also be automated, conserving water and allowing it to be used more wisely. When the volumetric water

content of the substrate falls below a setpoint, an irrigation controller opens a solenoid valve and applies watering to bedding plants impatiens, petunia, salvia, and vinca rosea. The escalating world water problem In addition to dealing with shortages and disputes between water users, the pollution levels have risen alarmingly, and the fresh water supply is further affected by the population of people and animals. If this keeps up, food production will be limited, which will have an impact on human productivity and, ultimately, the health of the whole ecosystem. The population has grown significantly and at a pace that is higher than the rate of food production, which is the main and most significant cause of this issue. Its expansion on the globe map will be strongly impacted by this population rise, particularly in nations with limited water resources[3], [4].

For the predicted population increase, the food production must be boosted by at least 50%. 85% of the world's freshwater usage is accounted for by agriculture. This causes an issue with water supply and necessitates an effort to use water sustainably. Due to a number of factors, it will only be possible to expand irrigated agriculture to provide a fraction of this increasing demand; the remaining percentage will need to come from an improvement in the productivity of rain-fed agriculture. Without coordinated planning and unprecedented levels of international collaboration, a number of serious water-related issues will arise during the next 50 years, endangering the health of many terrestrial ecosystems and severely affecting human health, especially in the world's poorest areas. This article discusses a clever and intelligent agricultural system that may assist the farmer in using the water level wisely while also taking care of other discrepancy elements, such as unnecessary animal access into the fields. The system comprises of a microprocessor and several sensors, including but not limited to those for wetness, temperature, humidity, and motion. The sensors, microcontroller, and internet are all connected through wired and wireless connections in the system[8], [9].

The system also includes an android application that enables the user to provide input that will be used to regulate the watering. In this study, a smart agricultural system is suggested, which would make use of IOT, WSN, and cloud computing concepts to assist farmers in scheduling irrigation for their farms using editable agriculture profiles. An automated irrigation system is created to maximise the use of water for agricultural crops based on user input. For sensors measuring soil moisture and temperature that are positioned in the plant roots, the system features a dispersed wireless network. A gateway unit costs \$31.00. IEEE manages sensor data, activates actuators, and sends data to an online application. For the purpose of controlling the amount of water, a microcontroller-based gateway was designed with an algorithm that included temperature and soil moisture threshold values. For crops to grow properly, watering and fertiliser must be scheduled properly. The following variables may alter how much water crops need in different climates: temperature, humidity, sunshine, wind speed, passive infrared sensor, seed monitoring, pesticide.

It is possible to increase crop productivity by using the gathered and felt climatic data from the field coupled with meteorological data from online archives. Crops need a lot of water if the weather is hot, dry, windy, and sunny; but, if the weather is cold, humid, overcast, and with little wind, the requirement for water is lower. A system with six components monitoring,

management, planning, information distribution, decision support, and control action was abstracted in a previous research model. The research model described above analyses data to improve decision assistance. A GSM-based smart agriculture system was suggested for the automation of a number of agricultural chores. Smart irrigation equipment that operates on a mechanical bridge slider configuration is a proposal for automation. Through a GSM module, the smart irrigator gets signals from a smart farm sensing system. The detected information is sent to a central database, where all crop-related information is processed and sent to the irrigation system to carry out automated activities. IOT-based smart agriculture provides irrigation-related information as well as services like smart control and decision-making based on real-time data from the fields.

Any smart device situated remotely may control all of these processes, and the interface sensors are utilised to carry out tasks with Wi-Fi, actuators, and other hardware components. The complete system was built utilising infield sensors, which gather data from the farm and send it through GPS to the base station, where the required steps are decided to manage irrigation in accordance with the system's database. Researchers monitor soil-related variables like moisture and humidity since they are crucial to any crop's development. The system has two operating modes: Auto mode and Manual mode. Users may manage system operations via an Android app or instructions in auto and manual modes, respectively. The system makes its own judgements and manages the installed devices. Smart systems may be implemented at a low cost and with high reliability thanks to the Internet of Things [5]. Advanced rural connection is made possible in smart village systems by using web services and real-time environmental factor monitoring.

The work suggested in offers the use of IOT in almost all steps, including growing, harvesting, packing, and shipping. Farmers and all other stakeholders will benefit from having a thorough understanding of the product from production to sale thanks to real-time data given by sensors and RFID tags in all the aforementioned crop growing stages. The automated agricultural system suggested in uses actuators to regulate the motor and light sensors to determine whether to switch on or off the lights in the greenhouse depending on moisture readings. Undoubtedly, an automated method aids farmers in enhancing agricultural productivity.

Paper creates a human-centric agriculture paradigm for the Internet of Things. In order to address the insufficiency and lack of management that are the source of issues in agriculture, it integrates IOT and cloud computing on a global scale. The creation of a sensor- and microcontroller-based smart agricultural system inside an IOT system is demonstrated. The implementation's goal is to show off the microcontroller's clever and intelligent skills by enabling judgements to be made about when to water the plants based on ongoing monitoring of the field's environmental conditions. Additionally, it seeks to upload a predetermined watering schedule to an application created for the purpose, according to the convenience of the farmer. A distributed wireless network of soil moisture and temperature sensors placed in plant root zones make up the implementation, which is a photovoltaic-powered automatic watering system. These sensors function as an IOT gateway by continually monitoring the parameters and transmitting them to the Arduino board for further processing. By inserting a WiFi module, this gateway now has wireless capabilities and can update data to the cloud. Through the attached module, the IOT

gateway also provides GSM functionality. General packet radio service (GPRS), a packet-oriented mobile data service used in 2G and 4G cellular worldwide systems for mobile communications, is also included into this receiver unit as a duplex communication connection based on a cellular-Internet interface (GSM).

The user may continually check the parameters from the convenience. Android application thanks to the data being transferred to the cloud at home or when travelling. Based on user input provided by the farmer via the smart agriculture application, the system has the ability to adapt. According to the farmer may choose an irrigation profile depending on the crop and the season, and schedule and manage the water resource use wisely. One of the main indicators that water is needed for the crops is the volumetric water content of the soil. Without this technique, the farmer must personally check each crop by looking at the soil in the fields, which is laborious, time-consuming, and taxing. The sophisticated system that alerts the user whenever the water content drops below the cap established by the farmer himself can take care of this.

One of the main causes of disruption or disturbance to the yield is the entry of animals, particularly cows, monkeys, dogs, etc. into the fields. This would squander one person's productivity by requiring them to constantly watch the fields, which would be inaccurate. This may be avoided with the help of the device, which uses a motion sensor to identify any animals in the fields and alert the farmer when they are around. The farmer may be permitted to first define the distance range for which the animals must be detected in the application.

The system architecture is shown in and includes an Arduino Uno R3 microcontroller board, sensors such the LM35 temperature sensor, humidity, moisture, and motion sensor, an ESP8266 Wi-Fi module, and a GSM module. The programme is an Android application that allows you to build up a profile for seasonal or daily and weekly irrigation schedules that are predetermined. A control signal will be transmitted to the Arduino Uno to turn on or off the irrigation depending on the farmer's input. The software has also been configured to alert the farmer anytime the physical parameters measured fall below the threshold value.

The Arduino Uno board serves as the IoT gateway and manages all on-board operations. All physical characteristics are sensed by sensors, which translate their analogue values into digital values. In order to monitor the temperature and humidity on the field, relevant sensors are utilised. Capacitive soil moisture sensors are used to gauge the soil's moisture content. Additionally, the speed of the wind has an impact on crop productivity. As part of our created system, this is also measured. A RTC module is also added to record data from the sensors in real time. The IOT gateway receives this data after that. The data is subsequently sent to the cloud via the IOT gateway utilising the Wi-Fi module.

Our system's cloud will have a Web Server, a database, and decision logic. The data obtained from the IOT gateway will be maintained in the database. The decision logic then determines whether the farmer's action to water the plants is necessary. For instance, a temperature threshold in the created system is maintained at 25 °C. The database will initiate an action to the decision logic if the temperature rises beyond the threshold temperature, which then sends a notice to the

created Smart Farming Android application. A SMS will be sent to the farmer's registered mobile phone to notify him as well.

A signal will be transmitted to the cloud based on the farmer's decision to turn on or off the irrigation, and from there it will go to the gateway, which will then send a signal to activate the relay and turn on the water pump. Real-time data is utilised to make irrigation choices utilising an IOT-based smart agricultural system. Farmer first enters into the system using an Android app and his login information, including his username and password. After that, he is free to choose the crop for that year. The system is put into place in three stages are Information distribution, processing, and sensing[7], [10].

Temperature, wetness, humidity, and motion are just a few of the physical characteristics that are sensed during this phase. This microcontroller board, the Arduino Uno R3, is equipped with all of these sensors. As it has the ability to send data to the cloud, this board serves as the system's IOT gateway. Wi-Fi ESP8266 module is used to transmit this data.

In the cloud, processing takes happen. A web server, a database where the sensed data is stored, and decision logic that bases choices on the felt data make up the cloud. The output of the decision logic will be provided to the Android application and subsequently to the IOT gateway during the information dissemination phase. The following is the smart farming system's complete algorithm.

Continuously gather sensor data; convert sensed data to A/D on the Arduino Board; send the data to the cloud through the IOT Gateway; and, if the data is over the threshold, send it to the cloud.

If the user chooses Turn ON, a control signal is delivered to the cloud server and subsequently to the IOT gateway.

- The water pump is switched on when the relay is triggered by the IOT gateway.
- Otherwise, if the user chooses to switch OFF:
- Send a control signal to the cloud-based server;
- Send the control signal to the IOT gateway;
- The IOT gateway activates the relay, turning off the water pump.

Unless Else

Keep looking for the threshold condition if necessary. On the Android platform, the Smart Farming Application is created. The following functionalities are offered by this application:

1. Choosing whether to switch the water pump ON or OFF
2. Choosing an irrigation profile, where the farmer may specify the start and stop times of the irrigation on a given day. The farmer may now spend his time on other beneficial activities thanks to this. The farmer may pick the same schedule for a week or a month using the application profile.
3. Advice to the farmer to employ a certain herbicide on his or her crop
4. Inform the farmer of the animal invasion of the land.

Since excessive or insufficient irrigation is bad for agriculture, IoT-based smart agricultural systems may prove to be highly beneficial to farmers. Based on the local environmental circumstances, threshold values for climatic variables like humidity, temperature, and wetness may be established. The technology also detects animal incursion, which is the main cause of crop decrease. Based on data from the meteorological repository and data detected in real time from the field, this system develops an irrigation programme. This method may advise farmers on the need of irrigation. There must be constant internet access. To get around this, the system may be expanded such that recommendations are sent to the farmer directly through SMS on his mobile device using a GSM module rather than a mobile app.

REFERENCES:

- [1] A. Doni, C. MurthyMV, and M. Kurian, "SURVEY ON MULTI SENSOR BASED AIR AND WATER QUALITY MONITORING USING IOT," *Indian J.Sci.Res*, 2018.
- [2] J. H. Suh *et al.*, "Fully integrated and portable semiconductor-type multi-gas sensing module for IoT applications," *Sensors Actuators, B Chem.*, 2018, doi: 10.1016/j.snb.2018.03.099.
- [3] J. R. Stetter, D. Peaslee, V. Patel, and B. J. Meulendyk, "Wireless Zero-Power Air Quality Electrochemical Sensor Card for Iot Applications," *ECS Meet. Abstr.*, 2018, doi: 10.1149/ma2018-01/42/2418.
- [4] M. T. Bandy, "A study of current trends in the design of processors for the Internet of Things," in *ACM International Conference Proceeding Series*, 2018. doi: 10.1145/3231053.3231074.
- [5] C. Schmidt, C. Kottke, R. Freund, F. Gerfers, and V. Jungnickel, "Digital-to-analog converters for high-speed optical communications using frequency interleaving: impairments and characteristics," *Opt. Express*, 2018, doi: 10.1364/oe.26.006758.
- [6] P. Del Hougne and G. Lerosey, "Leveraging Chaos for Wave-Based Analog Computation: Demonstration with Indoor Wireless Communication Signals," *Phys. Rev. X*, 2018, doi: 10.1103/PhysRevX.8.041037.
- [7] P. Van Duijsen, J. Woudstra, and P. Van Willigenburg, "Educational setup for Power Electronics and IoT," in *Proceedings of the 2018 19th International Conference on Research and Education in Mechatronics, REM 2018*, 2018. doi: 10.1109/REM.2018.8421802.
- [8] M. Lim, "Roots, Routes, and Routers: Communications and Media of Contemporary Social Movements," *Journal. Commun. Monogr.*, 2018, doi: 10.1177/1522637918770419.
- [9] D. DARLIS, A. R. DARLIS, and M. H. ABIBI, "Implementasi Sistem Penyiaran Musik Digital di Kafe menggunakan Visible Light Communication," *ELKOMIKA J. Tek. Energi Elektr. Tek. Telekomun. Tek. Elektron.*, 2018, doi: 10.26760/elkomika.v5i1.60.
- [10] S. A. Strom and D. R. Loker, "BeagleBone black for embedded measurement and control applications," in *ASEE Annual Conference and Exposition, Conference Proceedings*, 2018. doi: 10.18260/1-2--29844.

CHAPTER 12

MODERN ENVIRONMENTAL RECORDING DEVICES

Dr. Vikas Sharma, Assistant Professor
Department of Computer Science and Engineering, Sanskriti University, Mathura, Uttar Pradesh, India
Email id- vikass.oeit@sanskriti.edu.in

This research presents an extremely low power acoustic wake-up detector based on high frequency signal analysis. Focused on Internet of Things (IoT) applications for the environment or the military, it intends to identify in real time the presence of certain animal species or drones for warning generation and for initiating power-consuming operations like high frequency signal recording only when necessary. This wake-up detector, which has strong frequency selectivity and a high frequency detection capacity, continually checks for the presence of certain frequencies in an analogue acoustic signal. It is based on a current-mirror, analogue timers, and comparators, together with an ultra-low analogue frequency to voltage converter. With a focus on long-term stealth environmental or military surveys, cutting down on power consumption helps keep the system's size and weight to a minimum. When powered by three coin cell CR2032 batteries, this power usage has been lowered to 34 W, resulting in a full year of autonomy, including the microphone.

Strong operational or environmental requirements, such as placing a device in a regulated region or a stringent nature reserve, are applied to Internet of Things (IoT) devices used for environmental and military assessments. Environmental and military research need the long-term recording of signals like sound several months or years. Due to data storage space or battery energy, these recording procedures are seldom compatible with low power and high frequency recording. For instance, a data acquisition system operating at a minimum of 240 kbps with a resolution of 24 bits for low level signal detection is required for the acoustic recording of animals such as bats or rats, having a communication and localization system emitting up to 120 kHz and aerial drones producing a characteristic noise around 40 kHz. As a result, 2.5GB of data are stored for each channel every hour.

It is almost hard to develop a portable autonomous long-term data collecting device that can record constantly under these circumstances. In order to raise alerts or discover intriguing occurrences, we must deal with a problem that is outlined in, useless data storage, and useless post-processing. This local pre-filtering procedure, which follows the growing notion of leveraging edge computing approaches, enables to identify only meaningful events, using less, conserving a significant amount of data storage, and extending the recorder's operating life.

Modern environmental recording devices need a common 12V 1.2Ah lead battery with a 14.4Wh global capacity to operate. Batteries would only last 30 hours in continuous high frequency recording, not adding the energy required to generate alarms. Fortunately, continuous recording is typically not required for environmental rare event detection and can instead be reduced to

interesting data periods, such as for detecting the invasion of a specific species into a strictly protected natural area or the malicious behaviour of aerial drones into a restricted military area.

Utilizing a wake-up detector that is triggered by the detection of a certain frequency on the acoustic signal and recording the signal only after the wake-up detector has been triggered enables long-term monitoring and alarm production.

There are low power wake-up systems based on raw frequency detection, although they are primarily focused on detecting a particular low frequency, or are radio frequency analysis specialists, such as RFID technology. There are also certain detectors, like, that use sophisticated digital processing methods and have more developed capabilities, including pattern identification, but with a lower sampling frequency or a greater total power consumption owing to analogue to digital conversions describes a method for sensing environmental occurrences that uses a digital wake-up detector that operates on high frequency sound signals[1], [2].

This system uses roughly 0.6 mW of power. That is equal to how much energy the utilise ultrasonic microphones consume (Knowles SPU0410LR5H). This microcontroller-based wake-up system can operate continuously for nearly 3 years on a 14.5Wh battery (traditional 12V 1.2Ah lead battery), as opposed to 30 hours of continuous high frequency recording with the majority of the time no meaningful signal. This is opening the way for long-term environmental survey techniques, but it has one significant drawback: the lead battery, which is 10 cm long and 600 g in weight, prevents it from being used in extremely light and compact embedded systems.

The high frequency signal wake-up detector we offer in this research is a unique analogue implementation based on discrete components. With an emphasis on the power consumption budget available for waking-up on intriguing signal detection and having this detector run in always-on mode, the overall design of the acquisition system is first given. The wake-up always on mode is what we call it. A second section describes the wake-up system's ultra-low power analogue implementation, which is based on frequency analysis. We intend to make the data gathering system smaller and lighter than earlier systems, as stated in the introduction, so that it may be embedded anywhere without endangering existing species.

By employing three common 3V 0.23Ah 0.69W h CR2032 batteries (each weighing 3g) instead of a traditional 12V 1.2Ah 14.4W h lead battery (weighing 600g), as shown in, we primarily concentrate on the battery size reduction. Battery capacity must be decreased by a factor of 10, while weight must be lowered by a factor of 100. The detecting system's lifespan must also be kept in wake-up, always-on mode for at least a year. This implies that in order to make up for the decreased battery capacity, power consumption must be lowered by about a factor of 10.

We may assume that the highest allowable average power consumption in wake-up detection mode is roughly equal to the battery capacity divided by the required autonomy of the system since warnings to be detected and recorded are seldom enough to be disregarded (i.e. 12 months). The same holds true for aerial drone detection systems given the rarity of incursions. For instance, using three CR2032-style coin batteries results in an average annual power budget of $3 \times 0.69 \times 24 \times 365 = 236$ W for the always-on wake-up detection mode with the microphone power supply. Given this restriction, it is not feasible to utilise the 500-Watt Knowles SPU0410LR5H

microphone that was used in. Instead, we went with the Knowles FG-23329-P07, a lower power microphone with a 200 W power consumption. Even though it is not mentioned in the relevant Knowles datasheet, this microphone has successfully undergone experimental validation for ultrasonic detection at 40kHz or higher. An are available for powering the wake-up always-on detector with this microphone.

System architecture

A general description of the recording and analysis system is shown in, although this study concentrates on the low power wake-up system based on frequency analysis. The remaining components of the high frequency recording system are coupled with the acoustic low power wake-up system based on frequency analysis utilising a low power device. Processing is done in three phases, each of which uses more energy:

A microphone first records the acoustic signal and sends it to our low power analogue wake-up detector via frequency analysis. A management system interrupt is delivered when the wake-up recognises a certain frequency sound that is characteristic of an animal. Upon receiving an interrupt, the management unit microcontroller shown in begins more advanced signal processing to determine whether the signal detected is a true alert or not. This processing may use traditional linear or nonlinear filters, neural networks, wavelets transform, or correlations. To enhance the accuracy of these extra calculations, other additional sensors may be employed. These processes are carried out as needed and use a significant amount of power—roughly 17.5mW. The management division may also send out an alert. The scope of this study does not include these filtering processes.

If the detection is successful, the management unit begins recording the microphone signal and saves it to an SD card for a predetermined period of time in order to capture any future occurrences of the intriguing signal. It's vital to note that since the signal for low power acoustic wake-up is lost, this method cannot be utilised to capture single-shot signals.

An analogue to digital signal buffer converter might be used to construct a low power acoustic wake-up system incorporated into the "Qualilife" recording system, however this would not be low power. To achieve the lowest power consumption, the analogue low power wake-up detector has been created with an emphasis on simplicity. It is based on converting frequency to voltage by driving a capacitor linearly at constant current using a monostable. Analog comparators periodically sample and retain the capacitor's voltage, which serves as an image of the input frequency, in order to compare it against thresholds.

This approach, which drastically reduces power consumption, was inspired by our earlier digital implementation on a PIC24FJ256 from Microchip analogue low power microphone signal is initially routed via a hysteresis comparator, as seen in. This comparator enables the removal of background noise by activating only when the US input signal is of a suitable level.

Low Pass Comparator 2 Low Pass Comparator 1 Signal Us Uh UM High Pass Comparator 1 High Pass Comparator .The monostable analogue timer will thus produce pulses UM with a constant high time but synced with the input signal thanks to the hysteresis comparator's output

Uh. At this stage, we can see that the UM average value is inversely related to the US frequency of the input signal. A simple RC filter may be employed at this stage, but because of the exponential charges of the RC filter, the frequency to voltage conversion would not be linear. Instead, a completely linear conversion is required in order to precisely estimate the input frequency.

Using a current mirror connected to capacitor C1, this linear conversion is carried out. This was motivated by our earlier approach, which is shown in [20]. The current mirror functions similarly to the Microchip microcontrollers' Charge Time Measurement Unit (CTMU) [27]. The left transistor of the current mirror maintains a steady current as a result of pulses from the monostable timer. The capacitor C1 is discharged when this current is reflected to produce IC1. As can be seen in Fig. 5, voltage UC1 drops linearly during the monostable pulses while being constant throughout the other phases where N is the number of pulses between two successive resets, TPW is the pulse duration, Um is a logical level 1 or 0, depending on the monostable output state, IO is the current during monostable pulses in the current mirror, FSH is the sample and hold frequency, and FS is the input signal frequency. The frequency may be seen in the UC1 voltage, which must be regularly read. This is accomplished by utilising a low frequency astable timer that generates a signal UA at a predetermined frequency on a regular basis.

Given that C1 capacitor value is much more significant than C2 capacitor value, UC1 voltage is sampled and held into UC2. In order to reset the voltage UC1 value at VCC after this sample and hold operation, the Q1 transistor is opened and the Q2 PMOS transistor is closed. As a result, UC2 voltage is a representation of input signal frequency. The process's last step involves comparing UC2 with preset values to ascertain if the observed frequency falls within or outside of a predetermined range. The frequency value might also be obtained using an ADC, but this would use far more power than our wake-up trigger does overall [3], [4].

The actualization

Utilizing very low power analogue components, an ultra-low-power wake-up detector was implemented on a PCB board. For instance, 3.3V reference voltage is achieved using the ultra low power regulator TPS783, which only uses 500nA to control the input voltage to 3.3V. Comparators for input, a hysteresis trigger is used to first process the input signal US. The Uh signal is produced by the hysteresis comparator. The hysteresis comparator will not be triggered by a little amount of background noise, removing input low level disturbances. The hysteresis comparator provides a more reliable noise rejection than the single comparators used.

A reference voltage produced by the supervisor's DAC may be used to change the hysteresis level in order to adapt filtering to various detection sensitivity levels. Due to the trade-off between operating frequency and power consumption, selecting the comparator is crucial. A promising contender is TVL3691, which has an extremely low power consumption (only 75nA). However, for high frequency activities like bat detection, its maximum switching frequency (30kHz) is inadequate (100kHz). Another reference has been selected, the Texas Instruments TLV7031, which has a propagation delay of 3 ns and a supply current of 335 nA. Signal processing at up to 300kHz is possible.

Timers: A crucial component of our analogue wake-up detector are ultra low power timers. They are used to produce astable sample and hold signals (UA), monostable pulses timed to the input signal's rising edges, and delayed signals (UR) that reset capacitor voltage after a sample and hold operation. Three timers are required for this. Power limitations led to the selection of the CSS555C, a very low-power version of the traditional 555 timer that can handle all of our requirements.

- **Monostable timer:** A monostable timer is triggered by the input comparators' signal U_h , which creates a rising edge U_M on each falling edge of the input signal. The hardware implementation utilising CSS555 relates pulse width (TPW) to: $L(RA + 2RB)CT = TPW$ (3)

Monostable Timer, with $L = 0.695$. TPW has been set at 0.66 s in order to process input signals at 100 kHz, resulting in $RA = 10$ pF, $RB = 0$ pF, and $CT = 100$ pF. It's important to note that while lower capacitor values CT were tried, the pulse width was less clearly specified since parasitic capacitors were not insignificant at these levels.

- **Low frequency astable timer:** A CSS555 timer may also provide an astable signal in the form of a periodic signal UA. Equation 4 is used to establish astable frequency:

$L = 0.695$ and $TOSC = L(RA + 2RB)CT$ (4). $RA = 700k$, $RB = 370k$, and $CT = 1nF$ have been selected to provide a sample and hold timer frequency of about 1kHz. The capacitor reset signal UR is produced for UA by utilising a CSS555 to create a pulse with a delay, as illustrated in Fig. 8. According to equation 5, the pulse width tPW and delay tD are set. The formula is $tD = 1.2 CT [tD0(RA / RF + RB) + (tD1RB)]$. (5) Where $L = 0.695$ and $tD0 = \ln(2.3) \ln(1.23 (RF + RA)/RF)$, $tPW = 1.2 CTL(RA / RF + 2RB)$.

The following settings were selected in order to have a delay of 20 seconds that would allow for a proper charge transfer from C1 to C2 before reset: RA is equal to 100k, RB to 10, RF to 510k, and CT to 100pF.

The Present Mirror The system's last key component is the current mirror. It is taking the place of the CTMU. For the purpose of draining the primary capacitor C1, the current mirror serves as a constant regulated current source that is powered by the monostable output U_M . Equation 7 demonstrates how the serial resistor and the monostable's output voltage, when triggered, determine the current value in the mirror I_0 .

The choice of the current mirror analogue component is crucial because mirror precision directly affects frequency measurement accuracy. Due to its cheap price, the BCV62 PNP current mirror has been tested for the first time. But because of its poor accuracy (only a 70% match between transistors T1 and T2), it was unsuitable for a precise frequency detection. Then, Texas Instrument's REF200 has been selected. With only 0.25% of matching between the two transistors, this expensive current mirror is very accurate.

For our 100kHz signal, it is more than capable up to 5MHz. Since the mirror only uses power when the monostable is activated, or seldom, power consumption is not a concern. The design is impacted by the REF200 selection. Capacitor C1 is being discharged by the mirror using NPN transistors, as opposed to charging the capacitor using a PNP mirror [5], [6].

Four) Capacitors and related currents: The analogue wake-up detector's central capacitor, C_1 , is charged linearly by subsequent phases. It's important to choose C_1 , C_2 , and I_0 's values carefully. Equation 2 results when the input frequency to be detected is 100 kHz, the sample and hold frequency is 1 kHz, the time between pulses (TPW) is 0.66 s, and the UC1 minimum value is 0. $I_0 C_1 = V_{CC} f_S f_{SH} TPW = 50000$. If the mirror current is restricted to $I_0 = 10 \text{ A}$, C_1 will conduct at 20 nF.

Following integration, the voltage in UC1 must be sampled and maintained in C_2 . Close Q1 PMOS to do this. Charges are moved from the C_1 to the C_2 , changing the value of UC1. The value of C_2 has to be decided to be much lower than C_1 and has been set at $C_2 = 1\text{nF}$ in order to make this shift as little as feasible[7], [8].

Output Comparators: After the UC1 has been sampled and held in the C_2 capacitor, the UC2 must be used in a highly effective and straightforward manner. As shown in Fig. 10, this is accomplished utilising comparators with very low power and low speed. A certain input frequency range may be accurately chosen in the output by combining two comparators. Both of the comparators' outputs will equal a logical 1 if the input signal frequency falls inside the chosen interval, which will cause an interrupt to be sent to the management unit. It is possible to create several comparison associations that will enable the detection of a signal across various frequency bands. To synchronise or trigger a wireless sensor network, as shown in, this may be utilised to detect produced frequencies.

It is not essential to utilise a quick comparator like the TVL7031 since the output comparators operate at a low frequency. The TVL3691 may be used in its place, which will result in an extra power decrease. Our ultra-low power wake-up detector can pick up sounds with frequencies as high as 300kHz. Three comparators TLV7031 are incorporated in the design, as shown in Fig. 4, and each one uses 0.335 A of power. The current mirror uses extremely little power since it is only ever used during very brief constable pulses and has a 10 A maximum active current. The resistors surrounding the CSS555C are also true in this regard. In contrast to the CSS555C, both MOSFETs are likewise used sparingly, which results in their very low power consumption. This results in an estimated total consumption of 36 W for the analogue wake-up detector when all power consumptions are added together.

The TLV7031 may be swapped out with the TLV3691, which consumes just 75nA but has a 30kHz frequency restriction, to minimize power consumption. Given that the last comparators operate at a low frequency, only those may be replaced (less than 1kHz). Power usage is lowered to 34 W with this replacement. This power use is comparable to the acoustic Wake-up detector microcontroller implementation shown in. It uses around 600 W of electricity. This indicates that the power consumption of our analogue wake-up detector is 18 times lower than that of the prior approach. Without taking into account the microphone, this enables the system to detect high frequency analogue wake-up events in continuous mode for 2.3 years on a single CR2032 coin battery with a 230mAh capacity. When coupled with Knowles' low power microphone FG-23329-P07, the power consumption rises to 230 W, allowing for 125 days of continuous detection on a single CR2032 coin battery. Three coin cells, totaling 9 grammes in weight, may provide a year's worth of autonomy.

The always-on, ultra-low power (34 W) wake-up detector described in this study is portable and compact. It may be used to military or environmental assessments, such as the covert intelligent recording of acoustic signals given out by drones or animals. It is employed as a prefiltering stage for identifying instants when an input signal of a specific frequency is present or anticipated to be there since it can detect high frequency acoustic waves in a very low power mode.

For long-term embedded stealth monitoring systems used in environmental or military applications, this approach is ideal. The Ilot Bagaud island, which is a part of France's Parc National de Port Cros, is protected against rat invasions by an analogue wake-up detector, which is used in conjunction with the Qualilife system for real-time recording, analysis, and warning transmission. Our analogue Wake-up detector may be used to create other applications for non-acoustic high frequency signal analysis and detection. Particularly, the use of photo-transistors rather than microphones enables the operation of a pulsed light wake-up system at a great distance without transmission delay. With this method, a complete wireless environmental sensor network may be concurrently triggered at a very low power consumption. Even in a thick setting, like a rain forest, this approach holds up. Trajectory applications in environmental surveys may be used in conjunction with this.

When a single transmitter and a single receiver interact with one another through a single link, it is said to be point-to-point communication. In this second category of communication networks, information-carrying signals often travel in both directions, necessitating the use of a transceiver (a transmitter and receiver) at each end of the link. An information source's message signal is transformed by the transmitter into a format that can be sent over the channel at a remote location. The receiver, who is situated at a separate location in space, receives the message signal after it has been sent by the channel. However, during signal transmission over the channel, channel flaws result in signal distortion. The output of the channel is also augmented with noise and interference signals from other sources, resulting in a distorted replica of the broadcast signal in the received signal. The receiver's job is to process the signal it receives in order to get close to the signal from the original message for the information user. Because of noise, interference, and bad channels, there will always be a little disparity between the transmitter input and the receiver output. This is why we use the phrase "estimate."

The radio may be used for broadcasting as well as point-to-point communication, depending on how it is used. Each of us is used to both AM and FM radio. (The abbreviations amplitude modulation (AM) and frequency modulation (FM) correspondingly. The two of them are constructed in an integrated form inside of a single unit, and we can find them in every house and on every car. We hear local, national, and international news, commentary, music, and weather forecasts on the radio that is broadcast by surrounding radio stations. Radios like AM and FM have traditionally been built using analogue technology. However, owing to the constantly advancing capabilities and cheap cost of digital circuitry, digital radio (in both AM and FM forms) is already in use today.

Radio transmits speech via electrical impulses. Television uses electrical impulses to transmit visual images, and it operates on similar electromagnetic and communication-theoretical

principles. Signal processing techniques are particularly suited to speech signals since they are by definition one-dimensional functions of time. On the other hand, a moving image is a two-dimensional function of time that demands deeper examination. Each image at any one time is really seen as a frame divided into a number of small squares called picture components, or pixels. The greater the resolution of an image, the more pixels are used to display it. By scanning the pixels in a predetermined sequence, the information in the image is converted into an electrical signal whose amplitude is proportional to the brightness level of each individual pixel. The visual stream is sent through the electrical signal generated at the scanner's output. The mapping process that results in the creation of the visual signal is well known to the receiver. Thus, using the video stream, the receiver may recreate the original image. The same great advancements in digital technology that have benefited digital radio also help television. These advancements, the employment of advanced digital signal processing techniques, and consumer demands led to the creation of high-definition television (HDTV), which considerably increases the quality of reconstructed visuals at the receiver output.

Our next destination is the point-to-point communication situation. Satellite communications and wireless communications are two more significant ways that radio has had an effect on our daily lives. Both the uplink and the downlink in satellite communications, which are centred on a satellite in geostationary orbit, need line-of-sight radio transmission in order to work. An uplink connects a transponder (the electrical circuitry of the satellite) to one Earth terminal, while a downlink connects a transponder to another Earth terminal. As a result, a signal conveying information is delivered from one Earth terminal to the satellite through the uplink, amplified in the transponder, and then sent back from the satellite via the downlink to the other Earth terminal.

In that both a downlink and an uplink are necessary, wireless communications operate somewhat similarly to satellite communications. The downlink is used for the forward-link radio transmission from a base station to its mobile users. The uplink manages the reverse-link radio transmission from mobile users to their base stations. Unlike satellite communications, which are dominated by the single-path phenomena, wireless communications are dominated by the multipath phenomenon because of reflections of the broadcast signal from objects (such as buildings, trees, etc.) that are in the propagation path. As a consequence, the receiver's performance often suffers, making the receiver's design a challenging task. Mobile communications, in any event, have a unique distinctive capability. Additionally, by using the cellular concept, the wireless communication system is able to reuse the radio spectrum across a sizable area as often as practical. The available communication resources inside a cell may be shared by mobile users operating inside of that cell[9]–[11].

The original version of the computer was envisioned as a solitary tool capable of doing mathematical calculations. However, it soon became apparent that, given a computer's inherent ability to carry out logical processes, it is ideally suited to the building of a communication network. Numerous routers, which are made up of clever processors like microprocessors, make up a communication network. The fact that these processors' primary duty is to route voice or data via the network is indicated by the name "routers." Every router has hosts attached to it

because a host is a device that connects with another host. The main purpose of a network is to transmit or exchange audio, video, or data between hosts, which is made feasible by the use of digital switching. The two primary forms of switching are circuit switching and packet switching.

Circuit switching creates specialised channels for message transmission between two or more stations, sometimes referred to as terminals. The communication circuit consists of a connected set of connections from source to destination. For instance, in time-division multiplexed systems, where several users may share a single channel, the connections might be made up of time slots. The most important thing to keep in mind is that, once set up, the circuit remains open during transmission. Circuit switching is often controlled by a centralised hierarchical control mechanism that is aware of the whole network's architecture. To establish a circuit-switched connection, a free channel over the phone network must be taken and then allotted to the two users who wish to talk exclusively. For instance, a call-request signal must reach its destination and be acknowledged before conversation can begin. At this stage, the users essentially "see through" the network, effectively "owning" the resources granted to the circuit for the length of the connection with the other user. This state continues until the circuit is broken.

Circuit switching is a suitable match for telephone networks, as voice transmission accounts for the bulk of network traffic. We make this assertion because voice conversations often take longer on average, roughly two minutes than the time required to configure the circuit. Speech also creates a stream of traffic (about 0.1 to 0.5 seconds). However, with packet switching, network resources are distributed in accordance with demand. As a result, packet switching is better than circuit switching in that Packet switching was developed by P. Baran in 1964 to fulfil a need for American national security. A distributed network with varying degrees of redundancy that is robust in the sense that it can withstand the loss of many nodes due to a coordinated attack while still enabling the remaining nodes to maintain intercommunication for carrying common and control information was the initial requirement.

The OSI reference model was developed by a division of the International Organization for Standardization (ISO) in 1977. For a description of the theories used to establish the first seven levels of the OSI model as well as an explanation of the layers themselves, see Tannenbaum (1996). When a connection has traffic to provide, it is often utilised more extensively. Contrary to oral communication, data transfers may occur in bursts.

The principle of packet switching networks is store and forward. Every message that is longer than a given size is divided into segments that do not exceed the necessary size before transmission, especially in a packet-switched network. Packets are the resultant pieces. At the destination, the original message is reassembled packet by packet after travelling via several network locations. As a result, the network may be seen as a set of network resources (such as channel bandwidth, buffers, and switching processors) that are dynamically shared by a number of competing sites that wish to join. This dynamic sharing of network resources contrasts strongly with the circuit-switched network, where resources are given to a pair of hosts for the duration of their interaction.

A data network is a kind of communication network in which computers and other terminals serve as the hosts. The design of such a network advances in an orderly fashion by thinking of the network in terms of a layered architecture, which is seen as a hierarchy of nested layers. A layer is a process or object designed to perform a certain function inside a computer system. A layer's developers will undoubtedly be familiar with the inner workings and intricate details. At the system level, where it is described in terms of inputs, outputs, and the functional connection between the inputs and outputs, the layer in issue is, however, solely visible to the user as a "black box." In a layered architecture, each layer perceives the layers below it as one or more "black boxes" with a predetermined set of functional needs that the layer above it may use. Thus, the very complex problem of communication in data networks is reduced to a manageable set of precisely defined, competitive roles. The open systems interconnection (OSI) reference model was developed as a result of this way of thinking. Given that the reference model and associated standards are followed, any two systems' capacity to join up is referred to as being "open."

The OSI reference model divides the functions of communication and associated connections into a number of layers with distinct interfaces. Each layer is created on top of the previous one. Each layer particularly performs a certain subset of fundamental operations and relies on the layer underneath it to do additional rudimentary functions. Each layer also offers certain services to the layer above it, shielding it from the mechanics of how those services are performed. Each pair of layers has an interface that describes the services that the lower layer provides to the upper layer.

The figure also outlines the functions of each of the model's component levels. Layer k on system A, for instance, communicates with layer R on system B according to a set of rules and specifications known as layer k protocol. Where $k = 1, 2, \dots, 7$. The term "protocol" is a borrowing from daily speech that relates to usual human social practice. Peer processes are the elements that different systems use to construct the proper levels. In other words, protocol-based peer-to-peer communication between systems A and B enables communication between them. Physical connection allowing end users access to the OSI environment between adjacent operations

Data transformation is the process of altering incoming data to provide the services that the application layer selects; encryption is one example of data transformation that provides security giving two collaborating users a control framework for communication and managing their conversation in an organized manner control over the entire communication chain, from source to destination, between users flow control and packet routing via the network are intended to ensure exceptional performance.

Unprocessed data bits are sent across a physical channel at layer 1, the physical layer, which also takes care of the functional, procedural, and mechanical requirements to access the channel. The second through seventh levels are virtually linked to their distant coworkers. Each of these last six tiers connects data and control with layers above and below through layer-to-layer interfaces. From the discussion of data networks that was just presented, one may access the Internet. In order to separate the present applications from the underlying network technology, the Internet paradigm uses an abstract notion of network service. We might elaborate by saying the following:

The network's construction technology has no bearing on how the applications operate. The three functional building blocks of an Internet application are hosts, subnets, and routers. The nodes of the network are the hosts where data is sent or received. Routers act as intermediate nodes to cross subnet boundaries. A subnet, for example, is a network of sites that directly exchange data with one another. A subnet's internal operation may be broadly classified into two types.

Connected method, where the connections are known as virtual circuits, in analogy with real telephone system circuits, and connectionless mode, where the independent packets are known as datagrams. Similar to earlier data networks, the Internet uses a hierarchy of protocols. The Internet protocol is especially used for data exchange between hosts and routers (IP). Making an addressing system that allows data packets to be sent from one node to another is simple. The routers choose the best path for packets travelling over a sub network border that are intended for a certain destination. This is sent using routing tables, which are produced by employing special protocols to exchange crucial information with other routers. The final result of employing the layered collection of protocols is the delivery of best effort service. In other words, each data packet will be sent across the Internet.

REFERENCES:

- [1] B. Mihajlovski, I. Minchev, I. Blinkov, and B. Simovski, "USE OF MODERN GEOMATIC TECHNIQUES FOR CREATING AND UPDATING A GREEN CADASTRE OF URBAN TREES AND SHRUBS: A CASE STUDY OF KUMANOVO CITY RIVER BANK," *For. Rev.*, 2018.
- [2] Z. Huang, J. Epps, D. Joachim, and M. Chen, "Depression detection from short utterances via diverse smartphones in natural environmental conditions," in *Proceedings of the Annual Conference of the International Speech Communication Association, INTERSPEECH*, 2018. doi: 10.21437/Interspeech.2018-1743.
- [3] A. V. J. Ratulangi, S. Pangemanan, and V. Tirayoh, "ANALISIS PENERAPAN AKUNTANSI LINGKUNGAN TERHADAP BIAYA OPERASIONAL PENGELOLAHAN LIMBAH PADA RUMAH SAKIT PANCARAN KASIH MANADO," *GOING CONCERN J. Ris. Akunt.*, 2018, doi: 10.32400/gc.13.03.20292.2018.
- [4] M. A. Bockbrader, G. Francisco, R. Lee, J. Olson, R. Solinsky, and M. L. Boninger, "Brain Computer Interfaces in Rehabilitation Medicine," *PM and R*. 2018. doi: 10.1016/j.pmrj.2018.05.028.
- [5] I. Trancoso, J. Correia, F. Teixeira, B. Raj, and A. Abad, "Analysing speech for clinical applications," in *Lecture Notes in Computer Science (including subseries Lecture Notes in Artificial Intelligence and Lecture Notes in Bioinformatics)*, 2018. doi: 10.1007/978-3-030-00810-9_1.
- [6] C. Bayes, "The Cyborg Flâneur: Reimagining Urban Nature through the Act of Walking," *M/C J.*, 2018, doi: 10.5204/mcj.1444.
- [7] K. Saravanan and S. Saraniya, "Cloud IOT based novel livestock monitoring and identification system using UID," *Sens. Rev.*, 2018, doi: 10.1108/SR-08-2017-0152.

- [8] A. V. Lindseth and P. S. Lobel, "Underwater soundscape monitoring and fish bioacoustics: A review," *Fishes*. 2018. doi: 10.3390/fishes3030036.
- [9] J. L. Bao and Q. F. Fu, "Cell-FET sensors and their potential application," *Progress in Biochemistry and Biophysics*. 2018. doi: 10.16476/j.pibb.2017.0162.
- [10] T. G. Laske *et al.*, "Development and utilization of implantable cardiac monitors in free-ranging American black and Eurasian brown bears: System evolution and lessons learned," *Animal Biotelemetry*. 2018. doi: 10.1186/s40317-018-0157-z.
- [11] P. Boissy, M. Blamoutier, S. Brière, and C. Duval, "Quantification of Free-Living Community Mobility in Healthy Older Adults Using Wearable Sensors," *Front. Public Heal.*, 2018, doi: 10.3389/fpubh.2018.00216.